Shabnam Homaei

TOWARDS RESILIENT BUILDING PERFORMANCE: DEFINITIONS, FRAMEWORKS, AND METRICS

Doctoral thesis

NTNU
Norwegian University of Science and Technology
Thesis for the Degree of
Philosophiae Doctor
Faculty of Engineering
Department of Civil and Environmental
Engineering

NTNU
Norwegian University of
Science and Technology

Shabnam Homaei

TOWARDS RESILIENT BUILDING PERFORMANCE: DEFINITIONS, FRAMEWORKS, AND METRICS

Thesis for the Degree of Philosophiae Doctor

Trondheim, June 2022

Norwegian University of Science and Technology
Faculty of Engineering
Department of Civil and Environmental Engineering

NTNU
Norwegian University of
Science and Technology

Preface

This work was carried out at the Department of Civil and Environmental Engineering at the Norwegian University of Science and Technology (NTNU) from October 2017 to December 2021.

This project was funded by the research center of Zero Emission Neighbourhoods in Smart Cities (FME ZEN) and performed at the Department of Civil and Environmental Engineering (IBM), NTNU, Trondheim. The work was supervised by Associate Professor Mohamed Hamdy from NTNU.

Seven peer-reviewed scientific papers are the core of the dissertation. Four of these papers are listed as primary papers, in which I collaborated as the first author. Three additional papers are appended as supporting papers, which demonstrate the application of the primary papers in collaboration with other researchers.

This PhD thesis is a great accomplishment for me personally, and I hope that it also inspires others to contribute to the transition of the building sector into a positive force towards a more sustainable future.

Trondheim, December 2021
Shabnam Homaei

Abstract

In recent years, resilience has become a relevant issue in the context of building performance , owing to the diverse future events, which includes climate change, extreme weather events, energy supply disturbances, and pandemics. In traditional building designs, building performance is typically estimated under a fixed set of assumptions. However, significant external factors can impact building performance during its operational phase but have not been considered by designers. Failure to protect building performance against these changes can lead to serious short- and long-term challenges, such as fails in meeting the demands of building occupants. Therefore, the resilience of building performance needs to be investigated such that its sensitivity to external factors, like climate change, is reduced.

In this thesis, a building is defined as resilient if it is able to prepare for, absorb, adapt to, and recover from disruptive events. Despite the potential of resilient building designs and their growing interest, an agreed-upon definition for resilience in the context of building performance requires further research, along with the development of methodologies for resilience quantification. This situation is partly due to the polysemic background of the resilience definition that is interpreted differently in various fields.

This thesis investigates resilience in the context of building performance and develops methodologies, frameworks, and metrics for the quantification of resilience on the building scale. This paper-based thesis first focuses on adapting the existing resilience definitions to the context of building performance. This procedure begins with four questions related to the concept of resilience, which are resilience of what? resilience to what, resilience in what state, and resilience based on what? The answers to these questions allow designers to establish the key parameters for a resilient design.

Resilient systems usually have a combination of attributes that influence resilience and contribute in the quantification of resilience level through the derivation and validation of a function form in regard to functionality and time. The second research activity identifies robustness and flexibility as two important attributes of resilient building design and develops methodologies for their quantification.

As the final step, a methodology is developed, focusing on a framework for the quantification of resilience itself. This step introduces a single metric

for thermal resilience quantification in the scale of buildings. The metric is implemented for resilience labeling. In the quantification methodologies, IDA Indoor Climate and Energy software (IDA-ICE) is used as a building performance simulation tool, and MATLAB is used as a numerical analysis tool. The developed quantification methodologies were tested on a case study of a Norwegian single-family house.

The results of this research led to seven peer-reviewed papers, in which four comprise the core of the thesis and are listed as primary papers. The other three papers, which are from collaborations with other researchers, are listed as supporting papers in this thesis. The results highlight the suitability of the proposed methodologies and metrics for the quantification of resilience and its attributes. For example, for the considered case study building in Norway, it has been shown that upgrading building design from the current minimum design to a passive design has a significant impact (71% improvement) on the thermal resilience against power failure during winter. Furthermore, the results of the case study implied that various building designs with the same energy consumption can behave differently when facing uncertainties in the future, such as changes in weather conditions, occupant behavior, and energy prices.

Uncertainties of the future highlight that the evaluation of energy performance by itself will not be enough in the energy performance certificates in the near future. Therefore, the evaluation of other concepts, such as building resilience (robustness and flexibility), is also needed. This thesis takes one step forward in this regard by developing metrics, quantification frameworks, and methodologies for the evaluation of robustness, flexibility, and resilience that can be easily used by architects, building designers, decision-makers, etc. to benchmark different building designs and technologies from these perspectives.

Acknowledgment

I still remember the first day of my PhD at NTNU on a cold and rainy October day in Trondheim. Today, I am at the end of my PhD with extensive new knowledge and expertise after many ups and downs and moments of both despair and hope. Countless people have supported me during this journey.

First of all, I would like to thank my supervisor Mohamed Hamdy for trusting me, believing in me, encouraging me to be ambitious, and teaching me how to be patient and develop good research. I admire his open-door policy, creativity, and engagement. Indeed, he had a significant role in shaping and developing of this PhD work.

Many thanks are given to all researchers and colleagues involved in the ZEN research center and IEA EBC Annex 80 for all motivational meetings and their valuable feedback.

These four years have been very enjoyable thanks to the amazing friends I made here, especially Matteo, Alla, Amin, Therese, Mina, Rozita, Siri, Camilla, and Coline. Our nice coffee and lunch breaks were invaluable.

I am also very appreciative for all of the support from my parents, Pari and Firouz, and my fantastic sister, Shamim. Almost 5000 kilometers separated us, but they were always there for me.

Last but not least, my warmest thanks and love go to my boyfriend, Reza, for his patience, unlimited support, and encouragement during my study. This would not be possible without his help.

Trondheim, December 2021
Shabnam Homaei

List of papers

Primary papers

Paper I:
Homaei S, Hamdy M. A robustness-based decision making approach for multi-target high performance buildings under uncertain scenarios. *Applied Energy*. 2020 Jun 1;267:114868.

Paper II:
Homaei S, Hamdy M. Quantification of energy flexibility and survivability of all-electric buildings with cost-effective battery size: methodology and indexes. *Energies*. 2021 Jan;14(10):2787.

Paper III:
Homaei S, Hamdy M. (2021). Developing a test framework for assessing building thermal resilience. *Proceeding of Building Simulation 2021 Conference*, Bruges, Belgium.

Paper IV:
Homaei S, Hamdy M. Thermal resilient buildings: How to be quantified? A novel benchmarking framework and labelling metric. *Building and Environment*. 2021 Jun 2:108022.

Supporting papers

Paper V:
Attia S, Levinson R, Ndongo E, Holzer P, Kazanci OB, Homaei S, Zhang C, Olesen BW, Qi D, Hamdy M, Heiselberg P. Resilient cooling of buildings to protect against heat waves and power outages: Key concepts and definition. *Energy and Buildings*. 2021 May 15;239:110869.

Paper VI:
Rahif R, Hamdy M, Homaei S, Zhang C, Holzer P, Attia S. Simulation-based framework to evaluate resistivity of cooling strategies in buildings against overheating impact of climate change. *Building and Environment*. 2021 Nov 19:108599.

Paper VII:
Moschetti R, Homaei S, Taveres-Chacat E, Grynning S. Assessing responsive building envelope designs through robustness-based multicriteria decision

making in zero-emission buildings. *Submitted to Journal of Energies.*

Abbreviations

Symbols

Ad	Adaptation
AHP	Analytical Hierarchy Process
ASHP	Air source heat pump
BPS	Building performance simulation
CHP	Combined heat and power
CO_2	Carbon dioxide
CPP	Critical peak pricing
DH	District heating
DHW	Domestic hot water
DM	Decision making
DR	Demand response
EPBD	Energy performance of building directive
EPC	Energy performance certificates
ER	Electric radiator
EV	Electric vehicle
IPCC	Intergovernmental Panel on Climate Change
IWEC	International Weather for Energy calculations
LED	Light emitting diode
MAUT	Multi-attribute utility theory
MCDM	Multi-criteria decision making
NMF	Neutral modeling format
NVE	Norwegian water resource and energy
P	Preparation
PD	Performance deviation
PR	Performance regret
PS	Performance spreed
PV	Photovoltaic
RES	Renewable energy source
RC	Resilience curves
RS	Recovery speed

STC	Solar thermal collector
SPM	Simple performance metric
T	Test condition
TCL	Thermostatically controlled loads
TEK	Norwegian building regulation
WHO	World health organization

Physical quantities

AoE	Amplitude of event
A_{AF}	Total floor area (m^2)
A_z	Area of each zone (m^2)
AC	Annual cost without shift (€/yr)
$ACES$	Annual cost with effective shift (€/yr)
$ACIS$	Annual cost with ideal shift (€/yr)
A_m	Maximum performance of design m across all scenarios
ASI	Active survivability index (%)
B_m	Minimum performance of design m across all scenarios
C_{Bat}	Cost effective battery size (kWh)
$CEFI$	Cost effective flexibility index (%/kWh)
C_n	Minimum performance of each scenario
COP	Coefficient of performance
CS	Collapse speed (°C/h)
D_i	Best performance of all designs across all scenarios
EHS	Effective heat shift (kWh/yr)
EPL	Expected performance loss (degree.hour)
$H(A_i)$	Hurwicz weighted average

	for alternative A_i
i	Segment counter
IHS	Ideal heat shift (kWh/yr)
IOD	Indoor overheating degree (°C)
$KPI_{i,m}$	Robustness margin
KPI_{rel}	Relative performance
$KPI_{m,n}$	Performance of design m across scenario n
$K\bar{P}I_i$	Mean of performance indicator (i)
	across scenarios
PSI	Passive survivability index (h)
P_{min}	Minimum building performance during disruption
P_n	Normal building performance
SI	Saving index (%)
SFP	Specific fan power (kWh/m^3)
SRI	Smart readiness indicator(%)
s_i	Area of segment i (m^2)
t_0	Disturbance start time (day)
t_1	Disturbance end time (day)
t_2	Test end time (day)
t_d	Delay time (h)
t	time (day)
T_{HT}	Temperature threshold for
	habitability (°C)
T_{min}	Minimum temperature during
	test period (°C)
t_R	Recovery time (h)
T_{RT}	Temperature threshold for
	robustness (°C)
T_{SP}	Setpoint temperature (°C)
U	U value W/m^2.K
W_E	Exposure time penalty
W_H	Hazard penalty
W_P	Phase penalty
$WUMTP$	Weighted unmet thermal performance
	(Degree.hours)

$WUMTP_{overall}$	Overall weighted unmet thermal performance (Degree.hours)
$WUMTP_{overall,r}$	Overall WUMTP of the reference building (Degree.hours)
WWR	Window to wall ratio
z	Zone counter
α	Weighted preference
σ	Standard deviation

Contents

List of Figures

List of Tables

CHAPTER 1

Introduction

1.1 Motivation

Buildings play important roles in addressing the fundamental needs of their occupants, such as health and comfort. In developed countries, people spend more than 87% of their time indoors [2], which highlights the need for safe buildings to protect occupants under various circumstances. Generally, buildings are designed based on fixed assumptions according to common standards and local regulations, and building performance is estimated based on these assumptions. However, the actual building performance can be different during its life span because of numerous changes that arise during the building's operational phase. These changes can be categorized as internal or external. Internal changes are related to the building itself (e.g., performance degradation of the building envelope and energy supply systems [3]) and are usually addressed in the design phase. External changes are related to external factors, such as changes in the building's environment (e.g., climate change [4, 5] and variation in occupant behavior [6]) or building requirements (e.g., new technologies such as 4th generation of district heating [7] or electric vehicles [8]). These external changes are rarely considered in the building design or renovation phases.

Climate change is one of the main sources of changes and it has a significant effect on building performance. Understanding the impact of climate change on building performance is extremely challenging, owing to the multivariate and multi-scale influence of the climate system [9]. Although designers consider the impact of climate change by using the normal climate data and the projections of climate change based on climate models, climate conditions far from the expected ranges may occur [10].

Buildings as facilities with significant investment costs need to be able to react to these changes and maintain performance and functionality. Therefore, research interest has expanded to push the building designs beyond

minimum standard requirements to meet performance targets even under potential future changes [11]. A decrease in the sensitivity of building performance against external factors and other uncertainties is vital. This can be achieved by considering the impact of changes and applying risk management strategies against them. In general, one approach to ensure system performance against future uncertainties, including disturbances and shocks, is mitigation in the form of protection: designing systems to withstand and absorb undesired events [12]. In this regard, emphasises haven been placed on the concept of resilience as a protection strategy due to its role in decreasing the risks associated with inevitable disturbances that can influence building performance.

In the context of the built environment, resilience as an integrated approach across different building systems, standards, and practices can be evaluated based on various performance criteria, such as energy, comfort, moisture, and environmental performance. Furthermore, in building construction, there is a great potential for specific design options and strategies, such as building envelope, energy systems, and backup and storage systems. These solutions can be introduced in the form of integrated building designs to improve a building's resilience. In this regard, building performance simulation (BPS) enables designers to simulate their design concepts and evaluate the corresponded resilience levels by considering the impact of the upcoming changes on design performance.

Despite the existence of resilience enhancement strategies, there is still a need for common, succinct definitions, frameworks, and tools that can be implemented for benchmarking, such that the resilience of different building designs and strategies can be compared. Such frameworks and tools are based upon resilience quantification indicators and metrics, which can be used by building designers and decision-makers to make effective decisions with respect to performance resilience.

This PhD work defines resilience in the context of building performance by introducing the abilities of resilient building designs and different attributes of resiliency in this context. In addition, methodologies are developed for the quantification of building resilience that can be implemented to benchmark and compare resilience levels of different building designs and strategies. The concept of building performance is a general concept, which allows for quantifying how well a building fulfils its function [13]. Literature shows that there is no generally accepted framework for evaluation of building performance. The reason behind this can be summarised in three main points:defining an ultimate list of performance criteria that needed to be considered is not an easy task, the evaluation process of building performance can be a challenging process to establish, and the last reason is

the challenge with different goals and ambitions of the building stakeholders. There are many examples of building performance criteria, which are related to a set of functions that the building is expected to provide such as energy performance, visual performance, acoustic performance, thermal comfort, indoor air quality, structural performance, etc. In this work, the word building performance is mainly focusing on the energy performance and thermal comfort aspects of the building. Building performance under upcoming uncertainties and potential disruptive events is evaluated with BPS tools. This provides a ground for developing frameworks and metrics to quantify resilience and other attributes, such as robustness and flexibility. In the end, the combination of the above-mentioned steps develops methodologies that can be used by architects, engineers, and other decision-makers to effectively consider the impact of future events on building performance in the design or renovation phases and achieve solutions that can prepare for, absorb, adapt to, and recover from disruptive events, which will be suggested as a definition for resilient building design in this work and will be explained later.

1.2   Objective of the study and research questions

The main objective of this thesis is to develop a modeling and simulation methodology for the evaluation of the resilience of integrated building designs that can be used by designers and decision-makers during design or renovation phases to achieve resilient building designs under future uncertainties and events. The overarching aim is to contribute to developing new knowledge about resilience and its evaluation to explore, improve, and assess the potential impact of different integrated building designs on building resilience. The research objective has developed into the following research questions:

- **RQ1:** What is the definition of resilience in the context of building performance?

- **RQ2:** What are the main sources of uncertainties, changes, and disruptive events that buildings face during their operational phases?

- **RQ3:** What are the abilities and attributes of a resilient building design?

- **RQ4:** How can decision-makers benchmark resilience levels and quantify those of integrated building designs?

1.3   Story line of the thesis

This work presents an extended summary of the research carried out during this thesis and builds on three peer-reviewed scientific journal papers and one conference paper. In addition, three more peer-reviewed scientific journal papers in collaboration with other researchers have resulted as supporting papers.

The thesis starts with the definition of building resilience and identification of resilience attributes in the context of building performance and ends with the quantification of resilience and its attributes.

First, resilience in the context of building performance is defined. An evaluation of existing literature shows the definition of resilience in various contexts involves different sets of questions. Hence, the thesis identifies four main questions to define the concept of resilience in the context of building performance, which are: resilience of what? resilience to what? resilience in what state? and resilience based on what? The answers to these questions reveal the different states a resilient building faces during disruptions, the abilities of a resilient building, and its attributes. These efforts answer RQ1, RQ2, and RQ3 of the thesis and related research is also reflected in Papers III, IV, and V.

Second, after defining resilience (i.e., phases, abilities, and attributes), two main attributes of resilient building design—robustness and flexibility—are studied in detail. Furthermore, methodological approaches are developed for the quantification of these two attributes to answer RQ3 and RQ4. Related research is published in Papers I and II, including the methodologies and application on a case-study building.

Finally, the thesis focuses on the quantification of building performance resilience and develops a methodology for the quantification and labeling of resilience level that can be used for assessing the resilience of different building designs and technologies. This effort answers RQ1 and RQ4, as reflected in Papers III and IV. Paper IV is considered the main outcome of this thesis, which was built upon the knowledge attained from the previous papers.

This thesis is expected to reach a diverse audience in the field of building design, owing to the multidisciplinary relevance of the work. Various stakeholders in building projects will find value in the results. For example, architects can implement the developed methodologies and evaluate different architectural designs from the resilience perspective. In addition, engineers can apply these methodologies to evaluate the impact of various technologies and strategies, including building envelope design, renewable energy sources, and electric vehicles, on building resilience. As an example in larger scales,

decision-makers can employ these methodologies and metrics in grid companies to evaluate the impact of interactions between buildings or with the grid, yielding guidelines for a resilient building design. This thesis consists of seven chapters, structured as follows:

Chapter 1 provides an introduction to the concept of resilient building design and the aims of the thesis.

Chapter 2 provides the theoretical background for the research. It contains a foundation that is needed to define resilience in the context of building performance, by introducing four questions, which are focusing on the disruptive events, abilities of a resilient building, and different attributes of resilience. Furthermore, the chapter provides states of the art of the disturbances that influence building performance and current resilience quantification metrics and methods. At the end of this chapter, the implemented workflow in the thesis has been described.

Chapter 3 introduces the concept of robustness as an attribute of resilient building design and develops a methodology for selecting high-performance and robust building designs.

Chapter 4 explains the concept of building energy flexibility as an attribute of resilient building design and its quantification.

Chapter 5 focuses on the quantification of resilience itself and develops a benchmarking framework and labeling metric to evaluate building resilience.

Chapter 6 presents main findings, concluding remarks, and suggestions for future work.

1.4 Contribution in the appended papers

Three journal papers and one conference paper build the foundation of this PhD thesis. Furthermore, the activities in this thesis led to collaborations with other researchers, yielding three more journal papers, which are listed as supporting papers. An overview of the papers and their links to the research questions are presented in Figure1.1. The main topics and author contributions to each paper are described below:

> ***Primary papers***

Paper I:
Homaei, Shabnam; Hamdy, Mohamed. "A robustness-based decision making approach for multi-target high performance buildings under uncertain scenarios." Applied Energy 267 (2020): 114868.

Paper II:
Homaei, Shabnam; Hamdy, Mohamed. "Quantification of eenergy flexibility and survivability of all-eelectric buildings with cost-effective battery size: methodology and indexes." Energies 14.10 (2021): 2787.

Paper III:

Homei, Shabnam; Hamdy, Mohamed, "Developing a test framework for assessing building thermal resilience.". Building Simulation 2021 conference, Bruges, Belgium, 2021.

Paper IV:

Homaei, Shabnam; Hamdy, Mohamed. "Thermal resilient buildings: How to be quantified? A novel benchmarking framework and labelling metric." Building and Environment (2021): 108022.

Contributions to primary Papers I–IV. For Papers I–IV, my collaboration with Mohamed Hamdy helped to conceptualize these works. I then developed algorithms to establish new indicators in MATLAB. In addition, I created and validated simulation models in IDA ICE. My work also included running the algorithms and simulations. Finally, I created supporting figures and wrote the original draft. The post-processing algorithm, analysis of the simulation results, revisions, and edits were performed in collaboration with Mohamed Hamdy.

Supporting papers

Paper V:

Attia, Shady; Levinson, Ronnen; Ndongo Eileen; Holzer, Peter; Berk Kazanci, Ongun; Homaei, Shabnam; Hamdy, Mohamed, et al. "Resilient cooling of buildings to protect against heat waves and power outages: Key concepts and definition." Energy and Buildings 239 (2021): 110869.

Paper VI:

Rahif, Ramin; Hamdy, Mohamed; Homaei, Shabnam; Chang, Chen; Holzer, Peter; Attia, Shady; "Simulation-Based Framework to Evaluate Climate Resistivity of Buildings." Submitted to the Journal of Building and Environment

Contribution to supporting Paper V and VI Papers V and VI resulted from collaborations with IEA EBC Annex 80 (Resilient Cooling of Buildings). For these works, I took part in conceptualization, reviewing, and editing with the other authors.

Paper VII:

Moschetti, Roberta; Homaei, Shabnam;Taveres-Chacat, Ellika; Grynning, Steinar. "."Assessing responsive building envelope designs through robustness-based multi criteria decision making in zero-emission buildings. Submitted to the Journal of Energy and Buildings.

Contribution to supporting Paper VII: Paper VII comes from a collaboration with SINTEF Community in Trondheim. For this work, I took

part in the simulation of the case-study building, conceptualization, visualization, reviewing, and editing with the other authors.
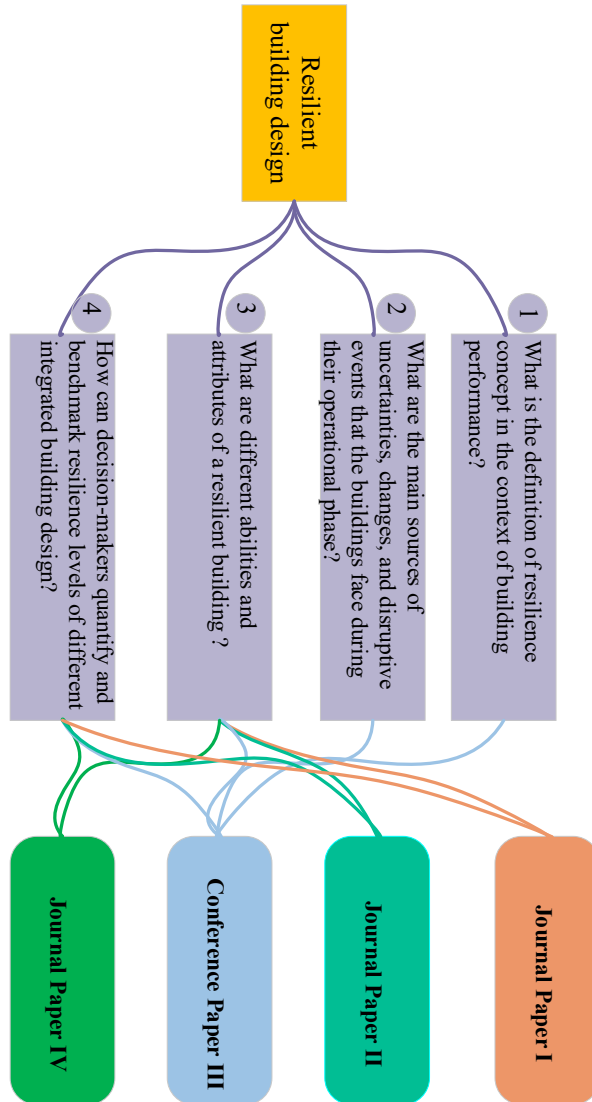
Figure 1.1: Organization of the research questions in the thesis and answers in the publication contributions.

CHAPTER 2

Research Context and Background

A report of the Intergovernmental Panel on Climate Change (IPCC) [14] showed that the severity and frequency of "low probability high impact events," such as natural disasters, are expected to increase because of climate change. Accordingly, extreme heat events are occurring more frequently and lasting longer with greater intensity in comparison to those in the pre-industrial era. For instance, the number of yearly heat waves in the United States (US) has increased steadily, from an average of two during the 1960s to six in 2010 [15]. Based on the report of the Copernicus Climate Change Service, 2019 was the warmest year on record for Europe, with June as the hottest month [16]. Furthermore, in recent decades, climate change has increased the frequency and severity of extreme cold events, such as windstorms and snowstorms [17]. A recent example is the record-low temperatures during the 2021 winter in Texas, US, which were followed by snow and blackouts, leaving millions of people without electricity during the COVID-19 pandemic [18]. Such events can disturb energy generation systems and lead to interruptions in meeting building occupants' needs. A report of the European Network of Transmission System Operators presented a significant growth in grid disturbance (30–60%) caused by environmental factors in the Nordic regions [19]. To protect building performance against disruptive events, attention is now being paid to the concept of resilience, but what is resilience exactly and how is it obtained? These questions will be answered in the next subsections.

2.1   Concept of resilience

A comprehensive definition of the concept of resilience is hard to obtain, since researchers with different academic backgrounds may have different objectives when investigating resilience. The word resilience stems from the Latin root "risilio" meaning "spring back". The common definition of re-

silience deals with "the ability of an entity or system to return to normal condition after the occurrence of an event that disrupts its state" [12]. In the context of the built environment, three main perspectives of resilience can be distinguished from the literature: engineering resilience, ecological resilience, adaptive resilience [20].

Engineering resilience is defined as the ability of a system to return to its pre-disturbance equilibrium state after facing the disturbance [21]. This definition focuses on the predictability of adverse events, assuming that human-made prediction systems are reliable in predicting these events. The speed of recovery is used as a measure of resilience with a focus on efficiency, constancy, and predictability, which are desired characteristics of a fail-safe engineering design [22].

In contrast, ecological resilience rejects single-state equilibrium and introduces multi-equilibrium and the possibility of changing between equilibrium states [23]. This type of resilience focuses on the system's capacity to absorb changes and retain its main structure and function [21]. The system may shift to a new equilibrium state as long as its structure and function are unchanged. Here, the magnitude of disturbance that can be absorbed before flipping to another equilibrium state is the measure of resilience, with the focus on persistence, change, unpredictability, and safe-fail designs [22].

Finally, adaptive resilience is defined for complex and dynamic socio-ecological systems that may change over time with and without external disturbances. Rather than returning to the normality, the definition entails the ability to change, adapt, and transform in response to a disturbance [23]. This refers resilience to short-term coping and long-term adaptation, which involves not only bouncing back but also bouncing forward [24]. Adaptive resilience emphasizes the importance of other fundamental attributes, such as adaptability, flexibility, self-organization, and ability to learn from disturbances [20].

Building performance faces a wide range of uncertainties (predictable and unpredictable), and adaptability, flexibility, and learning from disturbances are crucial when in the face of uncertainties, such as climate change. Therefore, adaptive resilience is implemented as a basis for building resilience definition in this work. Figure 2.1 shows three different forms of resilience based on the ball-and-cup model of system stability. Stable equilibrium is shown with the dark balls, while the light balls indicate the disturbed states. Engineering resilience refers to the movement of a system around only one stable equilibrium. While ecological resilience allows the transformation between multiple equilibrium states, in adaptive resilience, the equilibrium state along with the stability domain itself can adapt to disturbances.

The literature shows that resilience definitions typically include six main
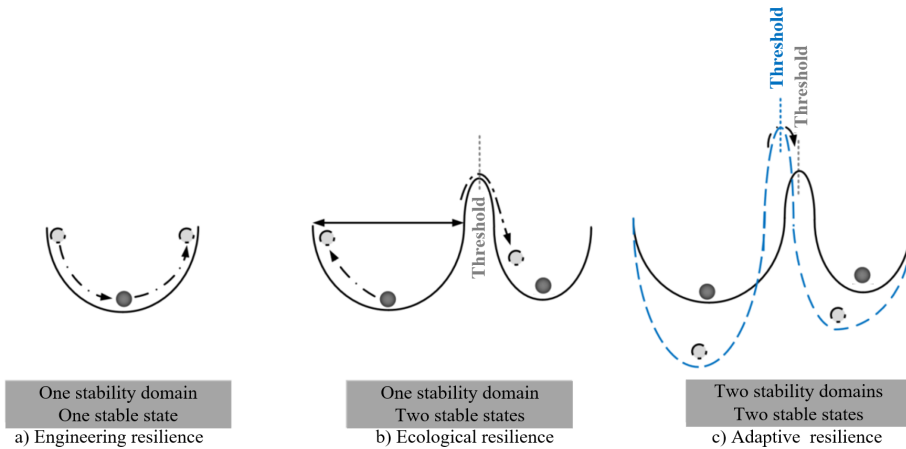
Figure 2.1: Visualization of resilience definitions based on the ball-and-cup model of system stability.

components, namely "the ability of the system to prepare, resist, absorb, respond to, adapt to, and recover from a disturbance" [25]. Based on the context and the characteristics of the system and the disruptive event, various combinations of these components have been used in the resilience definitions in different fields [26]. For example, Sharifi and Yamagata [20] suggested abilities of preparation, absorption, recovery, and adaptation for the sustainable and resilient urban system. Shandiz et al. [25] counted preparation, withstanding, adaptation, and recovery as important abilities of the energy-resilient communities. Nik et al.[27] divided the resilience characteristics into four main groups: planning and preparation, resisting, adapting to, and recovering from. Given this information, the resilient building has been defined as follows in this work:

For a building, in order to be resilient, the building should be able to prepare for, absorb, adapt to, and recover from the disruptive event.

Researchers have tried to ease the definition of resilience as a polysemic concept and create a clear definition by posing different questions. For instance, in the context of the built environment, Meerow et al. [28] concluded that the application of resilience requires answers to these questions: Resilience for whom and to what? When? Where? and Why? Sharifi and Yamagata [20] developed a framework for urban resilience forms by answering four questions: "Resilience of what?" "Resilience to what?""Resilience in what stage?" "Resilience for what?" Attia et al. [29] defined the concept of resilient cooling in buildings by answering three questions regarding resilience: "Resilience against what?", "Resilience at which scale? ", and "Resilience for
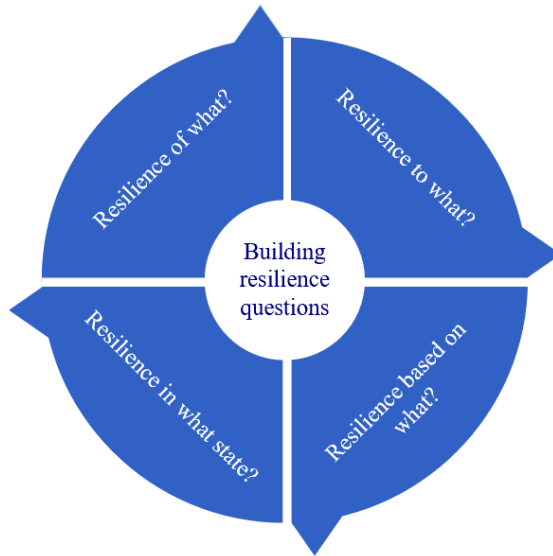
Figure 2.2: Fundamental questions related to the building resilience definition.

how long?" Inspired by these fundamental questions from the literature, this work poses four questions as follows: Resilience of what? Resilience to what? Resilience in what state? Resilience based on what? These questions are illustrated in Figure 2.2 and elaborated in the following sections:

2.2   Fundamental questions in the building resilience

2.2.1   Resilience of what?

The resilience of a system cannot be studied without a clear definition of the system scale, source of disruption, and its impact [29]. Utilization of the resilience concept requires specifying what will be resilient to what? The metaphor of "Resilience of what to what" has been used in different fields such as the evaluation of resilience for socio-ecological systems, technical systems, etc. It is crucial to elaborate on the scale of the system and the source of the disturbances, which are going to affect systems. In the context of built environment, resilience researchers [20, 30] considered different scales from micro (building or building element) to macro (district, city, or urban scale). For instance, on the macro scale, Meerow et.al [28] provided a detailed definition of "urban" trying to answer the question of the resilience of what in the concept of urban resilience. On the micro-scale,

IEA EBC Annex 80 focuses on the concept of resilient cooling of building within certain boundary conditions that are limited to the buildings [29]. In another study, Attia et al.[29] categorized the resilience evaluation scale into six different scales: a single zone, systems, buildings, neighborhoods, or larger scales, including urban districts or cities. When it comes to the buildings, the definition of resilience should reflect whether the disruption affects the performance of a single building element, a specific building service, or the entire building. Alfaridi and Boussabaine [31] address building resilience design in six categories: site, layout, structure, envelope, system, and operation. Based on their categories, the focus of this work will be mainly on the envelope, system, and operation. In the current work, resilience is evaluated on the scale of an entire building and its integrated energy systems. By integrated systems, we mean the heating and cooling generation and distribution systems, ventilation systems, air conditioning systems, hot water, and appliances inside the building.

2.2.2 Resilience to what?

Major sources of disruptive events are natural disasters. A report by the IPCC [14] shows that the severity and frequency of natural disasters are expected to increase because of climate change. Below et al. [32] divided natural disasters into six categories: meteorological, hydrological, geophysical, climatological, and biological events.A review of various disruptive events in the context of the built environment is summarized in Table 2.1. In this table, some studies were selected from the literature following with the purpose of the study and the types of disruptive events. Note that different kinds of resilience (e.g., seismic resilience and thermal resilience) were considered in this comparison.

Literature shows that, in general the disruptive events have been categorized into two different approaches. The first approach is the classification of disturbances based on their probability of occurrence and impact intensity, which classifies disturbances into two groups: low probability high impact events or high probability low impact events [27].In resilience evaluation, low probability high impact events have been used [17]. The second classification, which has been found is focusing on the impact intensity and duration of disruptive events [25].

Considering the classification suggested by Below et al. and other sources of disturbances identified in Table 2.1, disruption types are categorized into two groups in this work, as shown in Figure 2.3: natural and technological. Natural disruptions are further categorized into six groups based on [32]. As stated before, the performance of building is mainly being evaluated from energy and comfort perspective in this work. Natural disasters such as

13

Table 2.1: Review of selected studies on different types of disruptive events implemented in the resilience evaluation in the context of built environment.

Author	Purpose	Disruptive event	Ref
Li & Chan (2000)	Developing an index to define stressful weather condition	Weather stresses	[33]
Bruneau et al. (2003)	Developing a framework and measures for seismic resilience	Earthquake	[30]
Lomas & Ji (2009)	Resilience evaluation of naturally ventilated building under current and future climate	Climate change	[34]
Lomas & Giridharan (2012)	Evaluation of thermal resilience of free-running buildings against climate change	Climate change	[35]
Tokgoz & Gheorghe (2013)	Resilience quantification of residential buildings subject to hurricane winds	Hurricane winds	[36]
Alfaridi & Boussabaine (2015)	Suggesting a set of strategies for improving building resilience against climate change	Climate change	[31]
O'Brien & Bennet (2016)	Evaluation of thermal resilience of high-rise residential buildings	Power failure	[37]
Hamdy et al. (2017)	Evaluation of the impact of climate change in dwellings	Climate change	[38]
Lassandro & Di Turi (2017)	Evaluation of the impact of PCMs on resiliency of residential buildings	High temperature in summer	[39]
Baniasadi & Sailor (2018)	Assessing the trade-offs and synergies between energy efficiency and resilience to heat	Power failure coincide with extreme heat conditions	[40]
Baniasadi et al. (2019)	Evaluation of the effectiveness of PCMs in improving the resiliency of buildings during extreme events	24 hours AC loss (Power outage)	[41]
Katal et al. (2019)	Evaluation of the impact of retrofit measures on building resilience	Snowstorm leading to power failure (lasting for full ten days)	[42]
Rosales-Asensio et al. (2019)	Evaluation of the photovoltaic solar energy and electrochemical energy storage on the building resiliency for office buildings	Power outage	[43]
Sun et al. (2020)	Evaluation of the nexus of thermal resilience and energy efficiency of buildings	Extreme hot weather	[44]
Mehrjerdi & Saad (2020)	Evaluation of efficiency-resilience nexus in the building energy management	Failure in different energy supply systems in the building	[45]
Flores-Larsen & Filippin (2020)	Evaluation of energy and thermal resilience in low income houses	Extreme heat events	[46]

Author	Purpose	Disruptive event	Ref
Nik et al. (2020)	Defining resilience in the scale of urban energy systems	Climate change	[27]
Shandiz et al. (2020)	Developing a framework and metrics for resilience evaluation in the community level	Different hazards such as climatological events	[25]
Liu et al. (2021)	Evaluation of the impact of energy storage systems on the power resilience of a health care center	Power failure during pandemic	[47]
Attia et al. (2021)	Developing a definition and a set of criteria for assessing cooling resiliency against heat waves and power outages	Heat waves and power outage	[29]
O' Donovan et al. (2021)	Determining the resiliency of different passive cooling control strategies under current and future extreme conditions	Both current and future extreme conditions	[48]
Mehrjedi (2021)	Evaluation of the impact of vehicle-to-home charging (battery swapping mechanism) on building energy resilience	Power outage	[49]
Tian & Talebizadeh (2021)	Evaluation of energy resilience against natural disasters in buildings with shared parking stations for electric vehicles	Natural disasters leading to power outage	[50]
Schünemann et al. (2021)	Evaluation the impact of window ventilation on the heat resilience in the residential buildings	Projected warm summer considering urban heat island effect	[51]

pandemics (in the group of biological disruptions) can have huge impacts on the energy performance and comfort of the buildings. The study of [52] shows that during the full lock-down followed by the COVID-19 pandemic the residential space heating and cooling demand have been increased by 13% and 28% respectively, in a case study of a residential neighborhood in Switzerland. In the group of climatological disruption, attentions have been paid a lot to the heatwaves, which can be categorized based on their intensity(maximum temperature($°C$)), severity (degree. hours), and duration (days or hours)[53]. Critical heatwaves (long term or short term) can be followed by other kind of disruptive events such as power failures. This shows the sequence of disruptions which can make the objective of having a resilient performance more difficult to achieve.

Technological disruptions comprise two groups =: general and specific. One example of general technological disruption is a power failure, which can affect different parts of building performance. A specific technological dis-

ruption may be a failure in the heating or shading systems. In this work, power failure is considered a disturbance for building resilience evaluation.

2.2.3 Resilience in what state?

A major aspect of the resilience definition is the process that the observed system undergoes in response to a disruption, which is quantified by the measure of system performance in the disruption timeline. The time-dependent changes in the performance level of a system when facing a disruptive event can be conceptualized by different performance curves. These curves show that a disruption results in a performance loss, or "draw-down" state, which is followed by a bounce-back, or "draw-up" state. Both "draw-down" and "draw-up" states can exhibit various shapes depending on the characteristics of the system and disruptive event. The application of these performance curves and visualization of different system-performance states allows for the analysis of various resilience abilities and attributes by quantitative performance indicators. The performance of a system concerning a disruptive event as a function of time has been demonstrated with mainly two concepts in the literature—resilience triangle [30] and resilience trapezoid [17], which are widely used in various fields, such as seismic engineering and power engineering [17, 30]. The concept of the resilience triangle was first suggested by the Multidisciplinary Centre for Earthquake Engineering Research as a part of a framework for the quantification of seismic resilience [30]. The re-
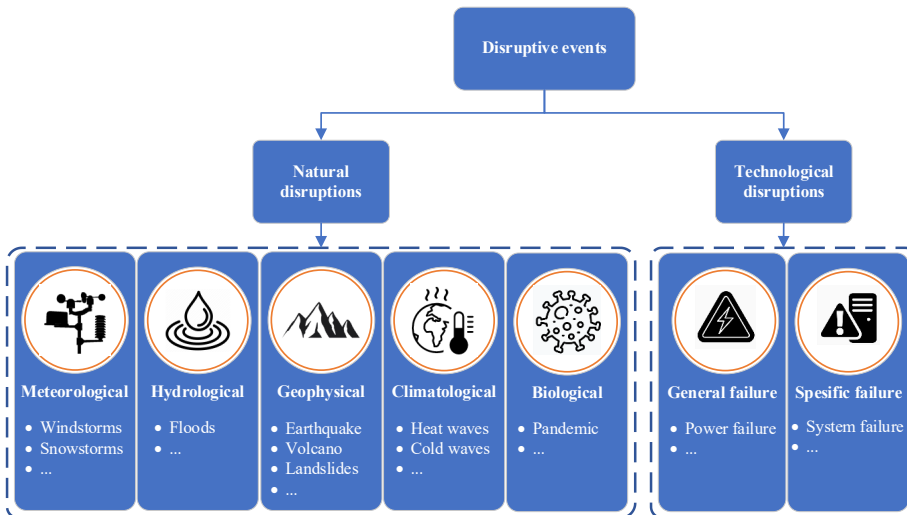
Figure 2.3: Categories and examples of disruptive events in the context of built environment.
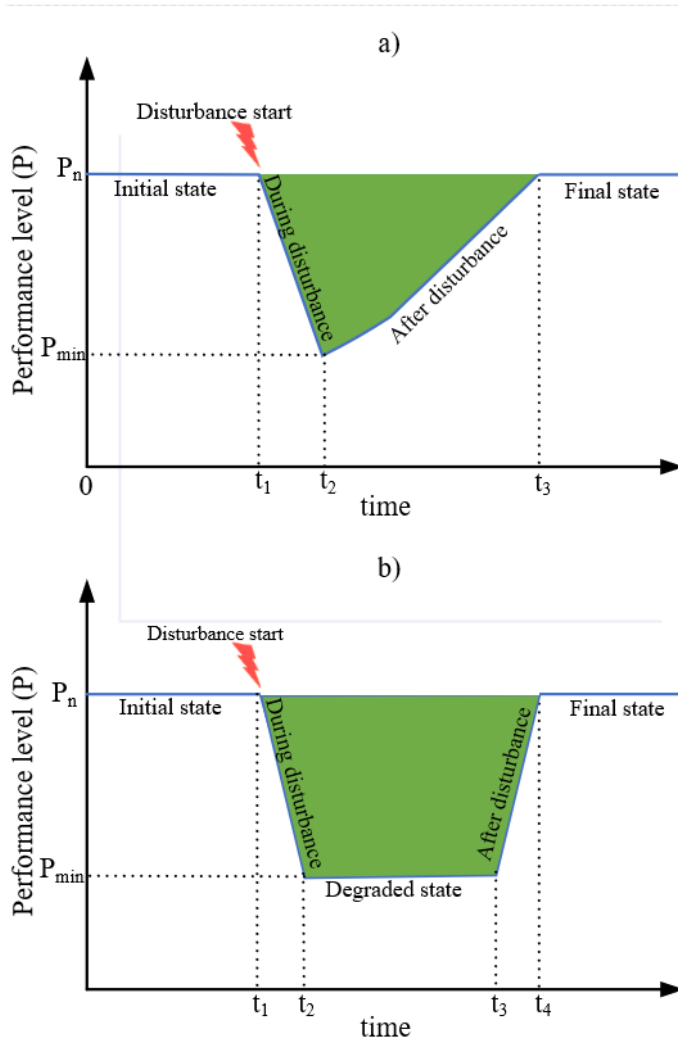
Figure 2.4: a) Resilience triangle and b) resilience trapezoid for a system facing a disruptive event.

silience triangle describes the deterioration of a system's functionality over the disruptive event timeline [54], as shown in Figure 2.4(a). The system experiences four states after being exposed to a disruptive event. The system operates with normal performance P_n before a disruptive event occurs (initial state). The disruptive event occurs at time t_1, and the system performance degrades, indicated as "during disturbance" in Figure 2.4(a), until it stops at time t_2 when the system experiences its worst performance level P_{min}. In the resilience triangle concept, immediate restoration actions are assumed to occur at the end of the disruptive event t_2, leading to gradual

17

improvements in the system performance, which are dependent on the implementation of the restoring actions, as shown by "after disturbance" in Figure 2.4(a). The restoration continues until the system achieves its pre-disturbance condition, which has a final-state performance P_n equal to that of its initial state.

The concept of the resilience triangle can be extended to the resilience trapezoid, which considers the degraded state that the system may experience when facing a disruptive event. In other words, in the resilience trapezoid, no immediate restoration actions occur at the end of disturbance t_2. This leads to a constant performance level, which is shown with the "degraded state" in the resilience trapezoid of Figure 2.4(b). For the first time, Panteli et al. used the concept of the resilience trapezoid to show different phases that a power system might experience during an extreme event [55].

The concepts of the resilience triangle and trapezoid and the pre-simulation results of building performance during a disruptive event indicate that buildings as dynamic systems degrade exponentially. Therefore, this work used a "multi-phase resilience curve" to show the performance of a building facing a disruptive event. Building performance can be measured by various metrics, and according to these metrics, building resilience with respect to different performance criteria can be quantified. This research assumed that immediate restoration action is taken into account after the disruptive event. However, the suggested curve may not show all possibilities of building performance but aims to capture key outcomes, including the abilities of a resilient building. The "multi-phase resilience curve" shows the two phases of the disruptive event—phases I, namely "during the disruptive event" and II, "after the disruptive event." Furthermore, the multi-phase resilience curve also shows the performance of building in initial and final states. The curve illustrates what happens to the building performance when faced with a disruptive event, as shown in Figure 2.5. Based on the definition that has been suggested for a resilient building in this work, the building is able to prepare in the initial state, absorb and adapt during the disruptive event (phase I), and recover after the disruptive event (phase II), which comprise the abilities of a resilient building. The states and phases can be described as follows.

- Initial state $(0 \leq t < t_1)$: During the initial state, the building continues normal operation until the disturbance occurs at t_1. Based on the resilient building definition provided in this work, the building can prepare itself for a disruptive event in this state.

- Phase I $(t_1 \leq t < t_2)$: Phase I is between the initiation and the end of the disruptive event, during which the building performance is usually degrading continuously. Based on the definition of resilient building,
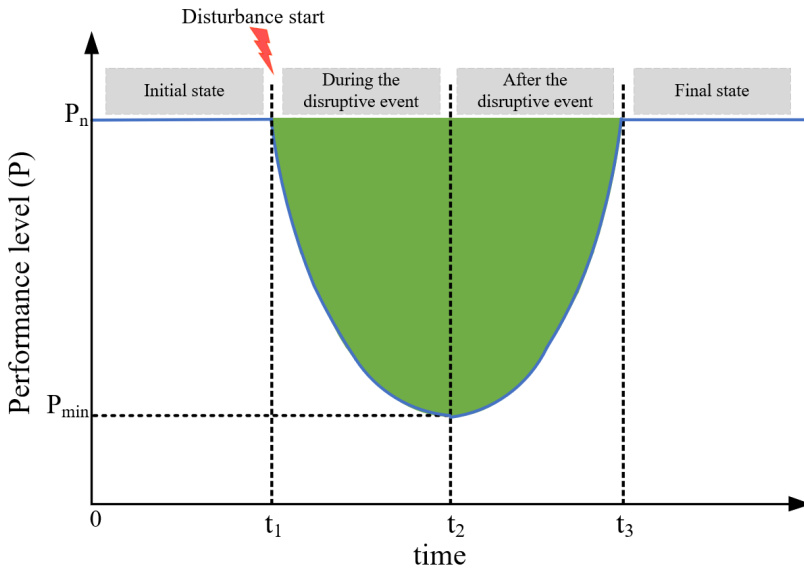
Figure 2.5: Multi-phase resilience curve, showing the performance of a building facing a disruptive event.

the building absorbs the impact of and then adapts to the disruptive event in this phase.

- Phase II $(t_2 \leq t < t_3)$: Phase II starts at the end of the disruptive event and lasts until the building reaches the normal performance level of the initial state. During this phase, the building performance is usually restoring continuously. Based on the definition of the resilient building, the building recovers from the disruptive event in this phase.

- Final state $(t > t_3)$: The final state begins after the full recovery of the building. In this state, the building operates at the normal performance level.

The literature concerning resilience in the context of buildings [56], urban planning [20], and energy systems [27] reveals that resilient systems typically have a combination of attributes that determine resilience and then derive and validate a function form that can be used to measure resilience in regard to functionality and time. The most-cited attributes that have the highest correspondence with components of building are listed below:

- Efficiency—Decreasing energy consumption (specifically during disruptions) by means of efficient production, distribution, and use.

- Robustness—Ability to withstand disruptions and remain within acceptable performance margins without suffering from major degrada-

19

tion by absorbing the impact of disruptions.

- Resourcefulness—Adequacy of readily available resources in times of need to appropriately prepare for an event and then respond and recover.

- Redundancy: Availability of backup or fail-safe strategies/technologies with a similar or even overlapping function as an alternative means to improve abilities of preparation for a disruption and absorbing it.

- Flexibility—Ability to adapt to changes and undergo a safe failure by restructuring its configuration and helping the building to return to its normal performance within a relatively short period.

- Adaptation—Ability to learn from a disruption experience to appropriately respond or change performance or structure during or following a disruptive event.

Each of these attributes can improve building resilience by harnessing the abilities of a resilient building. The relevance of attributes to abilities is shown in Table 2.2, which was adapted from [20]. For example, a high-efficiency building is able to better prepare, absorb, adapt, and recover from a disruptive event and therefore is more resilient.

In summary, the question of "Resilience in what state?" considers the states a building experiences surrounding a disruptive event, the abilities of the resilient building, and the attributes that contribute to the resilience of the building. These three factors are described in Figure 2.6.

2.2.4 Resilience based on what?

The final question in the resilience definition is related to resilience assessment. Several works have focused on the resilience assessment of systems in various fields. Hosseini et al. [12] separated resilience assessment approaches

Table 2.2: Resilience attributes and relationships with abilities of a resilient building.

Attributes	Preparation	Absorption	Adaptation	Recovery
		Relationship with abilities		
Efficiency	✓	✓	✓	✓
Robustness		✓		
Resourcefulness	✓			✓
Redundancy	✓	✓		
Flexibility				✓
Adaptation			✓	
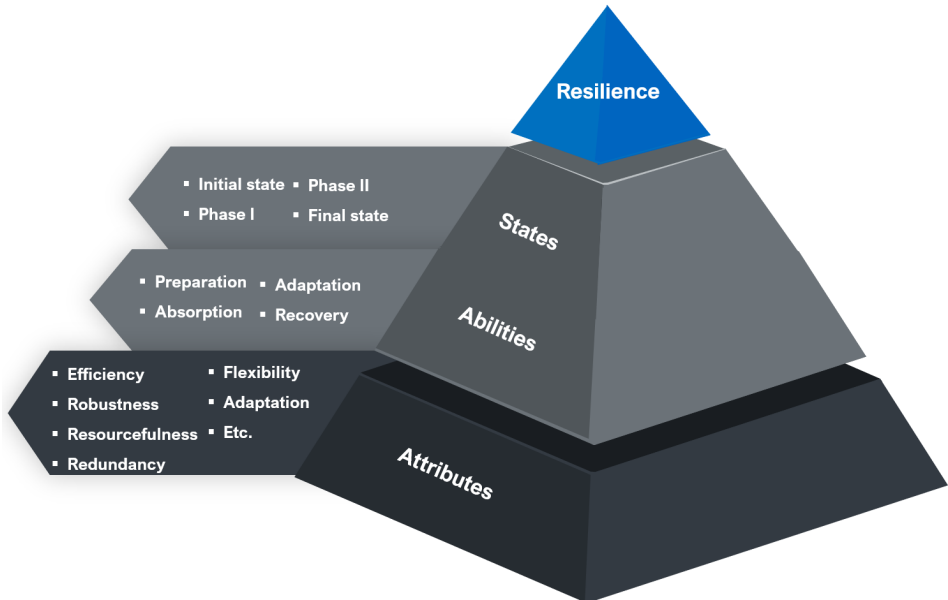
Figure 2.6: Illustration of resilient building states, abilities, and attributes.

into two categories: qualitative and quantitative. Qualitative approaches assess resilience without numeric descriptions. Quantitative approaches rely on numeric descriptions, in which resilience metrics are essential. Specific criteria are considered regarding resilience metrics, such as repeatability and comparability [57].

In the qualitative category in the context of the built environment, Sharifi and Yamagata [20] developed a conceptual framework for assessing urban energy resilience. In another framework, Nik et al. [27] divided the characteristics of resilient urban energy systems into four groups: planning and preparing for, resisting, adapting to, and recovering from disruptive events.

For quantitative resilience assessments, two groups of metrics are typical in the literature: metrics developed from the resilience curves (e.g., resilience triangle and trapezoid). For example, Bruneau et al. [30] developed a resilience loss index based on the resilience triangle in the field of seismology. Zobel [58] extended this metric by calculating the percentage of total possible loss over a long time interval. In a novel study, Panteli and Mancarella [55] applied the resilience trapezoid for the quantification of grid resilience with a set of time-dependent metrics called the $\Phi\Lambda E\Pi$ measurement system, based on the speed Φ and magnitude Λ of the damaged grid functionality, duration of the damaged state E, and recovery speed Π. In addition, Li et al. [59] evaluated the impact of energy storage systems for healthcare cen-

ters experiencing power failure during the pandemic using the resilience loss index and another index—the ratio of the supplied electric load to the total amount of electric load over a year. Similarly, Mehrjerdi [49] used the amount of energy not supplied to a building during a power outage as a resilience metric to quantify the building energy resilience based on the resilience triangle concept. Finally, Shandiz et al. used the resilience trapezoid and time-dependent resilience metrics to evaluate the energy resilience of communities [25].

The other group of quantitative resilience metrics focuses on the application of simple performance metrics in a single phase of the resilience curve (usually during the disruption phase). Specifically, typical simplified metrics have been used in the context of a building's thermal resilience based on simulation results. For instance, overheating risk [34, 60] and heat index [44, 63] are often applied to evaluate building thermal resilience against disruptions like climate change and heatwaves. Baniasadi et al. [41] implemented the reduction in the daily maximum temperature to quantify the effectiveness of phase-change material to improve the thermal resilience of residential buildings against heat waves. Additionally, two simplified metrics recently developed are passive survivability [37, 42, 43] and thermal autonomy [37].

However, these simplified metrics apply to the scale of one thermal zone and cannot unfold the resilience in the building level, called overall thermal resilience in this work, which considers all zones of the building. To overcome this issue, Hamdy et al. [38] introduced a new index called IOD (indoor overheating degree), which considers different thermal comfort limits depending on the zone, taking the intensity and frequency of overheating into account. Regarding building energy resilience, Gupta et al. [61] evaluated the extent of energy resilience through the application of photovoltaics (PVs) and smart batteries at the community level. The authors used more general measures related to PVs, such as self-consumption, as resilience metrics. In another study, Mehrjerdi [62] suggested the energy surplus on each time interval as a metric for energy resilience quantification against the power outage. Furthermore, Tian and Talebizadeh [50] considered the number of hours that the building can continue its expected operation with other energy sources in the case of a power outage as a resilience metric. A summary of selected metrics that have been implemented for resilience quantification in different contexts is reported in Table 2.3. The literature review on the resilience quantification approaches and metrics in different contexts highlights the following points:

- Resilience metrics should help decision-makers in the evaluation of the resilience level of different building designs in an informative and easy-to-understand approach.

Table 2.3: Review of selected studies on different resilience metrics implemented in the context of the built environment (In column Type, RC shows resilience curves and SPM show simple performance metric as type of metrics).

Author	Focus of the reference	Metric	Type
Bruneau et al. (2003) [30]	Community seismic resilience	Resilience loss metric (resilience triangle)	RC
Lomas et al. (2009) [34]	Building thermal resilience	Overheating risk	SPM
Zobel (2011) [58]	No specified area	Percentage of total possible loss (resilience triangle)	RC
Burman et. al (2014)[60]	Building thermal resilience	Overheating risk	SPM
O'Brien & Bennet (2016) [37]	Building thermal resilience	Passive survivability & thermal autonomy	SPM
Panteli et al. (2017) [55]	Power systems resilience	Set of time-dependent metrics (resilience trapezoid)	RC
Hamdy et. al (2017) [38]	Building thermal resilience	Indoor overheating degree	SPM
Baniasadi (2018) [41]	Building thermal resilience	Discomfort index	SPM
Baniasadi (2019) [40]	Building thermal resilience	Reduction in daily maximum indoor temperature	SPM
Katal et al. (2019) [42]	Building thermal resilience	Passive survivability	SPM
Rosales-Asensio et al. (2019) [43]	Building thermal resilience	Passive survivability	SPM
Gupta et al. (2019) [61]	Community energy resilience	PV self sufficiency	SPM
Shandiz et al. (2020) [25]	Community energy resilience	Time-dependent resilience metrics (resilience trapezoid)	RC
Sun et al. (2020) [44]	Building thermal resilience	Heat index	SPM
Liu et. al (2020) [59]	Building energy resilience	Resilience index (resilience triangle)	RC
Flores-Larsen et al. (2021) [46]	Building thermal resilience	Heat index	SPM
Mehrjeri (2021) [62]	Building energy resilience	Energy surplus over the time interval	SPM
Tian & Talebizadeh (2021) [50]	Building energy resilience	Number of hours that building can continue its operation with other electricity sources	SPM
Mehrjerdi (2021) [49]	Building energy resilience	Energy not supplied (resilience triangle)	RC

23

- Resilience metrics should capture the performance not only during the disruptive event but also after the disruptive event.

- Resilience metrics should focus on the building scale or, if limited to smaller scales, such as thermal zones, extend to the building scale.

- The metrics should result in different levels of resilience for various combinations of performance and time. Therefore, the metric should differentiate the impact and duration of the disruptive event and show how far and for how long the building performance deviates from the targets. In other words, the metric should be sensitive to the hazard level and exposure time to the disruptive event.

Given these points, this work develops metrics for the quantification of resilience and its different attributes, such as robustness and flexibility, in the context of building performance. The following chapters focus on the methodologies for the quantification of building robustness, flexibility, and resilience against disruptions that can affect building performance.

2.3 The implemented methodology

Based on the what explained until now, the implemented methodology for this work shows how resilience can be defined, assessed, and quantified in the context of building performance. The steps taken to develop the methodology are shown in Figure 2.7. The methodology has six main steps described as follows:

1. **Identify the building performance curve over a disruptive event**
   As explained in Section 2.2.3, the literature shows that the performance of systems surrounding a disruptive event can be described by concepts such as the resilience triangle and resilience trapezoid. An analysis of pre-simulation results of building performance during a disruptive event shows that buildings as dynamic systems exponentially degrade when faced with disruptive events, leading to the creation of the multiphase resilience curve, as shown in Figure 2.5. The performance of a building during a disruptive event is shown with this multi-phase resilience curve, which is implemented as a basis for defining resilience abilities and attributes and establishing their interrelationships.

2. **Identify abilities of the resilient building in the resilience curve**
   As defined earlier, a building is resilient if able to prepare for, absorb, adapt to, and recover from the disruptive event. These characteristics are considered the abilities of a resilient building.

3. **Select resilience attributes**

   The literature review in Chapter 2 shows that resilient buildings have various attributes that contribute to the resilience level by enabling the buildings to better prepare, absorb, adapt, and recover. Among the different attributes of resilience in the context of building performance, building robustness and flexibility are vital, gaining ground in the context of building performance. A robustness assessment has been considered a valuable tool in building performance evaluation in recent years. For example, in the context of building performance, this type of assessment has been implemented to create robust designs that can withstand disruptions [64], address shortcomings of the sustainability frameworks with respect to future uncertainties [65], reduce the performance gap between the estimated and actual building performance [66], and evaluate and benchmark the robustness of innovative technologies [67].

   Furthermore, the building sector has significant potential in energy flexibility plans [68]. Well-designed buildings and corresponding energy systems can provide flexible loads for effective use in power grid operation. The literature has shown some focus on the characterization of energy flexibility for buildings [69].

   Because of the importance of robustness and flexibility in resilience regarding building performance, these two attributes are evaluated in detail in this work. Efficiency is also discussed as a resilience attribute by creating a design space consisting of competitive designs from an energy-consumption perspective.

4. **Define resilience attributes**

   Resilience and its attributes are defined in more detail in the context of building performance.

5. **Develop frameworks and metrics for the quantification of resilience and its attributes**

   Frameworks, algorithms, and metrics are developed to aid building designers and decision-makers in the quantification of resilience (robustness and flexibility) of various building designs.

6. **Apply to the case study**

   Finally, the developed algorithms and metrics are tested by the application on buildings in a case study. The implemented case-study buildings are variations of Norwegian single-family houses that were modeled and simulated in IDA-ICE [70].

The selected attributes of resilient buildings, along with the developed methods for quantification of resilience and its attributes, are explained in
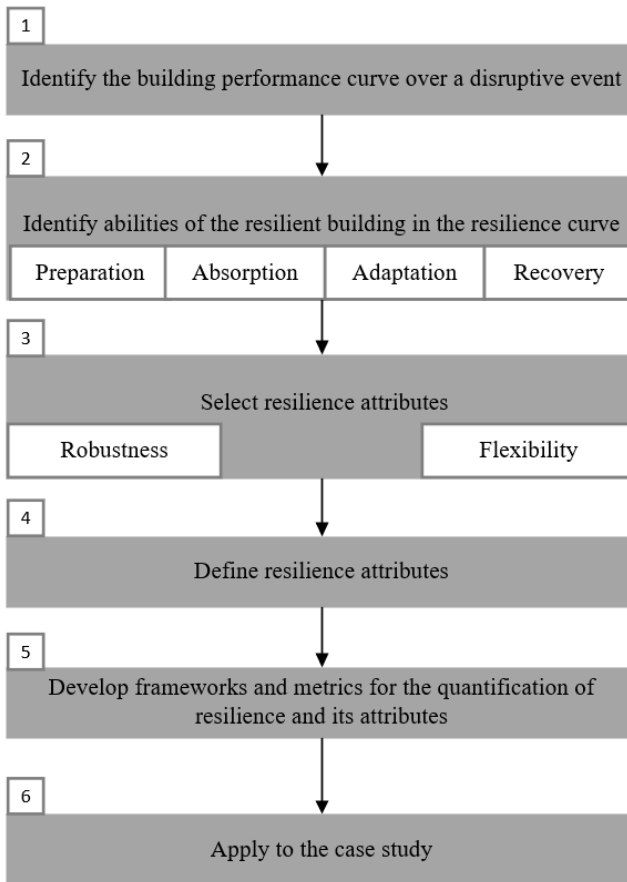
Figure 2.7: Flowchart of the implemented methodology in the thesis.

the Chapters 3,4,5.

Resilience Attribute I—Robustness

Robustness has been evaluated in the context of building performance in various studies, and different definitions exist for this concept in the context of building performance [10, 71, 72]. In this work, robustness is defined as a building's ability to perform effectively and remain within the acceptable margins under the majority of possible changes in the internal and external environments. Based on the definitions provided in this work, a robust building maintains its performance in an acceptable range and withstands a performance failure. On the other hand, a resilient building may face a complete performance failure and, in consequence, must recover from this failure. Therefore, a robust building can be resilient, but a resilient building may or may not be robust. This elaborates how robustness can thus improve a building's resilience by withstanding and absorbing the impact of a disruption, highlighting the value of a building robustness assessment. This assessment can reveal how various building designs can enhance the absorption ability in different manners.

3.1   Robustness assessment

In building energy performance, robustness assessments can be categorized into two groups: probabilistic and non-probabilistic approaches. In probabilistic approaches, the probabilities of uncertainties are known [73]. The probabilities of uncertainties are unknown in the non-probabilistic approaches [74], and scenario analyses are implemented to formulate alternatives with unknown probabilities [75]. The literature [71] shows that different robustness indicators were implemented with scenario analyses to help building designers and decision-makers select robust building designs. Some examples are the max–min, best-case and worst-case, and minimax regret methods.

For a high-performance and robust building design, three steps were commonly considered in the literature [76]. First, the building performance was

evaluated based on the results obtained from a BPS. Next, the robustness assessment of building performance was performed under different uncertainties. A robustness assessment can be achieved with respect to different performance criteria since building performance can be evaluated based on various performance criteria [77]. Therefore, a building-performance robustness assessment can be categorized as either single-criterion [71], where the performance robustness is assessed regarding one performance indicator, or multi-criteria [1], where the robustness is assessed based on multiple performance indicators. For instance, energy robustness, comfort robustness, and cost robustness can be assessed for a building. In the multi-criteria robustness, the assessment is repeated separately for each criterion, and the most robust design based on each criterion may differ [1]. Furthermore, the actual performance is an important criterion that should also be considered in the selection of a high-performance and robust building design. For the third step, multi-criteria decision-making (MCDM) is needed to support decision-makers in this selection. In MCDM, the high-performance and robust building design is determined based on the trade-offs between performance and corresponding robustness. The preferences of the decision-makers to specific performance criteria or robustness guides the design selection, which is achievable by applying a weight to each criterion in the decision-making process.

Some examples of MCDM are the Multi-Attribute Utility Theory (MAUT), Analytical Hierarchy Process (AHP), Fuzzy Set Theory, Weighted Sum Method, and Weighted Product Method. In the building performance context, AHP and MAUT are two of the most commonly applied methods in the literature. AHP is a well-known MCDM technique that helps decision makers to integrate different criteria into a single overall score for ranking decision alternatives through a pair-wise comparison [78]. In the building performance context, AHP has been used to develop a comprehensive indicator for indoor environment assessment [79], to select intelligent building systems [80],to develop a housing performance evaluation model that considers different criteria [81] , to rank and compare residential energy management control algorithms [82], and to select an optimal phase change material (PCM) for a ground source heat pump integrated with a PCM storage system [83]. The AHP method does not consider uncertainties. For this reason, Hopfe et al. extended the classical AHP for use with uncertain information [77] . The other commonly used MCDM method is "multi-attribute utility theory," which is a more precise methodology for incorporating uncertainty into MCDM [84]. In this method, the overall value of alternatives is defined in the form of a utility function based on a set of attributes. Multi-attribute utility theory has been applied to select cost-effective retrofit measures for

existing UK housing stock under uncertainty [85] and to perform a comparative assessment of energy efficiency alternatives with the aim of improving utility savings, and reducing embodied energy and investment cost [86]. In the context of robust design, Kotireddy et al.implemented Savage [71] that allows decision makers to select a design that has the least risk among alternative that are ranked based on regret. They also used Hurwicz [1] to select a robust design for low-energy buildings and consider decision makers attitudes toward risk. Nikolaidou et al. [87] also used Laplace, Wald, and Savage to find robust optimal Pareto solutions under uncertainty.

However, in practice, the selection of a robust and high-performance design is complicated and difficult, particularly with multiple, conflicting performance criteria. As the number of criteria and conflicts increases, the decision-making step becomes more difficult, requiring more experience to set the preference weight for each criterion [88]. Additionally, this design selection in the literature was based on the comparisons with different alternatives (i.e., building designs) rather than with the performance targets set by standards and regulations [1]. In that approach, the best design was defined based on the best alternative in the design space (i.e., minimum or maximum of each performance criterion), which might not meet performance targets. Therefore, the deviations of different alternatives from the performance target need to be considered in the selection of a high-performance and robust building design. At the same time, repeated robustness assessments that focus on different criteria can be computationally demanding, especially in cases with many designs and scenarios that need sampling techniques. In this work, a methodology was developed to overcome these issues and select high-performance and robust building designs against possible uncertainties.

3.2 Multi-target robustness-based decision-making

The developed methodology for selecting a high-performance and robust building design is called the T-robust approach, which integrates a multi-target robustness assessment into a MCDM process and includes performance targets in the decision-making. This methodology leads to five advantages:

- All assessed alternatives (i.e., building designs) are compared, not only to each other but also to the performance targets set by standards and regulations.

- The performances of alternatives are defined (penalized) based on deviations from the performance targets.

- The performance targets are based on regulations, standards, and laws and can be adapted according to specific occupants' needs.
- The robustness assessment is not repeated separately for each performance criterion.
- Criteria preferences are automatically established in the decision-making process by including performance targets.

The T-robust approach involves seven steps, as shown in Figure 3.1 and described as follows:

Step 1: Define designs and scenarios.
A robustness assessment evaluates the performance of a defined building design under specific possible uncertainties. The building designs can be defined based on the standards or regulations of each country or on the preferences of stakeholders. Different sources of uncertainties are prevalent in the context of building performance. Some examples include changes in occupant behavior [89], climate conditions [38], and economic factors [90]. A robustness assessment should be evaluated across all combinations of considered scenarios because the probability of occurrence of any combination is unknown. This can lead to high computational costs. The literature shows that different sampling strategies can be implemented to find representative samples for scenario combinations [91].

Step 2: Define key performance indicators and stipulated targets.
Because building performance can be evaluated from different perspectives, the second step specifies performance criteria to be considered in the robustness assessment. Furthermore, buildings must meet specific requirements according to regulations [92], building codes, and standards [93], referred to as "performance targets" in this study. Furthermore, the T-robust approach considers performance targets when the decision is being made. To evaluate robustness, another concept is defined, called the "robustness margin." Figure 3.2 shows the difference between the "performance target" and "robustness margin" for energy consumption. According to this figure, the building is robust from an energy perspective if its energy consumption does not exceed the robustness margin. The arrows in Figure 3.2 represent the changes that can occur during the building's operation and lead to an increase or decrease in its energy consumption.

Step 3: Define robustness assessment methods.
The performance robustness of a building can be assessed by various methods, and the method used is dependent on the purpose of the study, decision-makers, and their preferences [94]. Some examples of robustness assessment methods include max–min, best-case and worst-case, and minimax regret methods.
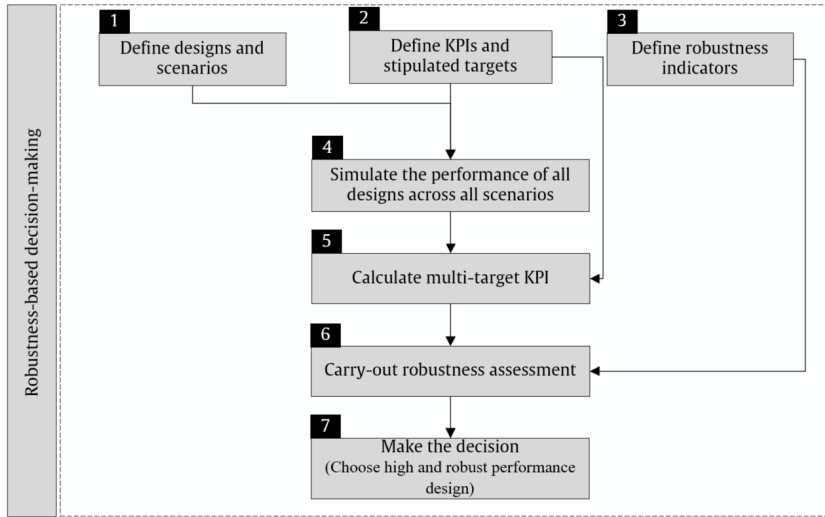
Figure 3.1: Diagram flow of the multi-target robustness-based decision-making approach.

Step 4: Simulate the performance of designs across all scenarios.
The performances of the suggested designs are simulated under each of the suggested scenarios with a BPS tool. Based on the defined performance indicators, the performance is extracted from the simulation result.

Step 5: Calculate the multi-target KPI.
The T-robust approach focuses on the integration of the robustness assessment into the decision-making process. This integration is accomplished with a new KPI, called the multi-target KPI (*MT-KPI*), which represents the building performance with respect to more than one criterion. In addition,
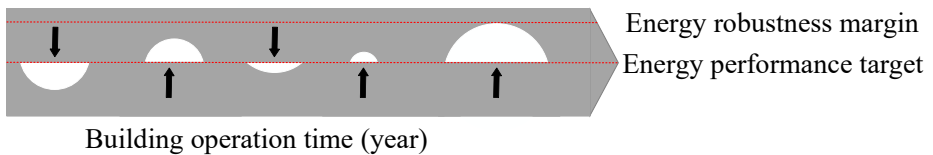
Figure 3.2: Illustration of performance target and robustness margin for energy consumption.

this KPI evaluates the performance and penalizes solutions that do not meet the robustness margin. These penalties can help differentiate feasible and infeasible solutions. In this work, the *MT-KPI* focuses on only two performance indicators (energy and comfort), but it can also be extended for more than two criteria. The *MT-KPI* is defined based on the robustness margin $KPI_{i,m}$ for each primary KPI, which is needed for penalizing infeasible solutions. Relative performance $KPI_{1,rel}$ with respect to each indicator can be defined as follows:

$$KPI_{1,rel} = \frac{KPI_1}{KPI_{1,m}} \times 100 \qquad KPI_{2,rel} = \frac{KPI_2}{KPI_{2,m}} \times 100 \qquad (3.1)$$

The comparison of building performance (KPI_i) and robustness margin (KPI_i, m) determines feasible solutions ($KPI_i < KPI_{i,m}$) and infeasible solutions ($KPI_i > KPI_{i,m}$). Figure 3.3 shows an example of building performance under 16 scenarios. Point (100,100) in the figure shows the relative margin point, at which the building performance regarding both indicators equals the robustness margin. Around the relative margin point, four performance zones are created, of which two (i.e., zones 2 and 4) are feasible regarding one KPI and infeasible regarding the other. Zone 3 is feasible for both KPIs, and zone 1 is completely infeasible. The calculation of the *MT-KPI* depends on the performance zones, as defined in Table 3.1.

Step 6: Carry out the robustness assessment. After the establishment of *MT-KPI* for each performance design under each scenario, the performance robustness assessment is conducted with the application of different robustness indicators. Assessing robustness for the *MT-KPI* not only selects the most robust design for multiple performance perspectives but also leads to a high-performance design by considering the actual performance in the decision-making process.

Step 7. Make the decision.
The best solution (i.e., high- and robust-performance design) is chosen based on the results of the robustness assessment with the *MT-KPI*.

3.3 Application of the T-robust approach on a case-study building

The developed T-robust approach was implemented for a case study of a Norwegian single-family house. The building model, different building designs, and uncertainty scenarios in this robustness assessment are explained in the following subsections:
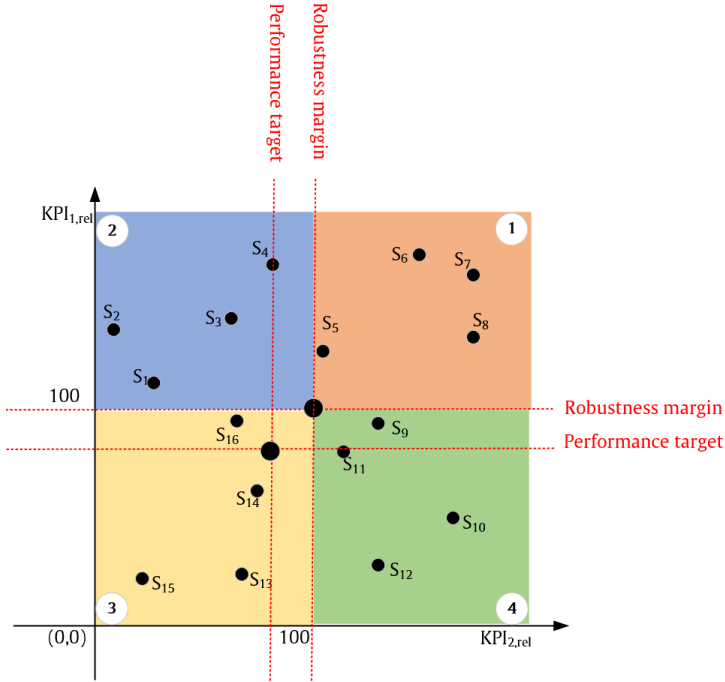
Figure 3.3: Illustration of the performance zones of one building design under 16 possible scenarios, where S_i represents the ith scenario.

Table 3.1: Calculation of *MT-KPI* in different performance zones.

Num	Performance zone	Feasibility	*MT-KPI*
1	$KPI_{1,rel} \geq 100$ $KPI_{2,rel} \geq 100$	Completely infeasible	$(KPI_1 - 100) + (KPI_2 - 100)$
2	$KPI_{1,rel} \geq 100$ $KPI_{2,rel} < 100$	Feasible for KPI_2	$(KPI_1 - 100) + (\frac{1}{100 - KPI_2})$
3	$KPI_{1,rel} < 100$ $KPI_{2,rel} \geq 100$	Feasible for KPI_1	$(\frac{1}{100 - KPI_1}) + (KPI_2 - 100)$
4	$KPI_{1,rel} < 100$ $KPI_{2,rel} < 100$	Completely feasible	$(\frac{1}{100 - KPI_1}) + (\frac{1}{100 - KPI_2})$

3.3.1 Building model

A representative model of Norwegian single-family houses [95] was used in the primary papers of this thesis, but the selections of design configurations differed based on the objective of each paper. This building is based on representative models in the project TABULA (Typology Approach for Building Stock Energy Assessment)[96], which aimed to develop building typologies for 13 European countries. The subject building is typical, with characteristics representative of the most common features found in Norwegian single-family houses based on the best available knowledge. The case-study building is a two-story building located in Oslo with a heated floor area of 162.4 m^2, divided into three zones in a detailed model using IDA-ICE software [70], which was validated using the BESTEST: Test Procedures [97]. The three zones comprise a representative dayroom (i.e., a combined zone for living room, kitchen, and entrance), bedroom, and bathroom. Occupancy schedules, domestic hot water distribution, and internal gains were derived from Nord et al. [98]. For the assessment using the T-robust approach, the design options include the building envelope, window-to-wall ratio (WWR), and building energy system (heating, ventilation, and domestic hot water (DHW) generation systems). Heating setpoints, window openings, and shading strategies are the scenario parameters, resulting in 16 uncertainty scenarios.

3.3.2 Building design variants

These design options lead to the eight configurations for the case-study building. The design space was developed such that all designs are competitive from an energy and comfort perspective, all meeting the same energy and comfort targets under the reference scenario. This allows for a robustness comparison of designs that perform the same in energy and comfort. The target set for annual energy consumption is 110 kWh/m^2 based on the TEK17 standard [92]. For thermal comfort, the number of unacceptable hours (including underheating and overheating hours based on the TEK17 standard) shall not exceed 5% of the occupied hours.

To meet these targets in all eight configurations, specific combinations are selected. For example, the targets can be achieved by combining the envelope with low insulation and high-efficiency energy and ventilation systems. In contrast, another design can achieve the targets via a highly insulated envelope and less efficient ventilation and energy systems. Note that the targets are only met in the reference scenario, and the building performance under uncertainty scenarios deviates from these targets. Therefore, the robustness

Table 3.2: Details of the eight competitive designs considered in the case study demonstration.

	Designs							
Design parameters	D_1	D_2	D_3	D_4	D_5	D_6	D_7	D_8
Overall U-value (W/m².K)	0.31	0.25	0.43	0.36	0.33	0.29	0.51	0.44
WWR (%)	30	30	30	30	40	40	40	40
Heating system	EB	EB	ASHP+EB	ASHP+EB	EB	EB	ASHP+EB	ASHP+EB
Ventilation system	Balanced	Exhausted	Balanced	Exhausted	Balanced	Exhausted	Balanced	Exhausted
Solar DHW system size (m²)	0	5	0	0	0	5	0	0
Lighting	Typical	LED	Typical	Typical	Typical	LED	Typical	Typical
KPI								
Total energy consumption (kWh/m²)	110	110	110	110	110	110	110	110
Unacceptable hours (h)	18	15	12	188	18	3	75	334

margin is considered in the definition of the *MT-KPI* to represent both the actual performance and performance robustness.

Table 3.2 shows the characteristics of each design and their performance from an energy and comfort perspective under the reference scenario. The first design (D_1) follows the recommendation of the TEK17 standard, the current minimum requirements in Norway [92]. From an envelope perspective, the U-values of the floor, walls, and roof; infiltration; and thermal bridges are variable, as indicated by the changing overall U-value. Two WWRs are considered in the design options.

The heating system is either an electric boiler (EB) or an air source heat pump (ASHP) with a COP (coefficient of performance) of 3.2 under the rated condition. In addition, heat emitters in the dayroom and bedroom are electric radiators (ERs), and the bathroom has electric floor heating. In the designs with ASHPs, an electric boiler is also implemented to accommodate the floor heating in the bathroom and compensate the drop on the COP of heat pumps during cold winter days.

Balanced mechanical ventilation with a heat recovery unit with an efficiency of 80% or mechanical exhaust ventilation without a heat recovery unit is employed. Domestic hot water in the building is generated with the EB. However, in two designs (D_2 and D_6), in order to compensate for the high energy consumption due to other design options, an auxiliary solar thermal collector (STC) is added.

Two lighting systems are also considered in the design options: typical lighting (luminous efficacy of 12 lm/W) and LED light (luminous efficacy of 60 lm/W), which is implemented in D_2 and D_6 to maintain a lower total energy demand.

3.3.3   Building performance scenarios

To understand how the building perform under the uncertainties, 16 uncertainty scenarios are created, focusing on two groups of parameters: occupant behavior and climate scenarios. Combinations of two heating setpoints, two

window-opening strategies, and two window-shading strategies led to eight occupant behavior scenarios. Additionally, two climate scenarios are considered. The details of these scenarios are as follows:

- Heating setpoints

The first option for the heating setpoint is taken from [95]. For more heating use, heating setpoints are increased in the second scenario based on the survey data taken from [99].

- Window-shading strategies

The first shading strategy is a temperature-based control, based on [95]. This strategy leads to moderate solar gain and, in consequence, the moderate usage of lighting in the building. The second strategy has a radiation-based control and an increased shading duration, which results in more lighting demand and less gain from solar.

- Window-opening strategies

The first window-opening strategy is based on [37], adapted with Norwegian context. The second strategy is a hybrid control strategy, which implements the first window-opening strategy in the dayroom and bathroom. For the bedroom, which experiences more overheating, the upper adaptive temperature limits proposed by [100] are applied. This strategy represents occupants who are sensitive to higher temperatures and prefer lower inside temperatures.

- Climate scenarios

To consider the impact of climate uncertainties, two weather files from the American Society of Heating, Refrigerating and Air-conditioning Engineers (ASHRAE), IWEC and IWEC2, are used from the library of IDA-ICE [70]. The 16 scenarios are summarized in Table 3.3.

3.3.4 Performance criteria and stipulated targets

The T-robust approach focuses on two performance criteria: total energy consumption and the number of unacceptable hours. The performance indicators and stipulated targets for these indicators are defined as follows:

Total energy consumption: Total energy consumption comes from space heating, heating for air ventilation, space cooling, domestic hot water, ventilation, lighting systems, and appliances over the course of a year. The equation for the total energy consumption in kWh/m^2 is based on the current minimum requirement in Norway (TEK17) is as follows [92]:

$$Total\ annual\ energy\ consumption = 100 + \frac{1600}{heated\ gross\ internal\ area} \quad (3.2)$$

Table 3.3: Summary of the occupant behaviors and climate parameters and their combinations into the 16 considered scenarios.

Parameter	Option	Scenarios															
		1	2	3	4	5	6	7	8	9	10	11	12	13	14	15	16
Heating setpoint	1) Bedroom, living room, bathroom 18, 21.5, 23°C	*	*	*	*					*	*	*	*				
	2) Bedroom, living room, bathroom 20, 23, 23°C					*	*	*	*					*	*	*	*
Window shading	1) Shading control On if T_{indoor} >23°C	*	*			*	*			*	*			*	*		
	2) Shading control on if radiation above 100 W/m²			*	*			*	*			*	*			*	*
Window opening	1) Open if T_{indoor} >T_{Out} and T_{indoor} >23°C for windows in all zones	*		*		*		*		*		*		*		*	
	2) Open if T_{indoor} >T_{Out} and T_{indoor} >23°C for day room and bathroom Open based on adaptive thermal model limits for bedroom		*		*		*		*		*		*		*		*
Climate	1) IWEC	*	*	*	*	*	*	*	*								
	2) IWEC2									*	*	*	*	*	*	*	*

where the heated gross internal area is in units of m². Following this equation for the case-study building yields 110 kWh/m² as the performance target for the total annual energy consumption for all designs to achieve in the reference scenario. Furthermore, to differentiate between the infeasible and infeasible solutions, a robustness margin is needed. The robustness margin for the energy performance of the building is assumed to include a 5% tolerance over the performance target, or 115 kWh/m².

Thermal comfort (unacceptable hours): The TEK17 standard recommends an operative temperature between 16 and 26°C for bedrooms in Norway [92]. Unacceptable hours include both overheating hours (T_{indoor} > 26°C) and underheating hours (T_{indoor} < 16°C) over the course of a year. Here, the indoor temperature is assumed to not fall outside of the TEK17′s comfort range for more than 5% of occupied hours. The robustness margin again includes a 5% tolerance over this limit for a solution to be considered feasible.

3.3.5 Robustness indicators

The T-robust approach integrates the robustness assessment into the decision-making process. Robustness indicators are important factors for the evaluation and optimization of a robust design. They can be selected based on several inputs, including the purpose of the study and the preferences of decision-makers [94]. Various robustness indicators were found in the literature [101].

In the building performance context, a robustness assessment is conducted with both probabilistic and non-probabilistic approaches. Hoes et

al.[101] were the first to investigate the Taguchi method, which uses the signal-to-noise ratio to decrease the variation in the signal (performance) from noise (uncertainty). Their robustness indicator was the standard deviation, which is similar to the signal-to-noise ratio. The application of the standard deviation of building performance as a robustness indicator revealed that the actual performance should also be considered.

Scenario analysis is a widely used method for robustness assessment. Some studies used probabilistic approaches, such as the comparison of mean and standard deviation across scenarios [102]. A non-probabilistic approach is another option for scenario analysis; for example, Kotireddy [103] implemented three robustness assessment methods—max–min, best-case and worst-case, and minimax regret— with scenario analysis. In the current work, these three non-probabilistic robustness assessment methods are implemented and compared with the probabilistic method (mean and standard deviation based on the Taguchi method). These robustness assessment methods are described below:

3.3.5.1 Max–min indicator

The max–min indicator describes the difference between the maximum performance A_m and minimum performance B_m of a design across all scenarios. The design with the smallest difference is the most robust design (Table 3.4). The calculation compares one design's performance across all scenarios without comparing different designs to each other. This indicator can be formulated as follows:

$$PS = A_m - B_m \tag{3.3}$$

where PS is the performance spread.

3.3.5.2 Best-case and worst-case indicator

The best-case and worst-case indicator indicates the difference between the maximum performance of each design A_m and the minimum performance of all designs across all scenarios (D). A design with the smallest difference between these two factors is the most robust design. This indicator can be formulated as follows:.

$$PD = A_m - D \tag{3.4}$$

where PD is the performance deviation.

3.3.5.3 Minimax regret indicator

The minimax indicator is the difference between the performance of each design and the minimum performance of each scenario across all designs

Table 3.4: Finding the maximum and minimum performances of a design across scenarios and best performance for designs and scenarios [1]

	Scenarios					Max and min performance across scenarios	
Designs	$S1$	$S2$	...	Si	Sn	Max(A)	Min(B)
D_1	KPI_{11}	KPI_{21}	...	KPI_{i1}	KPI_{n1}	A_1	B_1
D_2	KPI_{12}	KPI_{22}	...	KPI_{i2}	KPI_{n2}	A_2	B_2
...				...			
D_i	KPI_{1i}	KPI_{2i}	...	KPI_{ii}	KPI_{ni}	A_i	B_i
D_m	KPI_{1m}	KPI_{2m}	...	KPI_{im}	KPI_{nm}	A_m	B_m
Maximum performance for each scenario (C)	C_1	C_2	...	C_i	C_n		
Best performance of all designs across all scenarios (D)			D=Min(B)=Min(C)				

Table 3.5: Robustness calculations using max–min, best-case and worst-case, and minimax regret methods[1]

Design	**Performance Spread** (PI)	**Performance deviation** (PD)	**Performance regret** (PR)
D_1	$A_1 - B_1$	$A_1 - D$	$Max(R_{11}, ..., R_{n1})$
D_2	$A_2 - B_2$	$A_2 - D$	$Max(R_{12}, ..., R_{n2})$
...			
D_i	$A_i - B_i$	$A_i - D$	$Max(R_{1i}, ..., R_{ni})$
D_m	$A_m - B_m$	$A_m - D$	$Max(R_{1m}, ..., R_{nm})$
Robust design	Min(PS)	Min(PD)	Min(PR)

(C_n). This indicator can be formulated as follows:

$$PR = KPI_{mn} - C_n \qquad (3.5)$$

where PR is the performance regret and KPI_{mn} represents the performance of design m under scenario n. The maximum performance regret represents the highest deviation in each design, i.e., the largest difference between the worst and best performances. The most robust design has the smallest maximum performance regret across all designs. These calculations are shown in Table 3.6.

3.3.5.4 Mean and standard deviation based on the Taguchi method

In this probabilistic method, the mean and standard deviation are considered as robustness indicators. The most robust design has the smallest variation (standard deviation) around the target performance (mean) based on the Taguchi method, which has been implemented in product design for the first time. The calculations of these indicators are shown in Table 3.7.

3.4 Results of application on the case study building

The T-robust approach is applied to identify the robust and high-performance building design from an energy and comfort perspective and to measure the

Table 3.6: Calculation of performance regret of designs across all scenarios [1] .

Design	Scenarios			
	$S1$	$S2$	...	Sn
D_1	$R_{11} = KPI_{11} - C_1$	$R_{21} = KPI_{21} - C_2$	...	$R_{1n} = KPI_{n1} - C_n$
D_2	$R_{12} = KPI_{12} - C_2$	$R_{22} = KPI_{22} - C_2$	...	$R_{2n} = KPI_{n2} - C_n$
...		...		
D_i	$R_{1i} = KPI_{1i} - C_i$	$R_{2i} = KPI_{2i} - C_i$	...	$R_{ni} = KPI_{ni} - C_i$
D_m	$R_{1m} = KPI_{1m} - C_m$	$R_{2m} = KPI_{2m} - C_m$	...	$R_{nm} = KPI_{nm} - C_m$

Table 3.7: Robustness calculations using the Taguchi method [1].

Design	Scenarios						
	$S1$	$S2$	...	Si	Sn	Mean	standard deviation
D_1	KPI_{11}	KPI_{21}	...	KPI_{i1}	KPI_{n1}	$\bar{KPI}_1$	σ_1
D_2	KPI_{12}	KPI_{22}	...	KPI_{i2}	KPI_{n2}	$\bar{KPI}_2$	σ_2
D_i	KPI_{1i}	KPI_{2i}	...	KPI_{ii}	KPI_{ni}	$\bar{KPI}_i$	σ_i
D_m	KPI_{1m}	KPI_{2m}	...	KPI_{im}	KPI_{nm}	$\bar{KPI}_n$	σ_n
Robust design			Min ($KPI \cap \sigma$)				
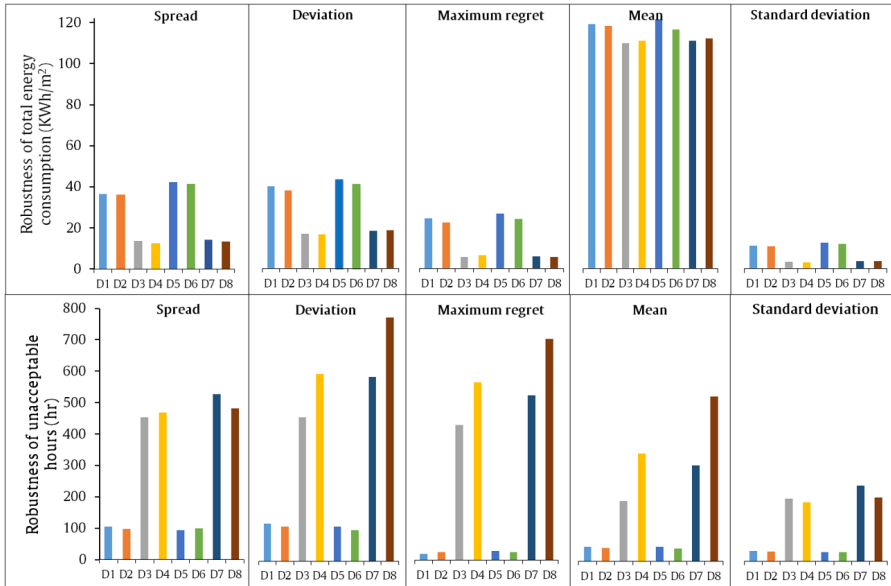
Figure 3.4: Robustness of total energy consumption and unacceptable hours using different robustness assessment methods for eight designs across considered scenarios.

robustness potential. After developing the design space and uncertainty scenarios (see Paper I for more details), each of the eight designs is simulated under 16 uncertainty scenarios, each spanning one year, totaling 128 an-

nual simulations. Subsequently, a robustness assessment is performed for the *MT-KPI* of each design under each scenario. Figure 3.4 shows the results of separate robustness assessments for each performance criterion (i.e., total energy consumption and unacceptable hours) using the various robustness indicators.

For both KPIs, two trends are evident among the robustness assessment indicators. First, the max–min and standard deviation behave similarly because indicators are calculated based on the variation. Second, the minimax regret method, best-case and worst-case method, and the mean follow similar trends because they all define robustness with respect to the optimal performance. Furthermore, the mean alone is not a good indicator for a robust design because the fluctuations across different scenarios are not reflected. Figure 3.4 indicates that the max–min, best-case and worst-case, and Taguchi methods select D_4 as the most robust design with respect to total energy consumption. On the other hand, the minimax regret, a less conservative indicator, selects D_3 as the most robust design.

For the unacceptable-hours the max–min, best-case and worst-case, and Taguchi methods select designs D_5 and D_6, which have better performance even in extreme cases, while the minimax regret as a less conservative indicator selects D_1. As shown in Figure 3.4, a design that is robust regarding both performance criteria is difficult to realize. In addition to robustness, the actual performance is crucial to a high-performance, robust building design. Therefore, a decision-making process is needed to make this selection based on these criteria. Furthermore, the process should prioritize each existing criterion.

The T-robust approach is implemented for this purpose, which integrates the performance targets into the decision-making and robustness assessment processes. Figure 3.5 shows the results of the T-robust approach for the *MT-KPI*. The max–min indicator finds D_1 as the most robust and high-performance building design. However, the best-case and worst-case, minimax regret, and Taguchi methods result in D_2 as the best choice. In the T-robust approach, the preferences are automatically incorporated into the *MT-KPI* by using a robustness margin. The selections of designs D_1 and D_2 show that the comfort criterion is prioritized in the robust design selection.

Analysing the results based on the exhaustive search and engineering knowledge (more details in Paper I) shows that there is a trade-off between D_2 and D_3 to be selected as the high-performance and robust design. D_3 performs better from an energy point of view across the scenarios. In contrast, D_2 has better performance from a comfort perspective. Figure 3.6 summarizes the results for all designs and scenarios using the same four performance zones defined in Figure 3.3. The results show that the effect of unaccept-
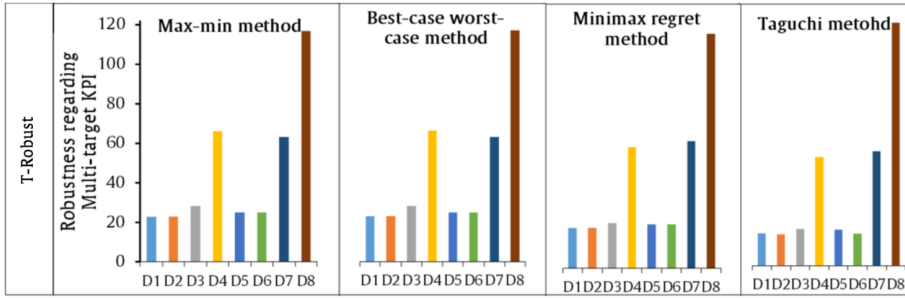
Figure 3.5: Robustness calculated using the T-robust approach with different robustness indicators.
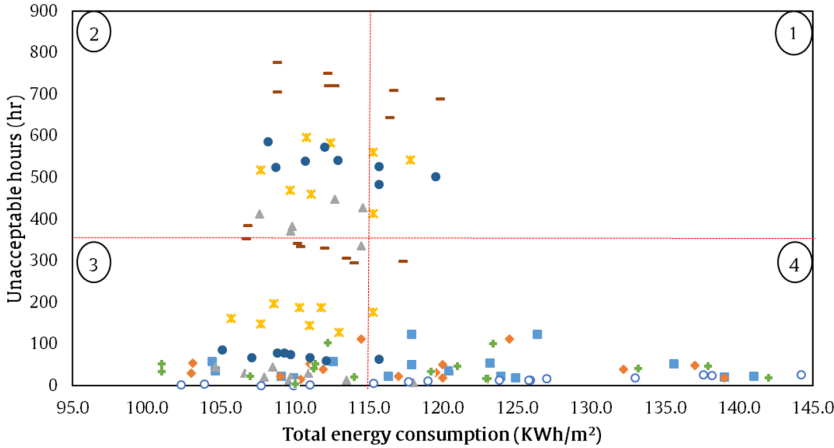
Figure 3.6: Unacceptable hours vs. total energy consumption of the eight designs under the 16 scenarios (red lines show the robustness margin for each indicator).

able hours ($\frac{Maximum\ unacceptable\ hours}{Unacceptable\ hours\ margin} = \frac{460}{330} = 1.40$) for D_3 is more severe than the effect of energy consumption ($\frac{Maximum\ energy\ consumption}{Energy\ margin} = \frac{139}{115} = 1.2\ 0$) for D_2. Furthermore, D_3 violates both the energy and comfort criteria (under different scenarios) because its performance is placed in zones 2 and 4. In contrast, D_2 only violates the energy criterion. The selection of D_2 indicates that the T-robust approach can accurately reflect the possible effects that can occur due to the severe deviations from target and the violation from two perspectives.

CHAPTER 4

Resilience Attribute II—Flexibility

As mentioned in Chapter 2, flexibility is another attribute that can affect the building resilience level by contributing to the recovery ability in Phase II (after the disruptive event). Therefore, the concept of building energy flexibility is studied, and methods for its quantification are developed. Recently, the application of renewable energy sources together with the electrification of buildings has led to an increase in clean and zero-carbon electricity. However, energy production from renewable sources is intermittent [104], variable [105], and difficult to forecast [106], and strategies for balancing supply and demand sides are required [107]. In addition, the electrification of residential heating and transportation can increase peak loads and require greater generation and grid capacity [108]. Demand-response (DR) programs can decrease the fluctuation in energy production via renewable sources, fully utilize the generated energy, balance the power grid, and relieve the grid during peak loads [109]. DR programs can lead to adjustments in power system supply and demand, known as flexibility [110].

This chapter describes a new methodology that aids building designers in the quantification of building energy flexibility based on signals coming from dynamic pricing tariffs as part of a DR program.

4.1   Background of building energy flexibility

The International Energy Agency (IEA) Energy in Buildings and Community Program (EBC) Annex 67 [111] defines buildings energy flexibility as "the building's ability to manage its demand and generation according to local climate conditions, user needs, and energy network requirements".In addition, the Energy Performance of Buildings Directive (EPBD) highlighted the importance of energy flexibility by introducing the Smart Readiness Indicator (SRI) in their recent recast [112]. The new recast introduces SRI to assess the capability of a building to adapt its operation to the needs of the

occupants and of the Grid. This contrasts with the earlier approach of the EPBD, which was only focusing on building energy labelling [113].IEA EBC Annex 67 proposed physical data and simulation-based approaches with quantitative indicators as a method for SRI quantification. Their method highlights not only the importance of smart technologies but also the significance of how the technologies are used in relation to boundary conditions such as occupant, climate and interconnected energy networks [113]. Several studies can be found in the literature focusing on the quantification of the energy flexibility of buildings. Reynders et al.[114] introduced a simulation-based method for the generic characterization of energy flexibility focusing on structural thermal storage in residential buildings. They developed indicators, which were based on the size, time and induced. Oldewurtel et al. [115] presented a unified framework for comparison of different DR programs and different flexibility assets such as batteries, plug-in electric vehicles (EV), commercial building thermal mass and thermostatically controlled loads (TCL).

DR programs aim to establish building energy flexibility by targeting different control objectives. Some examples of DR programs include peak shaving, load shifting, valley filling, and minimizing curtailment time [116].In general, DR programs can be categorized into two different groups [117]: incentive-based and price-based. Incentive-based DR programs focus on economic incentives provided by utilities or grid operators, which encourage customers to reduce their demand during a capacity shortage or times of high electricity prices. In price-based DR programs, customers change their normal electricity usage patterns in response to dynamic pricing tariffs. Dynamic pricing tariffs help customers manage their consumption more wisely and efficiently. Different schemes, such as time of year (seasonal) pricing, time of use pricing (daily or weekly), critical peak pricing, and real-time pricing [118] can be used in the dynamic pricing tariffs.

In residential buildings, loads related to household appliances (e.g., washing machines and dishwashers), EVs, and space or water heating systems are considered flexible. Studies in the literature evaluated the load shift with a focus on the white goods loads [119], EVs [120], and water heaters loads [121] in response to dynamic pricing tariffs.

Depending on the energy system and type of DR program, a storage system can be considered an asset for achieving flexibility in residential buildings. Two important categories of storage systems are electrical and thermal storage. In electric storage, batteries are implemented as flexibility assets to shift energy consumption from high to low-tariff periods or reduce the peak demand. In the literature, batteries were employed in combination with dynamic pricing tariffs to establish a dynamic interaction between the build-
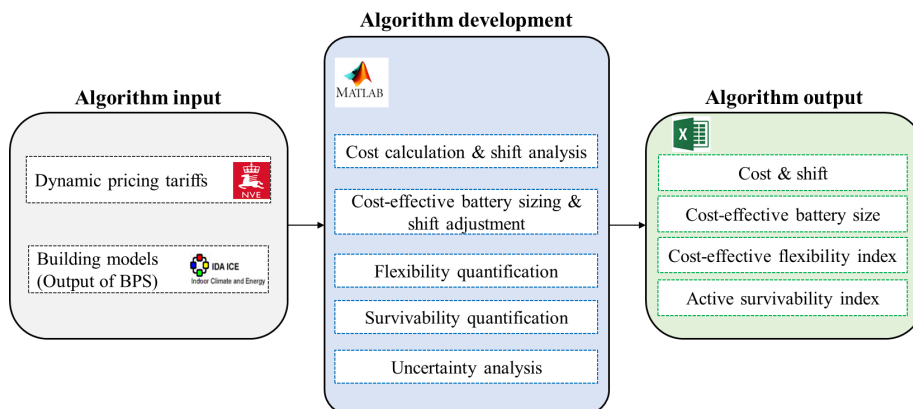
Figure 4.1: Conceptual framework of the developed methodology for the quantification of energy flexibility and survivability.

ing and smart grid [122]. Furthermore, batteries have been used as backup assets to provide power to customers during power outages [123, 124]. Understandably, batteries can act as "flexibility assets" for harnessing building energy flexibility and as "backup storage" for improving building survivability during power outages. Furthermore, battery capacity can aid in the quantification of energy flexibility and survivability. However, little attention has been paid to the energy flexibility and survivability trade-off from a cost-effectiveness perspective. For this purpose, a methodology was developed in this work to evaluate the trade-off between energy flexibility and survivability for all-electric buildings from a cost-effectiveness perspective in the context of dynamic pricing tariffs.

4.2 Methodology for the quantification of energy flexibility and survivability

The developed methodology for the quantification of flexibility and survivability consists of three stages, which focus on the quantification algorithm: algorithm input, algorithm development, and algorithm output, as illustrated in Figure 4.1. BPS and an in-house algorithm developed in MATLAB are used for this methodology. The stages of the methodology are defined in the following subsections.

4.2.1   Algorithm input

The algorithm input stage accepts the inputs needed to develop the algorithm: dynamic pricing tariffs, which act as signals for flexibility evaluations, and the building models, which represent the performances of different building designs.

4.2.1.1   Dynamic pricing tariffs

The current grid-rent tariff for Norwegian residential customers (i.e., Energy rate tariff model) is energy-based. This tariff consists of two parts: fixed and volumetric. The fixed part includes the annual costs associated with customer management and support, which is the same for all customers. The volumetric part is a charge associated with energy consumption that is user-dependent. Unfortunately, this tariff does not differentiate between the high and low power drains [125]. Therefore, dynamic pricing tariffs have been proposed to better incentivize grid utilization [126]. In Norway, three business models of dynamic pricing tariffs have been employed: time of use, which involves higher costs during higher demand periods; measured power rate; and tiered rate, both of which involve higher costs for a demand higher than a subscribed level. These tariffs are defined as follows:

Measured power rate tariff model: The measured power rate tariff is similar to the energy rate tariff with one addition; this tariff takes power into account based on the highest peak power drain during the measurement period. The Norwegian regulations recommend the power contribution be measured on a daily basis to match customer and grid demand [127].

Tiered rate tariff model: The tiered rate tariff assigns a higher cost to demands higher than a subscription level. This tariff includes two additional parts compared to the energy rate tariff model: capacity level (subscription limit) and overuse cost, which is the cost of consumption beyond the capacity level. In other words, the customer subscribes to a capacity level (subscription limit), and based on their excess use, a penalty (overuse) is charged. In this study, we used an individual annual subscription that either customers could select themselves or grid distribution companies could provide and it is not possible to change it over the course of a year. Norwegian regulators set a minimum usage of 1 kW but did not suggest exact power limits. However, this study considers ten limits. The appropriate power limit in this tariff needs to prevent high subscription or overuse costs.

Time of use tariff model: In the time of use tariff, the electricity price is differentiated between specific time periods, such as peak and off-peak hours, which can be recognized based on the historical data showing the grid pressure. Norwegian regulators suggested higher prices during winter

Table 4.1: Grid tariff rents for residential buildings in the Energy rate tariff, Measured power tariff, Tiered rate tariff, and Time of use tariff.

Energy Rate tariff			
Fixed cost (€/year)	Energy cost (€/kWh)	-	-
174.9	0.0194	-	-
Measured Power Rate tariff			
Fixed cost (€/year)	Energy cost (€/kWh)	Power cost (€/kWh/h)	-
174.9	0.005	0.186	-
Tiered Rate tariff			
Fixed cost (€/yr)	Energy cost (€/kWh)	Subscription cost (€/kWh/h)/year	Overuse cost (€/kWh/h)
174.9	0.005	68.9	0.1
Time of Use tariff			
Fixed cost (€/yr)	Summer energy cost (€/kWh)	Winter day energy cost (€/kWh)	Winter night energy cost (€/kWh)
174.9	0.0122	0.038	0.0152

days because of grid stress during these periods. Customers understand this tariff because it differentiates pricing according to blocks of time and offers pricing in terms of energy consumption (kWh) instead of power (kW), which is used in the two previous tariffs.

Table 4.1 shows the average values related to each tariff, which can vary between different distribution companies [125]. Other taxes and levies are added to the grid-rent tariff [128].

4.2.1.2 Building models

Another input to the algorithm is the building model. Here, BPS was used to estimate the building loads, such as space heating and DHW. The energy simulations for building models were conducted via the BPS software IDA-ICE, version 4.8 [70]. The results of simulations in IDA-ICE were input to the developed algorithm to calculate the shifted load, battery capacity, and other parameters. The simulations were conducted using a typical climate file (IWEC) from the IDA-ICE library [70].

4.2.2 Algorithm development

The MATLAB-based algorithm calculates the electricity cost, heat shifts, and cost-effective battery sizes for different dynamic pricing tariffs. Then, the algorithm quantifies the building energy flexibility and survivability for

the suggested tariffs. The steps toward this algorithm are explained in the following subsections.

4.2.2.1 Cost calculation and shift analysis

To calculate the energy costs of different building designs under the suggested dynamic pricing tariffs, the hourly energy demand resulting from the BPS and the cost parameters related to different tariffs are imported into this algorithm as input data. The algorithm then computes the energy costs for different building designs.

Load shifting is a strategy that can be used with price-based DR programs. In this work, the cost-effective load shift was implemented to shift the electric-based heating load (consisting of space heating and domestic hot water). The heating load was selected as the shiftable load because of its largest share in energy consumption in cold climate countries, such as Norway. Additionally, shifting the heating load is safer in comparison to other loads, such as appliances loads, which demand shifts at night time or when no occupants are present. However, this can lead to some disadvantages, such as fire risk. Therefore, the current work focuses on shifting the heating load without sacrificing thermal comfort and applying batteries as storage assets without using any thermal storage. The strategy behind the load-shift calculations in this work is called the cost-effective heat shift. To determine the cost-effective heat shift, the amount of ideal heat shift is first considered based on [129], and then it is adjusted based on the size of the cost-effective battery. The ideal heat shift is a theoretical optimum amount of shift that leads to the lowest costs with respect to the implemented tariff [129]. The assumptions for this ideal load shift are as follows:

- The ideal heat shift consists of the space heating and domestic hot water loads.
- The ideal heat shift does not sacrifice the occupant's comfort (regarding space heating and domestic hot water).
- The storage of the shifted load is daily-based (kWh/day).
- No losses occur during the ideal load shift.

The application of the ideal load shift yields specific load profiles and shift patterns for all tariffs, as shown in Figure 4.2. In the energy rate tariff, load shifting is not beneficial because the energy price is the same for all hours of the year. Therefore, the customer will not pay for the storage system if any benefit is not gained from the load shift. In the Measured power rate tariff, the daily peak power cost is included in the total cost and can be reduced without affecting the demand. If the daily peak decreases to the lowest possible value, the peak cost will minimize, resulting in a constant
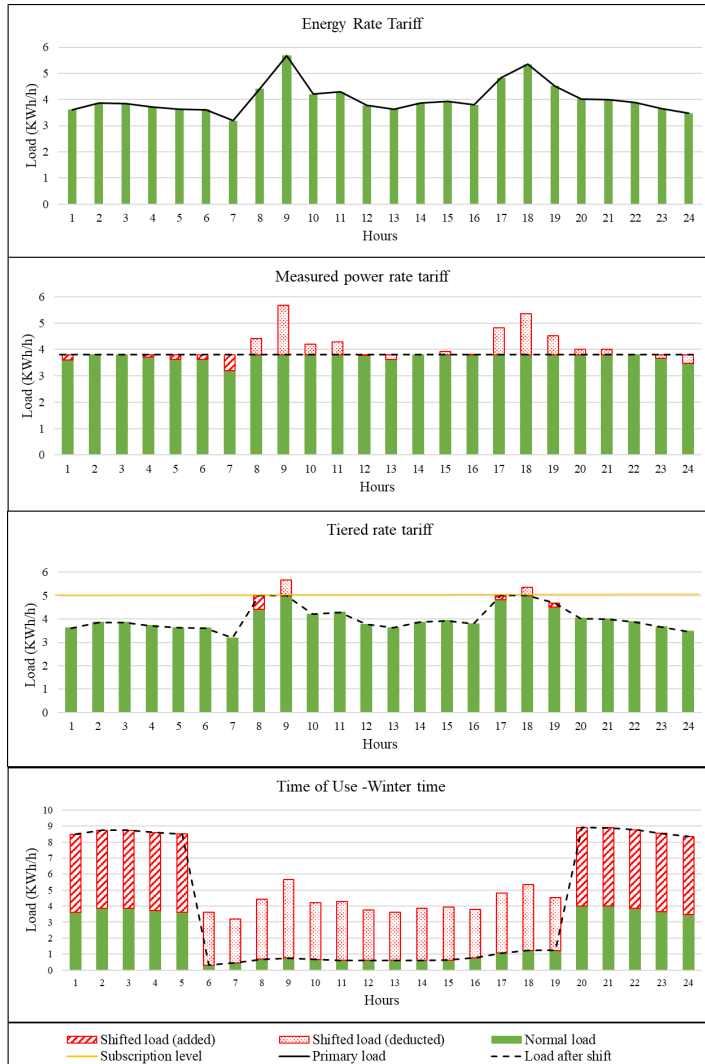
Figure 4.2: The winter load profiles for the ideal heat shifts of different business models of dynamic pricing tariffs.

load profile after the shift. The lowest possible peak is based on the maximum value between the plug loads and the daily average heating load. This value is selected to meet the plug load at any time and minimize the peak of the heating load. For the Tiered rate tariff, the overuse cost can be reduced without impacting the demand. Thus, the heating loads when demands are higher than the subscription level are shifted to the hours with loads below the subscription level, reducing the overuse cost to zero. For the Time of use
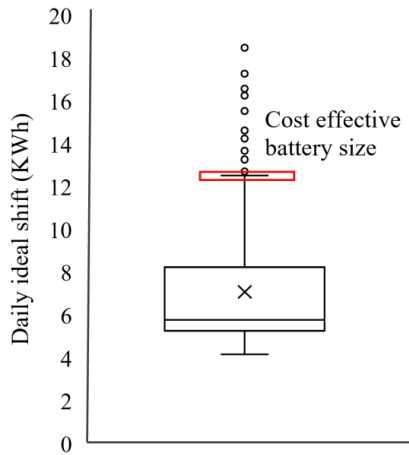
Figure 4.3: Illustration of the cost-effective battery sizing for a typical building.

tariff, the heating loads that occur during the penalized hours (winter days, red hours shading in Figure 4.2) are shifted to the normal hours (winter nights, green hours in Figure 4.2). Because all summer hours have the same energy costs, the ideal heat shift will have no impact during the summertime.

4.2.2.2   Cost-effective battery sizing and shift adjustment

After the calculation of the ideal heat shift, an adjustment is required based on the cost-effective battery size. The strategy used for battery sizing in this work is called cost-effective battery sizing. This strategy focuses on the daily capacity needed for shift storage. The battery size is selected based on the amount and distribution of the daily ideal heat shift over a year. The cost-effective capacity can cover the storage capacities that have a high probability of happening daily over the course of a year and will be enough for most of the days of the year (not all days of the year). Clearly, some days the cost-effective battery capacity will not be sufficient, but the storage capacities for these days are neglected because of their lower probabilities of occurrence.

Fig 4.3 shows a box plot of the daily storage capacity needed for the ideal heat shift in a typical building over a year. The selection of the cost-effective battery size based on the amount of daily storage and its distribution in Fig 4.3.The cost-effective battery capacity is selected based on the maximum capacity necessary in the box plot, which is indicated with a red box (C_{Bat}) in the figure. Note that by considering this value as the battery capacity, the

ideal heat shift in the outlier region is neglected because this type of shift is rare. The battery size can thus focus on cost-effectiveness. Therefore, if the distribution of the daily storage has some data in the outlier region, then the selected battery capacity may not be sufficient to store the entire ideal heat shift (*IHS*). This lack of storage will deduct part of the shift, creating an effective heat shift (*EHS*). Of note, when the box plot does not have an outlier section, the *EHS* is equal to the IHS, and in distributions with outliers, the *EHS* will be less than the IHS. Here, the cost-effective battery size can be used by designers and decision-makers in the conceptual design stage but does not capture the details related to the charge and discharge states of the battery, which may be needed in the detailed design stage.

4.2.2.3 Energy flexibility quantification

Energy flexibility potential can be quantified based on the signals coming due to dynamic pricing tariffs. The quantification determines a single indicator, the cost-effective flexibility index (*CEFI*), which shows the cost-effectiveness of the implemented battery for storing the heat shift as a flexibility asset. The *CEFI* equals the percentage of savings due to the effective heat shift divided by the cost-effective battery size. This index in %/kWh indicates the savings that can be guaranteed if the cost-effective battery size is implemented in the building. If the implemented battery is smaller than the cost-effective battery size, the percentage of savings will be lower.

4.2.2.4 Survivability quantification (active plus passive)

The literature defined passive survivability as the ability of a building to maintain the building in a safe and habitable thermal condition in the event of an extended power failure [130]. Previous work also refers to this concept as thermal resilience because of the focus on building survivability from a thermal perspective [131]. The "habitable thermal condition" in the passive survivability definition encompasses a wider range than the thermal comfort condition. In this work, the habitable thermal condition is $15°C<T_{indoor}<30°C$ [37], which is wider than the thermal comfort range for living rooms suggested by the Norwegian standard ($19°C<T_{indoor}<26°C$) [92]. The time required for a building to decrease from its setpoint temperature to $15°C$ is called winter passive survivability. In contrast, the time it takes a building to increase its temperature from the setpoint to $30°C$ is called summer passive survivability. The summation of these two values is referred to as passive survivability index (*PSI*) in this work (Equation 5.1). We calculated the winter passive survivability and summer passive surviv-

ability by simulating a six-day power failure during the coldest and warmest weeks of the winter and summer, respectively.

$$PSI= \textit{Summer passive survivability } + \textit{ Winter passive survivability} \quad (4.1)$$

As discussed, batteries can also be implemented as backup storage to improve building survivability in the case of a power outage. Given this, this work introduces a new kind of survivability for buildings equipped with batteries, called "active survivability" because batteries operate as active systems to protect building performance from power failure. In addition, this survivability considers more than the thermal condition as it evaluates the survivability of all end uses, such as lighting, appliances, and domestic hot water. We defined active survivability as the ability of the building and its storage system to maintain critical operations in the absence of grid power, and it is quantified by the active survivability index (ASI). The ASI equals the cost-effective battery capacity selected for the shift storage divided by the minimum energy needed for the building to maintain critical operations. The following assumptions are made for the calculation of the minimum energy consumption needed to maintain critical operations:

- A thermal setpoint temperature of 15 °C (the habitability threshold) is considered for the critical operation of the building.

- In the critical operation condition, the domestic hot water, lighting, and appliance demand are 25% of the values suggested by the Norwegian standard SN/TS 3031 [93].

The BPS under these assumptions estimates the minimum energy needed by the building in the critical operation.

4.2.3   Algorithm output

In this section, the outputs of the developed algorithm are defined:

1. AC: The annual energy cost of the building without considering a heat shift (€/yr), which can be calculated for each design under the business models of dynamic pricing tariff, as calculated in Section 4.2.2.1.

2. ACIS: The annual energy cost of the building using the ideal heat shift (€/yr), which can be calculated for each design under the business models of dynamic pricing tariff, as calculated in Section 4.2.2.1.

3. C_{Bat}: The cost-effective battery size (kWh) that is needed for storing the shifted heat, as determined in Section 4.2.2.2.

4. ACES: The annual energy cost of the building based on the effective heat shift (€/yr), as calculated in Section 4.2.2.2.

Table 4.2: Details of the ten competitive designs considered in the case study.

Design parameters	D_1	D_2	D_3	D_4	D_5	D_6	D_7	D_8	D_9	D_{10}
					Designs					
Overall U-value (W/m².K)	0.31	0.25	0.43	0.36	0.33	0.29	0.51	0.44	0.40	0.35
Normalized thermal bridge (W/m².K)	0.05	0.03	0.07	0.05	0.03	0.02	0.06	0.07	0.06	0.05
WWR (%)	30	30	30	30	40	40	40	40	30	30
Heating system	ER	ER	ASHP+ER	ASHP+ER	ER	ER	ASHP+ER	ASHP+ER	ER	ER
Ventilation system	Balanced	Exhausted	Balanced	Exhausted	Balanced	Exhausted	Balanced	Exhausted	Balanced	Balanced
Solar DHW system size (m²)	0	5	0	0	0	5	0	0	0	0
PV system size (m²)	0	0	0	0	0	0	0	0	40	20
Lighting	Typical	LED	Typical	Typical	Typical	LED	Typical	Typical	Typical	Typical
KPI										
Total energy consumption (kWh/m²)	110	110	110	110	110	110	110	110	110	110

5. E_{min}: The minimum energy needed by the building to maintain the critical operation (kWh), as determined in Section 4.2.2.4.

6. $SI = \frac{\Delta C}{AC} \times 100$: The savings index (%), which indicates the benefit of utilizing a building's flexibility by dividing the cost savings by the annual costs before the shift, as defined by [105].

7. $CEFI = \frac{SI}{C_{Bat}}$: The cost-effective flexibility index (%/kWh), which shows the cost-effectiveness of a building's flexibility by dividing the SI by the cost-effective battery capacity.

8. PSI: summation of the lengths of time that the building can remain in the habitable thermal condition ($15°C < T_{indoor} < 30°C$) following a grid power outage, in the coldest and hottest week respectively.

9. $ASI = \frac{C_{Bat}}{E_{min}} \times 100$: The active survivability index (%), which shows the percentage of the minimum energy needed in the critical condition that can be covered by the cost-effective battery used for shift storage. This value represents how the battery can enhance the building's survival in the absence of grid power.

4.3 Application to the case-study building

The case study used to test the methodology is the same case study introduced in Chapter 3 with the addition of two designs. For comparison purposes, these two designs are competitive, meaning they have the same energy target (110 kWh/m² based on the TEK 17 standard), but they are equipped with PV panels to assess their impact on the flexibility of the design. The designs are defined as competitive in order to create the opportunity of comparing the designs with the same energy target from the flexibility point of view. The characteristics of the ten designs are summarized in Table 4.2

4.4 The results of application on the case study building

In this section, selected results from the application of the developed methodology on the case-study building are shown (more detailed results can be
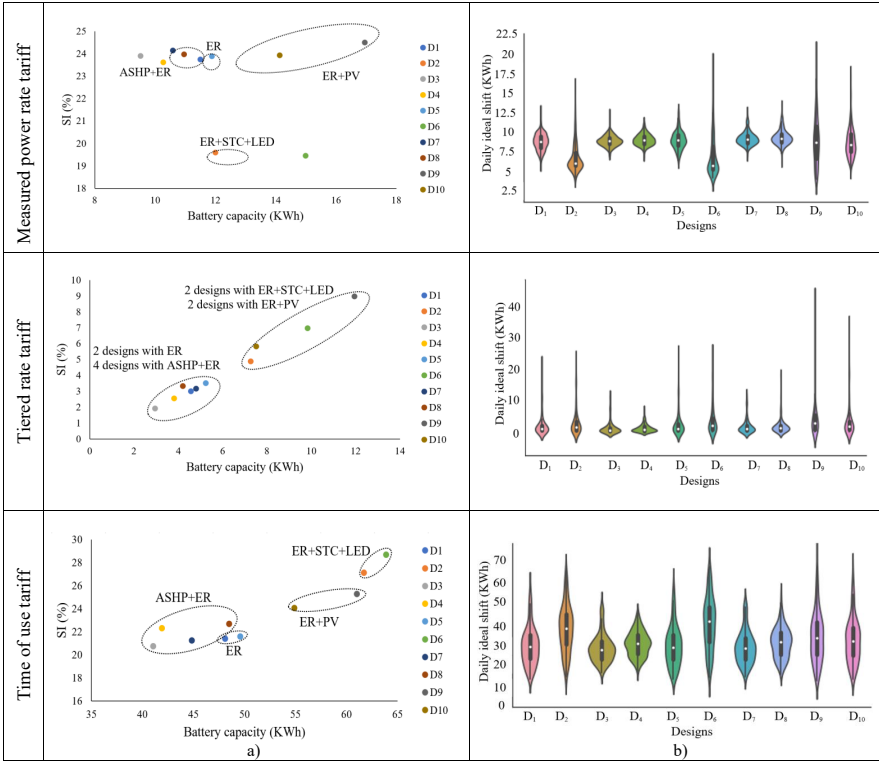
Figure 4.4: a) Relationship between the SI and C_{Bat} and b) violin plots of the daily shifts for the ten designs.

found in Paper II). Figure 4.4 shows the relationship between the *SI* and C_{Bat}, as well as a detailed comparison of the daily heat shift for different designs. Based on this figure, *SI* and C_{Bat} are directly proportional in all three tariffs. Time of use tariff has the highest *SI* and C_{Bat} because of its larger shift. The minimum *SI* and C_{Bat} correspond to the Tiered rate tariff, while Measured power rate tariff has values between those of the two other tariffs. The *SI* of Measured power rate tariff is similar to that of the Time of use tariff, but its C_{Bat} is significantly lower.

The battery capacity is determined according to the daily shift and its distribution. Hence, violin plots are used to demonstrate the distributions and probability densities of the daily shifts for the ten designs. A violin plot, similar to a box plot, provides a kernel density estimation of the underlying distribution. These violin plots, along with the relationships between SI values and cost-effective battery capacities for the tariffs in the reference

scenario, are shown in Figure 4.4. Note that the cost-effective batteries are only used for the storage of the shifted heat and not for storing energy produced by renewable energy sources.

In the Measured power rate tariff, D_2, D_6, D_9, and D_{10} have more distributed heat shifts with a high standard deviations. On the other hand, designs D_3, D_4, D_7, D_8 exhibit less daily storage, and their distributions are dense in the middle. These results reveal that the most influential parameter in the classification of the designs regarding the cost-effective battery capacity pertains to the energy system. Designs D_9 and D_{10} have weaker envelopes in combination with ERs, resulting in larger daily shifts and increased battery capacity. Even though D_2 and D_6 have smaller shifts, owing to lower summer usage, their shifts are larger during the winter because of the exhaust ventilation and ER, leading to increased battery capacity. The remaining designs, D_1 and D_5 show data distributed at a higher level in comparison to designs D_3, D_4, D_7, and D_8, leading to higher cost-effective battery capacities. The smallest battery capacities are assigned to the designs with the combination of an ASHP and ER because their daily storage values are concentrated at the lower levels (i.e., the heating demand created by a heat pump has less variation than the heat demand created by an ER, leading to smaller surpluses for the shift). For the designs without ASHPs, air-balanced ventilation results in smaller cost-effective battery capacities because of the fewer deviations in the heating demand over the year.

Time of use tariff focuses on the shift of the daily heat consumption. Thus, a design with higher daily heat consumption requires a higher battery capacity. Figure 4.4 shows that designs with higher heating demands also had shifts that were distributed more widely. These designs included those with weaker envelopes and ERs (D_9, D_{10}) or exhaust ventilation and an ER (D_2, D_6). Designs D_1, D_5 had greater shifts and more widely scattered daily storage requirements, resulting in mid-level cost-effective battery capacities and SI values. The smallest cost-effective battery capacities and SI values were present in the designs featuring ASHPs and ERs, owing to their smaller shifts and dense distributions. Design D_3, which uses a combination of an ASHP, ERs, and balanced ventilation, yields the minimum cost-effective battery capacity.

For the Tiered rate tariff, the shifts occur during random hours and more frequently during the peak hours in winter. Therefore, designs with higher demand during the winter have larger shifts and higher SIs, as seen in the designs D_2, D_6, D_9, and D_{10}, which have weaker envelopes with an ER or exhaust ventilation with an ER. On the other hand, these designs have more widely distributed daily storage and cost-effective battery sizes. Other designs with ERs or ASHP and an ER combinations have SIs and cost-

effective battery sizes smaller than those of the previous group. For this tariff, the minimum battery capacity is also assigned to design D_3, which has an ER, ASHP, and balanced ventilation.

The cost-effective battery capacity plays an important role in the calculation of the indexes developed in this work (i.e., *CEFI* and *ASI*). The trade-offs between cost-effective energy flexibility and survivability for the ten designs are shown in Figure 4.5 for the three business models of the dynamic pricing tariff. In this figure, the *ASI* and *CEFI* are shown along the x- and y-axes, respectively. As a third dimension, the bubbles indicate the relative values of the *PSI*s (number of hours that the building can survive). This figure reveals that between the three tariffs, Measured power rate tariff exhibits the highest *CEFI*, higher SI than the Tiered rate tariff, and a battery capacity as large as that of the Time of use tariff. The application of the ASHP and balanced ventilation leads to the highest *CEFI*s.

The *ASI* for the Time of use tariff is higher than that for the Measured power rate tariff, which is higher than that of the Tiered rate tariff, because of the highest cost-effective battery capacity achieved by the Time of use tariff. The higher the *ASI*, the higher the self-sufficiency of the building during a power outage. In other words, the building can survive with its own storage system without being dependent on large-scale centralized storage, such as that in neighborhoods.

The *PSI* for the current case study is calculated by applying a six-day-long power failure the coldest week in winter. Because the building is a heating-dominated building without a cooling system, the *PSI* calculation focuses on the winter passive survivability. Results in Figure 4.5 show that the building envelope and WWR are the most influential for passive survivability, as indicated by designs D_2 and D_6.

Illustrations such as Figure 4.5 can aid decision-makers in selecting the best design based on their preferences with respect to cost-effective flexibility and active and passive survivability. For example, buildings such as hospitals, care homes, and data centers prioritize survivability because they have a high potential of risk in the case of power failures. Figure 4.5 shows that under the Measured power rate tariff, if the decision-maker prefers a savings of more than 2% by utilizing each kWh stored in the cost-effective battery, the passive survivability is about one day, and the active survivability is low ($ASI < 17\%$). Such situation is evident in designs with ASHPs and can yield appropriate solutions if the *CEFI* is prioritized.

Another example involves prioritizing *ASI* under the Time of use tariff. If the decision-maker needs a high *ASI* (more than 75%), the *CEFI* is low, but the passive survivability is extended to four days, which applies to designs D_2, D_6, D_9, and D_{10}. Among these designs, designs D_2 and D_9 have the
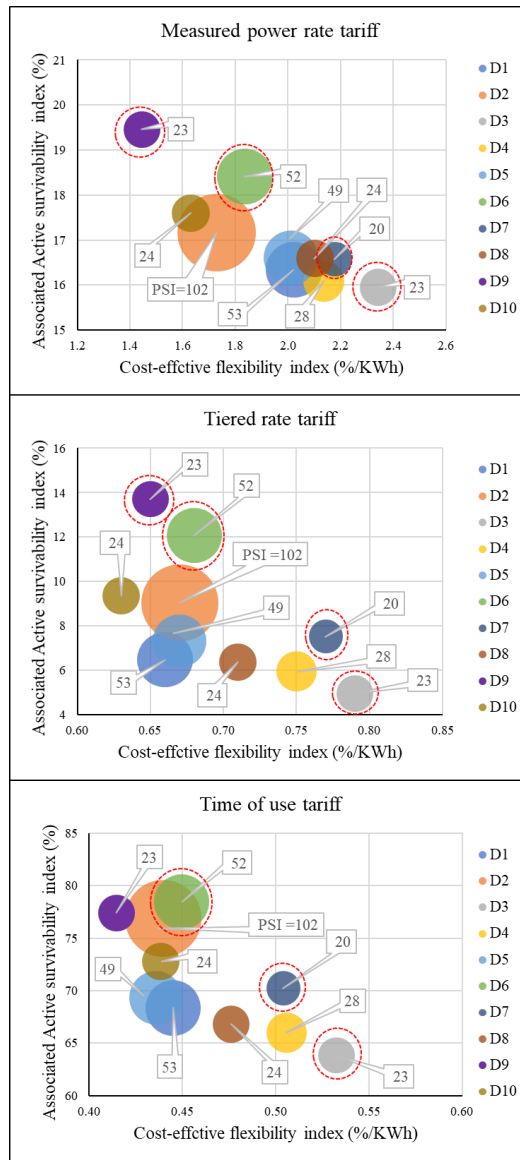
Figure 4.5: Trade-offs between cost-effective energy flexibility and survivability. The bubble size indicates the relative value of the passive survivability index.

greatest passive and active survivability indexes, respectively.

The competitive designs regarding flexibility and survivability are marked with red dotted circles in Figure 4.5, such as designs D_3, D_7, D_6, D_9 for the Measured power rate tariff. Both D_3 and D_7 use ASHPs and balanced ventilation and thus have higher *CEFI*s. On the other hand, D_6, with exhaust ventilation in combination with a strong envelope and STC, and D_9, having a weaker envelope and an ER, demand higher battery capacities (resulting in higher *ASI*s). Three of these designs have passive survivability values of roughly one day, and only D_6 has higher passive survivability. Hence, if the *CEFI* is prioritized under this tariff, D_3 and D_7 are appropriate solutions; if survivability is more important, D_2 or D_9 are good choices. In general, the methodology in this work provides allows decision-makers, such as grid companies, building designers, and homeowners, to set up trade-offs between energy flexibility and survivability from a cost-effective perspective. The decision-makers can select their preferred design based on prioritizations of the involved criteria.

Building Resilience Assessment

5.1 Overview

In the previous chapters, building robustness and flexibility as two main attributes of building resilience are discussed. This chapter focuses on the assessment of resilience itself for building performance. In this work, a resilient building is defined as follows:

- A resilient building is a building that is able to prepare for, absorb, adapt to, and recover from a disruptive event.

As mentioned in Chapter 2, four main questions are recognized for defining resilient buildings in this work. These questions are: Resilience of what? Resilience to what? Resilience based on what? Resilience in what state?

In this work, we have focused on the evaluation of the thermal resilience of a building and its integrated energy systems against power failure with a focus on both phases of the disruptive event based on some proposed resilience metrics.

In the context of the built environment, various simplified metrics have been implemented for the quantification of the thermal resilience of buildings. However, this topic still requires more research. Resilience quantification needs to capture resilience not only during the disruptive event but also after the disruptive event. The metrics should also indicate how far and for how long the building performance deviates from the targets. In other words, the metrics need to be sensitive to the event's hazard level and exposure time. Furthermore, a representation of thermal resilience on the scale of a thermal zone is necessary, as well as of the whole building. Given these points, methodologies that allow building designers and decision-makers to compare and benchmark different building and technology designs are developed from the thermal resilience perspective. This chapter is based on the research conducted in Papers III and IV. First, the developed methodology in Paper III, which focuses on extending the available concepts of resilience

and their associated metrics to the building thermal performance, is discussed. Then, a new methodology for the quantification of building thermal resilience, as developed in Paper IV, is presented.

5.2 Extension of the concepts of resilience triangle and trapezoid to the building thermal resilience

The resilience triangle and resilience trapezoid have been used to represent the performance of a system concerning a disruptive event [17, 30]. The resilience triangle concept is the foundation for the analytical assessment of resilience, describing the deterioration of a system's functionality over the duration of the disruptive event [54]. Immediate restoration actions are assumed to be taken at the end of the disturbance. The resilience triangle can be extended to the resilience trapezoid, which considers the degraded state that a system experiences when facing a disruptive event. Based on these two concepts, an analysis of pre-simulation results of building performance during a disruptive event shows that buildings as dynamic systems exponentially degrade after experiencing disruptive events. Thus, in this work, building performance concerning a disruptive event as a function of time is represented by a multi-phase resilience curve. Similar to the resilience triangle [30], immediate restoration actions are assumed to be taken at the end of the disturbance. Three phases are recognized in the multi-phase resilience curve, as shown in Figure 5.1 and described as follows:

1. Phase I: In the pre-disturbance Phase I, the building operates based on the setpoint temperature, which is considered the target, and for the example in Figure 5.1 is 21.5°C) before the disruptive event. Based on the definition of a resilient building, the building prepares for the disruptive event in this phase.

2. Phase II: At the beginning of Phase II, the disturbance progress phase, the disruptive event occurs. The building performance in terms of the indoor operative temperature usually decreases until the end of this phase. Based on the definition of a resilient building, the building absorbs the impact of and then adapts to the disruptive event in this phase.

3. Phase III: The post-disturbance Phase II shows the recovery process, in which the building's operative temperature returns to the set target or even more. Based on the definition of a resilient building, the building recovers from the disruptive event in this phase.

Figure 5.1 shows four performance thresholds in the multi-phase resilience curve, which are defined below:
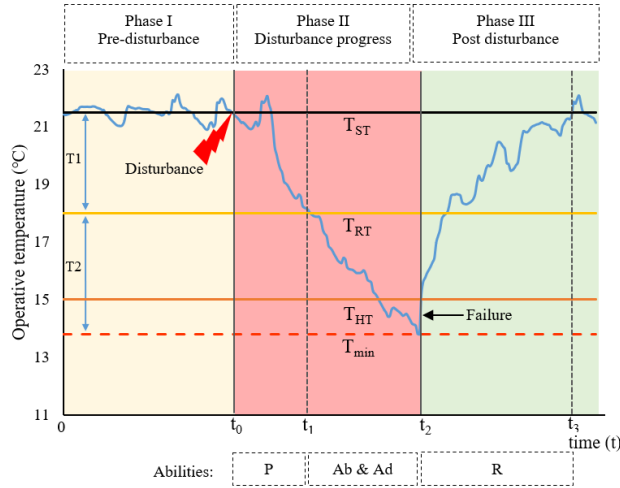
Figure 5.1: Multi-phase resilience curve (P: Preparation, Ab: Absorption, Ad: Adaptation, R: Recovery).

- T_{ST}: The setpoint temperature T_{ST} is the set target to achieve the desired building performance.

- T_{RT}: is the performance robustness threshold. Any performance (i.e., operative temperature) higher than T_{RT} is considered robust. An operative temperature less than T_{RT} indicates a non-robust performance.

- T_{HT}: The habitability threshold for the occupant is represented by the temperature T_{HT}. Exceeding this threshold shows that the building failed to provide the minimum required comfort condition for the occupants, and the building will not have a safe recovery. If the building manages to recover before reaching this habitability threshold, the building is considered thermally resilient.

- T_{min}: The minimum performance level caused by the disruptive event is represented by the temperature T_{min}.

Based on the definition that has been used for building performance resilience, which is in line with "Adaptive resilience", it is possible that the performance of the building experiences another level than T_{ST} after the disruption. Here, the performance of the building before and after the disruption is considered the same in order to ease their comparison.

Based on the three phases and four performance levels, the abilities of thermal resilient building in the action cycle of a disruptive event can be defined as follows:

- Preparation: This ability for preparation indicates how well the building is prepared for the disruptive event and how long it can perform higher than the robustness threshold, minimizing the potential for the adverse impact of the disruptive event. This ability depends on building characteristics such as the building envelope and storage systems, etc.

- Absorption and adaptation: Although the building is prepared for the disruptive event, the robustness threshold can still be crossed. Therefore, the building and its integrated systems should be configured such that they can absorb the impacts of the disruptive event and minimize the overall disruption. Furthermore, the building should be able to adapt to the impact of the disruptive event and modify its configuration.

- Recovery: Recovery is defined as the ability of the building to return to the set target performance level (T_{ST}) after the disruptive event. Restoration to the set target performance level depends on the impact intensity of the disruptive event and the levels of preparation, absorption, and adaptation.

5.3   Extension of the power system resilience metrics to the building thermal resilience

The resilience trapezoid was first implemented by [55] to quantify power system resilience. Time-dependent resilience metrics were developed to measure how fast and how low the resilience drops, how long the system remains in the degraded state, and how quickly it recovers. These metrics comprise the $\Phi\Lambda E\Pi$ system, in which Φ is the speed of damage, Λ is the magnitude of the damaged grid functionality, E is the duration of the damaged state, and Π is the recovery speed.

Based on the $\Phi\Lambda E\Pi$, we extended the system and adapted it to the context of building thermal performance. For this purpose, a test framework is introduced, which applies a fixed-duration power failure as a disruptive event to measure the thermal performance of the building resulting from the BPS tool (IDA-ICE). The test framework is applied to an all-electric building, with power failure as the disruptive event, which lasts for four full days during a typically cold winter (starting January 14). Furthermore, the four days before the disturbance (pre-disturbance phase) and four days after the disturbance (post-disturbance phase) are also evaluated in the test framework. In total, the test evaluation covers 12 days.

The set target in the test framework is based on the setpoint temperature suggested in the Norwegian standards [132]. In addition, the robustness

margin is assumed to have a 3.5°C tolerance from the set target (setpoint temperature based on the standard). The resultant robustness threshold is 18°C, which is a safe and well-balanced temperature to protect the health of the general populations in countries with temperate or cold climates [133]. A temperature of 15°C is selected as the habitability threshold based on a comprehensive review on the effect of low temperatures on elderly morbidity [134].

The adapted metrics from power system resilience represent thermal resilience in three phases, considering different abilities. Table 5.1 shows the metrics that extend from the power resilience analysis, which are used for the evaluation of thermal resilience in the suggested test framework. The robustness duration (RD) indicates the duration the building performance is maintained robust after experiencing the power failure. With a higher RD, the building is better prepared for disruptive events. The collapse speed (CS) indicates the speed with which the building performance drops from the set target. A lower CS implies that the building can absorb the impact of the event, and thus, the performance worsens at a lower rate. The amplitude of the power failure impact (AoE) is the minimum building performance after the power failure. A small AoE reflects the building's adequate ability to absorb the impact of the event and adapt. If AoE is greater than the difference between T_{ST} and T_{HT}, the building is not considered thermally resilient. The recovery speed (RS) in the restorative phase shows the rate at which the building can return to its set target after reconnecting to power. A higher RS shows that the building is better able to recover. The expected performance loss (EPL) considers both the impact intensity and duration of the power failure. A lower EPL shows that the performance deviated less from the target during the disruptive event, indicating a more resilient building.

The developed metrics were tested for the first two designs (D_1 and D_2) of the case study in Chapter 3. The building is all-electric, which means that electricity provides all of the demands in the building. Furthermore, the building is heating-dominated and does not have a cooling demand. The heating demand is based on direct electrical heating with ERs. In addition to

Table 5.1: Description of the suggested resilience metrics (P: Preparation, Ab: Absorption, Ad:Adaptation, R:Recovery).

Metric	Name	Unit	Equation	Phase	Ability
RD	Robustness Duration	h	$t_1 - t_0$	Phase II	P
CS	Collapse Speed	°C/h	$\frac{T_1+T_2}{t_2-t_0}$	Phase II	Ab and Ad
AoE	Amplitude of Event	°C	$T_1 + T_2$	Phase II	Ab and Ad
RS	Recovery Speed	°C/h	$\frac{T_1+T_2}{t_3-t_2}$	Phase III	R
EPL	Expected Performance Loss	degree.hour	$[\int_0^t (T_{ST} - T(t))\,dt]$	All phases	All abilities
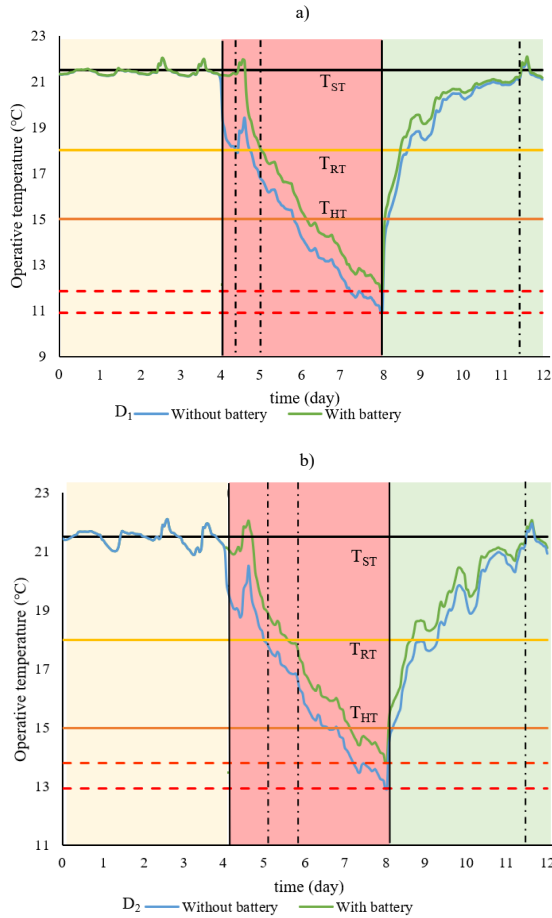
Figure 5.2: Multi-phase resilience curves for a)D_1 and b)D_2 with and without a battery.

the building design parameters, the impact of batteries as storage facilities on building resilience is considered for the two designs. For this purpose, the two competitive designs are equipped with batteries, the sizes of which are based on the cost-effective battery sizes, as explained in Chapter 4. The addition of the battery option results in four total designs for testing of the suggested metrics. Note that the developed metric is used for a single zone of the case-study building (living room). Figure 5.2 shows the multi-phase resilience curves for D_1, and D_2 with and without batteries.

The black dashed lines in Figure 5.2 show the RDs, which are reported in Table 5.2). D_2 has a longer RD in comparison to D_1 because of its stronger building envelope. In addition, the implementation of batteries for both cases

Table 5.2: Resilience metrics for D_1 and D_2 with batteries (WB) and without batteries (WOB).

Metric	D1		D2	
	WOB	WB	WOB	WB
RD (h)	9	24	23	38
CS (°C/h)	0.110	0.100	0.099	0.080
RS (°C/h)	0.120	0.115	0.102	0.086

increases the robustness of the building, and the building lasts for a longer time beyond the robustness margin. Based on Table 5.2, the battery implementation slows down the temperature reduction process. On the other hand, D_2 has a slower CS in comparison to D_1 because of higher U-values, which indicates a longer time to cool down the building. Therefore, a stronger envelope and the addition of a battery are effective design options for the building to better absorb and adapt to the impact of a power failure. A four-day power failure results in a 10.6 °C decrease from the setpoint temperature for D_1 without a battery and 9.6 °C with a battery. For D_2, the decrease is 8.6°C and 7.7°C, respectively, for the cases with and without the battery.

The time required for a design to return to the setpoint temperature is similar with and without the battery. Although the battery does not have a direct impact during Phase III, the AoE is smaller, and the RS is slower for both designs D_1 and D_2. Without batteries, the recovery time for D_2 is longer than that of D_1 because of the stronger building envelope in D_2, which means more time is needed to heat the building, and smaller AoE.

The combination of these two effects, make the recovery speed for D_2 slower than D_1. Finally, the EPL indicates how much of the performance is lost considering both impact intensity and duration of the power failure, as shown in Figure 5.3 for D_1 and D_2. The implementation of the battery decreases the EPL in both cases because the AoE is reduced and the temperature reduction process is delayed. Design D_2 has less performance loss than D_1, owing to its stronger envelope that can better absorb the impact of power failure.

The main issue with the current, developed metrics, which were adapted from power resilience, is that they quantify resilience on the scale of one thermal zone and cannot unfold resilience in the building level. Furthermore, most of these metrics focus on the evaluation of resilience in one of the phases of the event. For example, CS and RS only relate to Phases II and III of Figure 5.1, respectively. In addition, metrics such as EPL can yield the same levels of resilience for different combinations of performance
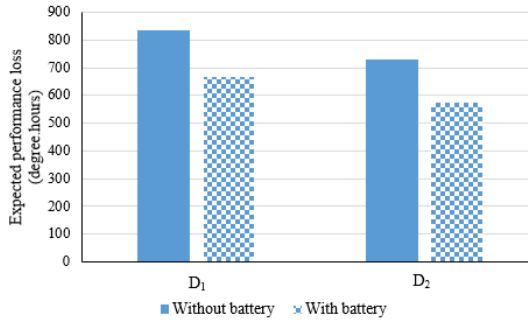
Figure 5.3: *EPL* for D_1 and D_2 with and without batteries.

and time. In other words, these kinds of metrics do not differentiate the impact intensity and duration of the disruptive event. Therefore, adapting the power resilience metrics to the building's thermal performance is enhanced with a new metric, the weighted unmet thermal performance (*WUMTP*), as explained in the following section.

5.4 Developed methodology for thermal resilience quantification

The *WUMTP* is a single metric that allows for the quantification of thermal resilience on the building scale, focusing on multiple phases of a disruptive event and considering the event's intensity and duration. For these purposes, changes are applied in the multi-phase resilience curve that we define in section 5.2. First, in the new multi-phase resilience curve, we assume that the phases occur between the start and end of the event, creating two phases for the disruptive event—Phase I during the disruptive event and Phase II after the disruptive event. In addition, the times before and after the disruptive event are referred to as the initial and final states, respectively. The phases and states are explained below:

- Initial state ($0 \leq t < t_0$): In the initial state, the building operates based on the setpoint temperature (which is considered the target) before the disruptive event. Based on the resilient building definition, the building is preparing for the disruptive event in this state.

- Phase I ($t_0 \leq t < t_1$): Phase I is between the initiation and the end of the disruptive event, during which the indoor operative temperature usually decreases continuously. Based on the definition of resilient building, the building absorbs the impact of and then adapts to the disruptive event in this phase.
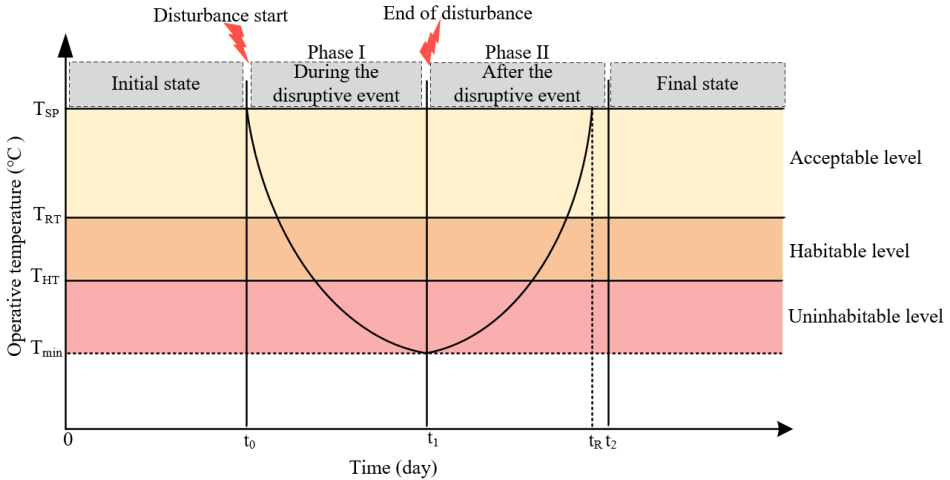
Figure 5.4: Illustration of a multi-phase thermal resilience curve of a building for the development of *WUMTP*.

- Phase II ($t_1 \leq t < t_2$): Phase II starts at the end of the disruptive event and lasts until the building reaches the same performance level as in the initial state. During this phase, the indoor operative temperature usually increases continuously. Based on the definition of the resilient building, the building recovers from the disruptive event in this phase.

- Final state ($t > t_2$): The final state begins after the building fully recovers. In this state, the building operates based on the setpoint temperature like in the initial state.

Based on the performance thresholds defined in Section 5.3, three performance levels are created. Building temperatures between T_{SP} and T_{RT} indicate an acceptable performance (acceptable level). Between T_{RT} and T_{HT}, the performance is at the habitable level, and any value less than T_{HT} indicates an uninhabitable level. Each level is shown with a different color in Figure 5.4.

To quantify building thermal resilience based on a multi-phase resilience curve, a test framework is introduced in the following subsection, establishing the requirements for thermal resilience quantification.

5.4.1 Resilience test framework

The developed test framework focuses on the evaluation of the effect of a fixed-duration disruptive event on the building performance, and three points are considered:

67

- We need to define when the disruptive event happens (t_0) and how long will it last ($t_1 - t_0$). In the suggested test framework, we assume a fixed-duration disruptive event.

- The thermal performance of the building after the disruptive event, i.e., during Phase II ($t_2 - t_1$), should be simulated to determine how the building can recover. For the suggested test framework, we assume Phase II lasts as long as Phase I to capture how the building recovers from the disruptive event.

- The range of performance levels should be specified when developing the test framework.

With the suggested test framework, the *WUMTP* measures the thermal resilience of the building with respect to changes in the building characteristics (including building envelope and systems) and the occupants of the building. The *WUMTP* focuses on the intensity and duration of the disruptive event, which can be different in each phase and each performance level. Therefore, the *WUMTP* is sensitive to deviations from the performance target in the various regions of the multi-phase resilience curve. The quality of performance deviation in the different regions can be differentiated with penalties based on the following factors, which indicate the scope of *WUMTP* quantification with respect to the event:

1. The phase of the event affects the *WUMTP*. The occupants' tolerations of the performance deviation during the disruptive event are more difficult in comparison to after the disturbance. This is a result of their possible mental states during each phase. In Phase I, the temperature continuously decreases while occupants face a pessimistic condition. In contrast, in Phase II, the temperature increases continuously, and occupants experience an optimistic situation, which is easier to bear. The application of the phase penalties yields different *WUMTP* calculations for each phase.

2. The hazard level of the event differs among the three different performance levels (acceptable, habitable, and uninhabitable). Thus, the calculation of *WUMTP* in each level relies on different hazard level penalties.

3. The exposure time to the event affects the *WUMTP*. Two sections—easy and difficult exposure—are possible for each phase and level, in which different exposure time penalties are applied.

5.4.2 *WUMTP* calculation

Penalties are defined for two phases, three performance levels, and two exposure times, totaling 12 segments, as shown in Figure 5.5. The lighter version
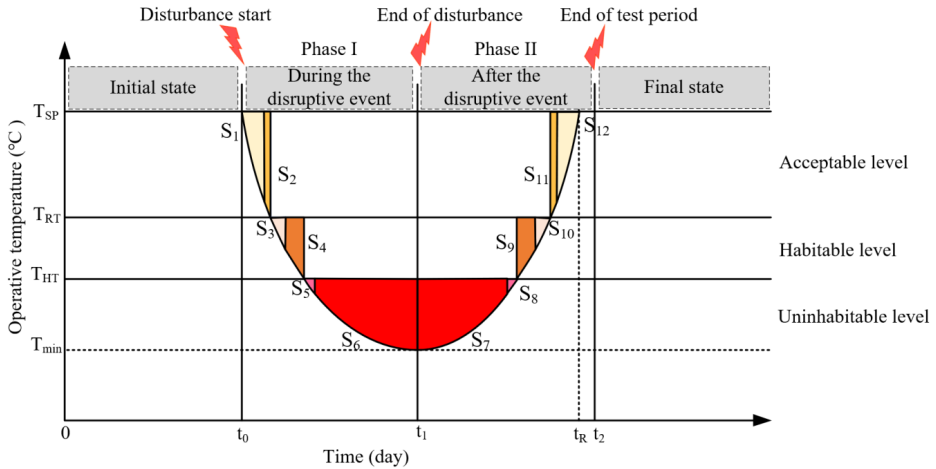
Figure 5.5: Illustration of the 12 segments in resilience test framework.

of each colors indicates the easy exposure sections, and the darker version colors shows the difficult exposure sections in each level. Three penalty types are considered for each segment: phase, hazard, and exposure-time penalties, as detailed in Table 5.3. The assigned values for each penalty are based on our logical assumptions. To the of best our knowledge, these penalties are not thoroughly discussed in the literature, and establishing a set of penalties still needs further attempts in the field of physiological research.

When defining the phase penalty, hazard level penalty, and exposure time penalty for each segment, the segment placement is critical. For example, a segment in Phase I receives a higher phase penalty in comparison to one in Phase II. Regarding hazard level penalty, a segment in an uninhabitable level is penalized more than a segment in the habitable level, which is penalized more in comparison to one in the acceptable level. The phase penalty is assigned as 0.6 for Phase I and 0.4 for Phase II. A hazard penalty of 0.1 is applied for an acceptable level and 0.2 and 0.7 for the habitable and uninhabitable levels, respectively.

The exposure time penalty is different for each section in each level. For comparable and informative results from the *WUMTP* calculation, note that the exposure time penalty is not on the same scale as the two other penalties. For example, in Phase I and the acceptable level, the assigned penalty for S_1 (easy exposure) is 2 and for S_2 (difficult exposure) is 8. The summation of exposure time penalties in each phase equals 100. The assigned penalties can be easily changed based on the priorities of each phase, hazard level, and exposure time.

Table 5.3: Associated penalties for different segments inside the resilience test framework.

Segment	Phase penalty (W_P)	Hazard penalty (W_H)	Exposure time penalty (W_E)
		Penalties	
S1	0.6	0.1	2
S2	0.6	0.1	8
S3	0.6	0.2	10
S4	0.6	0.2	20
S5	0.6	0.7	20
S6	0.6	0.7	40
S7	0.4	0.7	40
S8	0.4	0.7	20
S9	0.4	0.2	20
S10	0.4	0.2	10
S11	0.4	0.1	8
S12	0.4	0.1	2

Considering the specified penalties in Table 5.3 and the area of each segment resulting from the simulation-based test framework, the equation for *WUMTP* (Degree.hours) for a single zone is as follows:

$$WUMTP = \sum_{i=1}^{12} S_i W_{P,i} W_{H,i} W_{E,i} \qquad (5.1)$$

where i is the segments number and S_i is the area of segment i during the occupancy hours, which is calculated based on the hourly indoor operative temperature obtained in the BPS. The variables $W_{P,i}, W_{H,i}$, and $W_{E,i}$ represent the phase, hazard, and exposure-time penalties of the segment i, respectively. Within each segment, only occupied hours are considered in the calculation of the segment area. A building consists of various thermal zones, and different performance levels can be defined based on standards or the occupants' desires for each zone. The *WUMTP* accounts for these performance levels separately in each zone, but one overall metric is needed to evaluate the overall building. Based on the calculated *WUMTP* for each zone, the overall *WUMTP* (Degree.hours/m^2) of the building can be calculated based on the following equation:

$$WUMTP_{Overall} = \frac{\sum_{z=1}^{Z} A_z \times WUMTP_z}{\sum_{z=1}^{Z} A_z} \qquad (5.2)$$

where z is the building zone number, Z is the total number of zones in the building, and A_z is the area of each zone (m^2).
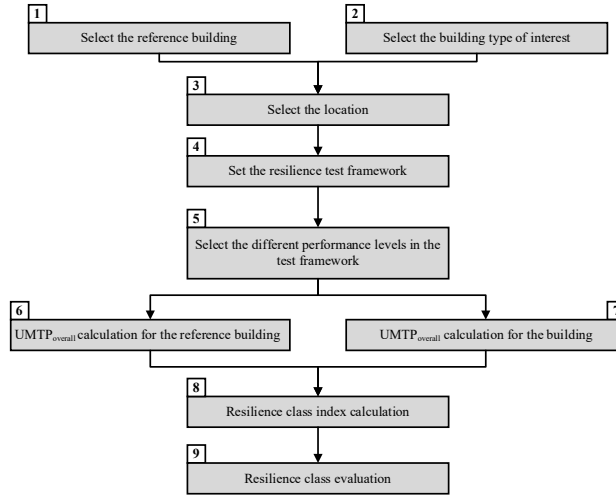
Figure 5.6: Steps of the resilience labeling methodology..

5.4.3 Resilience labeling

In this section, the *WUMTP*, as calculated in the previous section, is used to rate the building in a specific resilience class. A similar approach as the energy labelling is used (for more details, see Paper IV), as illustrated in Figure 5.6. The first step is to select one ideal reference building design based on the standards or regulations. The characteristics of this reference building regarding building envelope, systems, occupancy schedules, and internal load can be defined based on the recommendations from the country's standards. The second step is to select the building design to be rated for resilience. In the third step, the building's location is defined. Both the reference building and the building of interest should be in the same place. In step 4, both the reference building and the desired building are subjected to the same test framework, i.e., the same disruptive event. Step 5 involves the selection of the thermal performance levels for the different building zones. In steps 6 and 7, the $WUMTP_{overall}$ is calculated for both the reference and desired buildings. The $WUMTP_{overall}$ for the reference building is assumed to have a medium *WUMTP* level of class C. In step 8, the resilience class index (RCI) is determined by dividing the $WUMTP_{overall}$ of the reference building by the $WUMTP_{overall}$ of the desired building:

$$RCI = \frac{WUMTP_{overall,ref}}{WUMTP_{overall}} \qquad (5.3)$$

In step 9, the resilience class of the desired design is determined, as

71

Table 5.4: Resilience classes for building.

<3.6	RCI		Class A^+
<2.4	RCI	≤ 3.6	Class A
<1.5	RCI	≤ 2.4	Class B
<0.9	RCI	≤ 1.5	Class C
<0.6	RCI	≤ 0.9	Class E
	RCI	≤ 0.6	Class F

Table 5.5: Building element characteristics for the standard and passive designs.

	Standard design (TEK17 standard)	Passive design (Passive House standard)
U_{wall}[W/m^2.K]	0.19	0.12
U_{roof}[W/m^2.K]	0.13	0.09
U_{floor}[W/m^2.K]	0.1	0.08
U_{window}[W/m^2.K]	0.8	0.8
Thermal bridge[W/m^2.K]	0.07	0.03
Heat exchanger efficiency(%)	80	80
SFP ventilation [kW/m^3.s]	1.5	1.5
Air leakage 50 Pa [Airchange/hr]	0.6	0.6

presented in Table 5.4, where the subdivisions are multiples of 0.3. The range of class D is 0.3, but the ranges of classes C, B, and A increase to 0.6, 0.9, and 1.2, respectively. Therefore, improving from class B to A is more difficult than switching from class C to B.

5.5 Application of the *WUMTP* on a case-study building

The developed methodology for the quantification and labeling of the building's thermal resilience is tested on the same case-study building as described in Chapter 3. Two designs are considered for this case-study building to evaluate thermal resilience. First, the "standard design" in this work, is based on the conventional Norwegian building code from 2017 (TEK17) [92]. TEK17 is the current minimum energy requirement in Norway. The second design, called "passive design" in this work, is based on the Norwegian passive house standard NS3700 [135]. The building element characteristics for the TEK17 standard and passive house standard designs are shown in Table 5.5. The following points are considered in the establishment of the test framework for this case study.

- The building is all-electric, and the considered disruption is a power failure. The power failure starts on a day with high heating demand (January 14) and lasts for four full days. The duration of power failure is based on iterative simulations, which showed how long of a power failure would move a reference building (based on Norwegian standards) out of the habitability range.

- The same duration (four days) is used for the simulation of the building performance in Phase II.

- To gain a full perspective of building performance, the initial and final states are simulated for one day. This means that the building performance of the building is simulated for a total of ten days: one day in the initial state, four days during the power failure, four days after the power failure, and one day in the final state.

- The case-study building has three thermal zones, and the performance levels for these thermal zones are different. The first temperature threshold T_{SP} is selected based on [95]. The second performance threshold T_{RT} differentiates performance between robust and non-robust. Based on the recommendations of the World Health Organization (WHO) [133], 18°C is a safe and well-balancing temperature to protect the health of general populations during cold seasons in countries with temperate or cold climates. Therefore, 18°C is selected as T_{RT} for the living room zone, which creates a 3.5°C margin from the setpoint temperature for the robust performance in the living room. The same margin was applied to other zones. The last performance threshold T_{HT}, which differentiates between habitable and uninhabitable conditions for the occupant. A temperature of 15°C is selected as the habitability threshold for the living room based on a comprehensive review on the effect of low temperatures on elderly morbidity [134], resulting in a 3°C margin from the robustness threshold for the habitable performance in the living room. The same margin was applied to other zones. These assumptions lead to the values reported in Table 5.6. It has been decided to evaluate the thermal resilience in all of the thermal zones inside the building, in order to evaluate the resilience of building as an asset with less focus on how it is going to be implemented. It is obvious that in the critical condition facing a disruptive event back-up facilities can be implemented to heat essential rooms to save energy and keep the room warm enough for a longer period.

- The literature shows that exposure of one to two hours to low temperatures, such as 10°C [136], 11°C [137], and 12 °C [138] (all of which are in uninhabitable levels), has a significant impact on human health [139]. Therefore, the easy exposure section in the uninhabitable level is assumed to last for one hour, and the rest form the difficult exposure section. For the habitable and acceptable levels, the duration of the easy exposure sections are increased to two and three hours, respectively.

With these assumptions for the case-study building, the multi-phase resilience curve in the living room zone for the two designs are as follows:

Table 5.6: Three performance thresholds for different zones of the case-study building.

| | Zones | | |
Performance level	Living room	Bedroom	Bathroom
T_{SP} (°C)	21.5	18	23
T_{RT} (°C)	18	14.5	19.5
T_{HT} (°C)	15	11.5	16.5
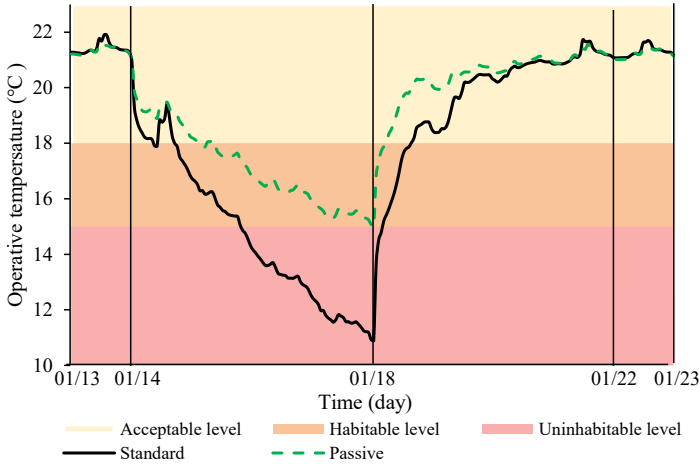
Figure 5.7: Comparison of multi-phase resilience curve for the standard and passive designs.

Figure 5.7 shows that the building envelope upgrade clearly has a huge impact on the resilience curve and consequently on the *WUMTP* calculation and resilience class evaluation. The multi-phase resilience curve of the standard design shows that this design experiences the uninhabitable level in the case of a four-day power failure. In contrast, the passive house design does not experience the uninhabitable level in the power failure in Oslo. The minimum temperatures in the living room for the standard and passive designs are approximately 11°C and 15°C, respectively. Despite this difference, the recovery times (the time to reach the setpoint temperature after the power failure) are approximately the same for both cases. This means that the recovery speed for passive design is slower than that of the standard design.

The $WUMTP_{overall}$ metric is calculated for the two building designs. This metric is multi-zone, and three different thermal zones were in the case-study building. Therefore, the suggested performance levels in Table

5.6 are used for the calculation, as reported in Table 5.7 for the two designs. The upgrade of the standard design to the passive design decreased the $WUMTP_{overall}$ by 80 degree-hours, a 71% reduction. Therefore, in the case of power failure during the cold winter, the passive design performs more closely to the targets compared to the standard design.

In this work, the suggested test framework and calculation of $WUMTP$ focuses on a cold event during winter. Hence, the $WUMTP$ during summer was not evaluated here and is out of the scope of the considered test framework. However, the event type can be changed to a hot event, such as a heatwave, but the framework needs specific adjustment accordingly. Although the passive design has a lower $WUMTP_{overall}$ than the standard design against a cold event, the situation may be different when a hot event is implemented in the test framework.

The lower $WUMTP_{overall}$ of the passive design in the current test framework is expected regarding the performance of standard and passive designs, as shown in the other works [37]. It should be noted that $WUMTP_{overall}$ benefits temperature as a performance indicator in this work and in consequence the resiliency is being evaluated with respect to thermal performance. This may not lead to resiliency with respect to other performance criteria and if needed resiliency should be evaluated with respect to those criteria separately. This may not lead to the resiliency with respect to other performance criteria and resiliency need to be evaluated with respect to those criteria separately. However, the developed test framework and calculation of $WUMTP$ can help designers and decision-makers compare different designs and enhancement strategies, such as the addition of battery storage or PV systems.

In resilience labeling, the design based on TEK 17 standard (standard design) [92], which is the minimum requirement in Norway, is used as the reference. The simulation of this design is conducted under the recommendations of NS3031 standard [93] with respect to the internal loads and other parameters. The RCI for the standard design is one, and its resilience is placed in class C. The RCI of other designs is calculated by dividing the $WUMTP_{overall}$ of the reference design by that of the other designs. The same building with the passive standards by itself is in resilience class A. Therefore, if the standard design is upgraded to the passive design without any other improvements, the resilience level improves by two levels (from class C to A). The thermal resilience and resilience class are considered for other designs with the resilience enhancement strategies and discussed in detail in Paper IV.

Despite its scientific approach, the developed methodology can be easily used by different stakeholders involved in real projects, such as building

Table 5.7: Calculated $WUMTP_{overall}$ for the two designs of the case-study building.

Num	Design	$WUMTP_{overall}$ (Degree.hours)
1	Standard	113
2	Passive	33

designers, engineers, decision-makers, and even building occupants. These resilience quantification and labeling methods can be effective for building designers and decision-makers to design resilient buildings to be prepared for, absorb the impact of, adapt to, and recover from disruptive events. The incorporation of thermal resilience labels in the design, planning, and operation phases of existing and new buildings and the addition of labels in energy performance certificates (EPCs) can be valuable. This information can provide a better understanding of the building performance under disruptive events and facilitate a design selection that not only performs well under design conditions but also withstands upcoming uncertainties.

CHAPTER 6

Conclusion And Future Work

Buildings do not behave with static performance during their operational phases, and their performances vary with changes in internal or external conditions. Dealing with these changes is challenging, but setting resilient solutions helps protect building performance against changes and uncertainties. The concept of resilience is not new, and it is widely applied in different fields. However, for building design, resilience needs to be clearly defined, and commonly agreed frameworks are required for its evaluation.

The work presented in this thesis spans the entire development of an evaluation approach of building resilience, starting with the definition of building resilience and identification of some of the resilience attributes in the context of building performance and ending with the quantification of resilience and its attributes. On a meta-level, this work attempts to protect building performance against upcoming changes (uncertainties). The innovative impacts of the thesis are summarized in the next section.

6.1   Innovative impacts

The main outputs of this thesis are the definitions of resilience (Chapter 2) and metrics for the assessment of resilience and its attributes in the context of building performance (Chapters 3, 4, and 5). These metrics were developed in the four primary papers and used in collaboration with other researchers in the supporting papers.

To obtain these outputs, the thesis first adapts the existing definitions of resilience into the context of building performance by posing four questions, which are focusing on resilience of what? resilience to what? resilience in what state? resilience based on what? The answers to these questions cover RQ1. It is defined that a building is resilient if able to prepare for, absorb, adapt to, and recover from the disruptive event. In addition to the primary papers, the efforts that have been done regarding the resilient building defini-

tion in this work created a collaboration opportunity with "IEA EBC Annex 80 Resilient Cooling of Buildings," which develops, assesses, and communicates solutions of resilient cooling and overheating protection. The result of this collaboration was published in a journal paper entitled "Resilient cooling of buildings to protect against heat waves and power outages: Key concepts and definition," which is listed as the first supporting paper of this thesis.

In the second step, the uncertainties, changes, and disruptive events that influence building performance during the operational phase are identified and categorized based on a literature review, addressing RQ2.

After defining the concept of resilience in the context of building performance and identifying possible changes that can influence building performance, different resilience attributes that correspond to buildings are identified from the literature. Each attribute can impact building resilience with specific abilities of a resilient building. Among these attributes, building robustness and flexibility are studied in more detail. Robustness and flexibility improve building resilience by providing absorption and recovery abilities. The evaluation of the resilience attributes and their relationships with the abilities of the resilient building addresses the RQ3.

Finally, methodologies are proposed for the quantification of resilience and its two attributes (i.e., robustness and flexibility). These methodologies yield additional metrics that cover the performance gaps related to existing quantification metrics in the literature. This step answers RQ4. These quantification methodologies are summarized as follows:

- The suggested methodology for robustness assessment involves the selection of a high-performance and robust building design with a focus on two performance perspectives. The proposed generic approach can be implemented for case studies of various backgrounds. In this thesis, a two-criteria (energy and comfort) robust design problem is assessed, but the methodology can be extended to address more than two criteria, as shown in collaboration with SINTEF, an independent research organization in Norway. A result of this collaboration is a journal paper submitted to the journal *Energies*, entitled, "Assessing responsive building envelope designs through robustness-based multi-criteria decision making in zero-emission buildings." and listed as the third supporting paper of his thesis. In this paper, the developed methodology for the robustness assessment was tested for a real case-study building, assessing three performance criteria: energy demand, thermal comfort, and energy flexibility. The case-study building was the Zero Emission Building Laboratory (ZEB-lab) office building located on the NTNU university campus in Trondheim, Norway.

- The suggested methodology for the flexibility assessment focuses on

sizing cost-effective batteries, which act as flexibility assets when they store the shifted heat in response to dynamic pricing tariffs (as a DR strategy). Furthermore, the methodology explores the trade-off between energy flexibility and survivability of all-electric buildings, which is identified as a research gap.

- A methodology is suggested for the quantification of the thermal resilience of buildings and labeling of buildings regarding resilience level. The thermal resilience quantification is based on a single metric, WUMTP, which calculates the deviations from the thermal targets for the whole building and penalizes them based on three factors: the phase, hazard level, and the exposure time of the event. The developed methodology gained interest from VTT (Technical Research Centre of Finland), and the candidate's research group will collaborate with VTT in continuing this research.

The innovative contribution of the developed methodologies along with their potential users (or future collaborators) and the results of the collaboration are shown in Figure 6.1.

6.2 Limitations and future discovery

Defining resilience and the abilities and attributes of a resilient building is a significant step toward the design of resilient buildings to decrease the impact of changes and uncertainties on building performance. The developed methodologies for the quantification of resilience and its attributes can help benchmark the resilience level of different building designs and technologies. However, these methodologies have limitations that should be mentioned:

Regarding the relationship between resilience and its attributes This work attempts to qualitatively identify the effect of each attribute on the abilities of the resilient building. Furthermore, Chapter 4 identifies the trade-offs between flexibility and resilience. The trade-off has been evaluated for different building designs and the best design is found to be dependent on the preference of the decision-makers with respect to flexibility and resilience.

Clearly, the quantitative relationships between resilience attributes and resilience itself are challenging to define and can be considered as a limitation of this work. Therefore, the resilience attributes and their influences on resilience should be studied in more detail in future works.

Regarding the scale of the work All the assessments in this work focus on the building scale. However, in the real world, buildings interact with each other and the connected grid. Therefore, the evaluation of resilience and other attributes on larger scales, such

Category	Innovative contribution	Potential user/ Future collaborator	Results
Resilience definition	• Introducing a claer defintion of resilient buildings by structuring it with four main question.	IEA EBC Annex 80 Resilient Cooling of Buildings	First supporting paper "Resilient cooling of buildings to protect against heat waves and power outages: Key concepts and definition" Published in the Journal of Energy and Building
Robustness assessment	• Development of a computational approach for selecting high performance and robust design, • Integration of multi-target robustness assessment into a multi-criteria decision making (MCDM), • Possibility of comparing design alternatives not only to each other but also to the performance target, • Automatic establishment of criteria preferences in the decision making process, • Removing the need for repeating robustness assessment.	SINTEF Community (an independent research organization with a close collaboration with NTNU)	Third supporting paper "Assessing responsive building envelope designs through robustness-based multicriteria decision making in zero-emission buildings and neighbourhoods" Submitted to the journal of Energy and Building
Flexibility assessment	• Formulation of a model to determine the cost-effective battery size needed for storing the shifted load, • Introduction of the concept of "active survivability" • Introduction of new flexibility and survivability indexes, • Exploreing the trade-off between the energy flexibility and survivability.	-	-
Resilience assessment	• Quantification of the thermal resilience of buildings, • Labelling of thermal resilience, • Developing a multi-zone metric for thermal resilience quantification, • Developing a multi-phase metric for thermal resilience quantification, • Sensitivity of the metric to the phase of the event, hazard level of the event, and exposure time of the event.	VTT (Technical Research Centre of Finland)	Based on the received interest from VTT, a future collaboration will be done in order to continue the work on the resilience quantification.

Figure 6.1: Innovative contributions of the developed methodologies in the thesis along with the potential users.

as neighborhoods and communities, is of interest. Other useful parameters may contribute to the resilience of buildings. For example, the application of central storage systems on larger scales, such as community storage, and their management can have a different impact than a single storage system applied in a single building.

Regarding the adaptability of the developed metrics for other events

The developed methodology for resilience quantification is a generic approach that can be used to assess building performance resilience. In this work, the methodology is applied to evaluate performance resilience from thermal and energy perspectives. However, other performance criteria such as the hydrothermal performance of the building is not considered but is a significant contributor to overall building performance. In addition, the developed methodology for thermal resilience quantification focuses on the quantification of the thermal resilience of residential buildings during cold seasons. While it can be implemented for thermal resilience quantification, wherever that there is a need for heating during cold seasons, but when it comes to evaluation of thermal resilience during the hot season requires an adjusted methodology. The evaluation of thermal resilience during hot and humid weather is an example. Therefore, future work can focus on the application of the developed methodology for the cooling season (summer) by adapting factors, including the performance indicator, temperature thresholds, and penalties. For example, this methodology only considers temperature in the evaluation of thermal resilience, while other factors, such as humidity, can also influence thermal resilience evaluation, demanding further research.

Bibliography

[1] R. Kotireddy, R. Loonen, P.-J. Hoes, J. L. Hensen, Building performance robustness assessment: Comparative study and demonstration using scenario analysis, Energy and Buildings 202 (2019) 109362.

[2] A.-T. Nguyen, S. Reiter, P. Rigo, A review on simulation-based optimization methods applied to building performance analysis, Applied Energy 113 (2014) 1043–1058.

[3] G. Eleftheriadis, M. Hamdy, Impact of building envelope and mechanical component degradation on the whole building performance: a review paper, Energy Procedia 132 (2017) 321–326.

[4] P. De Wilde, D. Coley, The implications of a changing climate for buildings (2012).

[5] D. Ramon, Towards future-proof buildings in belgium: Climate and life cycle modelling for climate robust office buildings (2021).

[6] D. Yan, W. O'Brien, T. Hong, X. Feng, H. B. Gunay, F. Tahmasebi, A. Mahdavi, Occupant behavior modeling for building performance simulation: Current state and future challenges, Energy and Buildings 107 (2015) 264–278.

[7] H. Li, N. Nord, Transition to the 4th generation district heating-possibilities, bottlenecks, and challenges, Energy Procedia 149 (2018) 483–498.

[8] S. Cao, The impact of electric vehicles and mobile boundary expansions on the realization of zero-emission office buildings, Applied Energy 251 (2019) 113347.

[9] K. Steinhaeuser, A. R. Ganguly, N. V. Chawla, Multivariate and multiscale dependence in the global climate system revealed through complex networks, Climate dynamics 39 (3-4) (2012) 889–895.

[10] A. Moazami, S. Carlucci, S. Geving, Robust and resilient buildings: A framework for defining the protection against climate uncertainty, in: IOP Conference Series: Materials Science and Engineering, Vol. 609, IOP Publishing, 2019, p. 072068.

[11]   S. Roostaie, N. Nawari, C. Kibert, Sustainability and resilience: A review of definitions, relationships, and their integration into a combined building assessment framework, Building and Environment 154 (2019) 132–144.

[12]   S. Hosseini, K. Barker, J. E. Ramirez-Marquez, A review of definitions and measures of system resilience, Reliability Engineering & System Safety 145 (2016) 47–61.

[13]   P. de Wilde, Ten questions concerning building performance analysis, Building and Environment 153 (2019) 110–117.

[14]   I. P. on Climate Change, Technical summary ipcc sr1.5 (2018).

[15]   USGCRP, Our changing planet: The u.s. global change research program for fiscal year 2020.
URL   https://www.globalchange.gov/browse/reports/our-changing-planet-fy-2020

[16]   C. C. C. S. C3S, C3s releases european state of the climate to reveal how 2019 compares to previous years.
URL   https://climate.copernicus.eu/c3s-releases-european-state-climate-reveal-how-2019-compares\-previous-years

[17]   M. Panteli, P. Mancarella, Modeling and evaluating the resilience of critical electrical power infrastructure to extreme weather events, IEEE Systems Journal 11 (3) (2015) 1733–1742.

[18]   The texas tribune.
URL   https://www.texastribune.org/series/winter-storm-power-outage/

[19]   F. H. Jufri, V. Widiputra, J. Jung, State-of-the-art review on power grid resilience to extreme weather events: Definitions, frameworks, quantitative assessment methodologies, and enhancement strategies, Applied energy 239 (2019) 1049–1065.

[20]   A. Sharifi, Y. Yamagata, Principles and criteria for assessing urban energy resilience: A literature review, Renewable and Sustainable Energy Reviews 60 (2016) 1654–1677.

[21]   T. Salgueiro, F. Erkip, Retail planning and urban resilience-an introduction to the special issue, Cities 36 (2014) 107–111.

[22] M. Abdulkareem, H. Elkadi, From engineering to evolutionary, an over-arching approach in identifying the resilience of urban design to flood, International journal of disaster risk reduction 28 (2018) 176–190.

[23] S. Davoudi, K. Shaw, L. J. Haider, A. E. Quinlan, G. D. Peterson, C. Wilkinson, H. Fünfgeld, D. McEvoy, L. Porter, S. Davoudi, Resilience: a bridging concept or a dead end?"reframing" resilience, Planning theory & practice 13 (2) (2012) 299–333.

[24] N. L. Engle, A. de Bremond, E. L. Malone, R. H. Moss, Towards a resilience indicator framework for making climate-change adaptation decisions, Mitigation and Adaptation Strategies for Global Change 19 (8) (2014) 1295–1312.

[25] S. C. Shandiz, G. Foliente, B. Rismanchi, A. Wachtel, R. F. Jeffers, Resilience framework and metrics for energy master planning of communities, Energy (2020) 117856.

[26] J. Carlson, R. Haffenden, G. Bassett, W. Buehring, M. Collins III, S. Folga, F. Petit, J. Phillips, D. Verner, R. Whitfield, Resilience: Theory and application., Tech. rep., Argonne National Lab.(ANL), Argonne, IL (United States) (2012).

[27] V. M. Nik, A. Perera, D. Chen, Towards climate resilient urban energy systems: a review, National Science Review (2020).

[28] S. Meerow, J. P. Newell, M. Stults, Defining urban resilience: A review, Landscape and urban planning 147 (2016) 38–49.

[29] S. Attia, R. Levinson, E. Ndongo, P. Holzer, O. B. Kazanci, S. Homaei, C. Zhang, B. W. Olesen, D. Qi, M. Hamdy, et al., Resilient cooling of buildings to protect against heat waves and power outages: Key concepts and definition, Energy and Buildings 239 (2021) 110869.

[30] M. Bruneau, S. E. Chang, R. T. Eguchi, G. C. Lee, T. D. O'Rourke, A. M. Reinhorn, M. Shinozuka, K. Tierney, W. A. Wallace, D. Von Winterfeldt, A framework to quantitatively assess and enhance the seismic resilience of communities, Earthquake spectra 19 (4) (2003) 733–752.

[31] Y. Alfraidi, A. H. Boussabaine, Design resilient building strategies in face of climate change, Int. J. Civ. Environ. Struct. Constr. Archit. Eng 9 (2015) 23–28.

[32] R. Below, A. Wirtz, D. Guha-Sapir, Disaster category classification and peril terminology for operational purposes, Tech. rep. (2009).

[33] P. Li, S. Chan, Application of a weather stress index for alerting the public to stressful weather in hong kong, Meteorological Applications 7 (4) (2000) 369–375.

[34] K. J. Lomas, Y. Ji, Resilience of naturally ventilated buildings to climate change: Advanced natural ventilation and hospital wards, Energy and buildings 41 (6) (2009) 629–653.

[35] K. J. Lomas, R. Giridharan, Thermal comfort standards, measured internal temperatures and thermal resilience to climate change of free-running buildings: A case-study of hospital wards, Building and Environment 55 (2012) 57–72.

[36] B. E. Tokgoz, A. V. Gheorghe, Resilience quantification and its application to a residential building subject to hurricane winds, International Journal of Disaster Risk Science 4 (3) (2013) 105–114.

[37] W. O'Brien, I. Bennet, Simulation-based evaluation of high-rise residential building thermal resilience., ASHRAE Transactions 122 (1) (2016).

[38] M. Hamdy, K. Sirén, S. Attia, Impact of financial assumptions on the cost optimality towards nearly zero energy buildings–a case study, Energy and Buildings 153 (2017) 421–438.

[39] P. Lassandro, S. Di Turi, Energy efficiency and resilience against increasing temperatures in summer: the use of pcm and cool materials in buildings, International journal of heat and technology 35 (S1) (2017) S307–15.

[40] A. Baniassadi, D. J. Sailor, Synergies and trade-offs between energy efficiency and resiliency to extreme heat–a case study, Building and Environment 132 (2018) 263–272.

[41] A. Baniassadi, D. J. Sailor, H. J. Bryan, Effectiveness of phase change materials for improving the resiliency of residential buildings to extreme thermal conditions, Solar Energy 188 (2019) 190–199.

[42] A. Katal, M. Mortezazadeh, L. L. Wang, Modeling building resilience against extreme weather by integrated cityffd and citybem simulations, Applied Energy 250 (2019) 1402–1417.

[43] E. Rosales-Asensio, M. de Simón-Martín, D. Borge-Diez, J. J. Blanes-Peiró, A. Colmenar-Santos, Microgrids with energy storage systems as a means to increase power resilience: An application to office buildings, Energy 172 (2019) 1005–1015.

[44] K. Sun, M. Specian, T. Hong, Nexus of thermal resilience and energy efficiency in buildings: A case study of a nursing home, Building and Environment 177 (2020) 106842.

[45] H. Mehrjerdi, M. Saad, S. Lefebvre, Efficiency-resilience nexus in building energy management under disruptions and events, IEEE Systems Journal (2020).

[46] S. Flores-Larsen, C. Filippín, Energy efficiency, thermal resilience, and health during extreme heat events in low-income housing in argentina, Energy and Buildings 231 (2021) 110576.

[47] J. Liu, L. Jian, W. Wang, Z. Qiu, J. Zhang, P. Dastbaz, The role of energy storage systems in resilience enhancement of health care centers with critical loads, Journal of Energy Storage 33 (2021) 102086.

[48] A. O'Donovan, M. D. Murphy, P. D. O'Sullivan, Passive control strategies for cooling a non-residential nearly zero energy office: Simulated comfort resilience now and in the future, Energy and Buildings 231 (2021) 110607.

[49] H. Mehrjerdi, Resilience-robustness improvement by adaptable operating pattern for electric vehicles in complementary solar-vehicle management, Journal of Energy Storage 37 (2021) 102454.

[50] M.-W. Tian, P. Talebizadehsardari, Energy cost and efficiency analysis of building resilience against power outage by shared parking station for electric vehicles and demand response program, Energy 215 (2021) 119058.

[51] C. Schünemann, D. Schiela, R. Ortlepp, How window ventilation behaviour affects the heat resilience in multi-residential buildings, Building and Environment (2021) 107987.

[52] V. Todeschi, K. Javanroodi, R. Castello, N. Mohajer, G. Mutani, J.-L. Scartezzini, Impact of the covid-19 pandemic on the energy performance of residential neighborhoods and their occupancy behavior, Sustainable Cities and Society (2022) 103896.

[53] A. Machard, C. Inard, J.-M. Alessandrini, C. Pelé, J. Ribéron, A methodology for assembling future weather files including heatwaves for building thermal simulations from the european coordinated regional downscaling experiment (euro-cordex) climate data, Energies 13 (13) (2020) 3424.

[54] E. Hossain, S. Roy, N. Mohammad, N. Nawar, D. R. Dipta, Metrics and enhancement strategies for grid resilience and reliability during natural disasters, Applied Energy 290 (2021) 116709.

[55] M. Panteli, P. Mancarella, D. N. Trakas, E. Kyriakides, N. D. Hatziargyriou, Metrics and quantification of operational and infrastructure resilience in power systems, IEEE Transactions on Power Systems 32 (6) (2017) 4732–4742.

[56] O. Ladipo, G. Reichard, A. McCoy, A. Pearce, P. Knox, M. Flint, Attributes and metrics for comparative quantification of disaster resilience across diverse performance mandates and standards of building, Journal of Building Engineering 21 (2019) 446–454.

[57] P. Trimintzios, Measurement frameworks and metrics for resilient networks and services: technical report, Eur. Netw. Inf. Secur. Agency (2011) 109.

[58] C. W. Zobel, Representing perceived tradeoffs in defining disaster resilience, Decision Support Systems 50 (2) (2011) 394–403.

[59] J. Liu, L. Jian, W. Wang, Z. Qiu, J. Zhang, P. Dastbaz, The role of energy storage systems in resilience enhancement of health care centers with critical loads, Journal of Energy Storage (2020) 102086.

[60] E. Burman, J. Kimpian, D. Mumovic, Reconciling resilience and sustainability in overheating and energy performance assessments of non-domestic buildings, Centre for Urban Sustainability and Resilience, UCL (University College London), 2014.

[61] R. Gupta, A. Bruce-Konuah, A. Howard, Achieving energy resilience through smart storage of solar electricity at dwelling and community level, Energy and buildings 195 (2019) 1–15.

[62] H. Mehrjerdi, Resilience oriented vehicle-to-home operation based on battery swapping mechanism, Energy 218 (2021) 119528.

[63] S. Flores-Larsen, C. Filippín, Energy efficiency, thermal resilience, and health during extreme heat events in low-income housing in argentina, Energy and Buildings 231 110576.

[64] A. H. Wiberg, L. Georges, T. H. Dokka, M. Haase, B. Time, A. G. Lien, S. Mellegård, M. Maltha, A net zero emission concept analysis of a single-family house, Energy and buildings 74 (2014) 101–110.

[65] P. Tuohy, Regulations and robust low-carbon buildings, Building Research & Information 37 (4) (2009) 433–445.

[66] P. De Wilde, The gap between predicted and measured energy performance of buildings: A framework for investigation, Automation in construction 41 (2014) 40–49.

[67] R. C. Loonen, F. Favoino, J. L. Hensen, M. Overend, Review of current status, requirements and opportunities for building performance simulation of adaptive facades, Journal of Building Performance Simulation 10 (2) (2017) 205–223.

[68] H. Tang, S. Wang, H. Li, Flexibility categorization, sources, capabilities and technologies for energy-flexible and grid-responsive buildings: State-of-the-art and future perspective, Energy (2020) 119598.

[69] R. G. Junker, A. G. Azar, R. A. Lopes, K. B. Lindberg, G. Reynders, R. Relan, H. Madsen, Characterizing the energy flexibility of buildings and districts, Applied energy 225 (2018) 175–182.

[70] Equa solutions ab ida indoor climate and energy (version 4.8).
URL https://www.equa.se/en/ida-ice.

[71] R. Kotireddy, P.-J. Hoes, J. L. Hensen, A methodology for performance robustness assessment of low-energy buildings using scenario analysis, Applied energy 212 (2018) 428–442.

[72] B. P. Jelle, E. Sveipe, E. Wegger, A. Gustavsen, S. Grynning, J. V. Thue, B. Time, K. R. Lisø, Robustness classification of materials, assemblies and buildings, Journal of Building Physics 37 (3) (2014) 213–245.

[73] L. Van Gelder, H. Janssen, S. Roels, Probabilistic design and analysis of building performances: Methodology and application example, Energy and Buildings 79 (2014) 202–211.

[74] P. Hoes, M. Trcka, J. Hensen, B. H. Bonnema, Optimizing building designs using a robustness indicator with respect to user behavior, in: Building simulation proceedings of the 12th conference of the international building performance simulation association, 2011, pp. 1710–1717.

[75] C. Struck, J. Hensen, Scenario analysis for the robustness assessment of building design alternatives–a dutch case study, Proceedings of CISBAT 2013 (2013) 939–944.

[76] R. H. Moss, J. A. Edmonds, K. A. Hibbard, M. R. Manning, S. K. Rose, D. P. Van Vuuren, T. R. Carter, S. Emori, M. Kainuma, T. Kram,

et al., The next generation of scenarios for climate change research and assessment, Nature 463 (7282) (2010) 747–756.

[77] C. J. Hopfe, G. L. Augenbroe, J. L. Hensen, Multi-criteria decision making under uncertainty in building performance assessment, Building and environment 69 (2013) 81–90.

[78] T. L. Saaty, Multicriteria decision making: The analytic hierarchy process: Planning, priority setting, Resource Allocation 2 (1990) 1–20.

[79] C.-M. Chiang, C.-M. Lai, A study on the comprehensive indicator of indoor environment assessment for occupants' health in taiwan, Building and Environment 37 (4) (2002) 387–392.

[80] S. H. Kim, G. Augenbroe, Decision support for choosing ventilation operation strategy in hospital isolation rooms: A multi-criterion assessment under uncertainty, Building and environment 60 (2013) 305–318.

[81] S.-S. Kim, I.-H. Yang, M.-S. Yeo, K.-W. Kim, Development of a housing performance evaluation model for multi-family residential buildings in korea, Building and environment 40 (8) (2005) 1103–1116.

[82] F. Omar, S. T. Bushby, R. D. Williams, Assessing the performance of residential energy management control algorithms: Multi-criteria decision making using the analytical hierarchy process, Energy and Buildings 199 (2019) 537–546.

[83] M. K. Rathod, H. V. Kanzaria, A methodological concept for phase change material selection based on multiple criteria decision analysis with and without fuzzy environment, Materials & Design 32 (6) (2011) 3578–3585.

[84] M. Velasquez, P. T. Hester, An analysis of multi-criteria decision making methods, International journal of operations research 10 (2) (2013) 56–66.

[85] A. Booth, R. Choudhary, Decision making under uncertainty in the retrofit analysis of the uk housing stock: Implications for the green deal, Energy and Buildings 64 (2013) 292–308.

[86] D. D'Agostino, D. Parker, P. Melia, Environmental and economic implications of energy efficiency in new residential buildings: A multi-criteria selection approach, Energy Strategy Reviews 26 (2019) 100412.

[87] E. Nikolaidou, J. Wright, C. Hopfe, Robust building scheme design optimization for uncertain performance prediction (2017).

[88] K. Mela, T. Tiainen, M. Heinisuo, Comparative study of multiple criteria decision making methods for building design, Advanced engineering informatics 26 (4) (2012) 716–726.

[89] L. C. Felius, M. Thalfeldt, L. Georges, B. D. Hrynyszyn, F. Dessen, M. Hamdy, Wood burning habits and its effect on the electrical energy demand of a retrofitted norwegian detached house, in: IOP Conference Series: Earth and Environmental Science, Vol. 352, IOP Publishing, 2019, p. 012022.

[90] A. Rysanek, R. Choudhary, Optimum building energy retrofits under technical and economic uncertainty, Energy and Buildings 57 (2013) 324–337.

[91] R. Kotireddy, P.-J. Hoes, J. L. Hensen, Integrating robustness indicators into multi-objective optimization to find robust optimal low-energy building designs, Journal of Building Performance Simulation 12 (5) (2019) 546–565.

[92] Byggteknisk forskrift (tek 17)., `https://dibk.no/byggereglene/byggteknisk-forskrift-tek17/14/14-2/` (2020).

[93] Standardnorge(2016)sn/ts3031:2016 calculation of energy needs and energy supply.
URL `https://www.standard.no/nyheter/nyhetsarkiv/bygg-anlegg-og-eiendom/2016/snts-30312016-for-beregning-av-energibehov-og-energiforsyning/`

[94] S. Polasky, S. R. Carpenter, C. Folke, B. Keeler, Decision-making under great uncertainty: environmental management in an era of global change, Trends in ecology & evolution 26 (8) (2011) 398–404.

[95] I. S. Øystein Rønneseth, Method for modelling norwegian single-family house in ida ice (2018).

[96] Iee project tabula (2009 - 2012), `https://episcope.eu/iee-project/tabula/`.

[97] Validation of ida indoor climate and energy 4.0 build 4 with respect to ansi/ashrae standard 140-2004, Tech. rep., Equa Simulation AB (2010).

[98] N. Nord, L. H. Qvistgaard, G. Cao, Identifying key design parameters of the integrated energy system for a residential zero emission building in norway, Renewable Energy 87 (2016) 1076–1087.

[99] H. M. D. Bente Halvorsen, Ta hjemmetempen (2012).

[100] L. Peeters, R. De Dear, J. Hensen, W. D'haeseleer, Thermal comfort in residential buildings: Comfort values and scales for building energy simulation, Applied energy 86 (5) (2009) 772–780.

[101] R. Kotireddy, Towards robust low-energy houses: a computational approach for performance robustness assessment using scenario analysis (2018).

[102] V. M. Nik, E. Mata, A. S. Kalagasidis, Assessing the efficiency and robustness of the retrofitted building envelope against climate change, Energy Procedia 78 (2015) 955–960.

[103] R. Kotireddy, P. Hoes, J. L. Hensen, Simulation-based comparison of robustness assessment methods to identify robust low energy building designs, in: Proceedings of 15th IBPSA conference, SanFrancisco, CA, USA, International Building Performance Simulation Association (IBPSA), 2017, pp. 892–901.

[104] J. Clauß, S. Stinner, I. Sartori, L. Georges, Predictive rule-based control to activate the energy flexibility of norwegian residential buildings: Case of an air-source heat pump and direct electric heating, Applied Energy 237 (2019) 500 – 518. `doi:https://doi.org/10.1016/j.apenergy.2018.12.074`.

[105] R. G. Junker, A. G. Azar, R. A. Lopes, K. B. Lindberg, G. Reynders, R. Relan, H. Madsen, Characterizing the energy flexibility of buildings and districts, Applied Energy 225 (2018) 175 – 182. `doi:https://doi.org/10.1016/j.apenergy.2018.05.037`.

[106] J. Niu, Z. Tian, Y. Lu, H. Zhao, Flexible dispatch of a building energy system using building thermal storage and battery energy storage, Applied Energy 243 (2019) 274 – 287. `doi:https://doi.org/10.1016/j.apenergy.2019.03.187`.

[107] K. Foteinaki, R. Li, A. Heller, C. Rode, Heating system energy flexibility of low-energy residential buildings, Energy and Buildings 180 (2018) 95 – 108. `doi:https://doi.org/10.1016/j.enbuild.2018.09.030`.

[108] A. Arteconi, A. Mugnini, F. Polonara, Energy flexible buildings: A methodology for rating the flexibility performance of buildings with electric heating and cooling systems, Applied Energy 251 (2019) 113387. `doi:https://doi.org/10.1016/j.apenergy.2019.113387`.

[109] G. Strbac, Demand side management: Benefits and challenges, Energy Policy 36 (12) (2008) 4419 – 4426, foresight Sustainable Energy Management and the Built Environment Project. `doi:https://doi.org/10.1016/j.enpol.2008.09.030`.

[110] P. D. Lund, J. Lindgren, J. Mikkola, J. Salpakari, Review of energy system flexibility measures to enable high levels of variable renewable electricity, Renewable and Sustainable Energy Reviews 45 (2015) 785 – 807. `doi:https://doi.org/10.1016/j.rser.2015.01.057`.

[111] S. Ø. Jensen, A. Marszal-Pomianowska, R. Lollini, W. Pasut, A. Knotzer, P. Engelmann, A. Stafford, G. Reynders, Iea ebc annex 67 energy flexible buildings, Energy and Buildings 155 (2017) 25–34.

[112] Directive, (eu) 2018/844 of the european parliament and of the council of 30 may 2018 amending directive 2010/31/eu on the energy performance of buildings and directive 2012/27/eu on energy efficiency. off j eur union, 75–91.
URL `https://eur-lex.europa.eu/eli/dir/2010/31/oj`

[113] S. Jensen, H. Madsen, R. Lopes, R. G. Junker, D. Aelenei, R. Li, S. Metzger, K. Lindberg, A. Marszal, M. Kummert, et al., Energy flexibility as a key asset in a smart building future: Contribution of annex 67 to the european smart building initiatives (2017).

[114] G. Reynders, J. Diriken, D. Saelens, Generic characterization method for energy flexibility: Applied to structural thermal storage in residential buildings, Applied energy 198 (2017) 192–202.

[115] F. Oldewurtel, T. Borsche, M. Bucher, P. Fortenbacher, M. G. V. T. Haring, T. Haring, J. L. Mathieu, O. Mégel, E. Vrettos, G. Andersson, A framework for and assessment of demand response and energy storage in power systems, in: 2013 IREP Symposium Bulk Power System Dynamics and Control-IX Optimization, Security and Control of the Emerging Power Grid, IEEE, 2013, pp. 1–24.

[116] A. Vandermeulen, B. van der Heijde, L. Helsen, Controlling district heating and cooling networks to unlock flexibility: A review, Energy 151 (2018) 103 – 115. `doi:https://doi.org/10.1016/j.energy.2018.03.034`.

[117] H. T. Haider, O. H. See, W. Elmenreich, A review of residential demand response of smart grid, Renewable and Sustainable Energy Reviews 59 (2016) 166 – 178. `doi:https://doi.org/10.1016/j.rser.2016.01.016`.

[118] G. Dutta, K. Mitra, A literature review on dynamic pricing of electricity, Journal of the Operational Research Society 68 (10) (2017) 1131–1145.

[119] J. Schofield, R. Carmichael, S. Tindemans, M. Woolf, M. Bilton, G. Strbac, Residential consumer responsiveness to time-varying pricing, Tech. Rep. A3, Low Carbon London Learning Lab, LCNF project: Imperial College London (2014).

[120] N. Nezamoddini, Y. Wang, Risk management and participation planning of electric vehicles in smart grids for demand response, Energy 116 (2016) 836 – 850. `doi:https://doi.org/10.1016/j.energy.2016.10.002`.

[121] A. Moreau, Control strategy for domestic water heaters during peak periods and its impact on the demand for electricity, Energy Procedia 12 (2011) 1074 – 1082, the Proceedings of International Conference on Smart Grid and Clean Energy Technologies (ICSGCE 2011. `doi:https://doi.org/10.1016/j.egypro.2011.10.140`. URL `http://www.sciencedirect.com/science/article/pii/S1876610211019667`

[122] A. D. Georgakarakos, M. Mayfield, E. A. Hathway, Battery storage systems in smart grid optimised buildings, Energy Procedia 151 (2018) 23 – 30, 3rd Annual Conference in Energy Storage and Its Applications, 3rd CDT-ESA-AC, 11–12 September 2018, The University of Sheffield, UK. `doi:https://doi.org/10.1016/j.egypro.2018.09.022`.

[123] Y. Yang, H. Li, A. Aichhorn, J. Zheng, M. Greenleaf, Sizing strategy of distributed battery storage system with high penetration of photovoltaic for voltage regulation and peak load shaving, IEEE Transactions on Smart Grid 5 (2) (2013) 982–991.

[124] E. W. Prehoda, C. Schelly, J. M. Pearce, Us strategic solar photovoltaic-powered microgrid deployment for enhanced national security, Renewable and Sustainable Energy Reviews 78 (2017) 167–175.

[125] H. Sæle, Consequences for residential customers when changing from energy based to capacity based tariff structure in the distribution grid, in: 2017 IEEE Manchester PowerTech, 2017, pp. 1–6.

[126] H. Sæle, O. H. ivik, D. E. Nordgård, Evaluation of alternative network tariffs — for residential customers with hourly metering of electricity consumption, in: CIRED Workshop 2016, 2016.

[127] A. B. Eriksen, H. Hansen, J. Hole, T. Jonassen, V. Mook, S. Steinnes, L. Varden, Rme horingsdokument, endringer i nettleiestrukturen (2020).
URL `http://publikasjoner.nve.no/rme_hoeringsdokument/2020/rme_hoeringsdokument2020_01.pdf`

[128] Smart metering(ams), `https://www.nve.no/energy-market-and-regulation/retail-market/smart-metering-ams/`, accessed: 2020-10-08.

[129] S. S. Karlsen, M. Hamdy, S. Attia, Methodology to assess business models of dynamic pricing tariffs in all-electric houses, Energy and Buildings 207 (2020) 109586. `doi:https://doi.org/10.1016/j.enbuild.2019.109586`.
URL `http://www.sciencedirect.com/science/article/pii/S0378778819304578`

[130] A. Baniassadi, D. J. Sailor, E. S. Krayenhoff, A. M. Broadbent, M. Georgescu, Passive survivability of buildings under changing urban climates across eight us cities, Environmental Research Letters 14 (7) (2019) 074028.

[131] A. Ozkan, T. Kesik, A. Z. Yilmaz, W. O'Brien, Development and visualization of time-based building energy performance metrics, Building Research & Information 47 (5) (2019) 493–517.

[132] Byggteknisk forskrift (tek 17)., `https://dibk.no/byggereglene/byggteknisk-forskrift-tek17/14/14-2/` (2020).

[133] Who housing and health guidelines, https://www.who.int/publications/i/item/9789241550376 (2018).

[134] K. Collins, Low indoor temperatures and morbidity in the elderly, Age and Ageing 15 (4) (1986) 212–220.

[135] Criteria for passive houses and low energy buildings - residential buildings.
URL `https://www.standard.no/no/Nettbutikk/produktkatalogen/Produktpresentasjon/?ProductID=636902`

[136] J. A. Wagner, S. M. Horvath, K. Kitagawa, N. W. Bolduan, Comparisons of blood and urinary responses to cold exposures in young and older men and women, Journal of gerontology 42 (2) (1987) 173–179.

[137] J. B. Mercer, B. Østerud, T. Tveita, The effect of short-term cold exposure on risk factors for cardiovascular disease, Thrombosis research 95 (2) (1999) 93–104.

[138] K. Collins, J. Easton, H. Belfield-Smith, A. Exton-Smith, R. Pluck, Effects of age on body temperature and blood pressure in cold environments., Clinical science (London, England: 1979) 69 (4) (1985) 465–470.

[139] P. H. England, Minimum home temperature thresholds for health in winter – a systematic literature review (2014).
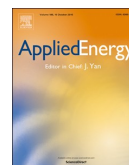
Research Publications

Paper I

A robustness-based decision making approach for multi-target high performance buildings under uncertain scenarios

Shabnam Homaei and Mohamed Hamdy

A robustness-based decision making approach for multi-target high performance buildings under uncertain scenarios

Shabnam Homaei*, Mohamed Hamdy

Norwegian University of Science and Technology (NTNU), Department of Civil and Environmental Engineering, Trondheim, Norway

HIGHLIGHTS

- A novel approach is introduced for building performance robustness assessment.
- Robustness assessment and decision making are integrated to select robust designs.
- A case study is conducted to demonstrate the value of the approach.
- Impacts of occupancy and weather scenario on building performance are analyzed.
- Robustness of competitive designs with the same performance level are compared.
- The results are compared to the Hurwicz criterion as a decision making method.

ARTICLE INFO

ABSTRACT

Considering the diverse uncertainties in building operations and external factors (i.e., occupancy and weather scenarios that can impact a building's energy and comfort), performance robustness has become as important as the building performance itself. Selecting a robust and high performance building design is challenging, particularly when multiple performance criteria should be fulfilled. It requires performance evaluation, robustness assessment, and multi-criteria decision making in three sequential steps. The current study introduces a new robustness-based decision making approach that integrates the robustness assessment and decision making steps and is more transparent than previously used approaches. The proposed approach normalizes each objective function based on its defined target and combines them into one comprehensive indicator. Moreover, it penalizes solutions that do not meet the targeted margins. The new approach is tested on a case study of a single-family house, where eight competitive designs and 16 occupant and climate scenarios are investigated. Exhaustive searches and sophisticated engineering analysis are applied to validate the logic behind the approach's results. In addition, a test framework is used to validate the reliability of the approach under different combinations of scenarios. The results show that the proposed approach can select a high performance and robust building design simultaneously with less analysis effort (no need for weighting the objectives nor for conducting a robustness analysis for each objective separately) and with much trustworthy rate (selecting solution in comparison to the defined targets and with less dependency on the scenario conditions) compared to one frequently used approach (i.e., the Hurwicz criterion).

1. Introduction

1.1. Background

Improving the energy performance of buildings is an essential goal in environmentally conscious societies. One of the actions that societies take to achieve this is to establish stricter standards and requirements for building components and performance [1]. Although there has been an increase in the construction of environmentally friendly buildings, these buildings do not always perform as expected, e.g., variations in thermal comfort [2], energy, or costs [3]. Designers estimate how a building should perform, but their estimates often deviate from the actual energy consumption when the building is in operation because uncertainties in the design or renovation phase are not adequately considered. The notion of uncertainties in the building context can be related to changes in the building environment, including climate

---

Nomenclature

AHP	Analytical Hierarchy Process	RA	Robustness assessment
ASHRAE	The American Society of Heating, Refrigerating and Air-Conditioning Engineers	TEK	Norwegian building regulation
		WWR	Window to wall ratio
ASHP	Air source heat pump	A_m	Maximum performance of design m across all scenarios
BPS	Building performance simulation	B_m	Minimum performance of design m across all scenarios
COP	Coefficient of performance	C_n	Minimum performance of each scenario
DHW	Domestic hot water	D_i	Best performance of all designs across all scenarios
DM	Decision making	$H(A_i)$	Hurwicz weighted average for alternative A_i
EB	Electric boiler	$KPI_{i,rel}$	Relative performance for indicator i
IWEC	International Weather for Energy Calculations	$KPI_{m,n}$	Performance of design m across scenario n
KPI	Key performance indicator(s)	$KPI_{i,m}$	Robustness margin for indicator i
LED	Light emitting diode	$K\bar{P}I_i$	Mean of performance indicator (i) across scenarios
MAUT	Multi-Attribute Utility Theory	PD	Performance deviation
MCDM	Multi-criteria decision making	PR	Performance regret
PA	Performance assessment	PS	Performance spread
PCM	Phase change material	T	Test condition
		α	Weighting preference
		σ	Standard deviation

changes [4], variations in occupant behaviour [5], and changes in economic factors [6]. Uncertain environments are rarely considered in the first steps of the design phase, so decisions based on these designs will be sensitive to uncertainties, leading to a gap between the estimated and observed energy performance [7]. Therefore, there is a need to reduce the sensitivity of a building's energy performance to an uncertain environment. Reducing sensitivity to a changing environment can be done by taking robustness assessment into account during the design or renovation phase [8]. In this work, robustness is defined as the ability of a building to perform effectively and remain within the acceptable margins under the majority of possible changes in internal and/or external environments. In the context of building energy performance, robustness can be assessed using probabilistic approaches for cases where the probabilities of uncertainties are known [9] and non-probabilistic approaches where the probabilities of uncertainties are unknown [10]. In the latter approach, the assessment is done based on a scenario analysis, in which scenarios are implemented to formulate alternatives with unknown probabilities [11]. The aim of using scenarios is to better understand the impact of uncertainties and to help decision makers select designs that perform robustly under the uncertainties [12]. There are different robustness assessment methods based on scenario analysis that can aid decision makers in selecting a robust design. Some examples include the max–min, best-case and worst-case, and minimax regret methods [13]. Furthermore, some studies use probabilistic approaches, such as assessing mean and standard deviation across scenarios [14].To select a high performance and robust building design, three main steps should be followed [12]. The first step is to evaluate the performance of the building based on the results obtained from a building performance simulation (BPS). As a building's performance must respond to multiple criteria [15], as the second step robustness is assessed regarding these criteria under various uncertainties. Building performance robustness assessments can be categorized as either single-criterion [16], or multi-criteria [17], where the performance robustness of the building is assessed regarding one or multiple performance criteria, respectively. For instance, energy robustness, comfort robustness, and cost robustness can be assessed for a building. Multi-criteria robustness assessment requires the robustness assessment to be repeated separately for each criterion, and the designs selected as robust based on each criterion may not be the same [17]. In the reported research, a design that is robust for energy consumption is not robust for overheating, and one that is robust for overheating is not robust for cost. Furthermore, it is important to consider the actual performance of selected robust designs and compare them to the performance targets; otherwise, the process can lead to unrealistic designs [16]. Together with both single-criterion and multi-criteria robustness

assessments, a multi-criteria decision making (MCDM) step is used as the third step for supporting decision-makers in selecting a robust and high performance building design. The selection of this design in MCDM is based on the trade-off between performance and corresponding robustness. The Hurwicz criterion [17], Minimin, Laplace, Wald [18], and Savage [16] are some examples of decision making strategies that have been implemented to select a robust building design. Based on the preferences of decision-makers, the impacts of different types of performance robustness or actual performance of the building can be prioritized by weighting them in the decision making process. Weights and other preferences data aid decision makers in tuning the selection of the best design (i.e., a high and robust performance design). However, in practice, selecting a robust and high performance design is a complicated and difficult task, particularly when multiple and conflicting performance criteria should be fulfilled. As the number of criteria and/or the conflicts among them increase, the decision making step becomes more difficult and requires more experience in order to set the preference weights for each criterion [19]. Furthermore, in the existing literature, a high performance and robust building design is selected by comparing different alternatives (i.e., building designs) to each other without comparing them with the performance targets set by standards and regulations [17]. In this approach, the best alternative is defined based on the best alternative in the design space (i.e., minimum or maximum of each performance criterion), which may be undesirable in comparison with performance targets. Furthermore, deviations of different alternatives from the performance target can be necessary in some cases. At the same time, repeating robustness assessments focusing on different criteria can be demanding from the computational point of view, especially in cases with a huge number of designs and scenarios that need sampling techniques.

1.2. Contribution of this paper

To bridge the abovementioned gaps, this paper introduces a computational approach, the T-robust approach, that integrates a multi-target robustness assessment into a multi-criteria decision making (MCDM) process and includes performance targets when the decision is being made. There are five main advantages to this approach:

- All assessed alternatives (i.e., building designs) are compared, not only to each other but also to the performance targets set by standards and regulations.
- The performances of alternatives are defined (penalized) based on deviations from the performance targets.

- The performance targets are based on regulations, standards, laws and can be adapted according to specific occupants' needs.
- The robustness assessment is not repeated separately for each performance criterion.
- Criteria preferences are automatically established in the decision making process by including performance targets.

This approach can aid building performance decision makers in selecting robust designs under possible uncertainties (possible scenarios). The integration of robustness assessment into the MCDM is done by introducing a multi-target key performance indicator, which is defined based on the design's performance regarding two different criteria. This indicator penalizes designs that do not meet the robustness margins for different key performance indicators (KPIs). This penalty differentiates between the solutions with performance less than the robustness margin (called feasible solutions in this paper) and solutions with performance greater than the robustness margin (called infeasible solutions). The robustness margins for each KPI are defined based on the requirements specified by regulations for each criterion. The introduced approach is evaluated with four different robustness assessment methods; three of them are non-probabilistic methods, while the last is a probabilistic one. To validate the introduced approach, it was also compared with a commonly used MCDM approach (the Hurwicz criterion) under a test framework. The test framework consists of eight test conditions, which are different combinations of implemented scenarios in the robustness assessment. The present approach can support designers and decision-makers in the design or renovation phase in identifying robust, high performance building designs that meet requirements even under changing conditions.

The paper is organized as follows. Section 2 reviews existing multi-criteria decision making methods in the field of building performance. In addition, different robustness assessment methods that quantify the impact of uncertainties are presented in this section. Section 3 describes the steps toward the multi-target robustness-based decision making approach and the test framework. In Section 4, the introduced approach is demonstrated using a case study. The design options and future scenarios, KPIs, and targets for each indicator are described in this section. Section 5 analyses the results obtained from the introduced approach and compares them with those from the Hurwicz decision making method through the test framework. A summary of the methodology, along with the main conclusions, is presented in Section 6.

2. Literature review

2.1. Review of multi-criteria decision making methods

In the building performance context, the best solution can be selected based on a trade-off between performance and corresponding robustness [17]. When considering multiple criteria, this can be achieved using a framework that makes it possible to compare different designs for various criteria. For such a comparison, the designs and performance criteria are shown in a decision making matrix, and because assessed criteria have different dimensions, a criteria normalization is applied. This allows different criteria to be translated to dimensionless criteria. In the next step, by applying preference weights to each criterion, different alternatives are compared to each other and the best one is selected based on an optimality function. This framework can be obtained through "multi-criteria decision-making" (MCDM) methods. These methods provide a solution to problems that are often associated with a trade-off between the performances of available alternatives under conflicting criteria. In the existing literature, MCDM methods are applied in different fields including energy planning [20], building performance simulation [21], and risk management [22]. Some examples are the Multi-Attribute Utility Theory (MAUT), Analytical Hierarchy Process (AHP), Fuzzy Set Theory, Weighted Sum Method, and Weighted Product Method. In the building performance

context, AHP and MAUT are two of the most commonly applied methods in the literature. AHP is a well-known MCDM technique that helps decision makers to integrate different criteria into a single overall score for ranking decision alternatives through a pair-wise comparison [23]. In the building performance context, AHP has been used to develop a comprehensive indicator for indoor environment assessment [24], to select intelligent building systems [25], to develop a housing performance evaluation model that considers different criteria [26], to rank and compare residential energy management control algorithms [27], and to select an optimal phase change material (PCM) for a ground source heat pump integrated with a PCM storage system [28]. The AHP method does not consider uncertainties. For this reason, Hopfe et al. extended the classical AHP for use with uncertain information [15]. The other commonly used MCDM method is "multi-attribute utility theory," which is a more precise methodology for incorporating uncertainty into MCDM [29]. In this method, the overall value of alternatives is defined in the form of a utility function based on a set of attributes. Multi-attribute utility theory has been applied to select cost-effective retrofit measures for existing UK housing stock under uncertainty [30] and to perform a comparative assessment of energy efficiency alternatives with the aim of improving utility savings, and reducing embodied energy and investment cost [31].There are also several other well-known decision making approaches, such as the Laplace [32], Wald [33], Hurwicz criterion [34], and Savage [35] methods. For example, Raysanek et al. [36] used classical decision theories like the Wald, Savage, and Hurwicz criterion approaches to find the optimum building energy retrofits under technical and economic uncertainty. In the context of robust design, Kotireddy et al. implemented Savage [16] that allows decision makers to select a design that has the least risk among alternative that are ranked based on regret. They also used Hurwicz [17] to select a robust design for low-energy buildings and consider decision makers attitudes toward risk. Nikolaidou et al. [18] also used Laplace, Wald, and Savage to find robust optimal Pareto solutions under uncertainty. The weaknesses of most of the methods that have been previously used to find high performance and robust designs under uncertainty are as follows. First, one of the criteria for finding a high performance robust design is the performance (with respect to energy consumption, comfort, cost, etc.) of each design across the assessed scenarios, which can be expressed by different indicators such as, mean, median, standard deviation. This can be confusing for a decision maker who wants to find the best indicator to reflect the design performance across all scenarios. Moreover, the concept of performance targets that are based on standards and regulations have not been used in previous studies, and the ideal alternative is determined based on the best performance (i.e., maximum and minimum value among all alternatives). This is in contrast with reality, in which the ideal alternative of some criteria does not have the minimum or maximum value. Furthermore, finding the optimal preference criteria can be a difficult task, particularly when multiple conflicting criteria should be fulfilled. In order to show the differences between the proposed approach and previously used methods, the results of the proposed approach are compared with the results of robustness assessment and decision making based on the Hurwicz criterion. This criterion states that the best alternative is the one located in a middle ground between the extremes posed by the optimist and pessimist criteria. The first step for the Hurwicz criterion is to calculate a weighted-average return for each alternative. This calculation averages the minimum and maximum of each alternative using α and $1-\alpha$ as weights; α $(0 \leq \alpha \leq 1)$ is the Hurwicz index and reflects the decision-makers' personal attitude toward risk taking. A Hurwicz weighted average can be calculated as below for each alternative (A_i):

For positive $-$ flow payoffs:

$$H(A_i) = \alpha(\text{maximum of row}) + (1 - \alpha)(\text{minimum of row})$$

(1)

For negative − flow payoffs:

$$H(A_i) = \alpha(\text{minimum of row}) + (1 - \alpha)(\text{maximum of row}) \tag{2}$$

The best Hurwicz score is the one with the maximum H for positive-flow payoffs and minimum H for negative-flow payoffs.

2.2. Introducing robustness assessment methods

The selection of robustness assessment methods is related to the purpose of the study, the decision-makers, and their preferences [37]. In the building performance context, robustness assessment is done with both probabilistic and non-probabilistic approaches. Hoes et al. [38] were the first to investigate the Taguchi method, which uses the signal-to-noise ratio value for decreasing variation in the signal (performance) due to the noise (uncertainty) in the building performance context. The robustness indicator implemented by Hoes et al. [38] is the relative standard deviation, which is similar to the signal-to-noise ratio. This indicator leads to designs that are robust for one performance indicator and sensitive for others (e.g., overheating hours). The conclusion of that study highlights the importance of considering the actual performance in addition to the relative robustness. Different robustness assessment methods have been implemented in the literature, such as Chinazzo et al. [39], Buso et al. [40], Karjalainen [41] and Gang et al. [42] implemented the spread of box plot (max–min), relative standard deviation referred to the basic model, best-case and worst-case, and minimax regret methods as robustness assessment methods respectively. Scenario analysis is one of the most widely used methods for robustness assessment. Some studies use probabilistic approaches such as comparison of mean and standard deviation across scenarios [14]. Nik et al. [43] used the mean across scenarios as a robustness indicator for robustness assessment of energy retrofits when considering climate scenarios as a source of uncertainty. Hoes et al. [10] also used relative standard deviation in the optimization of design robustness. This approach is questionable because the likelihood of occurrence of different scenarios is unknown. Thus, considering the mean and standard deviation across all scenarios does not represent the impact of each scenario, and the fluctuation between different scenarios will not be depicted. Furthermore, Li et al. [44] found that it is not suitable to adopt the standard deviation of building annual or hourly energy demand as an optimization objective function to select a robust optimal design of

zero/low energy buildings. Another option is implementing a non-probabilistic approach with scenario analysis; for example, Kotireddy [13] implemented three robustness assessment methods—max–min, best-case and worst-case and minimax regret—with scenario analysis. In the present paper, the same three non-probabilistic robustness assessment methods (max–min method, best-case and worst-case method, and minimax regret method) are implemented. These methods are compared with one probabilistic method (mean and standard deviation based on the Taguchi method) as a frequently used method. The implemented robustness assessment methods are described below.

2.2.1. The Max-Min method

This method is based on the difference between the maximum performance for each design (A_m) and the minimum performance for each design across all scenarios (B_m), as shown in Appendix I. The design with the smallest difference is the most robust one. In this method, the performance of a single design is only compared between different scenarios, without comparison between different designs. This indicator is calculated as in Eq. (3), in which PS is an abbreviation of performance spread.

$$PS = A_m - B_m \tag{3}$$

2.2.2. The best-case and worst-case method

This method is based on the difference between the maximum performance of each design (A_m) and the minimum performance of all designs across all scenarios (D), as shown in Appendix I. The design that has the smallest difference between these two factors is the most robust. This indicator is calculated as below, in which PD is an abbreviation of performance deviation.

$$PD = A_m - D \tag{4}$$

2.2.3. The minimax regret method

This method is based on the difference between the key performance indicator (KPI) value for each design and the minimum performance of each scenario across all designs (C_n). This indicator is calculated as below, in which PR is an abbreviation of performance regret and KPI_{mn} represents the performance of design m under scenario n.
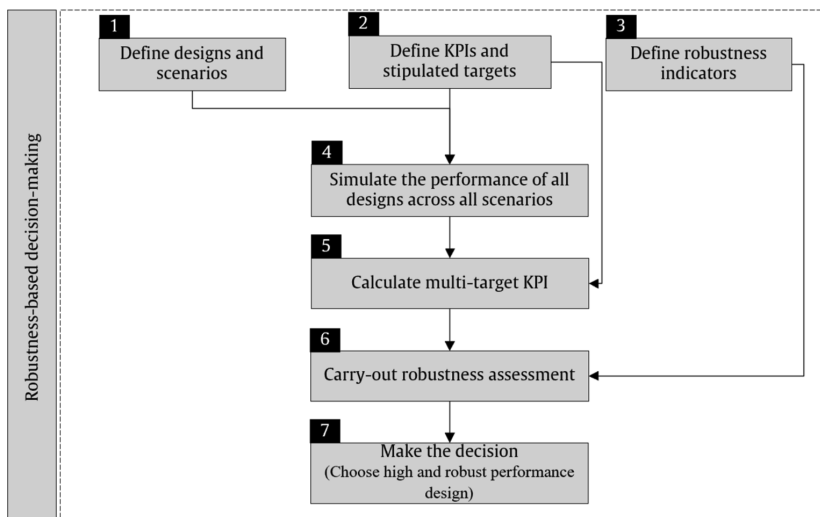
$$PR = KPI_{mn} - C_n \tag{5}$$

Fig. 1. Diagram flow of the multi-target robustness-based decision making approach.

The maximum performance regret represents the highest deviation in each design, i.e., the largest difference between the worst performance and the best performance. The most robust design is then the one with the smallest maximum performance regret across all designs. Appendix I shows the calculation of performance regret for designs across all scenarios.

2.2.4. The mean and standard deviation based on the Taguchi method

In this method, mean and standard deviation are considered as robustness indicators. The most robust design is the design that has the smallest variation (standard deviation) around the target performance (mean) based on the Taguchi method, which is also called the Robust Design Method. This method was used for the first time in product development [45]. The calculation of this indicator is shown in Appendix I.

3. Methodology

This section is divided into two major parts. The first section will focus on introducing the multi-target robustness-based decision making approach, and the second section will focus on validating of this approach under different test conditions (various sets of scenarios) in a test framework. Steps toward developing the approach are shown in Fig. 1 and in more detail in the following subsections.

3.1. Multi-target robustness-based decision making approach (T-robust)

In this section, the robustness-based decision making approach, which is called the T-robust approach in this paper, is introduced. This approach integrates robustness assessment into the decision making process. It considers multiple criteria for building performance and applies penalties if the robustness margins for them are not met. There are seven steps to this approach (Fig. 1), which are described below.

Step 1: Define designs and scenarios

Different possible designs for a building should be defined based on the preferences of the stakeholders who are involved in the project. Furthermore, designs are defined based on the building regulations and requirements of each country [46]. Designers also need to define scenarios for formulating alternative future conditions, considering the effects of various uncertainties in a building's energy performance during its lifespan. For instance, changes in occupant behaviour are one of the significant factors that impact a building's energy consumption [47]. Other external factors can also have effects on building performance, e.g., changes in climate conditions [48] and changes in economic factors [36]. Robustness assessment should be evaluated across the combination of all considered scenarios because the probability of occurrence of any combination is unknown. This can lead to high computational cost. The literature shows that different sampling strategies can be implemented in order to find samples that are representative of all scenario combinations [49].

Step 2: Define key performance indicators and stipulated targets

The performance of a building can be measured based on different indicators. These indicators can be related to objectives that originated from demands, such as energy consumption, thermal comfort, and cost. Indicators can be defined based on the preferences of the decision-makers involved in the building project or by considering the existing risks and technical problems in the building. Furthermore, buildings must meet specific requirements according to regulations [50], building codes, and standards [51]. In this paper, requirements are called performance targets, and the performance of the building under the design conditions (reference scenario) should not exceed the performance target. However, as stated before, the performance of buildings deviates from the performance target during operation, and this is where the robustness is needed. In order to evaluate robustness in this paper, another concept is defined, which is called the robustness margin. Fig. 2 shows the difference between "the performance target" and "the robustness margin" for energy consumption. According to this figure, the building will be robust from an energy perspective if its energy consumption does not exceed the robustness margin. The arrows in Fig. 2 represent the changes that can occur during the building's operation and lead to an increase or decrease in its energy consumption.

Step 3. Define robustness assessment methods

The performance robustness of a building can be assessed by various methods. These methods are introduced in Section 2.

Step 4. Simulate the performance of designs across all scenarios

In this step, the performance of each design across the formulated scenarios is simulated in simulation software, and based on the defined performance indicators, the results are extracted from the software.

Step 5. Calculate Multi-target KPI

In order to integrate the robustness assessment into the decision making process, a new KPI is developed called a multi-target KPI (MT-KPI). This KPI reflects the performance of the building regarding multiple criteria and penalizes the solutions that do not meet the robustness margin. In this way, it can differentiate between feasible and infeasible solutions. In the current paper, the development of the MT-KPI focuses on only two performance indicators (energy and comfort), but it can also be extended for more than two criteria. The vital point in the definition of this KPI is considering the robustness margin ($KPI_{i,m}$) for each primary KPI for penalizing infeasible solutions. Considering $KPI_{i,m}$, two parameters can be defined as below, which represent the relative performance of each indicator.

$$KPI_{1,rel} = \frac{KPI_1}{KPI_{1,m}} \times 100 \qquad KPI_{2,rel} = \frac{KPI_2}{KPI_{2,m}} \times 100 \qquad (6)$$

Implementing the robustness margin leads to differentiating between the feasible solutions (KPIi < KPIi,m) and infeasible solutions (KPIi > KPIi,m). Fig. 3 shows an example of the performance of a building under 16 scenarios. Point (100,100) in Fig. 3 shows the relative margin point, at which the performance of the building regarding both indicators is equal to the robustness margin. Around the relative margin point, four different performance zones are created, of which two (i.e., zones 2 and 4) are feasible regarding one KPI and infeasible regarding the other, one (zone 3) is feasible for both KPIs, and the last
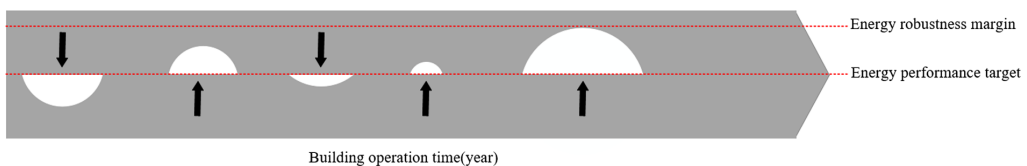

Fig. 2. Conceptual illustration of performance target and robustness margin for energy consumption.
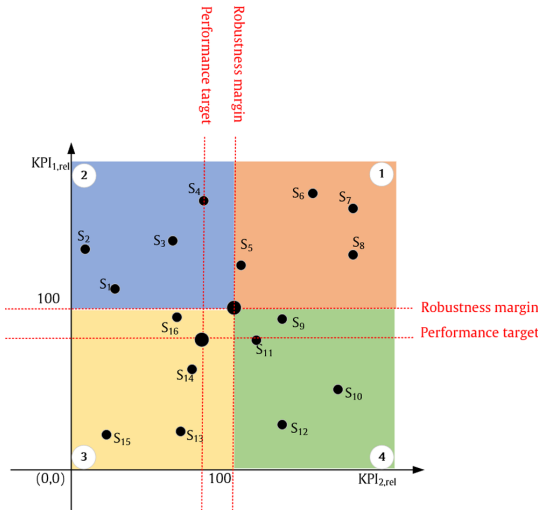
Fig. 3. Illustration of the performance zones of one design under 16 possible scenarios.

zone (zone 1) is completely infeasible.

The calculation of the MT-KPI depends on the performance zones, and is defined in Table 1. As can be seen from Fig. 3 and Table 1, in the completely infeasible zone (zone 1), the MT-KPI is the sum of the KPIs' difference with their corresponding robustness margins. This is applied as a penalty for the infeasibility of both indicators. In the completely feasible zone (zone 3), the MT-KPI is the sum of the inverted difference between indicators and their corresponding robustness margins. Inverting the differences is used in order to differentiate the feasible designs. For the other two zones, which are feasible for one KPI and infeasible for the other (zones 2 and 4), a penalty is applied only for the infeasible solutions, and the MT-KPI is defined based on Table 1.

Step 6. Carry out robustness assessment

In this step, the performance robustness of buildings is assessed with the mentioned robustness indicators for the MT-KPI. Assessing robustness using this KPI reflects not only robustness for multiple criteria but also the actual performance of the building because of the incorporation of the robustness margins in the definition of the MT-KPI.

Step 7. Make the decision

In this step, the best solution (i.e., high and robust performance design) is chosen based on the results of the robustness assessment with the MT-KPI.

3.2. The test framework

The combination of scenarios for a robustness assessment can vary based on the knowledge of the designers. A combination of a huge

number of scenarios can lead to high computational costs. On the other hand, decreasing the number of scenarios will remove some useful information, and this can affect the selection of a robust design. The literature shows that considering extreme scenarios (low–high scenarios) can be sufficient for performance robustness assessment [49]. In order to test the validation of the T-robust approach, a test framework was developed. For this purpose, the robustness assessment in the previous section was considered as input data, and the designs selected as robust under different scenario combinations (test conditions) were compared, as shown in Fig. 4. The steps of developing the test framework are described below.

Step 1: Develop test conditions

To test the performance of the robustness assessment methods, test conditions are needed. The original set of scenarios suggested for robustness assessment is called a reference test condition. This condition is the most informative condition, and other test conditions have fewer scenarios than the reference one. In the limited number of scenarios, extreme scenarios (low–high scenarios) can be identified based on the comparison of performance across scenarios. For cases with a high number of scenarios, extreme scenarios can be found using special sampling techniques [16]. In this study, test conditions were created based on a random combination of extreme and non-extreme scenarios. Notably, each test condition must have some extreme scenarios in order to sufficiently assess robustness.

Step2: Repeat robustness-based decision making for each test condition

In this step, the robustness assessment is repeated for the created test conditions in order to determine how different robustness assessment methods behave when the combination of scenarios is changed from the reference condition to other test conditions.

4. Demonstration of the T-robust approach using a case study

A representative model of Norwegian single-family houses [52] was chosen as the case study building. This model is based on representative models in the IEEE project TABULA (Typology Approach for Building Stock Energy Assessment) [53], which aimed to develop building typologies for 13 European counties. A synthetic average building is defined for each building type, whose characteristics are representative of the most common features found in that building type based on the best available knowledge. This building is a two-story building located in Oslo with a floor area of 162.40 m^2, and is divided into three zones in a detailed model in IDA Indoor Climate and Energy software (IDA-ICE) [54] which is validated using the BESTEST: Test Procedures [55]. The zones consist of a representative day room (i.e., a combined zone for living room, kitchen, and entrance), bedroom, and bathroom. Occupancy schedules, domestic hot water distribution, and internal gains are derived from Nord et al. [56]. The building envelopes, window to wall ratio, and building energy systems (heating system, ventilation system, and DHW generation system) are considered as design options and will vary between eight competitive designs. Heating set-points, window opening, and shading strategies are considered as scenario parameters

Table 1
Calculation of MT-KPI in different performance zones.

Num	Performance zone	Feasibility	Mt-KPI
1	$KPI_{1,rel} > 100$ and $KPI_{2,rel} > 100$	Completely infeasible	$(KPI_{1,rel}\text{-}100) + (KPI_{2,rel}\text{-}100)$
2	$KPI_{1,rel} > 100$ and $KPI_{2,rel} \leq 100$	Feasible for KPI_2	$(KPI_{1,rel}\text{-}100) + (1/(100\text{-}KPI_{2,rel}))$
3	$KPI_{1,rel} \leq 100$ and $KPI_{2,rel} \leq 100$	Completely feasible	$(1/(100\text{-}KPI_{1,rel})) + (1/(100\text{-}KPI_{2,rel}))$
4	$KPI_{1,rel} \leq 100$ and $KPI_{2,rel} > 100$	Feasible for KPI_1	$(1/(100\text{-}KPI_{1,rel})) + (KPI_{2,rel}\text{-}100)$
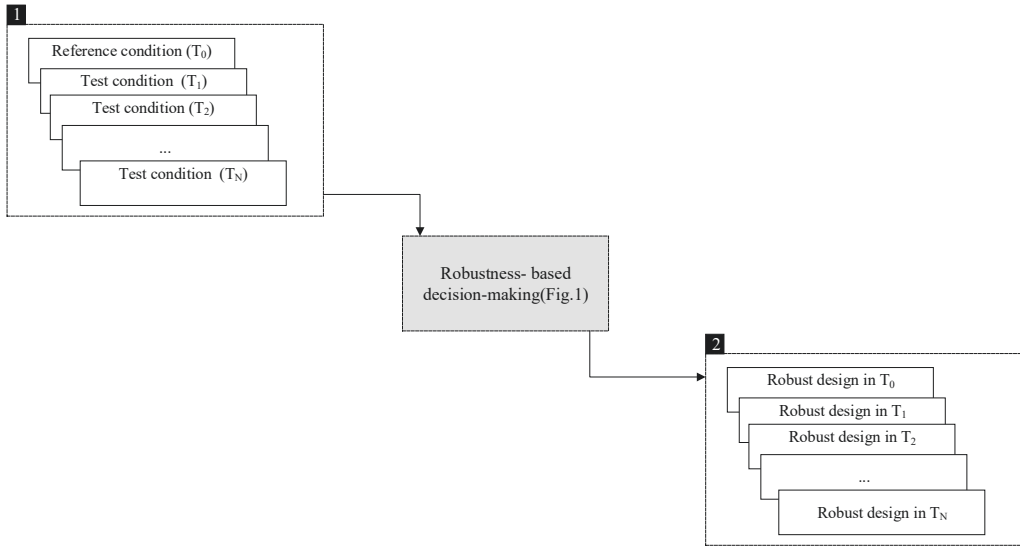
Fig. 4. Flow diagram of the test framework.

and 16 scenarios are created, which will be explained in the upcoming sections. Fig. 5 shows a screenshot of the IDA-ICE model and the building layout, which has a window to wall ratio of 30%. Steps toward the T-robust approach and test framework are described below for the considered case study.

4.1. Description of case study

4.1.1. Design variants and scenarios
4.1.1.1. *Competitive designs.* In this study, eight design configurations

are considered for the case study building. The same energy and thermal comfort targets are set for all of the design configurations under the reference scenario (S_1). This creates the opportunity to compare the robustness of designs with the same performance targets across the considered scenarios. The target set for annual energy consumption is 110 KWh/m^2 based on the TEK17 standard [50]. For thermal comfort, the number of unacceptable hours (including underheating and overheating hours based on the TEK17 standard) should not exceed 5% of occupied hours. To achieve these energy and thermal comfort targets, the building envelope, window to wall ratio,
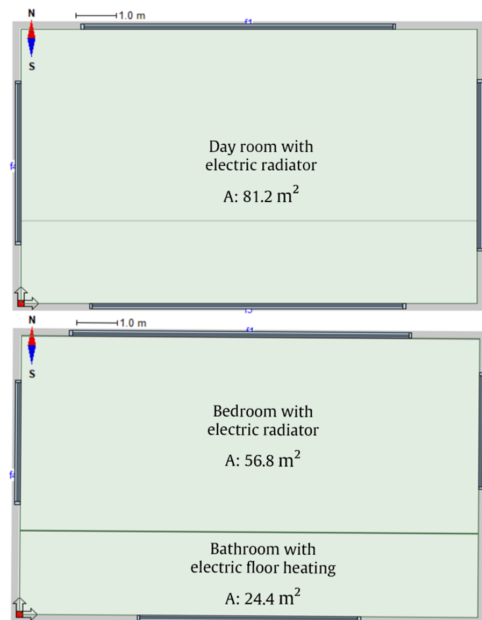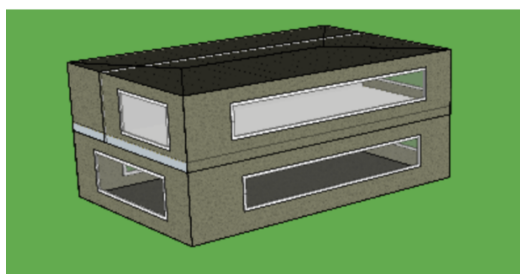
Fig. 5. Layout and appearance of a representative single-family house with a floor area of ca. 162 m^2.

and energy systems are considered as design options for the competitive designs. For example, the targets can be achieved by combining the envelope with low insulation and very efficient energy and ventilation systems. In contrast, another design can achieve the targets via a highly insulated envelope and less efficient ventilation and energy systems. However, targets are met only in the reference scenario, and when uncertainties arise, designs can have different magnitudes of performance deviations from the energy and comfort targets. Hence, the robustness margin is considered in the definition of the MT-KPI in order to select a design based on both its actual performance and performance robustness. Table 2 shows the details of the designs and the assessed KPIs under the reference scenario (S_1). The building envelope of D_1 is based on the TEK17 standard, the current minimum requirement in Norway [50]. In the building envelope, the U-values of the floor, walls, and roof, infiltration, and thermal bridges are variable, and the overall U-value shows the effect of these changes. Two WWR values are considered in the design options. The heating system options are an electric boiler and an air source heat pump with a COP (coefficient of performance) of 3.2 under the rating condition. The heat emitter are electric radiators in the living room and bedroom and electric floor heating in the bathroom. It should be noted that in the designs with the air source heat pump, the heat pump is used in combination with an electric boiler, which is used to generate heat for the electric floor heating in the bathroom. Options for the ventilation system are balanced mechanical ventilation with a heat recovery unit that has an efficiency of 80% and mechanical exhaust ventilation without a heat recovery unit. Domestic hot water in the building is generated with the electric boiler, but in some of the designs (i.e., D_2 and D_6), in order to compensate for the high energy consumption due to other design options, an auxiliary solar thermal collector is added. For lighting, in most of the designs, typical lighting (luminous efficacy of 12 W/m) is implemented, but in the designs with high energy demand (i.e., D_2 and D_6), LED light (luminous efficacy of 60 W/m) is used in order to keep the total energy demand lower.

4.1.1.2. Scenarios. The scenarios that are considered in this paper include two groups of parameters: occupant behaviour and climate scenarios. The eight occupant behaviours consist of eight possible combinations of two heating setpoints, two window opening strategies, and two window shading strategies. In the climate group, two climate scenarios are considered, which leads to a total of 16 scenarios. Table 3 summarizes the scenario parameters and combinations of them across the 16 scenarios.

i. Heating setpoints

The first option for heating setpoint is taken from [52]. In order to create an option with more heating use, heating setpoints are increased in the second scenario based on the survey data taken from [57].

ii. Window shading strategies

The first window shading strategy, taken from [52], is based only on temperature control. This strategy creates a moderate usage of lighting and moderate solar gain. The second scenario increases the shaded time during the day, leading to more lighting use and less solar gains from the window.

iii. Window opening strategies

The first window opening strategy is based on [58], and is adapted with the Norwegian scale. The second option is a hybrid option that uses the first option for window opening in the day room and bathroom. In contrast, in the bedroom, which faces more overheating, it uses the upper limits of the adaptive temperature limits proposed by [59] and is developed by a macro control in IDA ICE. This reflects a group of occupants who prefer a lower inside temperature.

iv. Climate scenarios

To consider the effect of climate uncertainties, two climate files from The American Society of Heating, Refrigerating and Air-Conditioning Engineers (ASHRAE), IWEC and IWEC2, are used from the library of IDA ICE [54]. The IWEC file is derived from up to 18 years of DATSAV3 hourly weather data from 227 locations, originally archived at the National Climatic Data Center (NCDC), and the IWEC2 file is derived from Integrated Surface Hourly (ISH) weather data for 3012 locations, also originally archived at the NCDC. Direct radiation parameters in the IWEC weather file have a strong negative bias of approx. 20 to 40% for Northern Europe [60]. The difference between dry-bulb temperature and direct normal radiation in the IWEC and IWEC2 weather files is shown in Fig. 6. These are the parameters with the strongest effects on the simulation results regarding energy consumption and thermal comfort, and for this reason, other parameters (e.g., relative humidity, etc.) are not compared in this paper.

4.1.2. Simulation model validation

The simulated model is validated using two different approaches. The first approach is to compare the amount of annual energy consumption to the calculated value based on the TEK 17 standard [50]. The comparison shows that if the model implements all of the requirements of TEK 17 standard (D_1 in the considered case study), it can meet the targeted value for annual energy consumption based on that standard, which is 110 KWh/m^2 for the considered case study. Furthermore, the annual energy consumption is compared with that of a similar building from [61]. Karlsen et al. [61] evaluated the annual energy consumption of a Norwegian single family house with two different envelope levels: typical '60 s buildings and TEK 17 standards. Their results show that the range of energy consumption for the Norwegian single-family house based on the TEK 17 standard and without electric vehicles is varing from 100 to 200 KWh/m^2. This is in line with the estimated energy consumption for the current case study, which is 110 KWh/m^2. The second approach focuses on the energy use of

Table 2
Details of the eight competitive designs considered in the case study demonstration.

Design parameters	Designs							
	D_1	D_2	D_3	D_4	D_5	D_6	D_7	D_8
Overall U-value (W/m². k)	0.31	0.25	0.43	0.36	0.33	0.29	0.51	0.44
WWR (%)	30	30	30	30	40	40	40	40
Heating system	EB	EB	ASHP + EB	ASHP + EB	EB	EB	ASHP + EB	ASHP + EB
Ventilation system	Balanced	Exhausted	Balanced	Exhausted	Balanced	Exhausted	Balanced	Exhausted
Solar domestic hot water system size (m²)	0	5	0		0	5	0	0
Lighting	Typical	LED	Typical	Typical	Typical	LED	Typical	Typical
KPIs	D_1	D_2	D_3	D_4	D_5	D_6	D_7	D_8
Total energy consumption (KWh/m²)	110	110	110	110	110	110	110	110
Unacceptable hours (hr)	18	15	12	188	18	3	75	334

ASHP: Air source heat pump, EB: Electric boiler.

Table 3
Summary of the considered occupant behaviour and climate parameters and their combinations in the 16 considered scenarios.

Parameter	Options	Scenarios															
		1	2	3	4	5	6	7	8	9	10	11	12	13	14	15	16
Heating setpoint	1) Bedroom, Living room, bathroom 18 ,21.5 ,23 °C (291.15, 294.65, 296.15 K)	×	×	×	×					×	×	×	×				
	2) Bedroom, Living room, bathroom 20 ,23 ,23 °C (293.15, 296.15, 296.16 K)					×	×	×	×					×	×	×	×
Window shading	1) Shading control On if $T_{indoor} > 23$ °C (296.15 K)	×	×			×	×			×	×			×	×		
	2) Shading control On if radiation above 100 W/m^2			×	×			×	×			×	×			×	×
Window opening	1) Open if $T_{indoor} > T_{out}$ and $T_{indoor} > 23$ °C (296.15 K) for windows in all zones	×		×		×		×		×		×		×		×	
	2) Open if $T_{indoor} > T_{out}$ and $T_{indoor} > 23$ °C (296.15 K) for day room and bathroomOpen based on adaptive thermal model limits for bedroom		×		×		×		×		×		×		×		×
Climate	1) IWEC	×	×	×	×	×	×	×	×								
	2) IWEC2									×	×	×	×	×	×	×	×

internal gains. Norwegian standard SN/TS 30301:2016 [46], which was developed for the calculation of the energy performance of buildings with standardized requirements, considers internal gains as fixed average values per square meter of the building which is shown in Appendix II. In the considered simulation model, these values are based on realistic values for each zone in order to increase the reliability of the energy demand profile in the model. In this validation approach, the energy consumption caused by realistic schedules is compared with the fixed values from the standard. The comparison shows that the range of simulation results is close to the reference values (Appendix II).

4.1.3. Performance indicators and stipulated targets

A building's performance robustness may be evaluated in terms of different key performance indicators. In this paper, it is evaluated for two KPIs, annual energy consumption and thermal comfort, the latter of which is evaluated in terms of unacceptable comfort level hours.

i. Total energy consumption

Total net specific energy use, which includes space heating, heating for ventilation air, space cooling, domestic hot water, ventilation, lighting systems, and appliances, is considered as the first performance indicator. TEK17 (the current minimum energy requirements in Norway) states that the total net specific energy use for a single-family house is derived from the following equation [50]:

$$\text{Total net specific energy use} = 100 + \frac{1600}{\text{heated gross internal area}} (KWh/m^2) \quad (7)$$

Considering this equation, total energy use for the case study building shall not exceed 110 KWh/m². This target is the one that all eight designs should not exceed under the reference scenario. As stated before, infeasible solutions are penalized based on the robustness

margin in the definition of the multi-target KPI. In this paper, the robustness margin allows 5% tolerance from the energy consumption target (110 KWh/m²), which sets115 KWh/m² as the robustness margin.

ii. Thermal comfort (unacceptable hours)

Energy-robust buildings are only effective when the users of the building feel comfortable. This leads us to adopt thermal comfort as the second performance indicator in this paper, which is only evaluated for the bedroom zone. TEK17 recommends an operative temperature between 16 and 26 °C (289.15 and 299.15 K) for bedrooms in Norway [50]. Unacceptable hours include both overheating hours ($T_{indoor} > 26$ °C, 299.15 K) and underheating hours ($T_{indoor} < 26$ °C, 299.15 K). In this paper, the indoor temperature should not fall outside of TEK17's comfort range for more than 5% of occupied hours. Furthermore, the robustness margin allows 5% tolerance from this limit for a solution to be considered feasible.

4.2. Validation under the test framework

Since excluding extreme scenarios may lead to designs that are more sensitive to change, all of the created test conditions should include some extreme scenarios. For this reason, test conditions are a combination of random extreme and random non-extreme scenarios. Because there are limited numbers of scenarios in this paper, extreme scenarios were identified by observing and comparing the performance across scenarios, as can be seen in Fig. 7. Extreme scenarios that lead to the same robust design as all scenarios are S_6, S_9, and S_{11} for energy consumption and S_1, S_8, S_{12}, S_{13}, and S_{16} for thermal comfort. Since the case study for this paper is a heating-dominated building, a large portion of the unacceptable hours is related to underheating hours. The combination of underheating and overheating hours makes the identification of extreme scenarios more complex. Fig. 8 represents the
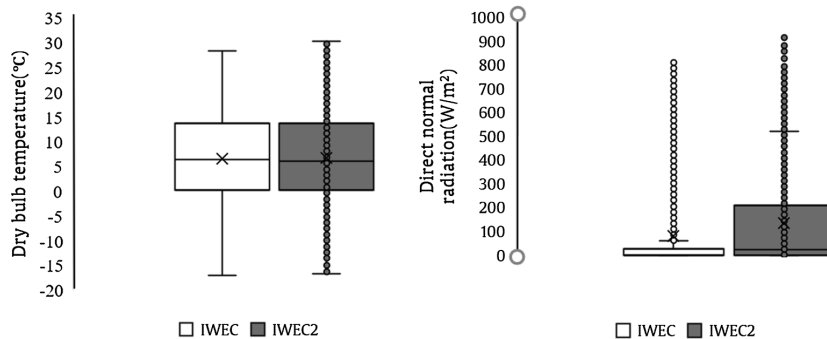
Fig. 6. Temperature and radiation differences in the IWEC and IWEC2 weather files.
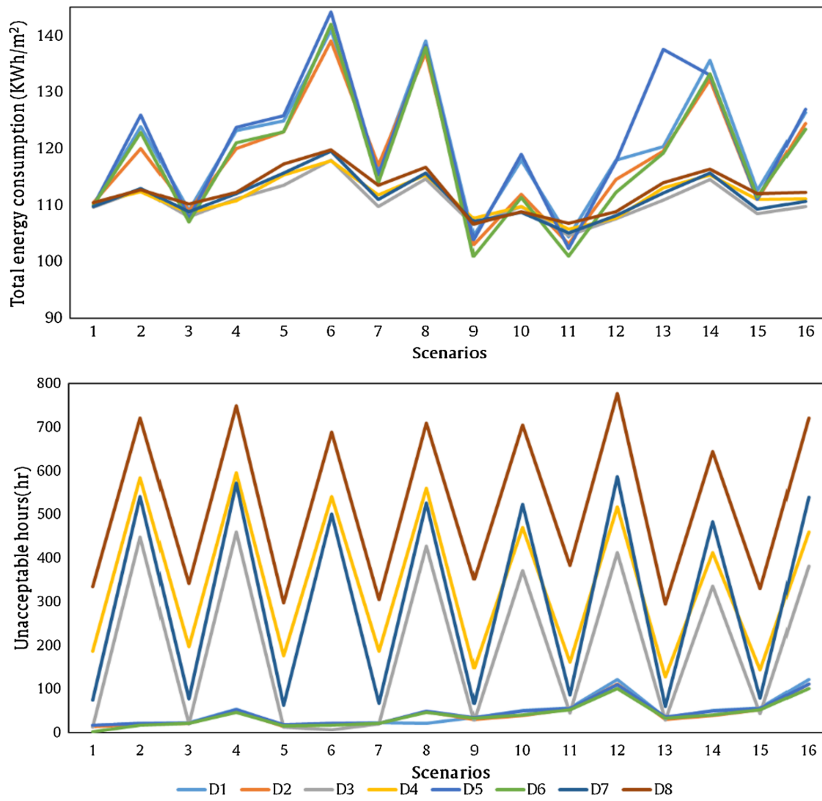
Fig. 7. Predicted performance (total energy consumption and unacceptable hours) of eight competitive designs across all scenarios.
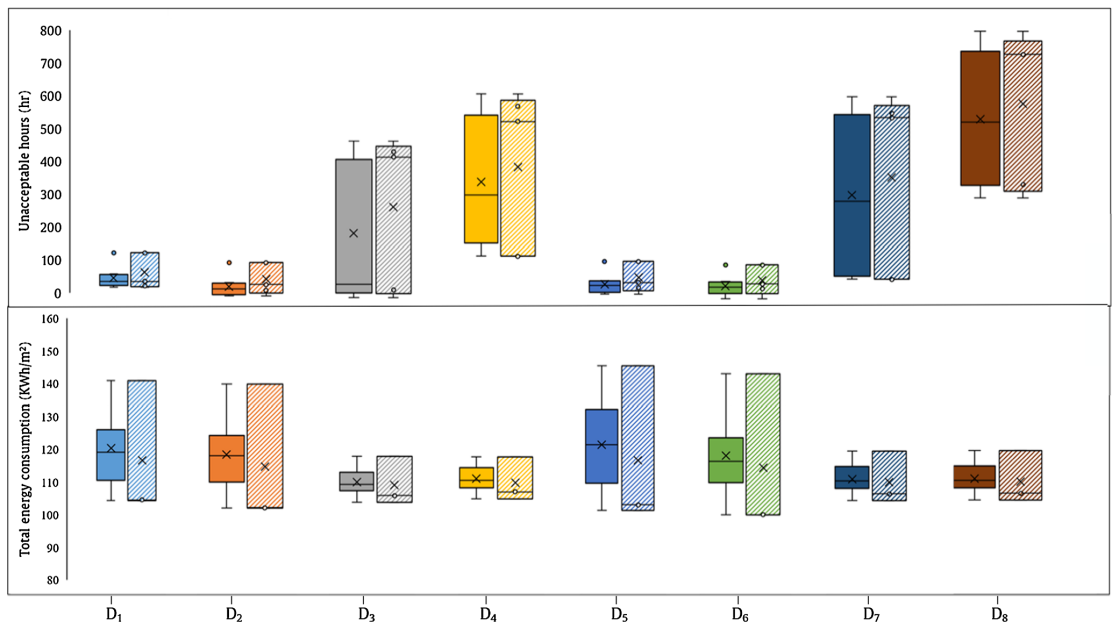
Fig. 8. Comparison of performance of eight competitive designs for combinations of all scenarios and extreme scenarios. The solid box represents all scenarios, and the hatched box represents extreme scenarios (S_6, S_9, and S_{11} for total energy consumption and S_1, S_8, S_{12}, S_{13}, and S_{16} for unacceptable hours).

comparison of building design performances from the energy and comfort perspectives for all scenarios and for extreme scenarios. As can be seen, the range of predicted performance with extreme scenarios is the same as the predicted performance across all scenarios. This shows that a test condition without any extreme scenarios cannot be sufficient for testing the performance of robustness assessment methods. So, in addition to the reference test condition (16 scenarios), eight test conditions are developed in this paper. The first test condition consists of all extreme scenarios, and the other test conditions consist of four random extreme scenarios and four random non-extreme scenarios. These combinations are shown in Table 4. Finally, robustness-based decision making was assessed for all developed test conditions with four proposed robustness assessment methods.

5. Results and discussion

5.1. Performance assessment for considered scenarios

Fig. 9 represents the variations in total energy consumption and unacceptable hours for the eight designs across the considered scenarios. The ranges of the boxes indicate the distribution of performance indicators. It can be inferred from Fig. 9 that the performance range of the designs with the electric boiler (D_1, D_2, D_5, D_6) is entirely different from that of the designs with the air source heat pump (D_3, D_4, D_7, D_8). D_3 has better predicted energy performance, and D_4 has the least variation in total energy consumption. So, it is not easy to determine which of them is the best design if total energy consumption is prioritized. If unacceptable hours are prioritized, it can be noted that D_1 has better performance and D_6 has the least variation. Fig. 9 shows that the designs with the air source heat pump (D_3, D_4, D_7, D_8) exhibit significant variation in the number of unacceptable hours. This is because the decrease in heat pump's COP (coefficient of performance) on cold winter days leads to more underheating hours during winter operation. So, if uncertainties are not considered in the performance prediction, the decision making process can select designs that lead to more underheating hours during winter operation. It can be concluded that selecting the best design based on performance cannot be achieved easily because some designs perform well but with significant variation across scenarios. So, robustness assessment is needed to facilitate the selection of designs that are robust under uncertainties and also have optimal actual performance.

5.2. Robustness assessment and robust design selection

In this section, the robust designs selected for the case study are compared based on four robustness assessment methods using two approaches:

- Choosing the best design based on robustness assessment and the decision making steps (Hurwicz criterion approach is used for the decision making step here.)
- Multi-target robustness-based decision making approach (T-robust approach)

5.2.1. Decision making based on the Hurwicz criterion

In this approach, first, robustness assessments are performed separately for total energy consumption and for unacceptable hours. Then, the design that is robust regarding both criteria is selected in a decision making step based on the Hurwicz criterion, with equal prioritization of energy and comfort. The robustness of the eight designs is calculated using the four robustness assessment methods in Fig. 10. It can be seen that for both KPIs, there are two trends among the robustness assessment methods. First, the spreads using the max–min method and standard deviation follow the same trend. This is because both of these robustness indicators are calculated based on the variation. Second, the maximum regret using the minimax regret method, the deviation using

the best-case worst-case method and the mean follow the same trend because all define robustness with respect to the optimal performance. Furthermore, it should be noted that considering the mean by itself cannot be a good indicator for selecting the robust design because that does not reflect the fluctuation across different scenarios. For this reason, the mean and standard deviation in the Taguchi method is considered as a robustness indicator in this paper. It can be inferred from Fig. 10 that D_4 is the most robust design regarding total energy consumption for the max–min, best-case and worst-case, and Taguchi methods, but the minimax regret method selects D_3 as the robust design. This is in line with what the literature states about the max–min and best-case worst-case methods as conservative approaches and the minimax regret method as a less conservative approach [13]. In this case, D_4 is a design that can exhibit the best performance even in extreme cases, and for this reason, it is selected by the conservative approaches. Similarly, comparing the robustness of unacceptable hours, it can be found that the max–min, best-case and worst-case, and Taguchi methods select designs D_5 and D_6, which have better performance even in extreme cases, and the minimax regret method selects D_1, which is less conservative. In order to select a robust and high performance design regarding both criteria, a decision making approach using a neutral Hurwicz criterion ($\alpha = 0.5$) is implemented. For this decision making, the actual performances regarding both KPIs and their corresponding robustness values are normalized, and a design score is calculated based on the following equation:

$$H(A_i) = \alpha(\text{maximum of row}) + (1 - \alpha)(\text{minimum of row}) \quad (8)$$

It should be noted that in this paper, all actual performance and corresponding robustness values are prioritized equally to simplify the demonstration. The design scores for all robustness assessment methods are calculated and presented in Fig. 11. The most robust design is the design with the highest score. It can be observed from Fig. 11.a that D_1 is the most robust design using the max–min method and D_3 is the most robust design using the best-case and worst-case, minimax regret, and Taguchi methods. It can also be seen that without prioritizing the performance criteria, the max–min method selects a design that performs better for unacceptable hours (D_1), and the other methods select a design (D_3) that performs better from the energy consumption perspective.

5.2.2. Multi-target robustness-based decision making

In this section, the results of the T-robust approach are presented. In this approach, based on the definition, MT-KPI differentiates between feasible and infeasible designs by considering the robustness margin. The results of the robustness assessment with MT-KPI are shown in Fig. 11.b, which indicates that the most robust designs regarding MT-KPI are D_1 for the max–min method and D_2 for the best-case worst-case, minimax regret and Taguchi methods. D_1 is a design that has better performance for MT-KPI even in extreme scenarios, and the selected designs show that regarding the MT-KPI, the max–min method selects the most robust design using a conservative approach. The max–min method selects D_1 in both the Hurwicz decision making and the T-

Table 4
Details of scenario combinations of the eight considered test conditions.

| Test condition	Number of scenarios	Extreme scenarios	Non-extreme scenarios
1	8	S_1, S_6, S_8, S_9, S_{11}, S_{12}, S_{13}, S_{16}	–
2	8	S_1, S_6, S_{13}, S_{16}	S_2, S_3, S_{14}, S_{15}
3	8	S_8, S_9, S_{11}, S_{12}	S_2, S_5, S_7, S_{10}
4	8	S_1, S_6, S_8, S_9	S_2, S_3, S_4, S_7
5	8	S_{11}, S_{12}, S_{13}, S_{16}	S_2, S_3, S_{10}, S_{14}
6	8	S_1, S_6, S_{11}, S_{12}	S_5, S_7, S_{10}, S_{15}
7	8	S_6, S_9, S_{13}, S_{16}	S_4, S_5, S_{14}, S_{15}
8	8	S_1, S_8, S_9, S_{12}	S_2, S_3, S_7, S_{10}
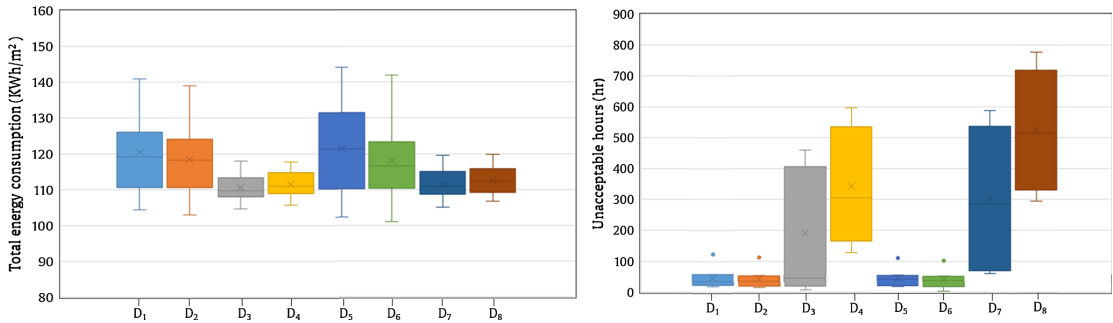
Fig. 9. Variation of total energy consumption and unacceptable hours for eight competitive designs across considered scenarios.

robust approaches; however, for the other indicators, the design selected using the Hurwicz method is D_3, but the one selected using the T-robust approach is D_2. In the T-robust approach, the preferences are automatically incorporated into the MT-KPI by using a robustness margin. Selecting designs D_1 and D_2 in the T-robust approach shows that the comfort criterion is prioritized in the robust design selection. This is in contrast with the designs selected using the Hurwicz criterion, in which all performance indicators are equally prioritized. In order to test the validity of the designs selected in the implemented approaches using different robustness assessment methods, the test framework was developed. The results for this test are represented in the next section.

5.3. Test results

As stated earlier, eight test conditions were generated in addition to the reference condition (T_0). The robustness assessment was repeated under the test conditions, and the results are shown in Table 5 for total energy consumption and unacceptable hours, respectively. It can be observed from this table that the design selected as most robust by all robustness assessment methods is repeated in conditions T_1, T_2 T_4, T_6, and T_7 for total energy consumption. In contrast, the designs selected as robust by the best-case worst-case method and the Taguchi method vary under conditions T_3, T_5, and T_8. So, for total energy consumption, the max–min and the minimax regret robustness indicators selected the same robust design across all generated test conditions. For the unacceptable hours, the T_1 and T_8 test conditions resulted in the selection of the same robust design as the reference condition for all robustness indictors. It can be inferred from Table 5 that the best-case worst-case and Taguchi methods selected the same robust design across all test conditions for unacceptable hours. A comparison of the robustness assessments for total energy consumption and unacceptable hours shows that one robustness assessment method can select the same design across all test conditions for one KPI but select different designs for the second KPI. For example, in this case study, the max–min method selects the same design across all test conditions for total energy consumption but different designs for unacceptable hours. Furthermore,
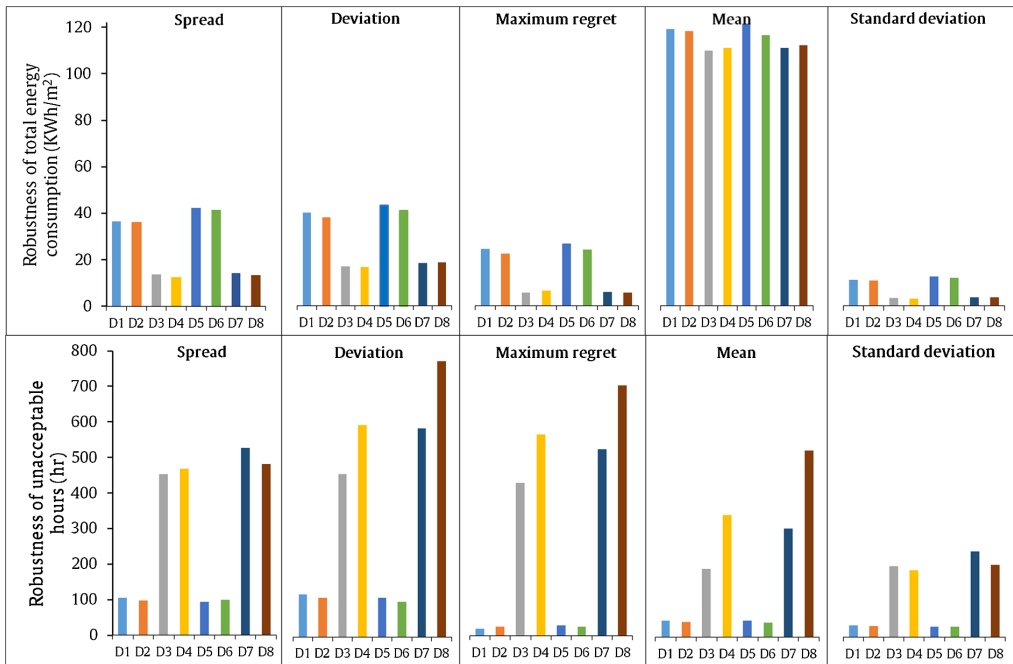
Fig. 10. Robustness of total energy consumption and unacceptable hours using different robustness assessment methods for eight designs across considered scenarios.
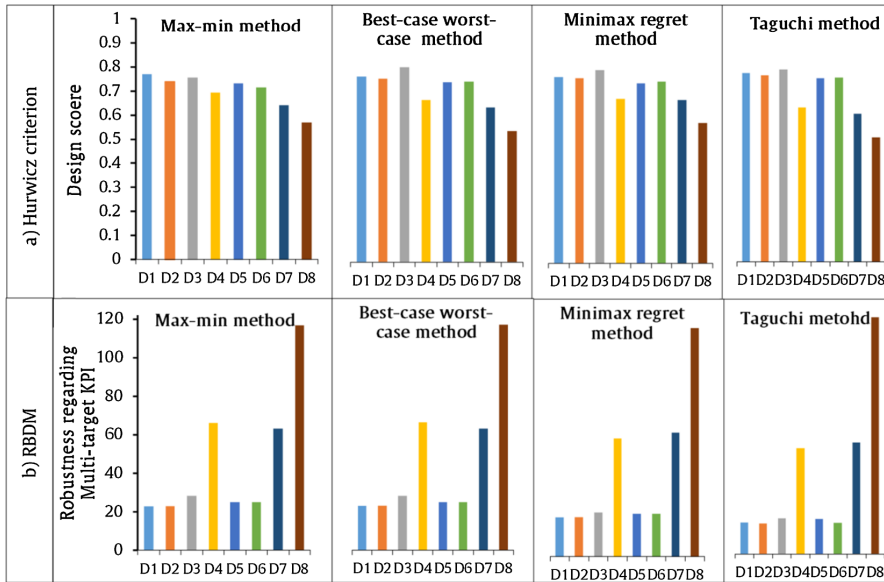
Fig. 11. (a) Design scores calculated using the Hurwicz criterion considering both performance indicators and corresponding robustness with different robustness assessment methods; (b) robustness calculated using the T-robust approach with different assessment methods.

between the implemented robustness methods, the Taguchi method selects different designs across test conditions regarding both total energy consumption and unacceptable hours. This shows that the Taguchi method is the most sensitive one regarding test conditions.

Table 6 shows the robust designs selected by the Hurwicz criterion and the T-robust approach across test conditions. The same designs that are selected as most robust by each robustness assessment methods under the Hurwicz criterion are also selected for conditions T_1, T_4, and T_7. No robustness assessment method generates the same result across every test condition in the Hurwicz decision making process, highlighting the complexity of the decision making process, which takes both indicators and their corresponding robustness into account. Even though there are some robustness assessment methods that perform consistently under different test conditions for individual KPIs, the design selected in the different test conditions is not the same when it comes to the decision making step. In the Hurwicz decision making process, D_1 is the most-selected design by the max–min method, and D_3 is the most-selected design by the other three methods. This is in line with the designs selected in the reference condition. Furthermore, the two designs selected most often by all methods across all test conditions, which are called the first and second dominant designs, are D_3

and D_1 for decision making based on the Hurwicz criterion. Regarding the T-robust approach, it can be observed that in this approach, as in the previous one, no assessment method selects the same design across all test conditions. In test conditions T_3 and T_4, all robustness assessment methods select the same design that they do in the reference test condition. The most-selected designs are D_1 for the max–min method and D_2 for the other three methods. In this approach, the designs selected most often by each robustness assessment method are again in line with the designs selected in the reference condition. In the T-robust approach, the first and second dominant designs are D_2 and D_3, respectively.

The differences between the two decision making approaches that can lead to diversity between the selected robust designs are summarized in Table 7. As can be seen from this table, the T-robust approach decreases the number of steps needed to find the best design from three to two steps by integrating the robustness assessment and decision making steps. Furthermore, the T-robust approach only assesses robustness for MT-KPI, instead of assessing it separately for energy and comfort. Performance and corresponding robustness in the Hurwicz criterion are normalized regarding the maximum performance among the alternatives. This makes the Hurwicz criterion dependent on the

Table 5
Designs selected as robust regarding total energy consumption and unacceptable hours under test conditions.

Test conditions	Total energy consumption				Unacceptable hours			
	Max-min	Best-case worst-case	Minimax regret	Taguchi	Max-min	Best-case worst-case	Minimax regret	Taguchi
T_0	D_4	D_4	D_3	D_4	D_5	D_6	D_1	D_6
T_1	D_4	D_4	D_3	D_4	D_5	D_6	D_6	D_6
T_2	D_4	D_4	D_3	D_4	D_6	D_6	D_1	D_6
T_3	D_4	D_3	D_3	D_3	D_5	D_6	D_1	D_1
T_4	D_4	D_4	D_3	D_4	D_6	D_6	D_6	D_6
T_5	D_4	D_3	D_3	D_3	D_6	D_6	D_6	D_6
T_6	D_4	D_4	D_3	D_4	D_5	D_6	D_6	D_6
T_7	D_4	D_4	D_3	D_4	D_6	D_6	D_6	D_6
T_8	D_4	D_3	D_3	D_3	D_5	D_6	D_1	D_6
Most selected	D_4	D_4	D_3	D_4	D_5	D_6	D_1	D_6
Dominant design	D_4				D_6			

Table 6
Selected robust design using the Hurwicz criterion and T-robust approach under test conditions.

Test conditions	Hurwicz criterion				T-robust approach			
	Max-min	Best-case worst-case	Minimax regret	Taguchi	Max-min	Best-case worst-case	Minimax regret	Taguchi
T_0	D_1	D_3	D_3	D_3	D_1	D_2	D_2	D_2
T_1	D_1	D_3	D_3	D_3	D_3	D_3	D_3	D_3
T_2	D_2	D_3	D_3	D_3	D_6	D_6	D_1	D_6
T_3	D_1	D_6	D_6	D_1	D_1	D_2	D_2	D_2
T_4	D_1	D_3	D_3	D_3	D_1	D_2	D_2	D_2
T_5	D_2	D_2	D_2	D_2	D_2	D_2	D_2	D_2
T_6	D_3	D_3	D_3	D_3	D_3	D_3	D_3	D_3
T_7	D_1	D_3	D_3	D_3	D_1	D_2	D_2	D_3
T_8	D_1	D_6	D_6	D_1	D_6	D_6	D_6	D_6
Most selected	D_1	D_3	D_3	D_3	D_1	D_2	D_2	D_2
First dominant	D_3				D_2			
Second dominant	D_1				D_3			

combination of performances in the solution space, and if the performance in the solution space change, the normalization process will be changed, which will affect the selected designs. In the T-robust approach, the normalization process is based on the performance targets and it does not vary with the changes in the combination of performances in the solution space. The last difference is related to the selection basis. In T-robust approach, the best design is selected by the integration of performance targets in the robustness assessment and there is no need for preferences in order to weight various criteria. This is exactly in contrast with the Hurwicz approach, where preference weights are needed for selecting the best design. For example, in the current case study, the energy and comfort criteria are weighted equally, and this can be one reason for differences between the designs selected by the two approaches. In order to validate the logic behind the selected designs and compare the dominant designs identified by the two approaches, the designs were ranked in an exhaustive search based on their physical meaning, as described in the next section.

5.4. Selection of the best design with an exhaustive search

In this section, the designs selected as robust using the Hurwicz criterion and T-robust approaches were compared via an exhaustive search. A limited number of designs was considered for the case study building in order to be able to analyse them with the exhaustive search and engineering knowledge. It is remarkable that in both approaches, designs D_1, D_2, D_3, and D_6 are selected by robustness assessment methods under different test conditions, but the dominant design in the Hurwicz criterion is not the same as in the T-robust approach. This difference can be attributed to the approach of quantifying the MT-KPI,

which takes a robustness margin into account and differentiates between feasible and infeasible solutions. This differentiation is done by penalizing infeasible solutions in the definition of the MT-KPI. To make the penalizing process more understandable, an exhaustive search was implemented for the proposed designs based on two performance criteria.

It should be noted that the exhaustive search could be done for this case study because it has a limited number of designs, but in cases with a large number of designs, it would be a tedious task to make a ranking based on design physical meaning and trade-off between different performance perspectives. This can lead to computational and practical difficulties. Furthermore, this search requires a deep understanding of the physical meaning of each design and expert knowledge. First, the most influential design options that can affect total energy consumption and thermal comfort were identified based on the physical meanings of designs. Then, the designs were ranked based on those options. The ranking is summarized in Table 8. Based on the evaluation of the simulation results (Figs. 8 and 9), the most influential design option for total energy consumption is implementing the electric boiler (D_1, D_2, D_5, D_6), and its effect is stronger when there is no solar thermal collector for generating hot water, which occurs in designs D_1 and D_5. On the other hand, designs with a higher U-value and larger WWR lead to higher energy consumption. So, of the two designs, D_5 consumes higher energy than D_1, because it has higher U-value and larger WWR. After D_5 and D_1, the next highest energy consumption is related to D_2 and D_6, but they consume less electricity because they have solar thermal collectors for generating hot water. The other designs consume less energy and are not considered in detail in the ranking for total energy consumption because they do not include the most influential options.

Table 7
Summary of differences between the Hurwicz and T-robust approaches.

Num	Criteria	Approaches	
		Hurwicz criterion	T-robust
1	No. of needed steps	3 steps (PA, RA, and DM)	2 steps (PA, integrated RA and DM)
2	No. of needed RAs	Dependent on the number of performance criteria (here 2)	1
3	Normalization basis	Maximum performance in the solution space	Performance targets
4	Selection basis	Weights of criteria are necessary(Equally prioritized for the current case study)	Weights are based on the required targets

No.: Number, PA: performance assessment, RA: Robustness assessment, DM: Decision making

Table 8

Design ranking based on total energy consumption and unacceptable hours.

Performance indicator	Most influential design options	Design ranking
Total energy consumption	1) Electric Boiler without solar thermal collectors 2) Higher U-value 3) Larger WWR	Bad → Good $D_5 > D_1 \gg D_6 > D_2 >$ other designs
Underheating hours	1) ASHP 2) Exhausted ventilation 3) Higher U-value 4) Larger WWR	Bad → Good $D_8 > D_4 > D_7 > D_3 >$ other designs
Overheating hours	1) Air balanced ventilation 2) Lower U-value	Bad → Good $D_1 > D_5 >$ other designs
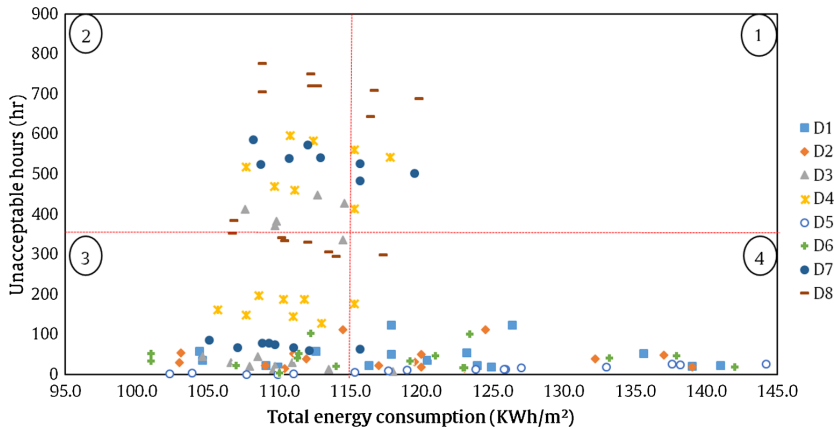
Fig. 12. Unacceptable hours vs. total energy consumption of the eight addressed designs under the 16 considered scenarios (the red lines show the robustness margin for each indicator). (For interpretation of the references to colour in this figure legend, the reader is referred to the web version of this article.)

Regarding underheating hours, the air source heat pump, which occurs in designs D_3, D_4, D_7, and D_8 is the most influential option for increasing underheating hours. The second influential parameter is exhaust ventilation, which can be found in D_8 and D_4, and the last options are higher U-value and larger WWR. So, the four designs with the most underheating hours are, in order, D_8, D_4, D_7, and D_3. Other designs have fewer underheating hours and are not considered in the ranking. Air balanced ventilation is the most influential parameter that increases overheating hours, and the second influential parameter is a lower U-value. This makes D_1 the design with the most overheating hours, followed by D_5. Fig. 12 summarises the results for all designs and scenarios using the same four performance zones defined previously in Fig. 3. Designs D_4, D_7, and D_8 are placed in zone 4 (infeasible for both criteria) for some scenarios, and for this reason, they are not preferable designs. D_1 is a design with high energy consumption and the highest overheating, so it cannot be selected as the best design, either. This is completely proven by both the T-robust and the Hurwicz approach, neither of which selected D_4, D_7, D_8, or D_1. The next design that cannot be selected as the best design is D_5, because it has the highest energy consumption and is ranked in the high overheating category. D_6 also cannot be selected as the best design because it has more energy consumption than D_2. The remaining candidates for selection as the best design are D_2 and D_3. The energy ranking shows that D_2 is the best design among the four designs considered from an energy perspective (D_5, D_1, D_6, D_2). On the other hand, based on the unacceptable hours ranking, D_3 is the best design among the four considered designs (D_8, D_4, D_7, D_3). This shows that there is a trade-off between the selection of D_2 or D_3 as the best design. The results show that the effect of unacceptable hours ($\frac{\text{Maximum unacceptable hours}}{\text{Unacceptable hours margin}} = \frac{460}{330} = 1.40$) for D_3 is more severe than the effect of energy consumption ($\frac{\text{Maximum energy consumption}}{\text{Energy margin}} = \frac{139}{115} = 1.2$) for D_2. Furthermore, D_3 violates

both the energy and comfort criteria (under different scenarios) because its performance is placed in zones 2 and 4. In contrast, D_2 only violates the energy criterion. The selection of D_2 by the T-robust approach proves that this approach can completely reflects the effects that can occur due to the sever deviations from target and the violation from two perspective. Nevertheless, selecting the best design between these two designs by ranking their performance regarding both criteria is not so easy, and this shows that D_2 and D_3 are the best two designs that can be selected by exhaustive search. This is also in line with the results of the designs selected by the Hurwicz and T-robust approaches. As stated before, the first dominant designs selected by the Hurwicz and the T-robust approaches are D_3 and D_2, respectively, which are also selected as the best design in the exhaustive search. Furthermore, the T-robust approach selects D_3 as the second dominant design. In contrast, the second dominant design selected by the Hurwicz approach is D_1, which is not a preferable design based on the results of the exhaustive search and the physical meaning of the designs because it results in high energy consumption and high overheating hours. One of the reasons for the selection of different designs by two approaches is that in the T-robust approach, preferences regarding energy and comfort are automatically included in the robustness assessment by using robustness margins in the definition of the MT-KPI. This is in contrast with the decision that is made by the Hurwicz approach with equally prioritized energy and comfort. This can be solved by prioritizing energy and comfort criteria using commonly agreed upon weights and preferences. However, in practice, identifying those preferences and tuning the decision making can be dependent on the project and vary for different objectives. Furthermore, finding the optimum weights that lead to the best design selection becomes more difficult when it comes to real-world problems that face a high number of conflicting criteria. Implementing the T-robust approach reflects the decision-makers'

preferences in a transparent way to ease the decision making process to select the best design without any guiding and tuning steps, at the same time reducing the computational cost.

The main contributions of this research are dual. First, it has proposed the T-robust approach, which allows a robust high performance building design to be selected by comparing assessed designs with performance targets. Second, the proposed approach was applied to a case study with eight competitive designs that all have the same energy and target requirement.

5.5. Practical use of the proposed approach

The proposed approach can be used by building designers, architects, engineers and other decision makers such as grid suppliers to find high performance and robust building designs. These designs can perform based on targeted requirements during operation while exhibiting minimal sensitivity to future uncertainties. Robust buildings can assure homeowners and building designers that the building will perform as expected against uncertainties, which can include changes in occupant behaviour, climate conditions, etc. As an example, it is documented that in identically constructed buildings, energy use can vary up to 17 fold due to the influence of occupants [62]. These fluctuations can be decreased by appropriately selecting robust designs. From broader perspective such as demand-side management, the energy consumption fluctuations created by uncertainties in the building sector can lead to issues such as grid failure and can increase grid stress. Thus, these fluctuations are not desirable for companies such as grid suppliers that are planning for current and future energy use in the building sector as the major energy consumer worldwide [63]. As an example, electricity demand can increase significantly during extreme weather conditions, which can be caused by buildings that are not designed for such conditions. This can leave thousands of buildings out of the comfort range and threaten the lives of vulnerable people. Furthermore, as demonstrated for the case study building, it is easier to compare designs based on the performance robustness of MT-KPI under uncertainty (Fig. 11.b), instead of comparing them regarding two different performance indicators (i.e. energy and comfort) across scenarios (Fig. 9). This comparison can be instrumental in decision making, especially when designs are going to be selected from a large design space. This approach also provides designers with information on which designs deviate more from the performance targets. This is done by penalizing the designs that do not meet the required targets.

6. Conclusion

This paper focuses on the selection of high performance and robust building designs under climate and occupant uncertainties. It introduces a new approach that integrates robustness assessment and decision making steps and selects the best design by not only comparing different designs to each other but also comparing them to performance targets that can be set by building regulations, standards or the desires of homeowners. The proposed approach comprises building performance simulation, scenario analysis, and different robustness assessment methods and then describes the robustness-based decision making approach based on the combination of these steps in a transparent and easy to understand way. This approach can be effectively used by building designers, architects, engineers, and decision-makers to select high performance and robust designs that can meet the established requirements even when considering possible changes in the internal and external environments.

The integration of robustness assessment into the decision making process is achieved using a multi-target key performance indicator, which takes multiple performances into account and differentiates between feasible and infeasible solutions using robustness margins. Using this approach also removes the need for repeated robustness assessments regarding multiple criteria. The introduced approach was assessed using four robustness assessment methods (i.e., max–min, best-case and worst-case, minmax regret and Taguchi methods) for a representative model of Norwegian single-

family houses as a case study under occupant behaviour and climate scenarios in order to identify the best design. The designs of the case study building are competitive designs and all of them met the same requirements for energy and comfort based on Norwegian standards under the reference scenario. In the demonstration example, performance robustness was assessed in terms of energy and thermal comfort. Furthermore, the introduced approach was compared to one of the frequently used methods for selecting robust designs (i.e., the Hurwicz criterion) in a test framework that consisted of different sets of scenarios (test conditions).

The following conclusions can be drawn based on this comparative study:

- The proposed approach can be used by designers and decision makers to select a robust and high performance building design by comparing designs not only to each other but also to performance targets based on standards, regulations or the desire of homeowners.
- The inclusion of the performance targets in the proposed approach can automatically establish the criteria preferences. This removes the need for a weighting process which requires high levels of experience and knowledge in real-world projects that face many conflicting criteria.
- Regardless of how many performance criteria are going to be evaluated, the proposed approach needs only one robustness assessment for the multi-target key performance indicator. This can reduce the demand for the computational cost.
- Implementation of the performance targets in the proposed approach can lead to the selection of different designs in comparison with the Hurwicz approach (D_2 in contrast with D_3 for the considered case study). This can be related to the differences in the selection basis; in the proposed approach, the designs are selected based on the performance targets, whereas the Hurwicz approach requires the weighting preferences in order to select the best design.
- Robustness assessment methods can exhibit different behaviours under test conditions when they are evaluating different key performance indicators. For example, in this case study, the max–min and minimax regret methods repeatedly selected the same design under all test conditions regarding total energy consumption. In contrast, they selected different designs under different test conditions when they were evaluating unacceptable hours. This also led to different designs being selected designs in the decision making process, which shows the complexity of multi-criteria decision making under uncertainty.
- In the introduced approach, the max–min method selected a design that can work for all scenarios, including extreme scenarios, and can thus be considered as a conservative method for this approach. Other methods (the best-case worst-case, minimax regret, and Taguchi methods) selected less conservative designs.

The proposed approach is a generic approach that can be implemented for case studies with different backgrounds. In this paper, it was assessed for a two-criteria (energy and comfort) robust design problem. In future works, this can be extended to address other criteria such as cost, which is an important perspective in high performance building design. Furthermore, in this paper, the context of the proposed approach is considered for a single building. In the real world, buildings interact with each other and with the connected grids. It is, therefore, an interesting option to consider this approach for larger scales, such as a neighbourhood scale.

CRediT authorship contribution statement

Shabnam Homaei: Conceptualization, Methodology, Software, Validation, Formal analysis, Investigation, Data curation, Writing - original draft, Writing - review & editing, Visualization. **Mohamed Hamdy:** Conceptualization, Methodology, Resources, Data curation, Writing - review & editing, Supervision.

Declaration of Competing Interest

The authors declare that they have no known competing financial interests or personal relationships that could have appeared to influence the work reported in this paper.

Acknowledgements

Appendix I. Calculation of implemented robustness indicators are shown in the following tables.

See Tables A1.1–A1.4.

Table A1.1
Finding the maximum and minimum performance of a design across scenarios and best performance for designs and scenarios [17].

Design	Scenarios					Max and Min performance across scenarios	
	S_1	S_2	...	S_i	S_n	Maximum performance (A)	Minimum performance (B)
D_1	KPI_{11}	KPI_{21}	...	KPI_{i1}	KPI_{n1}	$A_1 = \max(KPI_{11},...,KPI_{n1})$	$B_1 = \min(KPI_{11},...,KPIn1)$
D_2	KPI_{12}	KPI_{22}	...	KPI_{i2}	KPI_{n2}	A_2	B_2
...			...				
D_i	KPI_{1i}	KPI_{2i}	...	KPI_{i2}	KPI_{ni}	A_i	B_i
D_m	KPI_{1m}	KPI_{2m}	...	KPI_{3i}	KPI_{nm}	A_m	B_m
Minimum performance for each scenario (C)	$C_1 = \min(KPI_{11},...,KPI_{1m})$	C_2	...	C_i	C_n		
Best performance of all designs across all scenarios						$D = \min(B) = \min(C)$	

Table A1.2
Robustness calculation using max–min, best-case and worst-case, and minimax regret methods [17].

Design	Performance spread (PI)	Performance deviation (PD)	Performance regret (PR)
D_1	$A_1 - B_1$	$A_1 - D$	$\max(R_{11},...,R_{n1})$
D_2	$A_2 - B_2$	$A_2 - D$	$\max(R_{12},...,R_{n2})$
...			
D_i	$A_i - B_i$	$A_i - D$	$\max(R_{1i},...,R_{ni})$
D_m	$A_m - B_m$	$A_m - D$	$\max(R_{1m},...,R_{nm})$
Robust design	$\min(PS)$	$\min(PD)$	$\min(PR)$

Table A1.3
Calculation of performance regret of designs across all scenarios [17].

Designs	Performance regret(R) Scenarios			
	S_1	S_2	...	S_n
D_1	$R_{11} = KPI_{11} - C_1$	$R_{21} = KPI_{21} - C_2$	...	$R_{n1} = KPI_{n1} - C_n$
D_2	$R_{12} = KPI_{12} - C_1$	$R_{22} = KPI_{22} - C_2$	...	$R_{n2} = KPI_{n2} - C_n$
...			...	
D_i	$R_{1i} = KPI_{1i} - C_1$	$R_{2i} = KPI_{2i} - C_2$	...	$R_{ni} = KPI_{ni} - C_n$
D_m	$R_{1m} = KPI_{1m} - C_1$	$R_{2m} = KPI_{2m} - C_2$	...	$R_{nm} = KPI_{nm} - C_n$

Table A1.4
Robustness calculation using the Taguchi method [17].

Design	Scenarios					Mean	Standard deviation
	S_1	S_2	...	S_i	S_n		
D_1	KPI_{11}	KPI_{21}	...	KPI_{i1}	KPI_{n1}	$K\bar{P}I_1 = \frac{KPI_{11} + KPI_{12} + \cdots + KPI_{1n}}{n}$	$\sigma_1 = \sqrt{\sum_{i=1}^{n} \frac{(KPI_{1i} - K\bar{P}I_1)^2}{n}}$
D_2	KPI_{12}	KPI_{22}	...	KPI_{i2}	KPI_{n2}	$K\bar{P}I_2 = \frac{KPI_{21} + KPI_{22} + \cdots + KPI_{2n}}{n}$	$\sigma_2 = \sqrt{\sum_{i=1}^{n} \frac{(KPI_{2i} - K\bar{P}I_2)^2}{n}}$
D_m	KPI_{1m}	KPI_{2m}	...	KPI_{3i}	KPI_{nm}	$K\bar{P}I_m = \frac{KPI_{m1} + KPI_{m2} + \cdots + KPI_{mn}}{n}$	$\sigma_m = \sqrt{\sum_{i=1}^{n} \frac{(KPI_{mi} - K\bar{P}I_m)^2}{n}}$
Robust design						$\min(\bar{P}I \cap \sigma)$	

Appendix II

See Table A2.1.

Table A2.1

Comparison of load schedules based on SN/TS 3031:2016 (2016) [46] to simulated results for the case study building. For lighting only, the daily amount is used.

Hour	Equipment (Wh/m^2)	DHW (Wh/m^2)	Lighting (Wh/m^2)
1	0.96	0.00	0.3
2	0.96	0.00	0.3
3	0.96	0.00	0.3
4	0.96	0.00	0.3
5	0.96	0.00	0.3
6	0.96	0.96	0.3
7	0.96	6.87	1.7
8	1.92	0.96	1.7
9	1.92	0.96	1.7
10	0.96	0.96	1.7
11	0.96	0.96	1.7
12	0.96	0.96	1.7
13	0.96	0.96	1.7
14	0.96	0.96	1.7
15	0.96	0.96	1.7
16	2.88	0.96	1.7
17	4.81	0.96	1.7
18	4.81	13.74	1.7
19	4.81	13.74	1.7
20	4.33	1.37	1.7
21	4.33	1.37	1.7
22	2.40	1.37	1.7
23	2.40	0.96	1.7
24	0.96	0	0.3
Total daily operation (Wh/m^2)	48.05	68.67	31
Annual operation (KWh/m^2)	17.53	25.06	11.35
Annual operation based on simulationmodel (KWh/m^2)	17.56	26.56	11.29

References

[1] V.C. Hagen, Robustness assessment methods to identify robust high-performance building designs, Master thesis, Department of Civil and Environmental Engineering, Norwegian University of Science and Technology, 2018, doi:http://hdl.handle.net/11250/2559478.

[2] De Wilde P. The gap between predicted and measured energy performance of buildings: A framework for investigation. Autom Constr 2014;41:40–9. https://doi.org/10.1016/j.autcon.2014.02.009.

[3] De Wilde P, Tian W, Augenbroe G. Longitudinal prediction of the operational energy use of buildings. Build Environ 2011;46(8):1670–80. https://doi.org/10.1016/j.buildenv.2011.02.006.

[4] De Wilde P, Coley D. The implications of a changing climate for buildings. Build Environ 2012;55:1–7. https://doi.org/10.1016/j.buildenv.2011.02.006.

[5] Yan D, O'Brien W, Hong T, Feng X, Gunay HB, Tahmasebi F, et al. Occupant behavior modeling for building performance simulation: Current state and future challenges. Energy Build 2015;107:264–78. https://doi.org/10.1016/j.enbuild.2015.08.032.

[6] Hamdy M, Sirén K, Attia S. Impact of financial assumptions on the cost optimality towards nearly zero energy buildings–A case study. Energy Build 2017;153:421–38. https://doi.org/10.1016/j.enbuild.2017.08.018.

[7] Mavrotas G, Figueira JR, Siskos E. Robustness analysis methodology for multi-objective combinatorial optimization problems and application to project selection. Omega 2015;52:142–55. https://doi.org/10.1016/j.omega.2014.11.005.

[8] Leyten JL, Kurvers SR. Robustness of buildings and HVAC systems as a hypothetical construct explaining differences in building related health and comfort symptoms and complaint rates. Energy Build 2006;38(6):701–7. https://doi.org/10.1016/j.enbuild.2005.11.001.

[9] Van Gelder L, Janssen H, Roels S. Probabilistic design and analysis of building performances: Methodology and application example. Energy Build 2014;79:202–11. https://doi.org/10.1016/j.enbuild.2014.04.042.

[10] Hoes P, Trcka M, Hensen J, Bonnema B. Optimizing building designs using a robustness indicator with respect to user behavior, in: Building Simulation. Proceedings of the 12th conference of the international building performance simulation association. 2011. p. 1710–7.

[11] Struck C, Hensen J. Scenario analysis for the robustness assessment of building design alternatives–a Dutch case study. Proc CISBAT 2013;2013:939–44.

[12] Moss RH, Edmonds JA, Hibbard KA, Manning MR, Rose SK, Van Vuuren DP, et al. The next generation of scenarios for climate change research and assessment. Nature 2010;463(7282):747. https://doi.org/10.1038/nature08823.

[13] Kotireddy R, Hoes P, Hensen JL. Simulation-based comparison of robustness assessment methods to identify robust low energy building designs. Proceedings of 15th IBPSA conference, SanFrancisco, CA, USA. 2017. p. 892–901.

[14] Nik VM, Mata E, Kalagasidis ASJEP. Assessing the efficiency and robustness of the retrofitted building envelope against climate change. Energy Procedia, 78 2015:955–60. https://doi.org/10.1016/j.egypro.2015.11.031.

[15] Hopfe CJ, Augenbroe GL, Hensen JL. Multi-criteria decision making under uncertainty in building performance assessment. Build Environ 2013;69:81–90. https://doi.org/10.1016/j.buildenv.2013.07.019.

[16] Kotireddy R, Hoes P-J, Hensen JL. A methodology for performance robustness assessment of low-energy buildings using scenario analysis. Appl Energy 2018;212:428–42. https://doi.org/10.1016/j.apenergy.2017.12.066.

[17] Kotireddy R, Loonen R, Hoes P-J, Hensen JL. Building performance robustness assessment: Comparative study and demonstration using scenario analysis. Energy Build 2019;202:109362https://doi.org/10.1016/j.enbuild.2019.109362.

[18] Nikolaidou E, Wright JA, Hopfe CJ. Robust building scheme design optimization for uncertain performance prediction; 2017.

[19] Mela K, Tiainen T, Heinisuo M. Comparative study of multiple criteria decision making methods for building design. Adv Eng Inf 2012;26(4):716–26. https://doi.org/10.1016/j.aei.2012.03.001.

[20] Pohekar S, Ramachandran M. Application of multi-criteria decision making to sustainable energy planning—A review. Renew Sustain Energy Rev 2004;8(4):365–81. https://doi.org/10.1016/j.rser.2003.12.007.

[21] Hopfe CJ. Uncertainty and sensitivity analysis in building performance simulation for decision support and design optimization, PhD diss., Eindhoven University; 2009.

[22] Bertsch V. Uncertainty handling in multi-attribute decision support for industrial risk management. Univ.-Verlag Karlsruhe; 2007.

[23] Saaty TL. Multicriteria decision making: The analytic hierarchy process: Planning, priority setting. Resource Allocation 1990;2:1–20.

[24] Chiang C-M, Lai C-M. A study on the comprehensive indicator of indoor environment assessment for occupants' health in Taiwan. Build Environ 2002;37(4):387–92. https://doi.org/10.1016/S0360-1323(01)00034-8.

[25] Kim SH, Augenbroe G. Decision support for choosing ventilation operation strategy in hospital isolation rooms: A multi-criterion assessment under uncertainty. Build

Environ 2013;60:305–18. https://doi.org/10.1016/j.buildenv.2012.09.005.

[26] Kim S-S, Yang I-H, Yeo M-S, Kim K-W. Development of a housing performance evaluation model for multi-family residential buildings in Korea. Build Environ 2005;40(8):1103–16. https://doi.org/10.1016/j.buildenv.2004.09.014.

[27] Omar F, Bushby ST, Williams RD. Assessing the performance of residential energy management control Algorithms: Multi-criteria decision making using the analytical hierarchy process. Energy Build 2019;199:537–46. https://doi.org/10.1016/j.enbuild.2019.07.033.

[28] Yang K, Zhu N, Chang C, Wang D, Yang S, Ma S. A methodological concept for phase change material selection based on multi-criteria decision making (MCDM): A case study. Energy 2018;165:1085–96. https://doi.org/10.1016/j.energy.2018.10.022.

[29] Velasquez M, Hester PT. An analysis of multi-criteria decision making methods. Int J Oper Res 2013;10(2):56–66.

[30] Booth A, Choudhary R. Decision making under uncertainty in the retrofit analysis of the UK housing stock: Implications for the Green Deal. Energy Build 2013;64:292–308. https://doi.org/10.1016/j.enbuild.2013.05.014.

[31] D'Agostino D, Parker D, Melià P. Environmental and economic implications of energy efficiency in new residential buildings: A multi-criteria selection approach. 100412 Energy Strategy Reviews 2019;26. https://doi.org/10.1016/j.esr.2019.100412.

[32] P.S. marquis de Laplace, A philosophical essay on probabilities, Wiley; 1902.

[33] Wald A. Statistical decision functions which minimize the maximum risk. Ann Math 1945;265–80.

[34] Hurwicz L. The generalized Bayes minimax principle: a criterion for decision making under uncertainty. Cowles Comm Discuss Paper Stat 1951;335:1950.

[35] Savage LJ. The theory of statistical decision. J Am Stat Assoc 1951;46(253):55–67.

[36] Rysanek A, Choudhary R. Optimum building energy retrofits under technical and economic uncertainty. Energy Build 2013;57:324–37. https://doi.org/10.1016/j.enbuild.2012.10.027.

[37] Polasky S, Carpenter SR, Folke C, Keeler B. Decision-making under great uncertainty: environmental management in an era of global change. Trends Ecol Evol 2011;26(8):398–404. https://doi.org/10.1016/j.tree.2011.04.007.

[38] Kotireddy R. Toward robust low energy housing-A computaional approach for performance robustness assessment using scenario analysis, PhD diss, Eindhoven University of Technology; 2018.

[39] Chinazzo G, Rastogi P, Andersen M. Assessing robustness regarding weather uncertainties for energy-efficiency-driven building refurbishments. Energy Procedia 2015;78:931–6. https://doi.org/10.1016/j.egypro.2015.11.021.

[40] Buso T, Fabi V, Andersen RK, Corgnati SP. Occupant behaviour and robustness of building design. Build Environ 2015;94:694–703. https://doi.org/10.1016/j.buildenv.2015.11.003.

[41] Karjalainen S. Should we design buildings that are less sensitive to occupant behaviour? A simulation study of effects of behaviour and design on office energy consumption. Energy Efficiency 2016;9(6):1257–70.

[42] Gang W, Wang S, Xiao F, Gao D-C. Robust optimal design of building cooling systems considering cooling load uncertainty and equipment reliability. Appl Energy 2015;159:265–75. https://doi.org/10.1016/j.apenergy.2015.08.070.

[43] Nik VM, Kalagasidis ASJB. Environment, Impact study of the climate change on the energy performance of the building stock in Stockholm considering four climate uncertainties. Build Environ 2013;60:291–304. https://doi.org/10.1016/j.buildenv.2012.11.005.

[44] Li H, Wang S, Tang R. Robust optimal design of zero/low energy buildings considering uncertainties and the impacts of objective functions. 113683 Appl Energy 2019;254. https://doi.org/10.1016/j.apenergy.2019.113683.

[45] Fowlkes WY, MCreveling C. Engineering methods for robust product design: using

Taguchi methods in technology and product development. Addison-Wesley Publishing Company; 1995.

[46] Standard Norge (2016) SN/TS 3031:2016 Energy performance of buildings. [cited 2020 01/07]; Available from: https://www.standard.no/nyheter/nyhetsarkiv/bygg-anlegg-og-eiendom/2016/snts-30312016-for-beregning-av-energibehov-og-energiforsyning/.

[47] Felius L, Thalfeldt M, Georges L, Hrynyszyn B, Dessen F, Hamdy M, et al. Wood burning habits and its effect on the electrical energy demand of a retrofitted Norwegian detached house. IOP conference series: earth and environmental science. IOP Publishing; 2019. p. 012022.

[48] Hamdy M, Carlucci S, Hoes P-J, Hensen JL. The impact of climate change on the overheating risk in dwellings—A Dutch case study. Build Environ 2017;122:307–23. https://doi.org/10.1016/j.buildenv.2017.06.031.

[49] Kotireddy R, Hoes P-J, Hensen JL. Integrating robustness indicators into multi-objective optimization to find robust optimal low-energy building designs. J Build Performance Simul 2018:1–20. https://doi.org/10.1080/19401493.2018.1526971.

[50] Byggteknisk forskrift (TEK 17). [cited 2020 01/07]; Available from: https://dibk.no/byggereglene/byggteknisk-forskrift-tek17/14/14-2/.

[51] Standard Norge (2014) NS-EN 15251:2007 + NA:2014 Indoor environmental input parameters for design and assessment of energy performance of buildings addressing indoor air quality, thermal environment, lighting and acoustics. [cited 2020 01/07]; Available from: https://www.standard.no/nyheter/nyhetsarkiv/bygg-anlegg-og-eiendom/2012/norskstandard-for-inneklima/.

[52] Rønneseth Ø, Satrori I. Method for modelling Norwegian single-family house in IDA ICE. The research centre on zero emission neighbourhoods (ZEN) in smart cities. 2018.

[53] IEE Project TABULA (2009 - 2012). [cited; Available from: https://episcope.eu/iee-project/tabula/.

[54] EQUA Solutions AB Ida indoor climate and energy (version 4.8). [cited 2020 01/07]; Available from: https://www.equa.se/en/ida-ice.

[55] Standard 140-2001-standard method of test for the evaluation of building energy analysis computer programs, in, ASHRAE Engineers, AtlantaGA; 2017.

[56] Nord N, Qvistgaard LH, Cao G. Identifying key design parameters of the integrated energy system for a residential Zero Emission Building in Norway. Renewable Energy 2016;87:1076–87. https://doi.org/10.1016/j.renene.2015.08.022.

[57] H.M.D. Bente Halvorsen, Ta hjemmetempen, in, Statistics Norway; 2012.

[58] Bennet IOB. Whiliam, Simulation-based evaluation of high-rise residential building thermal resilience. ASHRAE Trans 2016;122.

[59] Peeters L, De Dear R, Hensen J, D'haeseleer W. Thermal comfort in residential buildings: Comfort values and scales for building energy simulation. Appl Energy 2009;86(5):772–80. https://doi.org/10.1016/j.apenergy.2008.07.011.

[60] Lukas L. Weather data for building simulation New actual weather files for North Europe combining observed weather and modeled solar radiation, School of Sustainable Development of Society and Technology, Mälardalen University of Sweden; 2012.

[61] Karlsen SS, Hamdy M, Attia S. Methodology to assess business models of dynamic pricing tariffs in all-electric houses. 109586 Energy Build 2020;207. https://doi.org/10.1016/j.enbuild.2019.109586.

[62] Kalkman A. Calculation of energy consumption in dwellings: theory and field data. In: Presented at the one day forum of the "5th meeting of IEA Annex 53", in, Rotterdam, The Netherlands; 2012.

[63] Thomas D, Deblecker O, Ioakimidis CS. Optimal operation of an energy management system for a grid-connected smart building considering photovoltaics' uncertainty and stochastic electric vehicles' driving schedule. Appl Energy 2018;210:1188–206. https://doi.org/10.1016/j.apenergy.2017.07.035.

Paper II

Quantification of energy flexibility and survivability of all-electric buildings with cost-effective battery size: methodology and indexes

Shabnam Homaei and Mohamed Hamdy

Quantification of Energy Flexibility and Survivability of All-Electric Buildings with Cost-Effective Battery Size: Methodology and Indexes

Shabnam Homaei * and Mohamed Hamdy

Department of Civil and Environmental Engineering, Norwegian University of Science and Technology (NTNU), 7491 Trondheim, Norway; Mohamed.hamdy@ntnu.no
* Correspondence: shabnam.homaei@ntnu.no; Tel.: +47-9251-5899

Abstract: All-electric buildings are playing an important role in the electrification plan towards energy-neutral smart cities. Batteries are key components in all-electric buildings that can help the demand-side energy management as a flexibility asset and improve the building survivability in the case of power outages as an active survivability asset. This paper introduces a novel methodology and indexes for determining cost-effective battery sizes. It also explores the possible trade-off between energy flexibility and the survivability of all-electric buildings. The introduced methodology uses IDA-ICE 4.8 as a building performance simulation tool and MATLAB® 2017 as a post-processing calculation tool for quantifying building energy flexibility and survivability indexes. The proposed methodology is applied to a case study of a Norwegian single-family house, where 10 competitive designs, 16 uncertainty scenarios, and 3 dynamic pricing tariffs suggested by the Norwegian regulators are investigated. The methodology provides informative support for different stakeholders to compare various building designs and dynamic pricing tariffs from the flexibility and survivability points of view. Overall, the results indicate that larger cost-effective batteries usually have higher active survivability and lower energy flexibility from cost-effectiveness perspective. For instance, when the time of use tariff is applied, the cost-effective battery size varies between 40 and 65 kWh (daily storage). This is associated with a cost-effective flexibility index of 0.4–0.55%/kWh and an active survivability index of 63–80%.

Keywords: energy flexibility; survivability; load shifting; tariff; battery sizing; cost-effectiveness; all-electric buildings

1. Introduction

1.1. Building Electrification

Electrification of the energy use in the final sectors has been highlighted as an important pathway to decarbonizing energy systems [1]. In particular, the heating [2] and transport [3] sectors are receiving considerable attention in the electrification era. Heating demand accounts for a significant share of total energy use in the European building sector [4], providing the grounds for moving toward building electrification and all-electric buildings. Currently, some end uses, such as lighting, appliances, and refrigeration are already dominated by electricity in the building sector. All-electric buildings use electricity for other end uses, such as heating, domestic hot water, cooking, and cooling, that are usually powered by other sources of energy (e.g., fossil fuels). Heat pumps are one of the enabling technologies for widespread building electrification and their growing usage at the EU level and in general are highlighted by the European Heat Pump Association (EHPA) [5] and the International Energy Agency (IEA) [6], respectively. So, electrification of the building sector plays an important role in the decarbonization process along with the application of other strategies such as providing building demands from hydrogen, waste-heat reuse [7], combined heat and power (CHP), and district heating systems (DH).

Implementation of renewable energy sources (RES) along with electrification will increase the share of clean and zero-carbon electricity in the grid during the operational phase. However, it should be noted that these energy sources actually consume a large amount of energy and emit emissions during their life cycle. Furthermore, energy production from renewable sources is intermittent [8], fluctuates [9], difficult to forecast [10], and requires strategies for balancing supply and demand [11]. In addition, electrification of residential heating and transportation can increase peak loads and require both greater generation and grid capacity [12]. Norway can be a good representative case for this condition. Norwegian power production is largely dominated by hydropower (95%) [13], and the electricity generated from hydropower is the main energy source for Norwegian dwellings. The availability of relatively cheap electricity has increased the usage of electric-based heating systems [14], the share of electric vehicles, and so on. For instance, 63.1% of the space heating and 96.2% of the domestic hot water (DHW) in Norway are produced by electricity [15]. Furthermore, Norway remained the global leader in terms of electric car market share at 56% of its new car sales in 2019, more than double the second-largest market share in Iceland at 22% [16].

1.2. Demand Response

Demand-response (DR) programs can be used to decrease the fluctuation in energy production via renewable sources, fully utilize the generated energy, and balance the power grid and relieve it during peak loads [17]. Different techniques, such as peak shaving, load shifting, valley filling, and minimizing curtailment time, can modulate building load in DR programs [18]. These programs are generally categorized into two groups [19]: incentive-based DR programs, where economic incentives are provided by utilities, load serving entities, or a regional grid operator in order to decrease customer demand during a capacity shortage or times of high electricity prices, and price-based DR programs, where customers change their normal electricity usage patterns in response to dynamic pricing tariffs. Both of these approaches have their own advantages and drawbacks [20]. Dynamic pricing tariffs are one of the most important DR programs and encourage users to consume more wisely and efficiently. They utilize different schemes, such as time of year (seasonal) pricing, time of use pricing (daily or weekly), critical-peak pricing, and real-time pricing [21]. There are some studies in the literature that have simulated households' behaviors under time-based prices [22]. Achieving energy efficient, renewably based, smart, and flexible buildings is one of the goals of the European Green Deal, which focuses on full decarbonization by 2050 [23].

1.3. Energy Flexibility

Application of DR programs can lead to adjustments in power system supply and demand, which is known as flexibility [24]. Flexible loads in residential buildings are related to household appliances (e.g., washing machines and dishwashers), electric vehicles, and space or water heating systems. There are survey-based studies that have shown that participants are willing to shift their white goods loads as flexible loads when it comes to variable pricing schemes [25]. Laicane et al. investigated the potential of demand side management with assessing load shifts in the washing machine and dishwasher usage and showed that these load shifts can decrease the dwelling peak load by 24% and 13.5%, respectively [26]. The participation of electric vehicles in the price-based DR programs in commercial, industrial, and residential areas is studied in [27], which concludes that there is a good efficiency in the reduction of electricity use when price-based demand response is used in combination with electric vehicles (EVs). Moreau evaluated the load shift for water heaters and proposed a control strategy in order to minimize the peak load at the end of shifting time [28]. In [29], Mancini and Nastasi evaluated the impact of energy retrofitting on the energy flexibility of dwellings in a scenario, which is focusing on greater electrification of consumption. They concluded that electrified systems are facing a considerable increase in flexible loads in comparison to the gas-fed systems. Achieving flexibility in residential buildings is generally possible when storage systems are used as

flexibility assets, depending on the energy system and types of DR programs [30]. Storage systems are categorized as electrical (e.g., batteries), active thermal, or passive thermal storage. These systems can be utilized as stand-alone storage systems or coupled with other technologies, such as heat pumps and combined heat and power systems (CHPs) [31,32]. Within the electrical storage category, battery storage is usually considered to be a flexibility asset with a time step of several hours, during which it can shift energy consumption from high-tariff to low-tariff periods or reduce the peak demand. Battery storage systems are modular and allow a wide range of applications. The falling cost of batteries and their combination with hybrid systems has made them an attractive storage option for homeowners [33]. A variety of optimization efforts in terms of sizing battery storage in combination with renewable energy sources have been undertaken for buildings [34–37]. For instance, Dmount et al. evaluated the integration of battery storage in a positive energy building equipped with energy systems, such as heat pumps and photovoltaic (PV) systems [38]. In addition, [39] implemented battery storage in combination with dynamic pricing tariffs in order to establish a dynamic interaction between the building and smart grid. Furthermore, it has been shown that batteries have great potential in terms of providing power for customers during power outages [40,41]. For instance, Tsianikas et al. [42] investigated optimized grid-outage resilient PV and battery systems from an economic point of view. The survivability of a solar energy system with local storage in the presence of a power outage was investigated in [43]. In this work, a certain percentage of battery capacity was reserved in case of a power outage. However, most studies on using batteries to achieve building survivability and resilience have focused on combinations of batteries (as storage systems) and renewable energy sources [44]. When put together, the above literature on building energy flexibility and survivability provides important insights into the application of batteries as "flexibility assets" for harnessing building energy flexibility and as "backup storage" for improving building survivability in the case of power outages. Furthermore, battery capacity can play an important role in the quantification of energy flexibility and survivability. However, far too little attention has been paid to the energy flexibility and survivability trade-off from a cost-effectiveness perspective.

1.4. Innovative Contributions

The aim of this work is to propose a methodology for exploring the trade-off between energy flexibility and survivability in all-electric buildings from a cost-effectiveness perspective in the context of dynamic pricing tariffs. The main contributions of this paper can be expressed as:

- Load shift calculation of electric-based heating demand in response to different business models for dynamic pricing tariffs.
- Formulation of a model to determine the cost-effective battery size needed for storing the shifted load.
- Introduction of the concept of "active survivability" in the context of all-electric buildings.
- Introduction of new flexibility and survivability indexes for the comparison of the possible designs for an all-electric building under different dynamic pricing tariffs.

These contributions have been achieved by developing a MATLAB-based algorithm. Two new indicators, the Cost-Effective Flexibility Index (CEFI) and Active Survivability Index (ASI), are introduced along with the proposed methodology. The CEFI allows the identification of energy flexibility in response to dynamic pricing tariff, and the ASI indicates the survivability of a building in the case of a power outage from an economical point of view. The CEFI and ASI generally depend on cost-effective sizes for the batteries selected for storing the heat shift and can be used in the case of power outages as backup storage. Furthermore, a set of designs known as competitive designs are implemented in this paper to allow comparisons of the energy flexibility and survivability of building designs with the same energy targets. In addition, uncertainties in building operation and external conditions can have an impact on the energy flexibility and survivability of

building designs under different dynamic pricing tariffs. For this reason, weather and occupant scenarios are created to gauge the impact of these uncertainties on energy flexibility and survivability under different dynamic pricing tariffs. Indeed, the main novelty of this work is the exploration of the trade-off between the energy flexibility and survivability of all-electric buildings, potentially opening the door to more complex concepts such as energy-resilient buildings. Furthermore, the algorithm developed in this paper can be adjusted for different dynamic pricing tariffs at the country, city, or neighborhood level and can be used for all-electric buildings, which represent a growing trend (both in heating-dominated building in cold climates and cooling-dominated buildings in hot climates). Different stakeholders in the grid markets, such as policy makers, grid companies, building designers, and homeowners, can take advantage of this algorithm to evaluate the performances of buildings from flexibility and survivability perspectives with two easy-to-understand indicators.

To achieve the above mentioned goals, three different business models of dynamic pricing tariffs suggested by the Norwegian regulators are considered, along with ten different building designs with the same energy target for an all-electric Norwegian single-family house. In order to investigate the impacts of uncertainties on energy flexibility and survivability, 16 scenarios (eight occupant scenarios × two weather scenarios) are proposed, and the impacts of these uncertainties on energy flexibility and survivability are evaluated. The paper proceeds as follows: Section 2 provides overviews of cost-effective battery sizing and the energy flexibility and survivability quantification method, along with the requirements for using it. In Section 3, the proposed method is investigated using a case study of an all-electric Norwegian single-family house involving detailed descriptions of 10 different building designs and 16 weather and occupant scenarios. The results of this case study are presented and discussed in Section 4. A summary of the methodology, along with the main conclusions, is presented in Section 5.

2. Methodology

In this section, we present the research methodology, including the study concept. This methodology combines building performance simulation (BPS) and an in-house algorithm developed in MATLAB. Figure 1 shows the conceptual framework of the study, which consists of three stages: algorithm input, algorithm development, and algorithm output. These parts will be described in the following subsections.
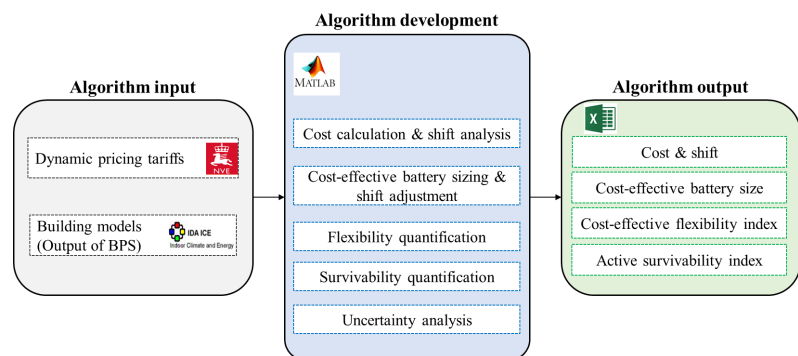
Figure 1. The conceptual framework of the study.

2.1. Algorithm Input

Different business models for the dynamic pricing tariffs and energy consumption resulted in building performance simulations are the required input data for the developed algorithm.

2.1.1. Business Models for Dynamic Pricing Tariffs in Norway

Today, Norwegian residential customers are faced with an energy-based grid rent tariff known as the "energy rate tariff model", which consists of two parts: one fixed part and one volumetric part [45]. The fixed part is an annual cost that covers the costs associated with customer management and support and is the same for all customers. The volumetric part is an energy charge that is user-dependent and reflects energy consumption. This grid tariff does not differentiate between high and low power drains [46]. To solve this issue, dynamic pricing tariffs are recommended to incentivize better grid utilization [47]. Therefore, the Norwegian Water Resource and Energy Directorate (NVE) has proposed a new grid rent tariff to incentivize load shifts and peak load reductions in buildings [48]. The new tariff combines three different business models that allow for either higher costs during high-demand periods (time of use tariff), or higher costs for the power demands that exceed higher than a subscribed level (measured power rate tariff and tiered rate tariff). These tariffs will be illustrated in the following parts and Figure 2. It should be noted that the values presented for each tariff (Table 1) are average numbers, which can vary between different distribution companies [46]. The other values related to taxes or levies are added to the grid rent tariff [49].

- Measured power rate tariff model.

This tariff consists of three different parts: a fixed part, an energy part, and a power part. The fixed part and the energy part are similar to parts in the energy rate tariff model, but the values can be changed. For instance, the value used in the energy part for the measured power rate tariff is less than that used in the energy rate tariff. The power part is determined based on the highest peak power outtake during the measurement period, and it is recommended that this part to be measured on a daily basis in the Norwegian regulations in order to match customer and grid peak demands [50]. However, for industrial customers, all of whom are using the measured power rate tariff currently, the highest peak period is measured on a monthly basis.

- Tiered rate tariff model.

This tariff consists of four different parts: a fixed part, a subscription limit, an energy part, and an overuse part. For this tariff, the customer subscribes to a capacity level (subscription limit), and, based on their violations of this level, a penalty (overuse part) is charged. In the short term, implementation of the penalty sends a price signal to the customer to reduce their consumption when it exceeds the subscription limit. On the other hand, in the long term, it helps customers to select a subscription limit leading to the lowest yearly costs. For most ordinary customers, the high and low power drains on the customer side are matched with high and low stress on the grid side, respectively. The overuse is applied to power drains above the limit, even when the grid has a good capacity. In this case, it will not create any benefits for the grid side. Furthermore, if the customer meets the subscription limit, he/she does not need to reduce his/her power drain, even when the grid is under high stress. These issues are the drawbacks of the tiered rate tariff model. In this study, we used an individual annual subscription that customers can select themselves or with help of grid distribution companies that cannot be changed over the course of a year. A Norwegian regulator sets a minimum usage of 1 kW but does not suggest exact power limits. This study considered ten limits. The appropriate power limit should be selected in this tariff to prevent high subscription or overuse costs.

- Time of use tariff model.

For this tariff, the electricity prices are set for specific time periods such as peak and off-peak hours. The peak hours are hours that have historically had high grid pressure, and the time of use tariff assigns higher energy prices to these hours. The time of use model suggested by the Norwegian regulator uses higher prices on winter days because they face grid stress [51]. Customers can understand this tariff easily because it differentiates pricing according to blocks of time and offers pricing terms of energy consumption (kWh)

instead of power (kW), which is used in the two previous tariffs. The dependence of the pricing on blocks of time (two peak and off-peak blocks) makes this tariff rather unfit going forward with a higher penetration of intermittent generation unless it is coupled with other dynamic pricing strategies, such as critical peak pricing (CPP). Illustrations of the introduced tariffs for typical winter and summer days, along with the values for the different parts of each tariff, are provided in Figure 2 and Table 1, respectively.
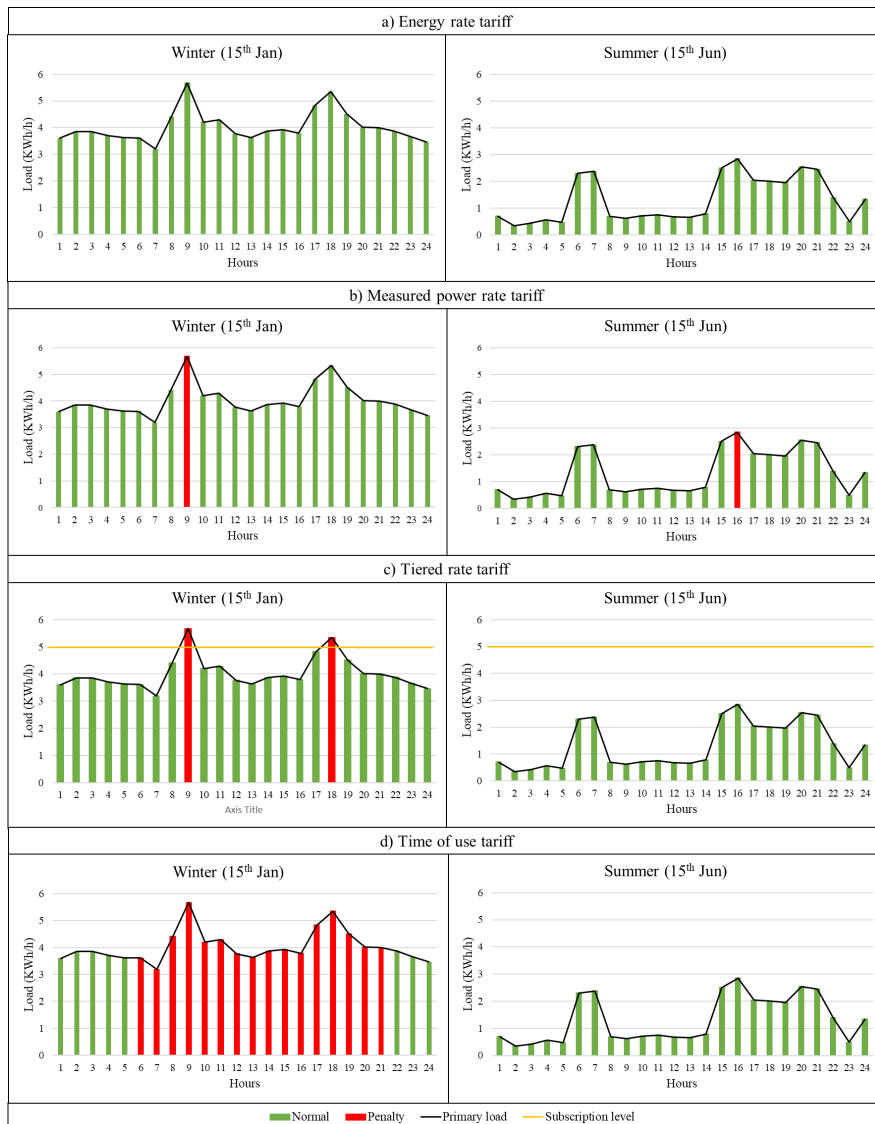
Figure 2. Illustration of: (**a**) Energy rate tariff, (**b**) measured power rate tariff, (**c**) tiered rate tariff, and (**d**) time of use tariff in typical winter and summer days. The illustration shows hourly loads over 24 h for the example single-family house. The penalized hours in each tariff are shown in red.

Table 1. Grid tariff rents for residential buildings in the energy rate tariff, measured power tariff, tiered rate tariff, and time of use tariff.

Energy Rate Tariff			
Fixed cost (€ /year)	Energy cost (€ /kWh)	-	-
174.9	0.0194	-	-
Measured Power Rate Tariff			
Fixed cost (€ /year)	Energy cost (€ /kWh)	Power cost (€ /kWh/h)	-
174.9	0.005	0.186	-
Tiered Rate Tariff			
Fixed cost (€ /year)	Energy cost (€ /kWh)	Subscription cost (€ /kWh/h)/year	Overuse cost (€ /kWh/h)
174.9	0.005	68.9	0.1
Time of Use Tariff			
Fixed cost (€ /year)	Summer energy cost (€ /kWh)	Winter day energy cost (€ /kWh)	Winter night energy cost (€ /kWh)
174.9	0.0122	0.038	0.0152

2.1.2. Building Models

Based on Figure 1, the building loads (including space heating, domestic hot water, etc.) are the second input of the developed algorithm. It is supposed that the building loads will be estimated in the early design phase using building performance simulation tools. The energy simulations for building models were conducted via the building performance simulation software IDA Indoor Climate and Energy (ICE), version 4.8 [52]. This dynamic, whole-building software applies equation-based modeling in Neutral Modeling Format (NMF) and has been validated using several validation tests [53,54]. A detailed dynamic of energy supply and system component can be simulated in this software, making it possible to evaluate the energy consumption and indoor climate of the building. In this study, the result of the simulation in IDA ICE was entered as an input to the developed algorithm to calculate the amount of shifted load and battery capacity and other parameters. The simulations were performed using a typical climate file (IWEC) from IDA ICE library [52].

2.2. Algorithm Development

The developed algorithm in this paper is a MATLAB-based (MATLAB 2017 [55]) algorithm coupled with IDA ICE, which is based on a previous work done at the Norwegian University of Science and Technology [51]. While the previous work focused on an Excel-based algorithm for calculating the costs and ideal heat shifts for each business models of dynamic pricing tariffs, the current MATLAB-based algorithm adjusts the ideal shift based on the cost-effective battery size and adds a method for the quantification of energy flexibility and survivability of all-electric buildings. In the first step, the building design and tariff to be used are selected. After this step, the algorithm takes the hourly energy demand simulated for the building design in IDA ICE and computes the building's energy costs under the selected tariff. After the cost calculation, the shifted load are calculated by implementing a signal referred to as the ideal heat shift signal (heat consists of electric-based space heating and the domestic hot water load), which is explained in more detail in Section 2.2.1. In the next step, the battery capacity for storing the shifted heat is determined based on the cost-effectiveness, producing the cost-effective battery size. The shift is then adjusted according to the cost-effective battery size. Thereafter, two new indexes are introduced for quantifying the energy flexibility and survivability of the building design under the selected tariff. In the last step, the building model and dynamic pricing tariff

will be changed, and the procedure continues until all building models under all tariffs have been considered. The flow diagram for this procedure is shown in Figure 3 and is explained in more detail in the upcoming sections.
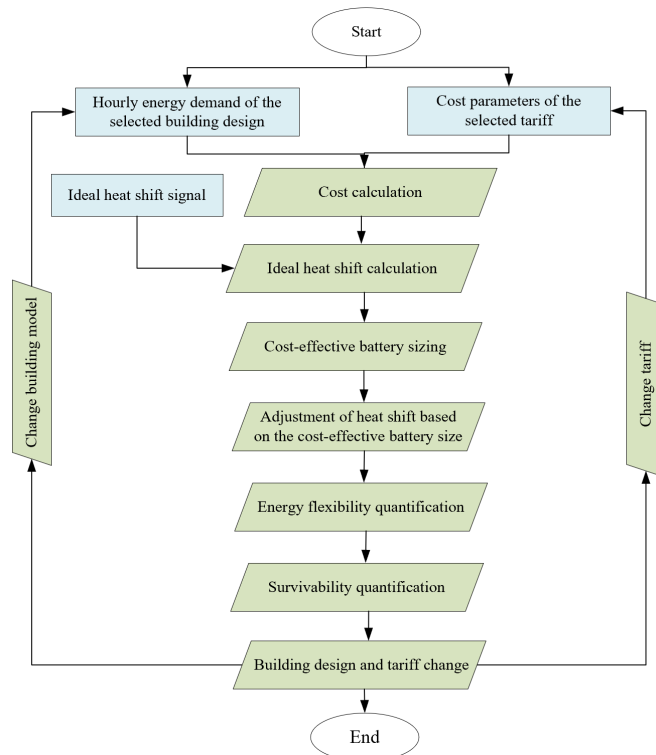
Figure 3. Flow diagram of the algorithm developed in MATLAB.

2.2.1. Cost Calculation and Shift Analysis

To calculate the energy costs of different building designs under the suggested business models for the dynamic pricing tariffs, the hourly energy demand taken from the building simulation (Section 2.1.2) and the values related to different parts of the dynamic pricing tariffs (Table 1) are entered as input data, and the cost calculation algorithm computes the costs of the different designs for each tariff.

Load shifting is one of the strategies that can be used with price-based DR programs. Flexible loads in the residential buildings can be categorized as belonging to household appliances, electric vehicles, space heating and cooling, and domestic hot water. Given the different business models for the dynamic pricing tariffs suggested by the Norwegian regulator, the electric-based heating load (consists of space heating and domestic hot water) is considered to be the shifted in this paper. This load has been selected for the following reasons: First, space heating and domestic hot water combine to form the largest share of a building's energy consumption in countries with cold climates, such as Norway. Second, shifting other loads, such as household appliances loads, amounts to running them at night or when no one is home. This strategy will lead to lower energy costs, but it has disadvantages, such as the risk of fire [51]. Furthermore, the energy source for most Norwegian residential buildings is electricity. Therefore, we can focus on electric-based heat shifting without sacrificing thermal comfort and use batteries without including thermal storage. The proposed methodology can also be adjusted and used for shifting the

cooling load in countries with hot climates. Based on the work of Karlsen et al. [51], the ideal heat shift is considered first in this paper. The ideal heat shift is a theoretical optimum amount of shift that leads to the lowest costs with respect to the implemented tariff [51]. In the next steps, the amount of this shift will be adjusted based on the cost-effective battery size that is selected for storing the shift. The assumptions for this ideal load shift are as follows:

- The ideal heat shift consists of the space heating and domestic hot water loads.
- The ideal heat shift will not sacrifice the occupant's comfort (regarding space heating and domestic hot water).
- The storage of the shifted load is considered in a daily-based manner (kWh/day).
- No losses are considered during the ideal load shift.

The implementation of the ideal load shift for each of the suggested business models of the dynamic pricing tariff leads to specific load profiles and shift patterns for each tariff, which are shown in Figure 4. The following points should be considered regarding the shifting patterns in each business model for the dynamic pricing tariffs.
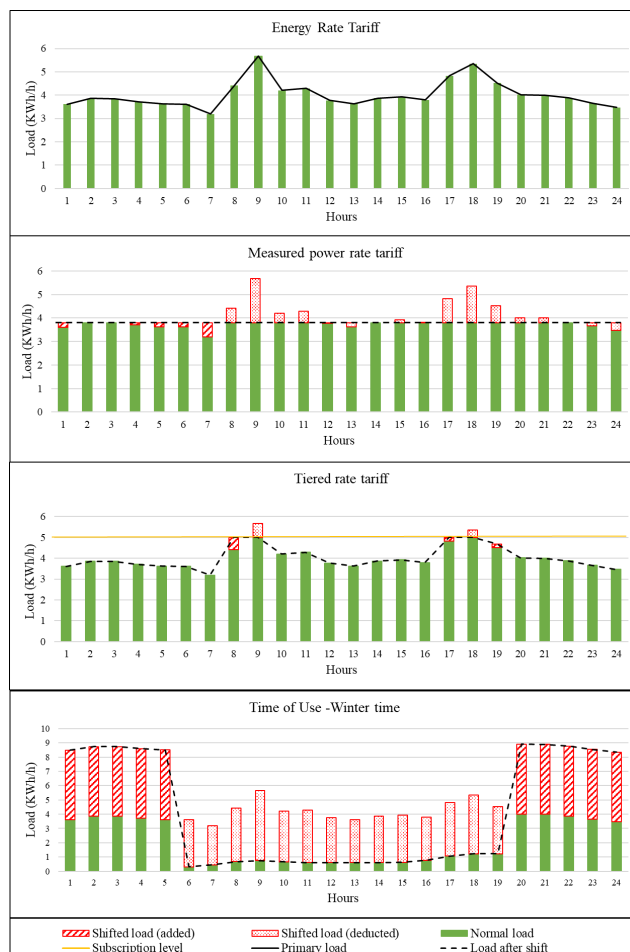
Figure 4. The winter load profiles for the ideal heat shifts of different business models of dynamic pricing tariffs.

- The energy rate tariff applies the same energy price during all hours of the year, so load shifting under this tariff will not be beneficial from the customer's point of view. Even though shifting can remove the stress from the grid in peak hours, no shifts will be implemented as long as they are not beneficial. In addition, no one will pay for the storage of the shifted load without receiving benefits. Hence, the load profile remains constant for the energy rate tariff.
- In the measured power rate tariff, the daily peak power cost is a part of the cost, which can be reduced without having an impact on the demand. The minimum daily peak cost can be achieved when the peak is as low as possible, thus creating a constant load profile after the shift. This constant value is the maximum of the plug load (plug load = total load − heating load) and the daily average heating load. This value is selected to meet the plug load during all hours of the day and minimize the peak of the heating load. If the load profile has smaller peaks distributed across a wide area, the cost reduction will be small. On the other hand, higher peaks of short duration can lead to greater cost reductions. So, the implementation of the ideal load shift is recommended for loads with high peaks with short duration.
- For the tiered rate tariff, the overuse cost can be reduced without impacting the demand. Thus, the heating loads for the hours with demands higher than the subscription level will be shifted to the hours with loads below the subscription level, reducing the overuse cost to zero.
- For the time of use tariff, the heating loads that occur during the penalized hours (winter days, red hours in Figure 2) should be shifted to the normal hours (winter nights, green hours in Figure 2). Because all summer hours have the same energy costs, the ideal heat shift will have no impact during the summer.

2.2.2. Cost-Effective Battery Sizing and Shift Adjustment

The implementation of battery storage, along with demand side management, is important in terms of increasing self-consumption and reducing peak power periods in the grid [56]. In the Norwegian context, reducing energy use during peak load hours is considered an important objective. For this reason, home storage solutions are gaining importance, and it has been suggested that storage capacities be added to building regulations [57]. Furthermore, the Research Center on Zero Emission Neighborhoods in Smart Cities (FMEZEN) indicates that the introduction of energy storage and smart control methods can be a useful option for reducing energy costs when the new tariffs suggested by the Norwegian regulator are implemented [56]. In addition, even though power outages are rare in high-income countries, batteries can play an important role in buildings' power supply stability [58]. This study focuses on batteries for storing the daily heat shift and using the stored shift in the batteries as backup storage in case of power outages. Even though, thermal storage (i.e., active or passive) can be considered as possible options for storing daily shift, the focus of this study is on batteries as electrical storage for the shift storage. The strategy used for battery sizing in this paper is called the "cost-effective battery sizing strategy". This strategy focuses on the daily capacity that is needed for shift storage and selects the cost-effective capacity based on the amount of daily shift storage and its distribution. The cost-effective capacity can cover the storage capacities that have a high probability of happening daily over the course of a year and will be enough for most of the days of the year (not all days of the year). Of course, there will be some days during the year that the cost-effective battery capacity will not be able to cover, but the storage capacities for these days are neglected because they have lower probabilities of occurrence.

The selection of the cost-effective battery size based on the amount of daily storage and its distribution is shown in Figure 5. For example, a design can have a daily storage distribution that is skewed toward the higher levels, leading to a higher battery capacity. Likewise, when the daily storage distribution is skewed toward the lower levels, a smaller battery capacity will be needed. Figure 5 shows the box plot of the daily storage capacity needed for the ideal heat shift in a typical building over the course of a year. The cost-

effective battery capacity is based on the maximum capacity necessary in the box plot, which is indicated with a red box (C_{Bat}) in Figure 5. It should be noted that this value is not the maximum value in the outlier part. The capacity data in the outlier part of the box plot are neglected in order to concentrate on cost-effectiveness. So, if the distribution of the daily storage has some data in the outlier part of the box plot, then the selected battery capacity may not be sufficient for storing the entire ideal shift (IHS). This lack of storage will deduct some part of the shift from the ideal heat shift, creating what will be called the effective heat shift (EHS) in this paper. It should be noted that when the box plot does not have an outlier section, the EHS will be equal to the IHS. In distributions with outliers, the EHS will be less than the IHS. The deducted part of the shift (the difference between the IHS and EHS) can be stored in large-scale, centralized neighborhood batteries. This paper focuses on just the cost-effective batteries at the building scale and does not consider large-scale, centralized batteries. Furthermore, it should be noted that the cost-effective battery capacity provides a battery size that can be used by designers and decision makers in the concept design stage and it is not capturing the details related to charge and discharge states of the battery, which may be needed in the detailed design stage. This can lead to some energy losses due to the charging and discharging efficiencies and can slightly increase the total energy use of the building, which has been neglected in this study.
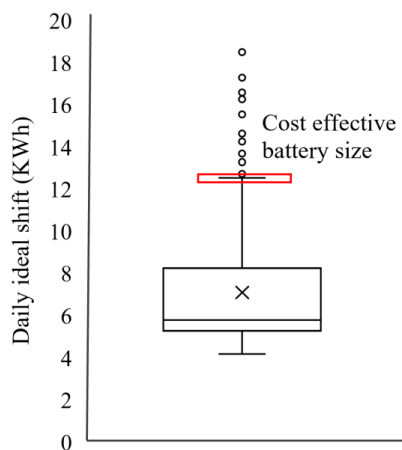
Figure 5. Illustration of determining the cost-effective battery sizing for a typical building.

2.2.3. Energy Flexibility Quantification

One of the approaches to analyzing energy-flexible buildings is the quantification of the flexibility potential of a building based on its response to a specific signal from energy systems [59,60]. In this approach, flexibility is quantified indirectly by analyzing the changes in the performance indicators, such as energy savings, peak power reductions, cost savings, and reductions in CO_2 emissions. The quantification method proposed in this study aims at calculating a single indicator (the cost-effective flexibility index (CEFI)), which shows the cost-effectiveness of the implemented battery for storing the heat shift as a flexibility asset. The CEFI divides the percentage of the cost savings achieved by the effective heat shift by the size of the cost-effective battery and creates an index in %/kWh that indicates the percentage savings that can be guaranteed if the cost-effective battery size is implemented in the building. If the implemented battery is smaller than the cost-effective battery size, the percentage of savings will be lower.

2.2.4. Survivability Quantification (Active + Passive)

A large part of the building literature is focused on the passive survivability of a building, which is defined as the ability to maintain the building in a safe thermal condition in the event of an extended loss of grid power [61]. This term is also known as thermal resilience because it focuses on building survivability from the thermal point of view only [62]. Passive survivability considers the length of time that a building remains in habitable thermal condition following a power outage from the grid [63]. The habitable thermal condition encompasses a wider range than the thermal comfort condition. For example, the habitable thermal condition in this paper is considered to be 15 °C $< T_{indoor} <$ 30 °C [63], which is wider than the thermal comfort range for living rooms suggested by the Norwegian standard (19 °C $< T_{indoor} <$ 26 °C) [64]. The length of time that passes between the onset of a power failure and when the temperature reaches 15 °C is called winter passive survivability. The time that passes between the power failure and when the temperature reaches 30 °C is called summer passive survivability. The sum of these two values constitutes the passive survivability index (PSI) in this work.

$$\text{PSI} = \text{Summer passive survivability} + \text{Winter passive survivability} \qquad (1)$$

The winter passive survivability and summer passive survivability are calculated by simulating a six-day power failure during the coldest and warmest weeks of the winter and summer, respectively. Because this study is focused on all-electric buildings, a new kind of survivability is introduced in this paper. This survivability is for all-electric buildings equipped with batteries and is called "active survivability". The term "active" is used here because batteries are added to the buildings as active solutions to protect them from power failures. Furthermore, this survivability focuses on more than the thermal condition, as it evaluates the survivability of all end uses, such as lighting, appliances, and domestic hot water. In this paper, active survivability is defined as the ability of the building and its storage system to maintain critical operations in the absence of grid power and is quantified with the "active survivability index (ASI)". The ASI divides the cost-effective battery capacity selected for the shift storage by the minimum energy needed for the building to maintain critical operations. Because the suggested survivability in this paper focuses on the survivability of all end uses in an all-electric building, the following assumptions are made when calculating the minimum energy consumption needed to maintain critical operations.

- The building heating setpoint is changed to 15 °C as the habitable threshold.
- The domestic hot water, lighting, and the appliance demand are decreased to 25% of the values suggested by SN/TS 3031 [65].

The simulation of the building designs under these conditions will calculate the minimum energy consumption necessary to maintain critical operations.

2.3. Algorithm Output

Based on the algorithm developed in the previous section, the following variables are defined in order to quantify the flexibility and survivability indexes.

i.   AC: The annual energy cost of the building without considering a heat shift (€/yr), which can be calculated for each design under the business models of dynamic pricing tariff. This value was calculated in Section 2.2.1.

ii.   ACIS: The annual energy cost of the building using the ideal heat shift (€/yr), which can be calculated for each design under the business models of dynamic pricing tariff. This value was calculated in Section 2.2.1.

iii. C_{Bat}: The cost-effective battery size (kWh), that is needed for storing the shifted heat. This value was determined in Section 2.2.2.

iv.   ACES: The annual energy cost of the building based on the effective heat shift (€/yr), which was calculated in Section 2.2.2.

v.　　E_{min}: The minimum energy needed by the building to maintain the critical operation (kWh), which is determined in Section 2.2.4.

vi.　　$SI = \frac{\Delta C}{AC} \times 100$: The savings index (%), which shows the benefit of utilizing a building's flexibility by dividing the cost savings by the annual costs before the shift, as defined by [9].

vii.　　$CEFI = \frac{SI}{C_{Bat}}$: The cost-effective flexibility index (%/kWh), which shows the cost effectiveness of a building's flexibility by dividing the SI by the cost-effective battery capacity.

viii.　　PSI : The length of time that the building can remain in the habitable thermal condition (15 °C< T_{indoor} < 30 °C) following a power outage from the grid.

ix.　　$ASI = \frac{C_{Bat}}{E_{min}} \times 100$: The active survivability index (%), which shows the percentage of the minimum energy needed in the critical condition that can be covered by the cost-effective battery used for shift storage. This value shows how helpful the battery can be in terms of the building's survival in the absence of power from the grid.

3. Application on the Case Study

A representative model of a Norwegian single-family house [66] was chosen as the case study building based on research conducted by Homaei and Hamdy [67]. This building is a two-story building located in Oslo. It has a floor area of 162 m^2 and is divided into three zones in a detailed model in the IDA ICE software. The zones consist of a representative dayroom (i.e., a combined zone for living room, kitchen, and entrance), bedroom, and bathroom. Occupancy schedules, domestic hot water distribution, and internal gains are derived from Nord et al. [68]. The developed model has been validated [67] and is flexible in terms of changing the design parameters and adding renewable energy sources (RES). Furthermore, external factors can be altered, such as occupant behavior and weather. This model is shown in Figure 6.
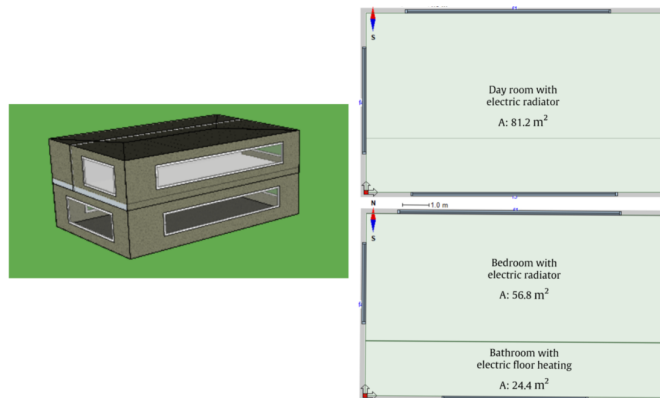
Figure 6. Layout and appearance of a representative single-family house with a floor area of 162 m^2.

Ten different building designs are suggested for this building model by changing the design parameters, including the building envelop, window-to-wall ratio (WWR), heating system, and implementation of RES. These designs are all competitive designs [67], which means that they all meet the same energy consumption and comfort requirement targets, which have been set based on the TEK 17 standard, the current set of minimum requirements in Norway [64]. For example, one design can achieve the target by combining a low-insulation envelope with very efficient energy and ventilation systems, while another design can achieve the targets via a highly insulated envelope and less efficient ventilation and energy systems. These competitive designs provide the opportunity to compare the flexibility and survivability of various designs having the same energy level. The characteristics of the ten designs are shown in Table 2. From the envelope point of view, the

overall U-value, the normalized thermal bridge, and the WWR ratio have been changed. The design options for heating system include direct electric heating with electric radiators with efficiencies near 99%, and the combination of electric radiators and indirect electric heating with an air source heat pump with a coefficient of performance (COP) of 3.2. Hence, the COP of the heat pump can decrease due to the low outside temperature during winter; as such, it has been combined with electric radiators in order to prevent undercooling. Options for the ventilation system include balanced mechanical ventilation with a heat recovery unit that has an efficiency of 80% and mechanical exhaust ventilation without a heat recovery unit. For lighting, in most of the designs, typical lighting (luminous efficacy of 12 W/m) is implemented, but in the designs with high energy demand, LED lighting (luminous efficacy of 60 W/m) is used in order to keep the total energy demand lower. In some designs, renewable energy systems such as solar thermal collectors (STC) or photovoltaics (PV) are implemented. Heat loss is neglected in all of the designs. It can be seen from Table 2 that all of these designs meet the energy consumption target for the building, which is 110 kWh/m^2 based on the TEK17 standard. Furthermore, buildings face various uncertainties during their operation and their performance can deviate from the set target. There are studies that evaluate the impacts of uncertainties on building performance. These uncertainties can be categorized as, for example, climate change [69], changes in economic factors [70], and variation in occupant behavior [71]. Other studies evaluate the impacts of uncertainties on the energy flexibility of buildings. For instance, Hu et al. [72] quantified the uncertainties related to occupancy and occupant behavior in terms of the aggregated energy flexibility in high-rise residential building clusters. Arteconi et al. [12] evaluated the influences of weather data and stratigraphy on the flexibility performances of buildings with electric heating and cooling systems. Hence, 16 different occupant behavior and weather scenarios are considered in this study. For the climate uncertainty, two climate files from The American Society of Heating, Refrigerating, and Air Conditioning Engineers (ASHRAE), IWEC and IWEC2, are used from the library of IDAICE [52]. For occupant behavior uncertainties, two heating setpoints, two shading strategies, and two window opening strategies were modeled. Further details regarding the modeling assumptions for occupant behavior and weather can be found in Homaei and Hmady's study [67] and Appendix A. The performance of each design was simulated across the 16 scenarios in IDA ICE. The total load profiles were then extracted from IDA ICE and imported into the algorithm developed in Section 2.2 to calculate the energy cost, the cost-effective battery size, and the CEFI, PSI, and ASI under the three dynamic pricing tariffs.

Table 2. Details of the ten competitive designs considered in the case study demonstration.

Design Parameters	Designs									
	D1	D2	D3	D4	D5	D6	D7	D8	D9	D10
Overall U-value (W/m^2·k)	0.31	0.25	0.43	0.36	0.33	0.29	0.51	0.44	0.40	0.35
Normalized thermal bridge (W/m^2·k)	0.05	0.03	0.07	0.05	0.03	0.02	0.06	0.07	0.06	0.05
WWR (%)	30	30	30	30	40	40	40	40	30	30
Heating system	ER	ER	ASHP + ER	ASHP + ER	ER	ER	ASHP + ER	ASHP + ER	ER	ER
Ventilation system	Balanced	Exhausted	Balanced	Exhausted	Balanced	Exhausted	Balanced	Exhausted	Balanced	Balanced
Solar DHW system size (m^2)	0	5	0	0	0	5	0	0	0	0
PV system size (m^2)	0	0	0	0	0	0	0	0	40	20
Lighting	Typical	LED	Typical	Typical	Typical	LED	Typical	Typical	Typical	Typical
KPI										
Total energy consumption (kWh/m^2)	110	110	110	110	110	110	110	110	110	110

4. Results and Discussion

As mentioned previously, in order to test the algorithm and evaluate the impacts of the occupant and weather uncertainties on a building's energy flexibility and survivability under different tariffs, the procedure explained in Section 2 was applied to the building models described in Section 3. The results are described in the following subsections. It should be noted that the results in each subsection are analyzed according to the designs and tariffs.

4.1. Cost and Shift Analysis

The energy demands of the ten designs have been investigated under 16 occupant and weather scenarios. The algorithm developed in MATLAB uses the hourly energy demand for each building design to compute its annual energy costs and the ideal and effective heat shifts for the four tariffs. Figure 7 shows the resulting annual costs (before and after the shifts) and effective load shifts. The following results can be obtained from Figure 7.
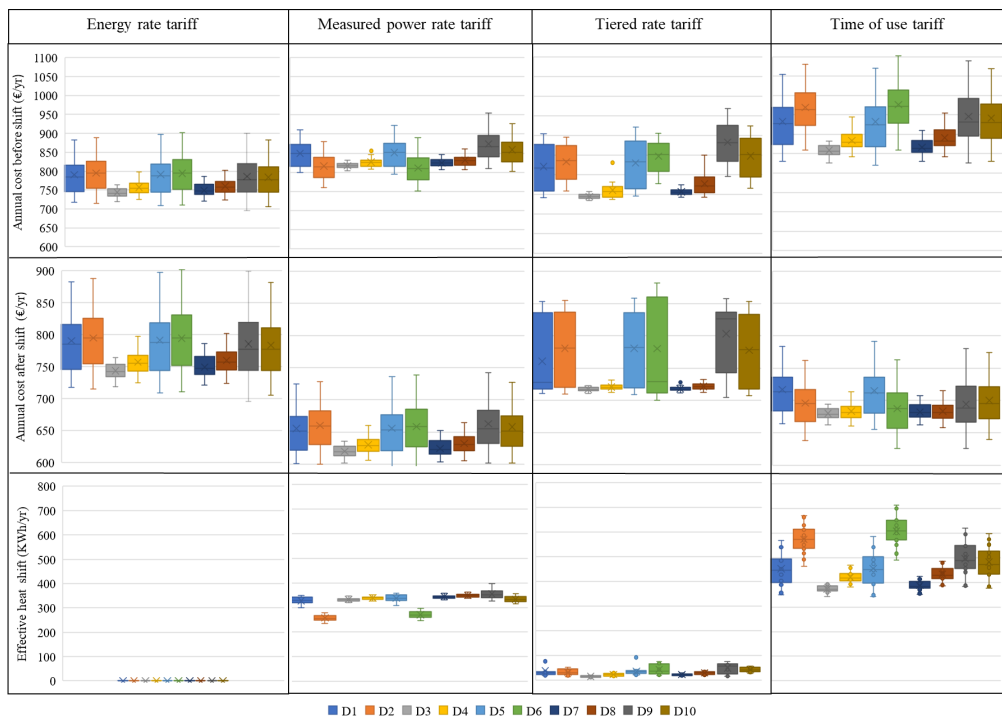
Figure 7. Annual costs (before and after shifts) and effective shifts for the ten designs across 16 scenarios and the different tariffs.

4.1.1. Annual Energy Costs before and after the Shift

First, the tariffs are compared in terms of costs, then a cost comparison is done for the different designs. In the base condition (without a shift), the cheapest tariff is the energy rate tariff across all design. This result makes sense because the energy rate tariff does not apply penalties and simply reflects the price of energy consumption. Furthermore, for most of the designs in the base condition, the most expensive tariff is the time of use tariff. A comparison of the tariffs without a shift shows that if customers do not change their load profiles under the tariffs, they will face an increase in grid rent. In other words, these tariffs should be viewed as incentives for the customers to change their consumption patterns. If the effective shift is applied, the energy rate tariff is the most expensive tariff because

it has no shift. The measured rate tariff has the minimum annual cost after the effective shift for most of the designs. The comparison of the annual costs before and after the shift reveals that the time of use tariff leads to the higher cost savings among the three tariffs with a shift. So, this tariff provides higher incentives for changing consumption patterns; however, it has a higher annual cost than the rest before the shift.

For the design comparison, the simulation results show that designs equipped with the combination of an electric radiator, ASHP, and balanced ventilation are less sensitive to uncertainties in comparison to the designs incorporating an electric radiator and exhaust ventilation. For example, in a scenario designed to increase the energy consumption, the increases in the amount of energy and the peak value needed for designs featuring an electric radiator will be greater than those for designs with an ASHP. The same holds true for balanced and exhaust ventilation. For this reason, Figure 7 shows that the average annual energy costs for the designs incorporating an ASHP (D_3, D_4, D_7, D_8) are less than the annual costs for the designs featuring just an electric radiator or exhaust ventilation (D_1, D_2, D_5, D_6, D_9, D_{10}) for the energy rate tariff, the time of use tariff, and the tiered rate tariff. Furthermore, for designs with the same energy system (e.g., D_3, D_4, D_7, D_8) and designs with air-balanced ventilation (e.g., D_3, D_7) have lower annual costs than the designs with exhaust ventilation (e.g., D_4, D_8). Under the measured power rate tariff, the situation is a bit different. For this tariff, the annual costs before the shift for designs D_2 and D_6 are less than the costs for other designs featuring an electric radiator. These two designs incorporate LED lights, and they have a smaller plug load compared to the other designs, decreasing their peak power costs during the summer compared to the other designs. In the other words, the main difference between D_2 and D_6 and the rest of the designs is that they require less peak power during the summer. A comparison of the daily shifts across a year for D_2, D_6, and D_1 (a typical design without LED lights) is shown in Figure 8. This figure shows that there are significant differences among the daily shifts for designs D_2, D_6, and D_1 during the summer. The LED lights, used to compensate for the higher demand (created by the implementation of the exhaust ventilation and electric radiator), are responsible for the observed differences.

If the effective shift is applied, the annual costs for the designs with a combination of an ASHP and electric radiator (D_3, D_4, D_7, D_8) are lower than the annual costs for the designs featuring an electric radiator only (D_1, D_2, D_5, D_6, D_9, D_{10}), except in the case of the energy rate tariff, for which no shift occurs. Furthermore, designs with higher costs in the base condition (without the shift) achieve greater cost reductions when the load shift is applied (e.g., designs featuring an electric radiator and exhaust ventilation).
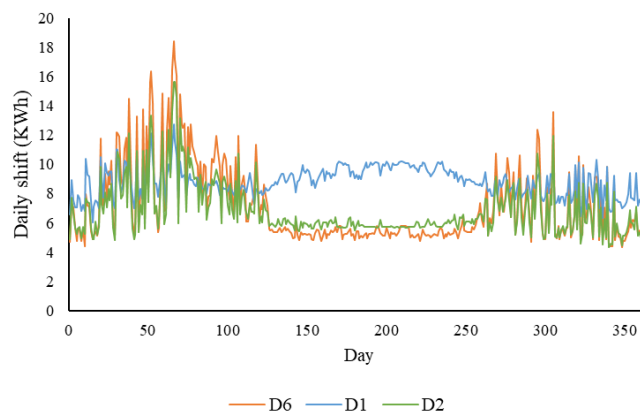
**Figure 8.** A comparison of the daily shifts for D_2, D_6, and D_1 under the measured power rate tariff.

4.1.2. Effective Heat Shift

A comparison of the effective shifts for the three business models of dynamic pricing tariff shows that based on cost-effective battery sizing, the effective shifts for the time of use tariff and the tiered rate tariff are the highest and lowest, respectively. The effective shift for the measured power rate falls between the shifts for these two tariffs. The time of use tariff shifts the total daily heating demands to the night periods. The case study building is a heat-dominated building, and the daily heating demand is a large part of its total energy consumption. Hence, the time of use tariff has the greatest effective heat shift. For the measured power rate tariff, all demand higher than the constant value (flat load profile) is shifted. Because the constant value is calculated based on a comparison of the daily heat average and plug loads, there is a surplus for all days of the year, but this surplus can vary from very low to high amounts. Hence, the shift is distributed across the year and creates a medium daily shift in comparison to the two other tariffs. Because the shift is distributed across the year, under the measured power rate tariff, the battery will go through more charge and discharge cycles, which can have negative effects on the battery life. For the tiered rate tariff, any demand exceeding the subscription level is shifted. Because the subscription level is not related to the daily distribution of load, the shift hours are random and skewed toward the winter peak consumption hours. This focus on the peak hours results in a lower daily shift for this tariff.

When it comes to the effective heat shift comparison between designs, it can be seen that for the measured power rate tariff, D_2 and D_6 have the smallest shifts. The shift for the measured power rate tariff is based on values that are higher than the constant value across the year. Thus, D_2 and D_6, which have lower plug loads, have smaller shifts during the summer compared to the other designs (Figure 8). Thus, they have the smallest shifts among all designs. Regarding the time of use tariff, because the daily heat consumption is shifted, designs featuring greater daily heat consumption have bigger shifts. These designs include those with weaker envelopes and electric radiators (D_9, D_{10}) or the ones with exhaust ventilation in combination with an electric radiator (D_2, D_6). As for the rest of the designs, the ones featuring just an electric radiator (D_1, D_5) have higher daily heating demands and consequently higher shifts than the ones using an ASHP and electric radiator (D_3, D_4, D_7, D_8). For the tiered rate tariff, the shift is focused more heavily on the peak hours during the heating period; hence, designs with more heating peaks will have greater shifts. These designs include those with weaker envelopes and combinations of electric radiators and exhaust ventilation systems. The smallest shifts under this tariff are seen for designs equipped with ASHP and an electric radiator. Designs with balanced ventilation have smaller shifts compared to the designs incorporating exhaust ventilation due to their lower peaks.

4.2. Cost-Effective Battery Size

The other important parameter, which was introduced in Section 2.3, is the cost-effective battery capacity for the shift storage. Figure 9 shows the relationship between the SI and cost-effective battery capacity as well as a detailed comparison of the cost-effective battery capacities for the ten designs across all tariff and reference scenario combinations. It can be seen that the SI and cost-effective battery capacity are directly proportional for all of the tariffs. Figure 9 reveals that the time of use tariff has the highest SI and cost-effective battery capacity due to the large shift for this tariff, which was discussed in Section 4.1.2. It should be noted that, in addition to the amount of the shift, the daily shift distribution also plays a role in determining the cost-effective battery capacity, as is discussed later. Under the time of use tariff, homeowners can achieve higher cost savings, but they will need greater storage capacity to do so. In contrast, the tiered rate tariff needs very low storage capacity, but it leads to lower cost savings due to its smaller shift. The measured power rate tariff falls between the other two tariffs in this regard. It has an SI in the range of the SI for the time of use tariff but a significantly lower cost-effective battery capacity featuring many charge and discharge cycles.
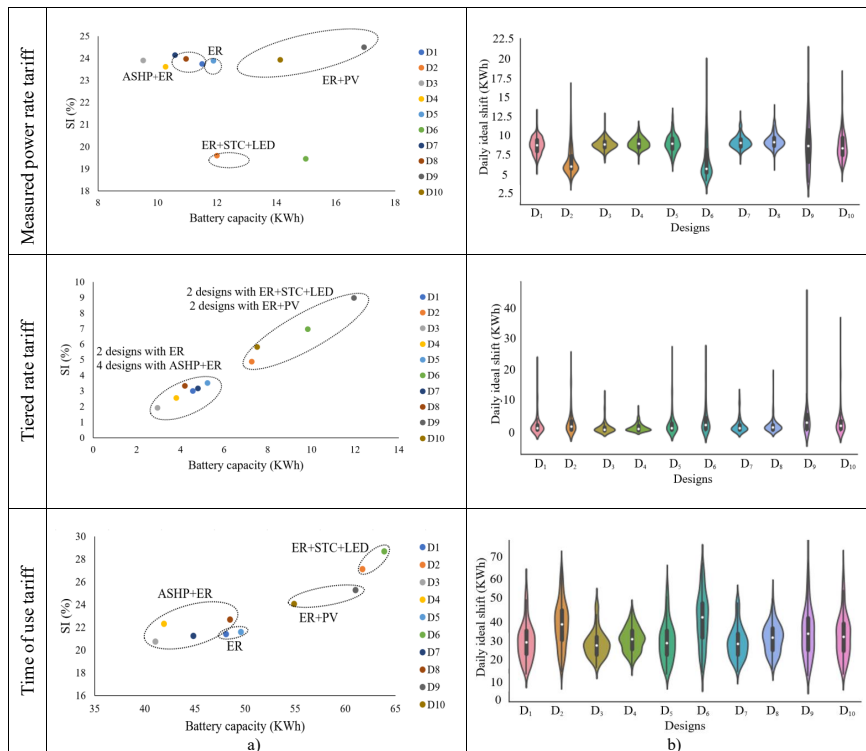
Figure 9. Visualization of designs based on SI, cost-effective battery size, and daily ideal shift (**a**) The relationship between the SI and cost-effective battery size. (**b**) The violin plots of the daily shifts for the ten designs in the reference scenario.

The battery capacity is determined according to the daily shift and its distribution. Hence, violin plots have been used to plot the distributions and probability densities of the daily shifts for the ten designs. The violin plot is similar to the box plot and provides a kernel density estimation of the underlying distribution. These violin plots, along with the relationships between SI values and cost-effective battery capacities for the tariffs in the reference scenario, are shown in Figure 9. Note that the cost-effective batteries are only used for the storage of the shifted heat and not for storing energy produced by renewable energy sources. Based on this figure, the measured power rate tariff produces more distributed daily storage in D_2, D_6, D_9, and D_{10}, and the standard deviations in the daily storage are higher for these designs in comparison to the other designs. In contrast, designs D_3, D_4, D_7, D_8 have less daily storage, and their distributions are dense in the middle. Thus, the most important parameter in the classification of the designs regarding the cost-effective battery capacity pertains to the energy system. Designs D_9 and D_{10} have a weaker envelope in combination with an electric radiator, resulting in higher daily shifts and increased battery capacity. Even though D_2 and D_6 have lower shifts due to lower summer usage, their shifts are higher during the winter due to the exhaust ventilation and electric radiator, leading to increased battery capacity. The remaining designs D_1 and D_5 have data distributed at the higher level in comparison to designs D_3, D_4, D_7, and D_8, leading to higher cost-effective battery capacities. The smallest battery capacities are assigned to the designs with the combination of an ASHP and electric radiator because their daily storage values are concentrated at the lower levels (the heating demand created by a heat pump has less variation than the heat demand created by an electric radiator, leading to smaller surpluses for the shift). For the designs without an ASHP, air-balanced ventilation leads to smaller

cost-effective battery capacities due to fewer deviations in the heating demand across a year. The shift in the time of use tariff is focused on daily heat consumption. So, designs with higher daily heat consumption will have higher battery capacities. Figure 9 shows that designs with higher heating demands also have shifts that are distributed more widely. These designs include those with will have higher battery capacities. Figure 9 (Dows D10) or the designs with high heating electric radiators (D2, D5, D7). The designs D1, D5 have widely shifts. These designs include those with storage requirements, resulting in mid-level cost-effective battery capacities and SI values. The smallest cost-effective battery capacities and SI values belong to the designs featuring ASHPs and electric radiators due to their smaller shifts and dense distributions. Design D4, which uses a combination of an ASHP, electric boilers and balanced ventilation, has the minimum cost-effective battery capacity.

For the Tiered rate tariff, the shifts occur during random hours and more frequently during the peak hours in the winter. For this reason, designs with higher demand during the winter will have greater shifts and higher SI values, as seen in the designs D2, D6, D9, and D10, which have weaker envelopes with an electric radiator or exhaust ventilation with an electric radiator. On the other hand, these designs have more widely distributed daily storage and cost-effective battery sizes. Other designs will have cost-effective battery sizes that are smaller than those for the previous group. For this tariff, the minimum battery capacity is also assigned to design D3, with the electric radiator, ASHP, and balanced ventilation.

4.3. Cost-Effective Flexibility Index (CEFI)

The cost-effective flexibility index (CEFI) is introduced in Section 2.3. This parameter indicates the percentage of savings that can be guaranteed if the cost-effective battery capacity is implemented. Figure 10 compares the CEFIs for the ten designs across the three business models of dynamic pricing tariff under the reference scenario. Comparing the tariffs reveals that in the reference scenario, the percentage of savings per kWh achieved by the cost-effective battery capacity across all of the designs is higher for the Measured power rate tariff. For this tariff, the cost savings are greater than those for the tiered rate tariff, and the battery capacity is as great as that for the time of use tariff, leading to the highest CEFI. The tariff with the next-highest CEFI is the Tiered rate tariff, while the time of use tariff has the minimum CEFI due to its very high battery capacity. Therefore, the measured power rate tariff saves more money at a smaller battery capacity.
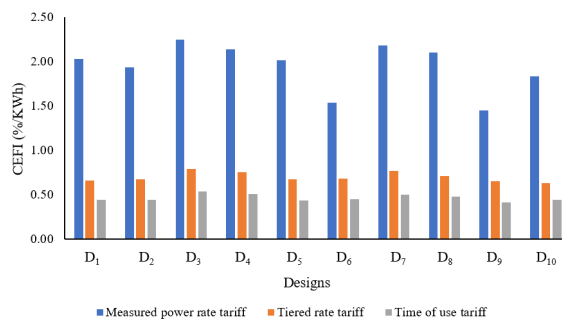
Figure 10. The CEFI values for the ten designs in the reference scenario and three tariffs.

When it comes to the design comparison across all of the tariffs, the highest CEFI is related to D3. The other designs with high CEFIs are D7, D4, and D8, all of which have an ASHP and electric radiator. Among these four designs, D3 and D7, which have air-balanced ventilation, have higher CEFIs compared to designs D4, D8. Of the remaining designs, those with weaker envelopes and electric radiators (D9, D10) or exhaust ventilation and electric radiators (D2, D6) have the smallest CEFIs. Based on the suggested design options

in this paper, it can be concluded that the most highly recommended design options for increasing the CEFI are those with ASHP and balanced ventilation. PVs must be paired with weaker building envelopes to meet the same energy target and for this reason, designs with PVs have larger battery size and smaller CEFI.

4.4. Survivability

The results related to the survivability can put into two categories: passive survivability and active survivability.

4.4.1. Passive Survivability

The case study building is a heat-dominated building and no cooling systems have been considered. In order to analyze passive survivability, a week is selected in each of winter and summer to run simulated grid power failures. The simulations are run by shutting off the power (for the HVAC and other energy-consuming equipment, such as appliances) during the warmest and coldest periods in summer and winter, which are selected from a typical year data in the IDA ICE weather file. For the summer passive survivability, a six-day power failure is applied starting on 15 July (the warmest week in the weather file). Because the building is a heat-dominated building, there is no need for cooling systems; hence, applying the power failure in the summer does not increase the temperature in the house to beyond the range of habitable conditions ($T_{Indoor} > 30\ °C$) in any of the designs. This means that all of the designs retain the habitable thermal condition in the case of a grid power failure in the summer. Thus, the PSI will reflect only the winter passive survivability for the current case study. For the winter passive survivability, a six-day grid power failure is applied starting on 15 Jan (the coldest week in the weather file). During this period, all of the designs experience temperatures below the habitable temperature ($T_{Indoor} < 15\ °C$). Figure 11 shows the winter passive survivability performances for the ten designs for a power failure starting on 15 January, Ozkan et al. indicate that the building envelope and WWR are the most effective parameters for increasing passive survivability [62]. The results achieved in this paper confirm this fact, and D_2, with the strongest building envelope and smaller WWR, has the best passive survivability performance. D_6 also has higher passive survivability due to having the second strongest envelope. D_1 and D_5 have mid-level survivability. The remaining designs, which have ASHPs, have lower survivability performances because the ASHP requires a weaker building envelope to meet the energy target. The designs with PV are in the same situation because they have weaker envelopes.
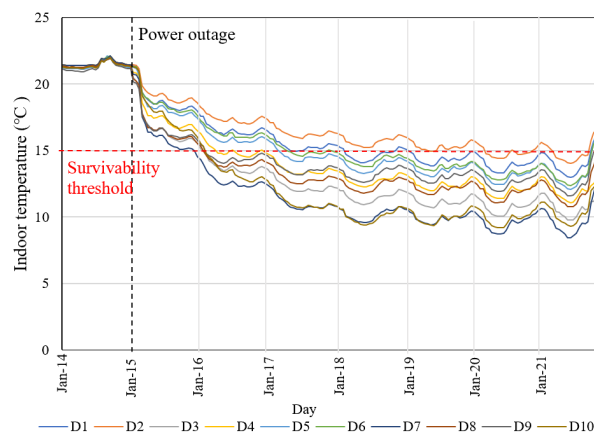
Figure 11. Winter passive survivability performances of the ten designs following a grid power outage in the winter.

4.4.2. Active Survivability

The ASI measures how much the cost-effective battery can contribute to the building's survival in the absence of grid power. The higher the ASI, the higher the self-sufficiency of the building during a power outage. This means that the building can survive with its own storage system, without being dependent on the centralized storage in the larger scales such as neighbourhoods. To calculate ASI, the minimum energy that is needed for survivability is estimated by running a simulation for each design in the critical condition. The ASI is calculated by dividing the cost-effective battery size by the minimum energy need for the design. The designs are then compared with respect to maintaining not only habitable temperatures but also meeting the minimum energy needed for other end uses, such as appliances, lighting, and domestic hot water. Figure 12 shows the ASIs for the ten designs for the reference scenarios and the three business models of the dynamic pricing tariffs.
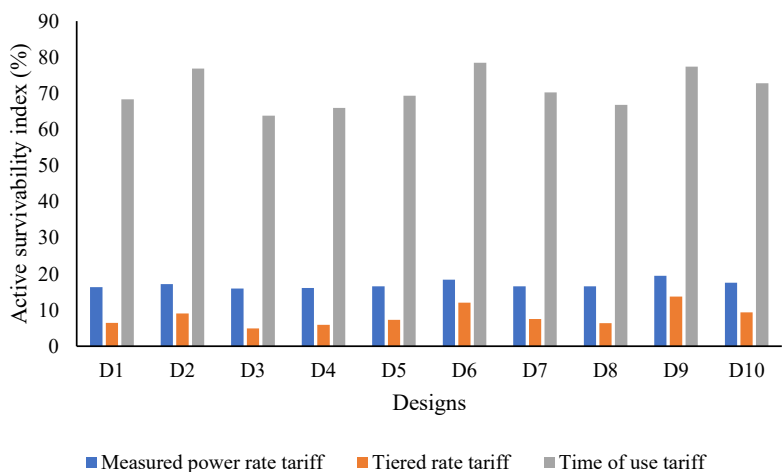
Figure 12. Active survivability indexes for the ten designs in the reference scenarios and three business models of dynamic pricing tariff.

It can be seen that the ASI for the time of use tariff is higher than that for the measured power rate tariff, which in turn is higher than that of the tiered rate tariff because, although the minimum energy needed for survivability is the same for all of the tariffs, the cost-effective battery size is the highest for the time of use tariff. In the higher cost-effective battery range, the building can survive longer on the stored shift in the battery when the grid power fails. Thus, when the time of use tariff is used, the building will be less dependent on large-scale, centralized storage. In contrast, if the tiered rate tariff is implemented, the building will be more dependent on centralized storage during a grid power failure. The ASI comparisons for the designs under each tariff are also informative. It should be noted that the minimum energy needed for survivability changes across the designs; however, the designs are competitive and have the same energy target, so the minimum energy needed for survivability does not vary much across designs. Thus, the cost-effective battery size is more influence on designs' ASIs and designs with the same energy target have the same trend. For example, the Measured power rate tariff designs D_2, D_6, D_9, and D_{10} have higher battery capacities in comparison to the designs D_3 and D_5 and the designs with an ASHP, namely D_3, D_4, D_7, and D_8. The same trend can also be observed for the ASI. The same trend occurs for the Tiered rate and the Time of use tariffs, and designs with weaker envelopes and electric radiators (D_9, D_{10}) or exhaust ventilation and electric radiators (D_2, D_6), which have higher shifts and battery capacities, have higher ASIs in comparison to the designs with ASHPs (D_3, D_3, D_7, D_8) or medium envelopes with balanced ventilation

(D_1, D_5). The bigger the cost-effective battery capacity, the longer the building will survive and the less dependent it will be on centralized storage when the grid power fails.

4.5. The Trade-Off between Energy Flexibility and Survivability

The trade-offs between cost-effective energy flexibility and survivability for the ten designs are shown in Figure 13 for the three business models of dynamic pricing tariff. In this figure, the ASI and the CEFI are shown along the x- and y-axes, respectively. The bubbles are added as a third dimension and indicate the relative values of the passive survivability indexes (number of hours that the building can survive). The larger the bubble size, the more passively survivable the building. This figure can help decision-makers to select the best design based on their preferences in terms of cost-effective flexibility, active survivability, and passive survivability. For example, for hospitals and care homes, where the risk associated with a grid power failure is high, the building survivability can be prioritized. In contrast, if the building should ensure a well-functioning DR program, energy flexibility becomes more important and can be prioritized. For example, under the measured power rate tariff, if the decision-maker prefers to achieve savings of more than 2% by utilizing each kWh stored in the cost-effective battery, the passive survivability will be in the range of one day, and the active survivability will be low (less than 17%). This situation comes up in designs with ASHPs and can yield appropriate solutions if the CEFI is prioritized. Another example involves desiring a high ASI value under the time of use tariff. If the decision-maker wants a high ASI value (more than 75%), the CEFI will be low, but the passive survivability can be extended to four days. This situation applies to designs D_2, D_6, D_9, and D_{10}. Among these designs, designs D_2 and D_9 have the greatest passive and active survivability, respectively. When considering all of the tariffs, it can be seen that designs with ASHP have the highest CEFIs and designs with PVs or STCs have the highest ASIs. The competitive designs from the flexibility and survivability points of view are marked with red dotted circles in Figure 13. The competitive designs under the measured power rate tariff are D_3 and D_7, both of which use ASHP and balanced ventilation and thus have higher CEFIs, as well as D_6, which has exhaust ventilation in combination with a strong envelope and STC, and D_9, which has a weaker envelope and an electric radiator and thus demands a higher battery capacity (which leads to higher active survivability). Three of these designs have passive survivability values of around one day, and only D_6 has higher passive survivability. Hence, if the CEFI is prioritized under this tariff, D_3 and D_7 can be appropriate solutions, while, if survivability is more important, D_2 or D_9 could be selected. Under the tiered rate tariff, the competitive designs remain the same due to their similar strategies for the heat shift. Under the time of use tariff, the situation is a bit different, and the competitive solutions are designs D_3, D_7, and D_6. Design D_9 is not in the group of competitive designs because the shift strategy for this tariff does not focus on peak demands and limits but rather the total amount of daily heat and shifting the load to the night. When the CEFI is prioritized, designs D_3 and D_7 are the suggested solutions, while, if survivability is more important, D_6 can be an appropriate solution. In general, the methodology in this paper provides information that allows decision-makers, such as grid companies, building designers, and home owners, to set up trade-offs between energy flexibility and survivability from a cost-effective perspective. The decision-makers should select their preferred design based on prioritizations of the involved criteria.
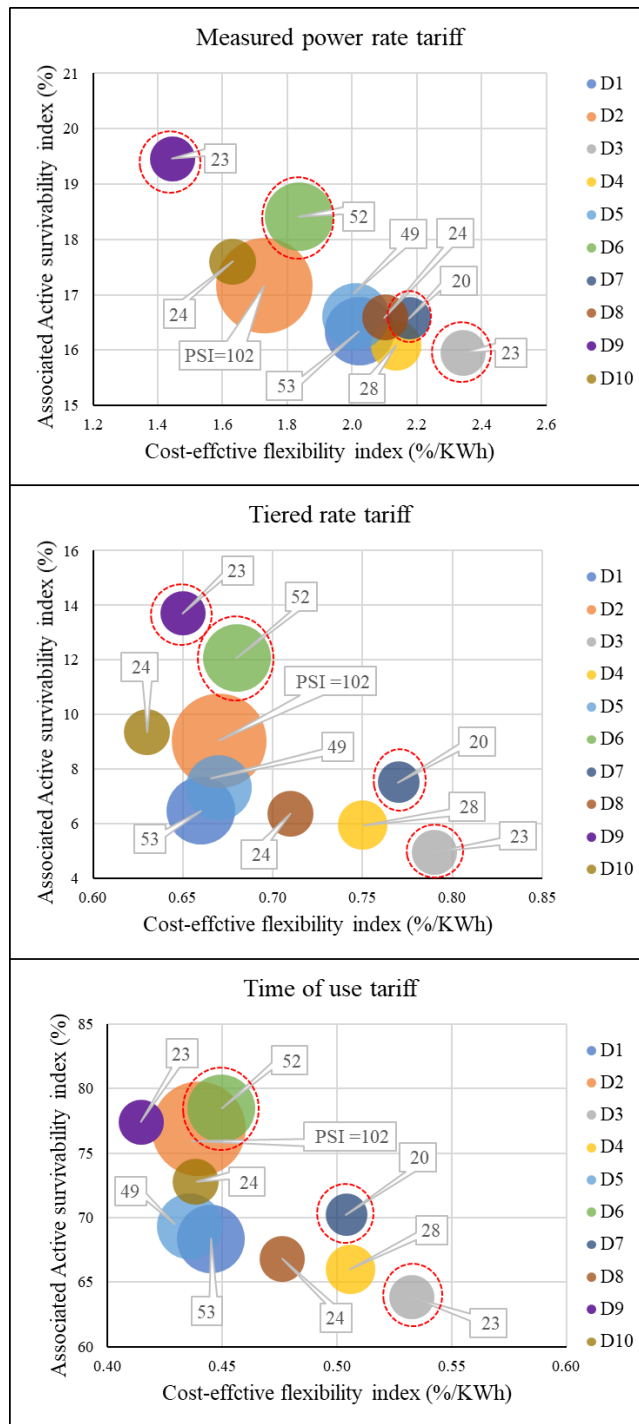
Figure 13. The trade-offs between cost-effective energy flexibility and survivability. The bubble size indicates the relative value of passive survivability index.

4.6. Impacts of Weather and Occupant Uncertainties

As stated previously, 16 uncertainty scenarios consisting of pairings of two climate scenarios with eight occupant scenarios are considered in this study in order to evaluate their impacts on the indexes under different tariffs. For example, Appendix A shows how annual energy consumption, SI, and cost-effective battery capacity change across the 16 scenarios for the measured power rate tariff. Based on this figure, there is an increase in the SI value and battery capacity, when the total energy consumption increases. In order to discover how these scenarios influence the cost-effective energy flexibility and the active survivability in the three business models for the dynamic pricing tariff, the CEFIs and ASIs are calculated for all designs across all scenarios. The uncertainties in the CEFIs and ASIs across the three business models are calculated and shown in Figure 14. The uncertainty in the CEFI is defined as follows [73]:

$$Uncertainty = \frac{CEFI_{max} - CEFI_{min}}{CEFI_{mean}} \% \tag{2}$$

where $CEFI_{mean}$ is the mean value of the CEFI of all designs across all scenarios and $CEFI_{max}$ and $CEFI_{min}$ are the maximum and minimum CEFI values for all designs and all scenarios. The same formulation is also used for the calculation of the uncertainty in the ASI. The maximum uncertainties for the CEFI and ASI occur under the tiered rate tariff because the annual subscription level's direct influence on the SI value, the cost-effective battery capacity, and thus the CEFI and ASI values make this tariff more sensitive to uncertainties in comparison to the other tariffs. In other words, under the tiered rate tariff, when the shift analysis is done, the values related to the CEFI and ASI will be very sensitive to future uncertainties. Hence, it is important to consider uncertainty scenarios when determining a subscription level. The measured power rate tariff has the smallest uncertainties for the ASI and CEFI. Furthermore, as mentioned earlier in Section 2.2.2, the cost-effective battery size covers the storage capacities that have a high probability of happening daily over a course of a year (the loads lower than the red box in Figure 5). With this strategy, there will be some days with low probable loads that the cost-effective battery capacity will not be able to cover them. Given this, uncertainties such as climate change can have some impacts on the battery size and in consequence on ASI and CEFI. If climate change leads to some low probable extreme condition, the cost-effective battery capacity will not get influenced and this is because the cost-effective battery size is independent of extreme conditions. However, if climate change leads to more probable extreme conditions and it completely changes the distribution of the daily loads, the cost-effective battery will not be reliable anymore for the new climate conditions. So, it is recommended to consider the impact of uncertainties on the battery size in the design step.
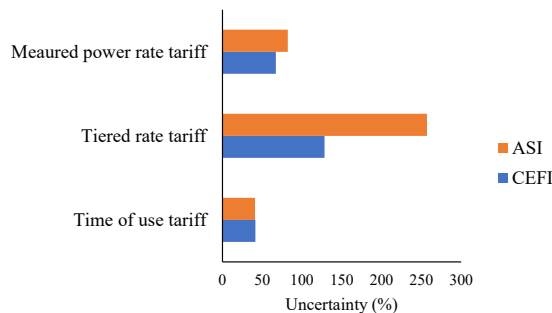
Figure 14. The uncertainties related to the CEFIs and ASIs for the three business models of dynamic pricing tariff.

5. Summary and Conclusions

This paper explores the trade-off between energy flexibility and survivability of all-electric buildings by suggesting a methodology for quantifying the energy flexibility and survivability. This quantification is done with a focus on sizing cost-effective batteries, which can be considered as flexibility assets when they store the shifted heat (as a DR strategy) in the response to a dynamic pricing tariff. In addition, these batteries can be used as backup storage systems for building survival during grid power failures. The energy flexibility is quantified as a single indicator (cost-effective flexibility index) reflecting the amount of cost savings that can be achieved by implementing the cost-effective battery. The active survivability of the building is also quantified as a single indicator (active survivability index) showing how well the cost-effective battery implemented for shift storage can cover the minimum energy needed in the case of a grid power failure. A MATLAB-based algorithm, coupled with dynamic building performance simulation software (i.e., IDA ICE), is used to determine the cost-effective battery size, CEFI, and ASI. This generic method can be used for buildings in cold or hot climates that use electricity as their source for heating and cooling demands. The suggested methodology can be used by different stakeholders in building projects, such as grid companies, building designers, and electric grid customers, including home owners, to estimate the energy flexibility and survivability of the building from a cost-effective perspective. In order to create the conditions necessary for comparing the energy flexibility and survivability of building designs with the same energy target, a unique design space with ten competitive designs is created for an all-electric Norwegian single-family house. Furthermore, 16 uncertainty scenarios are created to evaluate the impact of possible uncertainties on the introduced indexes under different dynamic pricing tariffs. The implementation of the suggested methodology in this case study has created the opportunity to compare three business models for the dynamic pricing tariff suggested by the Norwegian regulator and also to compare designs meeting the same energy target. The following conclusions can be drawn based on this study:

- For all of the suggested designs with the same energy target, the energy rate tariff and the time of use tariff are the cheapest and the most expensive tariffs, respectively. The high prices of the three suggested tariffs are exactly in line with the logic behind them, which is creating incentives and encouraging customers to change their energy consumption patterns.
- For the suggested case study building, which meets the TEK17's energy consumption target (110 kWh/m^2), the cost-effective battery sizes for the different designs under the measured power rate tariff is in the range of 10-18 kWh. For the tiered rate tariff, the range is from 2 to 12 kWh, while, for the time of use tariff, the cost-effective battery size varies between 40 and 65 kWh.
- The higher sizes of the cost-effective batteries under the time of use tariff are related to the shifting strategy used in this tariff, which focuses on shifting the heating demand away from the daytime and needs higher capacities to store it.
- In the suggested design space, designs with weaker envelopes or exhaust ventilation in combination with an electric radiator have higher heating demands and higher heat peaks, thus leading to higher daily shifts and increases in the cost-effective battery size, as in designs D_2, D_6, D_9, and D_{10}. In contrast, designs using an ASHP can use smaller batteries to shift the heat under all of the tariffs due to less variation and smaller peaks in the heating demand.
- When considering the three dynamic pricing tariffs, the highest CEFI is found for the measured power rate tariff, and its CEFI is significantly higher than those of the two other tariffs (1.4–2 %/kwh in comparison to 0.6–0.8 %/kWh for the tiered rate tariff and 0.4–0.55 %/kWh for the time of use tariff). In this tariff, neither the cost saving is as small as the tiered rate tariff, nor the battery capacity is as big as the time of use tariff.
- Of the ten designs with the same energy target, design D_3, which uses a combination of an electric radiator and ASHP as the energy system and air-balanced ventilation as

the ventilation strategy, has the maximum CEFI of the designs. Thus, in this design space, ASHP and air-balanced ventilation are the most important design options for obtaining a high CEFI value. However, the implementation of renewable systems, which are paired with weak building envelopes to meet the energy target, or exhaust ventilation in combination with an electric radiator leads to lower CEFI values.

- For the case study building, which meets the TEK17's energy consumption target (110 kWh/m^2), the ASIs of the different designs under the time of use tariff vary between 63–80%. For the measured power rate tariff and tiered rate tariff, the ASI values decrease to 16–20% and 4–14%, respectively. The high active survivability under the time of use tariff is the result of a higher cost-effective battery size compared to the battery sizes for the other tariffs.
- Designs with higher cost-effective battery capacities can help the building survive longer during grid power failures. The ASI is higher in the designs with higher cost-effective battery sizes, such as designs D_2, D_6, D_9, and D_{10}.
- The building envelope and WWR are the most important parameters influencing passive survivability.
- There is a trade-off between the defined energy flexibility and survivability of the all-electric building for the three business models for the dynamic pricing tariff. The preferred design should be selected based on the prioritization of the criteria. Designs with an ASHP are suggested when the CEFI value is prioritized over the survivability in the case of power failure. In contrast, designs with higher battery capacities (D_2, D_6, D_9, D_{10}) are suggested when survivability is prioritized over energy flexibility.
- The CEFI and ASI values for the tiered rate tariff are more sensitive to weather and occupant uncertainties. For this tariff, the heat shift, the corresponded savings, and the cost-effective battery size depend on the selected subscription level, making it far more sensitive to uncertainties from the flexibility and active survivability points of view.

In the context of operational applicability, the suggested methodology can be used by the different stakeholders in building projects, such as grid companies, building designers, and electric grid customers, including home owners, to classify the energy flexibility and survivability of buildings according to two easy-to-understand indicators hinging on cost-effectiveness. The application of this methodology is not limited to Norway and can be extended to other countries where electricity is used as a heating source, such as Kosovo, Malta, Sweden, and Finland. Furthermore, it can be extended to countries with hot climates that use electricity for cooling. In this paper, the proposed methodology is considered for a single building. In the real world, buildings interact with each other and with connected grids. It would, therefore, be interesting to consider this approach on a larger scale, such as a neighborhood scale, by extending the sizing to centralized storage systems. The energy flexibility and survivability of buildings can also trade-off with other building performance metrics, such as energy consumption and emissions. In future work, energy flexibility and survivability can be used, along with other performance criteria, in a multi-criteria assessment framework to help decision-makers prioritize and select building designs.

Author Contributions: Conceptualization, S.H. and M.H.; methodology, S.H. and M.H.; software, S.H.; validation, S.H.; formal analysis, S.H.; investigation, S.H.; data curation, S.H. and M.H.; writing— original draft, S.H.; Writing—review and editing, S.H. and M.H.; visualization, S.H.; resource, M.H.; supervision, M.H. All authors have read and agreed to the published version of the manuscript.

Institutional Review Board Statement: Not applicable.

Informed Consent Statement: Not applicable.

Conflicts of Interest: The authors declare no conflict of interest.

Abbreviations

The following abbreviations are used in this manuscript:

AC	Annual cost without shift
ACIS	Annual cost with ideal shift
ACES	Annual cost with effective shift
ASHP	Air source heat pump
ASI	Active survivability index
BPS	Building performance simulation
CEFI	Cost-effective flexibility index
CHP	Combined heat and power
CPP	Critical peak pricing
DH	District heating
DHW	Domestic hot water
DR	Demand response
EFS	Effective heat shift
ER	Electric radiator
EV	Electric vehicle
HVAC	Heating ventilation and air conditioning
IHS	Ideal heat shift
kW	Kilowatt
kWh	kilowatt-hour
LED	Light emitting diode
NMF	Neutral modeling format
NVE	Norwegian water resource and energy
PCM	Phase change material
PSI	Passive survivability index
PV	Photovoltaic
RES	Renewable energy sources
SI	Saving index
STC	Solar thermal collector
TEK17	Norwegian building regulation
WWR	window to wall ratio
C_{Bat}	Cost-effective battery capacity
CO_2	Carbon dioxide

Appendix A

The uncertainty scenarios related to the weather and occupant behavior are shown in Table A1. More information can be found in [67]. Furthermore, the impact of uncertainties on the total energy consumption, the SI, and the cost-effective battery capacity used in the measured power rate tariff is shown as an example in Figure A1.

Table A1. Summary of the occupant behaviors and climate parameters and their combinations into the 16 considered scenarios. * shows the chosen option for each parameters in the scenarios.

Parameter	Option	Scenarios															
		1	2	3	4	5	6	7	8	9	10	11	12	13	14	15	16
Heating setpoint	(1) Bedroom, livingroom, bathroom 18, 21.5, 23 °C	*	*	*	*					*	*	*	*				
	(2) Bedroom, livingroom, bathroom 20, 23, 23 °C					*	*	*	*					*	*	*	*
Window shading	(1)Shading control On if $T_{indoor} > 23$ °C	*	*			*	*			*	*			*	*		
	(2) Shading control on if radiation above 100 W/m²			*	*			*	*			*	*			*	*
Window opening	(1) Open if $T_{indoor} > T_{Out}$ and $T_{indoor} > 23$ °C for windows in all zones	*		*		*		*		*		*		*		*	
	(2) Open if $T_{indoor} > T_{Out}$ and $T_{indoor} > 23$ °C for day room and bathroom Open based on adaptive thermal model limits for bedroom		*		*		*		*		*		*		*		*
Climate	(1) IWEC	*	*	*	*	*	*	*	*								
	(2) IWEC2									*	*	*	*	*	*	*	*

Figure A1. The impacts of the 16 uncertainty scenarios on total energy consumption, cost-effective battery capacities, and the savings indexes of the ten designs for the measured power rate tariff.

References

1. Deason, J.; Wei, M.; Leventis, G.; Smith, S.; Schwartz, L. *Energy Analysis and Environmental Impacts Division Lawrence Berkeley National Laboratory Electricity Markets and Policy Group*; Technical Report; Lawrence Berkeley National Laboratory: Berkeley, CA, USA, 2018.

2. Lund, H.; Østergaard, P.A.; Connolly, D.; Ridjan, I.; Mathiesen, B.V.; Hvelplund, F.; Thellufsen, J.Z.; Sorknæs, P. Energy storage and smart energy systems. *Int. J. Sustain. Energy Plan. Manag.* **2016**, *11*, 3–14.

3. Clauß, J.; Stinner, S.; Solli, C.; Lindberg, K.B.; Madsen, H.; Georges, L. A generic methodology to evaluate hourly average CO_2eq. intensities of the electricity mix to deploy the energy flexibility potential of Norwegian buildings. In Proceedings of the 10th International Conference on System Simulation in Buildings, Liege, Belgium, 10–12 December 2018; pp. 10–12.

4. Persson, U.; Werner, S. *Quantifying the Heating and Cooling Demand in Europe*; Technical Report; Intelligent energy Europe program of the Europian Union: Halmstad, Sweden, 2018.
5. European Heat Pumps Association Website. Available online: https://www.ehpa.org/ (accessed on 8 October 2020).
6. International Energy Agency Website. Available online: https://www.iea.org/ (accessed on 8 October 2020).
7. Loibl, W.; Stollnberger, R.; Österreicher, D. Residential heat supply by waste-heat re-use: Sources, supply potential and demand coverage—A case study. *Sustainability* **2017**, *9*, 250. [CrossRef]
8. Clauß, J.; Stinner, S.; Sartori, I.; Georges, L. Predictive rule-based control to activate the energy flexibility of Norwegian residential buildings: Case of an air-source heat pump and direct electric heating. *Appl. Energy* **2019**, *237*, 500–518. [CrossRef]
9. Junker, R.G.; Azar, A.G.; Lopes, R.A.; Lindberg, K.B.; Reynders, G.; Relan, R.; Madsen, H. Characterizing the energy flexibility of buildings and districts. *Appl. Energy* **2018**, *225*, 175–182. [CrossRef]
10. Niu, J.; Tian, Z.; Lu, Y.; Zhao, H. Flexible dispatch of a building energy system using building thermal storage and battery energy storage. *Appl. Energy* **2019**, *243*, 274–287. [CrossRef]
11. Foteinaki, K.; Li, R.; Heller, A.; Rode, C. Heating system energy flexibility of low-energy residential buildings. *Energy Build.* **2018**, *180*, 95–108. [CrossRef]
12. Arteconi, A.; Mugnini, A.; Polonara, F. Energy flexible buildings: A methodology for rating the flexibility performance of buildings with electric heating and cooling systems. *Appl. Energy* **2019**, *251*, 113387. [CrossRef]
13. Statistics Norway. Available online: https://www.ssb.no/en/energi-og-industri/statistikker/elektrisitet/aar (accessed on 8 October 2020).
14. Bergesen, B.; Groth, L.H.; Langseth, B.; Magnussen, I.H.; Spilde, D.; Toutain, J.E.W. *Energy Consumption 2012 Household Energy Consumption*; Technical Report 16/2013; Norwegian Water Resources and Energy Directorate: Oslo, Norway, 2012.
15. Energy Consumption in Households. Available online: https://ec.europa.eu/eurostat/statistics-explained/index.php/Energy_consumption_in_households (accessed on 8 October 2020).
16. IEA. *Global EV Outlook 2020*; Technical Report; IEA: Paris, France, 2019.
17. Strbac, G. Demand side management: Benefits and challenges. *Energy Policy* **2008**, *36*, 4419–4426. [CrossRef]
18. Vandermeulen, A.; van der Heijde, B.; Helsen, L. Controlling district heating and cooling networks to unlock flexibility: A review. *Energy* **2018**, *151*, 103–115. [CrossRef]
19. Haider, H.T.; See, O.H.; Elmenreich, W. A review of residential demand response of smart grid. *Renew. Sustain. Energy Rev.* **2016**, *59*, 166–178. [CrossRef]
20. Shen, B.; Ghatikar, G.; Lei, Z.; Li, J.; Wikler, G.; Martin, P. The role of regulatory reforms, market changes, and technology development to make demand response a viable resource in meeting energy challenges. *Appl. Energy* **2014**, *130*, 814–823. [CrossRef]
21. Dutta, G.; Mitra, K. A literature review on dynamic pricing of electricity. *J. Oper. Res. Soc.* **2017**, *68*, 1131–1145. [CrossRef]
22. Gottwalt, S.; Ketter, W.; Block, C.; Collins, J.; Weinhardt, C. Demand side management—A simulation of household behavior under variable prices. *Energy Policy* **2011**, *39*, 8163–8174. [CrossRef]
23. *Communication from the Commission to the European Parliament, the European Council, the Council, the European economic and social committee and the Committee of the Regions, the European Green Deal*; Technical Report; European Commission: Brussels, Belgium, 2019.
24. Lund, P.D.; Lindgren, J.; Mikkola, J.; Salpakari, J. Review of energy system flexibility measures to enable high levels of variable renewable electricity. *Renew. Sustain. Energy Rev.* **2015**, *45*, 785–807. [CrossRef]
25. Schofield, J.; Carmichael, R.; Tindemans, S.; Woolf, M.; Bilton, M.; Strbac, G. *Residential Consumer Responsiveness to Time-Varying Pricing*; Technical Report A3; Low Carbon London Learning Lab, LCNF Project; Imperial College: London, UK, 2014.
26. Laicane, I.; Blumberga, D.; Blumberga, A.; Rosa, M. Reducing household electricity consumption through demand side management: The role of home appliance scheduling and peak load reduction. *Energy Procedia* **2015**, *72*, 222–229. [CrossRef]
27. Nezamoddini, N.; Wang, Y. Risk management and participation planning of electric vehicles in smart grids for demand response. *Energy* **2016**, *116*, 836–850. [CrossRef]
28. Moreau, A. Control Strategy for Domestic Water Heaters during Peak Periods and its Impact on the Demand for Electricity. *Energy Procedia* **2011**, *12*, 1074–1082. [CrossRef]
29. Mancini, F.; Nastasi, B. Energy retrofitting effects on the energy flexibility of dwellings. *Energies* **2019**, *12*, 2788. [CrossRef]
30. Chen, Y.; Xu, P.; Gu, J.; Schmidt, F.; Li, W. Measures to improve energy demand flexibility in buildings for demand response (DR): A review. *Energy Build.* **2018**, *177*, 125–139. [CrossRef]
31. Selinger-Lutz, O.; Groß, A.; Wille-Haussmann, B.; Wittwer, C. Dynamic feed-in tariffs with reduced complexity and their impact on the optimal operation of a combined heat and power plant. *Int. J. Electr. Power Energy Syst.* **2020**, *118*, 105770. [CrossRef]
32. Hamdy, M.; Sirén, K. A multi-aid optimization scheme for large-scale investigation of cost-optimality and energy performance of buildings. *J. Build. Perform. Simul.* **2016**, *9*, 411–430. [CrossRef]
33. Syed, M.; Hansen, P.; Morrison, G.M. Performance of a shared solar and battery storage system in an Australian apartment building. *Energy Build.* **2020**, *225*, 110321. [CrossRef]
34. Weniger, J.; Tjaden, T.; Quaschning, V. Sizing of Residential PV Battery Systems. *Energy Procedia* **2014**, *46*, 78–87. [CrossRef]
35. Hassan, A.S.; Cipcigan, L.; Jenkins, N. Optimal battery storage operation for PV systems with tariff incentives. *Appl. Energy* **2017**, *203*, 422–441. [CrossRef]

36. Heine, K.; Thatte, A.; Tabares-Velasco, P.C. A simulation approach to sizing batteries for integration with net-zero energy residential buildings. *Renew. Energy* **2019**, *139*, 176–185. [CrossRef]
37. Nastasi, B.; Mazzoni, S.; Groppi, D.; Romagnoli, A.; Garcia, D.A. Solar power-to-gas application to an island energy system. *Renew. Energy* **2021**, *164*, 1005–1016. [CrossRef]
38. Dumont, O.; Carmo, C.; Georges, E.; Balderrama, S.; Quoilin, S.; Lemort, V. Economic assessment of energy storage for load shifting in Positive Energy Building. *Int. J. Energy Environ. Eng.* **2017**, *8*, 25–35. [CrossRef]
39. Georgakarakos, A.D.; Mayfield, M.; Hathway, E.A. Battery Storage Systems in Smart Grid Optimised Buildings. *Energy Procedia* **2018**, *151*, 23–30. [CrossRef]
40. Yang, Y.; Li, H.; Aichhorn, A.; Zheng, J.; Greenleaf, M. Sizing strategy of distributed battery storage system with high penetration of photovoltaic for voltage regulation and peak load shaving. *IEEE Trans. Smart Grid* **2013**, *5*, 982–991. [CrossRef]
41. Prehoda, E.W.; Schelly, C.; Pearce, J.M. US strategic solar photovoltaic-powered microgrid deployment for enhanced national security. *Renew. Sustain. Energy Rev.* **2017**, *78*, 167–175. [CrossRef]
42. Tsianikas, S.; Zhou, J.; Birnie, D.P., III; Coit, D.W. Economic trends and comparisons for optimizing grid-outage resilient photovoltaic and battery systems. *Appl. Energy* **2019**, *256*, 113892. [CrossRef]
43. Ghasemieh, H.; Haverkort, B.R.; Jongerden, M.R.; Remke, A. Energy resilience modelling for smart houses. In Proceedings of the 2015 45th Annual IEEE/IFIP International Conference on Dependable Systems and Networks, Rio de Janeiro, Brazil, 22–25 June 2015; pp. 275–286.
44. Gupta, R.; Bruce-Konuah, A.; Howard, A. Achieving energy resilience through smart storage of solar electricity at dwelling and community level. *Energy Build.* **2019**, *195*, 1–15. [CrossRef]
45. UENTSO-E Overview of Transmission Tariffs in Europe: Synthesis. 2019. Available online: https://eepublicdownloads.blob.c ore.windows.net/public-cdn-container/clean-documents/mc-documents/190626_MC_TOP_7.2_TTO_Synthesis2019.pdf (accessed on 8 October 2020).
46. Sæle, H. Consequences for residential customers when changing from energy based to capacity based tariff structure in the distribution grid. In Proceedings of the 2017 IEEE Manchester PowerTech, Manchester, UK, 18–22 June 2017; pp. 1–6.
47. Sæle, H.; Høvik, Ø.; Nordgård, D.E. Evaluation of alternative network tariffs—For residential customers with hourly metering of electricity consumption. In Proceedings of the CIRED Workshop 2016, Helsinki, Finland, 14–15 June 2016.
48. Hansen, H.; Jonassen, T.; Løchen, K.; Mook, V. *Høringsdokument nr 5-2017: Forslag til Endring i Forskrift om Kontroll av Nettvirksomhet*; Technical Report; Norges Vassdrags—Ogenergidirektor: Oslo, Norway, 2017.
49. Smart metering (AMS). Available online: https://www.nve.no/energy-market-and-regulation/retail-market/smart-metering-ams/ (accessed on 8 October 2020).
50. Eriksen, A.B.; Hansen, H.; Hole, J.; Jonassen, T.; Mook, V.; Steinnes, S.; Varden, L. *RME HoRINGSDOKUMENT, Endringer i Nettleiestrukturen*; Norges Vassdrags-og Energidirektorat: Oslo, Norway, 2020.
51. Karlsen, S.S.; Hamdy, M.; Attia, S. Methodology to assess business models of dynamic pricing tariffs in all-electric houses. *Energy Build.* **2020**, *207*, 109586. [CrossRef]
52. EQUA Solutions AB Ida Indoor Climate and Energy (Version 4.8). Available online: https://www.equa.se/en/ida-ice (accessed on 8 October 2020).
53. Equa Simulation AB. Validation of IDA Indoor Climate and Energy 4.0 Build 4 with Respect to ANSI/ASHRAE Standard 140-2004. Technical Report. 2010. Available online: http://mail.ssf.scout.se/iceuser/validation/ASHRAE140-2004.pdf (accessed on 8 October 2020).
54. Equa Simulation AB. Validation of IDA Indoor Climate and Energy 4.0 with respect to CEN Standards EN 15255-2007 and EN 15265-2007. Technical Report. 2010. Available online: http://www.equaonline.com/iceuser/validation/CEN_VALIDATION_EN_15255_AND_15265.pdf (accessed on 8 October 2020).
55. *MATLAB Version 9.3.0.713579 (R2017b)*; The Mathworks: Natick, MA, USA, 2017
56. Rønneseth, Ø.; Haase, M.; Georges, L.; Thunshelle, K.; Holøs, S.B.; Fjellheim, Ø.; Mysen, M.; Thomsen, J. *Building Service Solutions Suitable for Low Emission Urban Areas*; Technical Report; The Research Center on Zero Emission Neighbourhoods (ZEN) in Smart Cities: Trondheim, Norway, 2020.
57. Immendoerfer, A.; Winkelmann, M.; Stelzer, V. *Energy Solutions for Smart Cities and Communities Recommendations for Policy Makers from the 58 Pilots of the CONCERTO Initiativ*; Technical Report; The Institute for Technology Assessment and Systems Analysis (ITAS) Karlsruhe Institute of Technology: Karlsruhe, Germany, 2014.
58. Wethal, U. Practices, provision and protest: Power outages in rural Norwegian households. *Energy Res. Soc. Sci.* **2020**, *62*, 101388. [CrossRef]
59. Reynders, G.; Lopes, R.A.; Marszal-Pomianowska, A.; Aelenei, D.; Martins, J.; Saelens, D. Energy flexible buildings: An evaluation of definitions and quantification methodologies applied to thermal storage. *Energy Build.* **2018**, *166*, 372–390. [CrossRef]
60. Oldewurtel, F.; Sturzenegger, D.; Andersson, G.; Morari, M.; Smith, R.S. Towards a standardized building assessment for demand response. In Proceedings of the 52nd IEEE Conference on Decision and Control, Firenze, Italy, 10–13 December 2013; pp. 7083–7088.
61. Baniassadi, A.; Sailor, D.J.; Krayenhoff, E.S.; Broadbent, A.M.; Georgescu, M. Passive survivability of buildings under changing urban climates across eight US cities. *Environ. Res. Lett.* **2019**, *14*, 074028. [CrossRef]

62. Ozkan, A.; Kesik, T.; Yilmaz, A.Z.; O'Brien, W. Development and visualization of time-based building energy performance metrics. *Build. Res. Inf.* **2019**, *47*, 493–517. [CrossRef]
63. O'Brien, W.; Bennet, I. Simulation-Based Evaluation of High-Rise Residential Building Thermal Resilience. *ASHRAE Trans.* **2016**, *122*, 455–468.
64. Byggteknisk Forskrift (TEK17). Available online: https://dibk.no/byggereglene/byggteknisk-forskrift-tek17/14/14-2/ (accessed on 8 October 2020).
65. Standard Norge (2016) SN/TS3031: 2016 Energy Performance of Buildings. Available online: https://www.standard.no/nyheter/nyhetsarkiv/bygg-anlegg-og-eiendom/2016/snts-30312016-for-beregning-av-energibehov-og-energiforsyning/ (accessed on 8 October 2020).
66. Rønneseth, Ø.; Sartori, I. *Method for Modeling Norwegian Single-Family House in IDA ICE*; Technical Report; The Research Center on Zero Emission Neighbourhoods (ZEN) in Smart Cities: Trondhiem, Norway, 2018.
67. Homaei, S.; Hamdy, M. A robustness-based decision making approach for multi-target high performance buildings under uncertain scenarios. *Appl. Energy* **2020**, *267*, 114868. [CrossRef]
68. Nord, N.; Qvistgaard, L.H.; Cao, G. Identifying key design parameters of the integrated energy system for a residential Zero Emission Building in Norway. *Renew. Energy* **2016**, *87*, 1076–1087. [CrossRef]
69. De Wilde, P.; Coley, D. The Implications of a Changing Climate for Buildings. *Build. Environ.* **2012**, *55*, 1–7. [CrossRef]
70. Hamdy, M.; Sirén, K.; Attia, S. Impact of financial assumptions on the cost optimality towards nearly zero energy buildings—A case study. *Energy Build.* **2017**, *153*, 421–438. [CrossRef]
71. Yan, D.; O'Brien, W.; Hong, T.; Feng, X.; Gunay, H.B.; Tahmasebi, F.; Mahdavi, A. Occupant behavior modeling for building performance simulation: Current state and future challenges. *Energy Build.* **2015**, *107*, 264–278. [CrossRef]
72. Hu, M.; Xiao, F. Quantifying uncertainty in the aggregate energy flexibility of high-rise residential building clusters considering stochastic occupancy and occupant behavior. *Energy* **2020**, *194*, 116838. [CrossRef]
73. Wang, A.; Li, R.; You, S. Development of a data driven approach to explore the energy flexibility potential of building clusters. *Appl. Energy* **2018**, *232*, 89–100. [CrossRef]

Paper III

Developing a test framework for assessing building thermal resilience
Shabnam Homaei and Mohamed Hamdy
Proceeding of Building Simulation 2021 Conference.

Developing a test framework for assessing building thermal resilience

Shabnam Homaei[1], Mohamed Hamdy[1]
[1]Norwegian University of Science and Technology, Trondheim, Norway ,

Abstract

Building performance can be affected by various events such as changing environment or changing requirements. Thus, buildings should react to these events to last their performance. In this regard, the concept of resilience is recently gaining ground in building design context. However, for the application of resilience in the building design, there should be a clear definition and an assessment framework. This paper develops a comprehensive definition of resilience and its assessment by answering four main questions. Furthermore, it introduces a multi-phase resilience curve and tests building thermal resilience using a test framework and a set of metrics. The developed test framework has been used for a case building facing a power failure lasting for four days. The results highlight the suitability of the proposed test framework and metrics to quantify building thermal resilience.

Key Innovations

- Developing a test framework for evaluating building thermal resilience.

- Quantification of building thermal resilience with a focus on different phases and abilities in the cycle of a disruptive event.

Practical Implication

- Aiding building designers and decision makers in selecting the most appropriate building designs and strategies by evaluation and quantification of building thermal resilience.

Introduction

In general, buildings are designed based on a group of fixed assumptions and conditions in the design or renovation phases. This is while in the operational phase, buildings are not performing under the fixed assumptions and conditions, which have been set by designers. Building performance can be affected by a wide range of changes that can arise during the operational phase. These changes can be categorized to changing environment (e.g., climate change, occupant behaviour changes (Homaei and Hamdy (2020)) or changing requirement (e.g., adding new technologies to the building or the integrated grid (Rønneseth et al. (2019)). For example, climate change is one of the main sources of uncertainty that can influence the performance of buildings, energy systems and in larger scales urban areas. Even though the impacts of climate change are considered by using the normal climate data and the projections of climate change, there can still be climate conditions far from the expected ranges in the future (Moazami et al. (2019)). Furthermore, the frequency and severity of extreme events have increased in the last 30 years (Kenward and Raja (2014)) leading to other consequences in energy systems such as major power failures that can be life-threatening and can cause to huge economic losses (Campbell and Lowry (2012)). Buildings are categorized in the group of facilities with a long life cycle and significant investment costs. For this reason, they should be able to perform well not only for the current condition but also for upcoming conditions in the future. In general, one of the strategies to ensure the performance of systems against future uncertainties, disturbances, and shocks is mitigation options in the form of protection: designing systems to withstand and absorb undesired events (Hosseini et al. (2016)), which can also be applied to buildings as systems. In the category of these options, the concept of resilience has gained much attention in recent years. The word resilience stems from the Latin root "risilio" meaning to "spring back".The common definition of resilience deals with "the ability of an entity or system to return to normal condition after the occurrence of an event that disrupts its state"(Hosseini et al. (2016)). The concept of resilience is polysemic and its interpretation can be changed based on the context and objectives in different disciplines. Nowadays, the concept of resilience has been used in diverse fields such as ecology (Holling (1973), psychology (Rutter (1987)), economy (Rose (2007)), seismic engineering (Bruneau et al. (2003)), and etc. The resilience studies were originated from the work of Holling in ecology during the 1970s (Holling (1996)) and other fields have borrowed this concept from ecology. Holling used resilience to describe the ability of an ecological system to maintain its function and structure by enduring the shocks and absorbing disturbances, but not necessarily remaining the same pre-disturbance state (Holling (1996)), which is known as ecological resilience. Several studies thus far have addressed the conceptualization of the resilience concept and its quantification in different fields. For example, concerning energy systems, the resilience of gas systems

(Cimellaro et al. (2015)) and power systems (Panteli et al. (2016))have been evaluated. The resilience triangle suggested by the Multidisciplinary Center for Earthquake Engineering Research was the first effort for measuring the seismic resilience (Bruneau et al. (2003)). This has been extended by the concept of resilience trapezoid, which divides the system's performance response into three stages: pre-disturbance, disturbance progress, and restorative stages to consider the degraded state in case of no immediate restoration actions after disturbance (Panteli et al. (2016, 2017)). Resilience trapezoid has been implemented for quantifying resilience in different contexts such as power systems (Panteli et al. (2016)), multi-energy systems (Bao et al. (2020)), urban infrastructure, and energy resilience modeling of communities (Shandiz et al. (2020)). Implementation of resilience triangle and resilience trapezoid in different fields has led to the introduction of various indices for resilience quantification. For example, Tierney and Bruneau (2007) measured a system's resilience through the state of functionality of the system after the disaster and the time it takes to go back to the normal condition. Panteli et al. (2016) introduced time-dependent resilience metrics (named $\Phi\Lambda E\Pi$ metric system) for quantification of infrastructure resilience in power systems, which is based on the speed (Φ) and the magnitude (Λ) of the damaged grid functionality, the duration of the damaged state (E), and the recovery speed (Π). In the context of the built environment, the literature concerning resilience can be categorized into the urban or building scale. For instance, urban energy resilience has been defined and evaluated against climate change (Nik et al. (2020)) and other threats such as cyber-attacks, terrorism, etc (Sharifi and Yamagata (2016)). In the building scale, passive survivability and thermal autonomy have been used as measures to quantify thermal resilience against to power failures and extremely hot (Baniassadi and Sailor (2018)) and cold (Ozkan et al. (2019)) weather. These two measures are only focusing on the disturbance propagation phase in the resilience trapezoid and they are not reflecting other characteristics related to resilience in the pre-disturbance and post-disturbance phases. This paper will focus on the building thermal resilience and introducing the multi-phase resilience curve based on the results of building performance simulation. This multi-phase curve will ease the application of resilience metric for building thermal resilience. Furthermore, a test framework is applied to conceptualize the application of the resilience metrics on the multi-phase resilience curve. This test framework applies a duration of 12 days test of building thermal performance by considering a disturbance with a duration of four days.

Resilience in the built environment

Even though there are various definitions of resilience in the literature, building resilience requires more research. The resilience of building can be defined based on its characteristics (e.g. building envelope, energy systems, storage and backup systems, etc.) and the nature of disruption, which affects the building. For example, a building can be resilient to extreme hot weather but not to extreme cold weather. In most of the definitions of resilience, there are six components which are known as "abilities of system to prepare, resist, absorb, response to, adapt to, and recover from a disturbance" (Carlson et al. (2012)). Based on the context, a different combination of these abilities can be implemented for the definition and conceptualization of resilience. To achieve a comprehensive definition and assessment for building resilience, four main questions have been raised and answered in this paper: "Resilience of what?", "Resilience to what?", "Resilience in what stage?", "Resilience based on what?". These questions will be answered as follows:

- Resilience of what?

In the context of built environment resilience can be evaluated in different scale: single zone, systems, building, neighbourhoods, or even larger scales such as urban scale or cities. Furthermore, the resiliency of occupants as one of the important players in the building can be evaluated (Pisello et al. (2017)). In this paper, the thermal resilience of the building and its integrated systems has been evaluated. Here, the performance is evaluated based on indoor operative temperature resulted from a building performance simulation tool.

- Resilience to what?

Understanding the source of disturbances and shocks is essential for resilient building designs and protect-
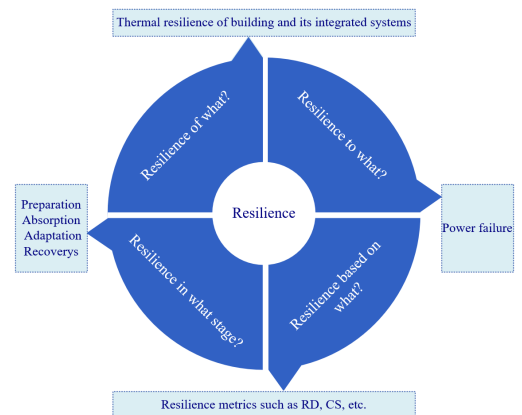

Figure 1: Resilience questions and answers in this paper.

ing buildings against disturbances. Several types of disturbances can influence the building performance. These disturbances have been classified into two different approaches in the literature. The first approach is the classification of disturbances based on their probability of occurrence and impact intensity, which classifies disturbances into two groups: low probability high impact events or high probability low impact events (Nik et al. (2020)). In resilience evaluation, low probability high impact events have been used (Panteli and Mancarella (2015)). The second classification, which has been found is focusing on the impact intensity and duration of disruptive events (Shandiz et al. (2020)). For example, this can classify heat waves to high impact heat waves with a short duration time, or low impact heat waves with a long duration time. Different events that can disrupt the building performance can be found in the literature such as fires, windstorms and hurricanes, flooding, heat waves, ice storms, power outage, and pandemic situation Shandiz et al. (2020). In this paper, the thermal resilience of the building and its systems has been evaluated against a power failure, which will last for four days.

- Resilience in what stage?

The other important component in defining resilience is identifying the stages, which a resilient building is facing in the cycle of disruptive events. These stages are also known as resilient system abilities. As stated before, there are six main abilities for a resilient system, and different combination of these abilities have been selected in resilience definition in different fields. For example, Sharifi and Yamagata (2016) suggested abilities of preparation, absorption, recovery, and adaptation for the sustainable and resilient urban system. Shandiz et al. (2020) counted preparation, withstanding, adaptation, and recovery as important abilities of the energy resilient communities. Nik et al. (2020) divided the resilience characteristics to four main groups: planning and preparation, resisting, adapting to, and recovering from. Based on the context of current work, which is focusing on a single building, and to make the suggested resilience metrics more understandable, four main abilities (stages) are suggested in this paper. Based on these abilities, in order to be resilient, the building should be able to prepare, absorb, adapt to, and recover from the disruptive event for protecting building's occupant from health injuries due to the disruptive event. These abilities will be discussed in the next section.

- Resilience based on what?

The last essential question is related to the metrics for measuring resilience. Different types of resilient measures such as time-dependent measure have been introduced in various fields (Panteli et al. (2016)).

Metrics, which have been used here for quantification of building thermal resilient against power failure will be explained in the next section. Figure1 shows the four main questions and their answers, which have been considered in this paper.

Test framework and metrics

Illustration of building thermal resilience

In order to illustrate the thermal resilience of buildings, i.e., the ability of buildings to prepare, absorb, adapt to, and recover from the disruptive event, the multi-phase performance curve is used to conceptualize the resilience phases and abilities and quantify the thermal resilience of buildings. This curve is inspired by resilience triangle and resilience trapezoid and uses the results of the dynamic building performance simulation for curve establishment. The performance can be measured by different indicators, here the indoor operative temperature resulted in the building performance simulation is considered as an indicator. Figure 2 shows the multi-phase resilience curve with the placement of phases and abilities during the time. Every solid line in this figure shows a parameter, which is fixed based on the assumptions and the dashed lines are the variables, which are case-dependent and they will be changed based on the impact of the event and the building characteristics. Three phases can be seen in the multi-phase performance curve of the building.

1. Phase I: Pre-disturbance phase: In this phase, the building is operating based on the set point temperature (which is considered as the target and for example in Figure 2 is 21.5°C) before the disruptive event.

2. Phase II: Disturbance progress phase: The disruptive event occurs at the beginning of this phase and the performance of the building (the indoor operative temperature) decreases until the end of this phase.
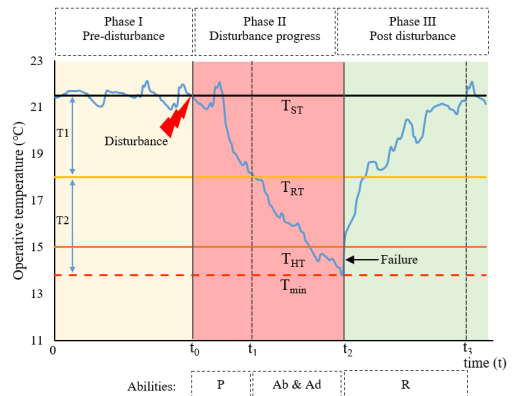

Figure 2: The multi-phase resilience curve (P: Preparation, Ab: Absorption, Ad:Adaptation, R:Recovery).

3. Phase III: Post disturbance phase: This phase shows the recovery process, which the building operative temperature is going to be improved and come back to the set target or even more. Post disturbance phase consists of two parts: the restoration part, which the temperature increases until the set target and post-restoration, which happens after passing the set target.

In addition to these phases, it can be seen that there are four different performance levels in the multi-phase performance curve. These performance levels can be defined as below:

- T_{ST}: is the set target (the setpoint temperature), which is needed for the desired performance of the building.
- T_{RT}: is the performance robustness threshold. Any performance(i.e., operative temperature) higher than this value will be a robust performance and if the operative temperature is less than T_{RT}, the performance will not be robust.
- T_{HT}: is the habitability threshold for the occupant. Passing this threshold shows that the building has been failed in providing the minimum required comfort condition for building's occupant. If the performance of the building (i.e., indoor operative temperature) passes this threshold, the building will not manage to have a safe recovery. But if the building manages to recover before reaching the habitability threshold, the building will be thermally resilient.
- T_{min}: is the minimum performance level caused by the disruptive event.

Considering three phases and the four performance levels, the thermal resilient building's abilities in the action cycle of facing a disruptive event can be defined as follow:

- Preparation: This ability shows by design how much the building is prepared for the disruptive event and for how long it can perform higher than robustness threshold and minimize the potential adverse impact of the disruptive event. This depends on the building characteristics such as building envelope, storage systems, etc.
- Absorption and adaptation: Although the building is prepared for the disruptive event, still the robustness threshold can be crossed. Therefore, the building and its integrated systems should be configured in a way that they can absorb the impacts of the disruptive event and minimize the overall disruption. Furthermore, the building should be able to adapt to the impact of the disruptive event and modify its configuration.
- Recovery: The ability of the building to return back to the set target performance level (T_{ST}) after the disruptive event. Restoration to the set target performance level depends on the impact

intensity of the disruptive event, the degree of previously mentioned abilities e.g., preparation, absorption, and adaptation.

In the next section, a test framework will be introduced to implement the resilience metric for the multi-phase resilient curve.

Four days test framework

Based on the introduced phases, abilities and performance levels, a test framework is developed for evaluation of building thermal resilience in three phases and considering different abilities. This framework implements the building performance regarding the indoor operative temperature, which is resulted in a dynamic building performance simulation tool (i.e., IDA ICE). In this framework, a fixed duration power failure is applied as a disruptive event. The following assumptions can be considered regarding the test framework:

1. The test framework can be applied for all-electric buildings, which are using electricity for providing all types of demand in buildings.
2. The disruptive event is a fixed duration power failure, which will last for four days. Furthermore, four days before the disturbance (pre-disturbance phase) and four days after the disturbance (post disturbance phase) have been evaluated in the test framework. In total, the test evaluation will take 12 days.
3. The set target in the test framework is based on the setpoint temperature suggested in the Norwegian standards(TEK (2020)).
4. It is assumed that the robustness margin allows 3.5°C tolerance from the set target (setpoint temperature based on the standard).

A set of metrics inspired by power resilience (Panteli et al. (2016)) and adapted to the building context, has been used to quantify building thermal resilience in the suggested test framework. These metrics should be able to represent thermal resilience in different phases and considering abilities. Table 1 shows the set of metrics that have been used for the evaluation of thermal resilience in the suggested test framework. Robustness duration (RD) shows for how long the building performance can be maintained robust after facing power failure. The higher robustness duration, the building will be more prepared for facing the disruptive event. CS shows the collapse speed, means how fast the building performance will drop from the set target. Lower values for CS shows that the building can absorb the impact of the event and for this reason, the performance will be decreased with a lower speed. AoE shows the amplitude of the power failure impact (the minimum performance of the building that will be experienced after power failure). Smaller AoE reflects that the building is better able to absorb the impact of the event and adapt to

Table 1: Description of resilience metrics (P: Preparation, Ab: Absorption, Ad:Adaptation, R:Recovery).

Metric	Name	Unit	Equation	Phase	Ability
RD	Robustness Duration	hr	$t_1 - t_0$	Phase II	P
CS	Collapse Speed	°C/hr	$\frac{T_1 + T_2}{t_2 - t_0}$	Phase II	Ab and Ad
AoE	Amplitude of Event	°C	$T_1 + T_2$	Phase II	Ab and Ad
RS	Recovery Speed	°C/hr	$\frac{T_1 + T_2}{t_3 - t_2}$	Phase III	R
EPL	Expected Performance Loss	degree.hour	$\left[\int_0^t (T_{ST} - T(t))\, dt\right]$	All phases	All abilities

it.If AoE is greater than the difference between T_{ST} and T_{HT}, the building will not perform thermally resilient. RS is the recovery speed in the restorative phase, which shows how promptly the building can restore to its set target, after connecting the power after four days. Higher RS shows that the building has a better ability for recovery. EPL represents the expected performance loss considering both impact intensity and duration of the power failure. The lower EPL shows that the performance deviated less from the target during the disruptive event and this will lead to a more resilient building.

Case study

To assess the suitability and usability of the proposed multi-phase resilience curve and test framework, they are demonstrated for a case study of Norwegian single-family house, with two different competitive designs and possibility of implementation of storage technology. A representative model of the Norwegian single-family house is chosen as the case study building. It is a two-story building located in Oslo, and the layout of the building is the same as (Homaei and Hamdy (2020)). This building is divided into three thermal zones in IDA Indoor Climate and Energy software (IDA-ICE) (IDA (2020)) to calculate the temperature and energy demand of each zone. The first floor consists of the living room, and the bedroom and bathroom are placed on the second floor. The building is an all-electric building, which means that electricity is used for providing all of the demands in the building. Besides, it is a heating-dominated building and it does not have cooling demand. The heating demand is based on direct electrical heating with electric radiators. Occupancy schedules, domestic hot water distribution, and internal heat gains are based on (Nord et al. (2016)). Heating set points, window opening strategy, and window shading is based on scenario 1 in (Homaei and Hamdy (2020)) and IWEC weather file from the library of IDA ICE has been used for running the simulations. Two designs regarding the building envelope and ventilation systems have been considered for testing. These designs are competitive, means that both of them are meeting the energy target of TEK17 standard (the current minimum requirement in Norway)(TEK (2020)). In the first design, design parameters (e.g., building envelope, ventilation, etc) are based on the recommended parameters in TEK 17 standard, but the second design is meeting the

Table 2: Details of the two competitive designs considered in the case study demonstration.

Design parameters	D_1	D_2
Overall U-value $(w/m^2.K)$	0.31	0.25
Ventilation system	Balanced	Exhausted
Solar thermal collector size (m^2)	0	5
Lighting	Typical	LED light
Energy consumption(kWh/m^2)	110	110
Battery size (kWh)	48	62

energy target of TEK 17 with using of other combination of design parameters. The energy system in both designs are electric radiators, while D_1 is using balanced mechanical ventilation with a heat recovery unit that has an efficiency of 80% and D_2 has mechanical exhaust ventilation without a heat recovery unit. The details of each design are shown in Table2. To compensate higher energy consumption resulted by the implementation of the exhausted ventilation, solar thermal collectors and LED lights have been added to D_2. In addition to the building design parameters, the impact of batteries as storage facilities on the resiliency of the building have been considered for the two designs. For this purpose, the two competitive designs have been equipped with batteries. The size of the battery for these two design is based on (Homaei and Hamdy (tted)), which in batteries are used for storage of the generated heat shift based on the implementation of dynamic pricing tariffs, suggested by the Norwegian regulator. Homaei and Hamdy suggested a new approach for battery sizing, which is called "cost-effective battery sizing strategy". The interested reader is referred to (Homaei and Hamdy (tted)) for more details. The battery size for each design is reported in Table 2. Considering the battery option will lead to in total of four designs for testing of the suggested method. The disruptive event for this case study is the grid power failure, which will last for days in typical cold days during winter (starting 14th January). In this work, the thermal resilience has been evaluated for one zone in the building (here the living room with a set point temperature of 21.5 °C based on TEK17 standard). The hourly indoor operative temperature resulted in IDA ICE has been used for calculating thermal resilience metrics. In the next section, the test framework will be applied for the two introduced designs with and without considering battery for them, and the suggested metrics will be calculated.

Results

Building thermal resilience can be dependent on different parameters such as building envelope, ventilation system, heating systems, and storage systems in a design package. Within this context, two competitive designs, with the possibility of implementation storage capacity developed to evaluate the impact of design options on thermal resilience and test the suitability of the proposed test framework. Figure 3 and Figure 4 shows the time-dependent multiphase resilience curve for the D_1 and D_2, respectively. Each curve has the performance with and without the implementation of battery. The shape of the curve shows the actual performance of the building during the disturbance and it enables the metric quantification. The three phases can be clearly identified. The duration of each phase is four days as suggested in the resilience test framework.

Resilience metrics

The first metric to evaluate is the robustness duration (RD), i.e., for how long the temperature of the building will not pass the robustness margin. Based on the recommendations of the World Health Organization (WHO (2018)), 18°C is a safe and well-balancing temperature to protect the health of general populations during cold seasons in countries with temperate or cold climates. For this reason, 18°C has been selected as robustness threshold. Furthermore, 15°C has been selected as the habitability threshold based on a comprehensive review on the effect of low temperatures on elderly morbidity (Collins (1986)). RD for the two designs with and without batteries can be seen with dashed black lines in Figure 3 and Figure 4. Furthermore, the values related to RD for both designs with and without a battery can be found in Table 3. This table shows that D_2 has higher RD in comparison to D_1, because of encompassing stronger building envelope. Besides, the implementation of
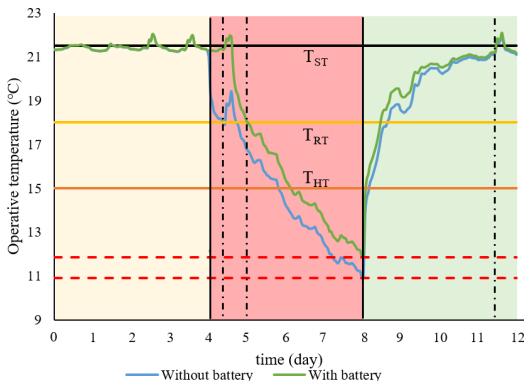
Figure 4: The multi-phase resilience curve for D_2 with and without battery.

Table 3: Resilience metrics for two introduced designs(WB: With battery, WOB:Without battery).

Metric	D1		D2	
	WOB	WB	WOB	WB
RD (hr)	9	24	23	38
CS (°C/hr)	0.110	0.100	0.099	0.080
RS (°C/hr)	0.120	0.115	0.102	0.086

batteries for both cases has increased the robustness of the building and the building will last for a longer time above the robustness margin. For example, for D_1, RD increases from 9 hours to 24 hours, while for D_2 it increases from 23 to 38 hours when the battery is implemented. It can be concluded that stronger envelope and battery storage will aid the building to be more prepared for facing the power failure. Figure 3 and Figure 4 shows that both designs do not have a safe recovery after facing power failure for four days even with the application of batteries.

The second metric to evaluate within the test framework is collapse speed (CS) i.e., how fast the resilience drops in phase II. Table 3 shows CS for both designs with and without battery. Based on this table, battery implementation will make the temperature reduction process slower. On the other hand, D_2 has a smaller CS in comparison to D_1. This is because of higher U-values in D_2, which will lead to a longer time to cool down the building. So, a stronger envelope and the battery are effective design options for helping the building to better absorb the impact of the power failure and adapt to it.

AoE (which shows how low the performance drops in phase II) can be seen from Figure 3 and Figure 4. For case of D_1 without battery, AoE is 10.6 °C. This means that if a TEK 17 design, faces with four days power failure, its temperature will be decreased until 10.9 °C from the setpoint temperature, which is 21.5

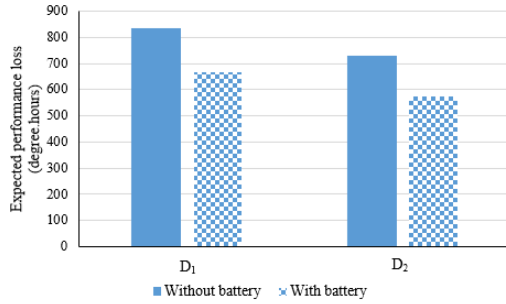Figure 3: The multi-phase resilience curve for D_1 with and without battery.

Figure 5: Expected performance loss(EPL) for the two designs.

°C. If D_1 is equipped with the battery, the amplitude of the event will be decreased to 9.6°C and the minimum temperature during the disturbance propagation phase will be 11.9°C. For D_2, AoE for the case with and without the battery is 8.6°C and 7.7°C, respectively. This means that the minimum temperature during the disturbance propagation phase will be 12.9 °C and 13.8 °C for D_2, with and without battery, respectively.

The next metric to evaluate in the test framework is the recovery speed (RS), i.e., how fast the resilience will be recovered in phase III. RS values have been showed in Table 3. The time duration that takes for a design to come back to the set point temperature, is in the same range for both cases, with and without the battery. This is because of using battery does not have a direct impact on phase III, but it decreases the AoE and Smaller AoE will lead to smaller RS. For this reason, the RS in the case with battery is lower than the case without battery for both designs D_1 and D_2. When it comes to comparing RS for D_1 and D_2 (without battery), it should be noted that the recovery time for D_2 is higher than D_1. The reason is the stronger building envelope in D_2, which will lead to a longer time to heat the building. On the other hand, AoE value for D_2 is smaller. The combination of these two effects, make the recovery speed for D_2 slower than D_1.

The last metric in the test framework is the expected performance loss (EPL), i.e., how much of the performance has been lost considering both impact intensity and duration of the power failure. EPL has been shown in Figure 5 for D_1 and D_2. Implementation of the battery, decreases EPL in both D_1 and D_2. This happens because the battery will decrease the amplitude of the event and also delays the temperature reduction process. When it comes to the comparison between D_1 and D_2, D_2 has less performance loss, because of having stronger envelope that can absorb the impact of power failure in a higher level.

Conclusion

A multi-phase resilience test framework for evaluating building thermal resilience has been introduced in this paper. The test framework, which is called the "four days test" consists of three different phases:pre-disturbance phase, disturbance progress phase, and post disturbance phase, which each of them will last for four days, leading to in total test duration of 12 days. The considered disturbance in this test framework is the power failure and the performance indicator, which is used here is the indoor operative temperature resulted from building performance simulation in IDA ICE. Thermal resilience in the proposed test framework has been quantified using a set of resilience metrics. These metrics show for how long the building is thermally robust (RD metric), how fast (CS metric) and how low (AoE metric) the thermal resilience will drop after a facing the disturbance, how fast the building performance will be back to it pre-disturbance state (RS metric), and how much of the performance has been lost by the disruptive event (EPL metric). These metrics can be used as useful tools to show the effect of different building designs options such as building envelope, storage systems, backup systems, etc. This can be beneficial for designers and decision-makers to identify the impact of different design options and strategies in improving building thermal resilience. The trade-off between building thermal resilience and other performance criteria (e.g., efficiency, comfort, robustness, cost,) will help the decision-makers to select the most appropriate building design in different circumstances. A case study building has been used here to show the impact of building envelope and the battery storage on the different resilience metrics. The results show the suitability of the suggested test framework and metrics to quantify building thermal resilience, and evaluate the effect of different design strategies on the building thermal performance when it is facing to disruptive events. The test framework in this paper is applied for evaluating thermal behaviour of the building when it is exposed to power failure, but it also can be extended to evaluate other performance criteria such as energy and other disruptive events such as extreme weather events. The focus of this paper was in evaluating the thermal resilience for a single zone in a multi-zone building. The future work will be continued to find out how the thermal resilience metrics can be generalized to represent the building's overall thermal resilience.

Acknowledgment

References

(2018). Who housing and health guidelines. https://www.who.int/publications/i/item/9789241550376.

(2020). Byggteknisk forskrift (tek 17). `https://dibk.no/byggereglene/byggteknisk-forskrift-tek17/14/14-2/`.

(2020). Equa solutions ab ida indoor climate and energy (version 4.8). `https://www.equa.se/en/ida-ice`.

Baniassadi, A. and D. J. Sailor (2018). Synergies and trade-offs between energy efficiency and resiliency to extreme heat–a case study. *Building and Environment 132*, 263–272.

Bao, M., Y. Ding, M. Sang, D. Li, C. Shao, and J. Yan (2020). Modeling and evaluating nodal resilience of multi-energy systems under windstorms. *Applied Energy 270*, 115136.

Bruneau, M., S. E. Chang, R. T. Eguchi, G. C. Lee, T. D. O'Rourke, A. M. Reinhorn, M. Shinozuka, K. Tierney, W. A. Wallace, and D. Von Winterfeldt (2003). A framework to quantitatively assess and enhance the seismic resilience of communities. *Earthquake spectra 19*(4), 733–752.

Campbell, R. J. and S. Lowry (2012). Weather-related power outages and electric system resiliency. Congressional Research Service, Library of Congress Washington, DC.

Argonne National Lab.(ANL), Argonne, IL (United States) (2012). *Resilience: Theory and Application.*.

Cimellaro, G. P., O. Villa, and M. Bruneau (2015). Resilience-based design of natural gas distribution networks. *Journal of Infrastructure systems 21*(1), 05014005.

Collins, K. (1986). Low indoor temperatures and morbidity in the elderly. *Age and Ageing 15*(4), 212–220.

Holling, C. S. (1973). Resilience and stability of ecological systems. *Annual review of ecology and systematics 4*(1), 1–23.

Holling, C. S. (1996). Engineering resilience versus ecological resilience. *Engineering within ecological constraints 31*(1996), 32.

Homaei, S. and M. Hamdy (2020). A robustness-based decision making approach for multi-target high performance buildings under uncertain scenarios. *Applied Energy 267*, 114868.

Homaei, S. and M. Hamdy (Submitted). Quantification of energy flexibility and survivability of all-electric buildings with cost-effective battery size : Methodology and indexes. *Applied Energy*.

Hosseini, S., K. Barker, and J. E. Ramirez-Marquez (2016). A review of definitions and measures of system resilience. *Reliability Engineering & System Safety 145*, 47–61.

Kenward, A. and U. Raja (2014). Blackout: Extreme weather climate change and power outages. *Climate central 10*, 1–23.

Moazami, A., S. Carlucci, and S. Geving (2019). Robust and resilient buildings: A framework for defining the protection against climate uncertainty. In *IOP Conference Series: Materials Science and Engineering*, Volume 609, pp. 072068. IOP Publishing.

Nik, V. M., A. Perera, and D. Chen (2020). Towards climate resilient urban energy systems: a review. *National Science Review*.

Nord, N., L. H. Qvistgaard, and G. Cao (2016). Identifying key design parameters of the integrated energy system for a residential zero emission building in norway. *Renewable Energy 87*, 1076–1087.

Ozkan, A., T. Kesik, A. Z. Yilmaz, and W. O'Brien (2019). Development and visualization of time-based building energy performance metrics. *Building Research & Information 47*(5), 493–517.

Panteli, M. and P. Mancarella (2015). The grid: Stronger, bigger, smarter?: Presenting a conceptual framework of power system resilience. *IEEE Power and Energy Magazine 13*(3), 58–66.

Panteli, M., C. Pickering, S. Wilkinson, R. Dawson, and P. Mancarella (2016). Power system resilience to extreme weather: fragility modeling, probabilistic impact assessment, and adaptation measures. *IEEE Transactions on Power Systems 32*(5), 3747–3757.

Panteli, M., D. N. Trakas, P. Mancarella, and N. D. Hatziargyriou (2017). Power systems resilience assessment: Hardening and smart operational enhancement strategies. *Proceedings of the IEEE 105*(7), 1202–1213.

Pisello, A., F. Rosso, V. Castaldo, C. Piselli, C. Fabiani, and F. Cotana (2017). The role of building occupants' education in their resilience to climate-change related events. *Energy and Buildings 154*, 217–231.

Rønneseth, Ø., N. Holck Sandberg, and I. Sartori (2019). Is it possible to supply norwegian apartment blocks with 4th generation district heating? *Energies 12*(5), 941.

Rose, A. (2007). Economic resilience to natural and man-made disasters: Multidisciplinary origins and contextual dimensions. *Environmental Hazards 7*(4), 383–398.

Rutter, M. (1987). Psychosocial resilience and protective mechanisms. *American journal of orthopsychiatry 57*(3), 316–331.

Shandiz, S. C., G. Foliente, B. Rismanchi, A. Wachtel, and R. F. Jeffers (2020). Resilience framework and metrics for energy master planning of communities. *Energy*, 117856.

Sharifi, A. and Y. Yamagata (2016). Principles and criteria for assessing urban energy resilience: A literature review. *Renewable and Sustainable Energy Reviews 60*, 1654–1677.

Tierney, K. and M. Bruneau (2007). Conceptualizing and measuring resilience: A key to disaster loss reduction. *Scopus*.

Paper IV

Thermal resilient buildings: How to be quantified? A novel benchmarking framework and labelling metric
Shabnam Homaei and Mohamed Hamdy
Building and Environment. 2021 Jun 2.

Thermal resilient buildings: How to be quantified? A novel benchmarking framework and labelling metric

Shabnam Homaei *, Mohamed Hamdy

Norwegian University of Science and Technology (NTNU), Department of Civil and Environmental Engineering, Trondheim, Norway

ARTICLE INFO

ABSTRACT

The resilient building design has become necessary within the increasing frequency and intensity of extreme disruptive events associated with climate change. Since thermal comfort is one of the main requirements of occupants, evaluating building resilience from a thermal perspective during and after disruptive events is necessary. Most of the existing thermal resilience metrics focus on thermal performance only during disruptive events. Building designers are still seeking metrics that can capture thermal resilience in both phases (i.e. during and after the disruptive events). This paper introduces a novel benchmarking framework and a multi-phase metric for thermal resilience quantification. The metric evaluates thermal resilience concerning building characteristics (i.e. building envelope and systems) and occupancy. It penalises for thermal performance deviations from the targets based on the phase, the hazard level , and the exposure time of the event. The introduced methodology is validated by quantifying the thermal resilient performance of six building designs against a four-day power failure as a disruptive event. The six designs represent minimum and passive building requirements with and without batteries or photovoltaics as resilience enhancement strategies. For the considered case study, upgrading the building from the minimum to the passive design has a huge impact (71%) on resilience improvement against power failure in winter. The application of the battery and PVs can improve the thermal resilience of the two designs in the range of 19%–27% and 44%–60%, respectively. Findings can provide a useful reference for building designers to benchmark the building's thermal resilience and constitute resilience enhancement measures.

1. Introduction

1.1. Scope

Building performance (including energy and comfort) can be affected by a wide range of foreseen and unforeseen changes during operation, such as environment effects (e.g. extreme weather due to the climate change [1]) or new requirements (e.g. new technologies or policies [2,3]). Buildings as facilities with significant investment costs should be able to react to these changes and maintain their performance and functionality. For this reason, interest has been growing to push the building designs beyond the minimum standard requirements to meet performance targets even under future changes [4]. In general, one strategy for adequate future building performance in the face of changes and disruptive events is mitigation in the form of protection [5]. Recently, in this approach, attention is being paid to the concept of resilience, which involves "low probability high impact scenarios". The report of Intergovernmental Panel on Climate Change

(IPCC) [6] shows that the severity and frequency of these scenarios, such as natural disasters, are expected to increase in the following years because of climate change. In comparison to the pre-industrial era, extreme heat events are occurring more frequently, lasting longer, with greater intensity. For instance, the average number of heatwaves in the United States (US) has increased from two in 1960 to six in 2010 [7]. Based on the report of the Copernicus Climate Change Service, 2019 was the warmest year on record for Europe, with June as the hottest month on record [8].

Furthermore, in the past decades, climate change has increased the frequency and severity of extreme cold events, such as windstorms and snowstorms [9]. A recent example is the record of low temperatures during the 2021 winter in Texas, US. The low temperatures were followed first by snow and then by the blackouts, leaving millions of people without access to electricity during the COVID-19 pandemic [10]. Such events can, on the one hand, disturb the energy generation systems and, on the other hand can lead to thermal

Nomenclature

A_{AF}	Total floor area
A_z	Area of each zone
EPC	Energy performance certificates
i	Segment counter
IOD	Indoor overheating degree
IPCC	Intergovernmental Panel on Climate Change
PV	Photovoltaic panel
RCI	Resilience class index
SFP	Specific fan power
S_i	Area of segment i
t	Time
t_0	Disturbance start time
t_1	Disturbance end time
t_2	Test end time
t_d	Delay time
TEK	Norwegian building regulation
T_{HT}	Temperature threshold for habitability
T_{min}	Minimum temperature during test period
TMY	Typical meteorological year
t_R	Recovery time
T_{RT}	Temperature threshold for robustness
T_{SP}	Setpoint temperature
U	U-Value
WUMTP	Weighted unmet thermal performance
$WUMTP_{Overall}$	Overall weighted unmet thermal performance
$WUMTP_{Overall,ref}$	Overall weighted unmet thermal performance of the reference building
W_E	Exposure time penalty
W_H	Hazard penalty
WHO	World Health Organization
W_P	Phase penalty
z	Zone counter

discomfort in buildings. In developed countries, more than 87% of time is spent indoors [11], and indoor thermal comfort is one of the main requirements of building occupants. A survey-based study shows that disruptions in acoustic quality and thermal comfort are the most disruptive factors, which can affect the productivity of buildings occupants [12]. This highlights the evaluation of building performance resilience from a thermal perspective. The report of the European Network of Transmission System Operators shows significant growth in grid disturbance (30%–60%) caused by environmental factors in the Nordic regions [13]. These phenomena, in parallel with the penetration of electrification in buildings, can cause huge losses [14] in the building sector. So, resilient building design against these inevitable events is imperative. In this paper, the building is defined to be resilient if it is able to prepare for, absorb, adapt to and recover from the disruptive event [15]. The building response after facing a disruptive event can be divided into two phases: (i) during the disruptive event and (ii) after the disruptive event. So far, some efforts have been made to improve building resilience, but quantifying these improvements during both phases (i.e. during and after the disturbance) still requires more research. In cold climate countries, such as Norway, a large share of annual energy consumption in buildings is related to the heating seasons [16], in which the heating demand is provided for the building. So, evaluating a building's thermal resilience during heating seasons is important. Furthermore, it is assumed that during the low probable high impact

events, which are needed for resilience evaluation, people will spend most of their time at homes and this highlights the evaluation of thermal resilience for residential buildings. For these two reasons, this study will focus on evaluating the thermal resilience of residential buildings during heating seasons. It is noteworthy that the developed methodology in this study can be used for thermal resilience evaluation during the heating seasons in any geographical area that the building demands heating.

1.2. Resilience quantification

In general, several works have focused on the resilience assessment of systems in various fields. Hosseini et al. [5] separated resilience assessment approaches into two major categories: qualitative and quantitative. The qualitative approaches are based on assessing resilience without numeric descriptions. Methods such as conceptual frameworks and semi-quantitative indices can be placed in this group. In the field of the built environment, Sharifi and Yamagata [17] developed a conceptual framework for assessing urban energy resilience. In another framework, Nik et al. [18] divided the characteristics of resilient urban energy systems into four main groups: planning and preparation, resisting, adapting to and recovering from.

The quantitative approaches assess resilience with respect to numeric descriptions and are divided into two subcategories: general and structural-based modelling. The general approaches are based on empirically observable metrics of system performance without considering specific system characteristics. The resilience triangle developed by Bruneau et al. [19] in the field of seismic resilience is the most representative general-based method, which uses the total impact (i.e. performance losses during and after disruptions) to measure seismic resilience. The resilience trapezoid model [9] is another well-known general-based method, which considers the degraded state that the system experiences when facing a disruptive event. Panteli and Mancarella [20] were the first to use the resilience trapezoid for quantification grid resilience by the introduction of a set of time-dependent metrics called the $\Phi \Lambda E \Pi$ metric system, which is based on the speed Φ and the magnitude Λ of the damaged grid functionality, the duration of the damaged state E, and the recovery speed Π.

In the context of the built environment, Homaei and Hamdy [15] have adjusted these metrics for the quantification of different resilient abilities (i.e. preparation, absorption, adaptation, recovery). Li et al. [21] evaluated the impact of energy storage systems for health care centres facing power failure during the pandemic using the total impact approach and introducing a resilience index (the ratio of the supplied electric load to the total amount of electric load over a year). Shandiz et al. used the resilience trapezoid and time-dependent resilience metrics for evaluating the energy resilience of communities [22].

In structural-based approaches, system characteristics and behaviour need to be modelled or simulated to examine how the system's structure can influence its resilience. Simulation models are structural-based approaches in which simulations are used to represent uncertain behaviour of the system in resilience quantification [23]. For the built environment, dynamic building performance simulations are vital in the estimation of the building performance during normal and abnormal conditions. For example, Katal et al. [1] calculated the building thermal resilience in terms of winter passive survivability for the 1971 Montreal snowstorm by combining CityFFD (City Fast Fluid Dynamics) and CityBEM (City Building Energy Model) simulations. O'Brien et al. [24] used Energy Plus building performance simulation software for simulating the performance of high-rise residential buildings in Canada in case of power failure during winter and summer. They applied passive survivability and thermal autonomy as metrics for resilience evaluation.

Resilience metrics are essential in the quantification of resilience based on simulation results. Specific criteria should be considered

regarding resilience metrics, such as repeatability and comparability [25]. Furthermore, resilience quantification needs to not only capture resilience during the disruptive event, but also after the disruptive event. The metric should also indicate how far and for how long the building performance is deviated from the targets. In other words, the metric should be sensitive to the hazard level and exposure time to the disruptive event.

Some typical simplified metrics have been used in the context of a building's thermal resilience based on simulation results. For instance, overheating risk [26,27] and heat index [28,29] are most used for evaluating building thermal resilience against disruptions like climate change and heatwaves. Another two simplified metrics that have been developed recently are passive survivability [1,24,30] and thermal autonomy [24]. The main issue with these simplified metrics is that they need to be used in the scale of one thermal zone and cannot unfold the resilience in the building level, called overall thermal resilience in this paper, which considers all zones of the building. To overcome this issue, Hamdy et al. [31] introduced a new index called IOD (indoor overheating degree), which considers different thermal comfort limits depending on the zone and takes the intensity and frequency of overheating into account. Furthermore, simplified metrics such as passive survivability and thermal autonomy only focus on thermal performance during the disruptive event. So far, little progress has been made on developing metrics that capture resilience in both phases of the disruptive event. Therefore, crucial information related to the post-event phase and building recovery can be lost. Putting together the literature on the resilience quantification approaches and metrics in the field of building thermal performance provides insights on the importance of resilience quantification with an appropriate set of metrics. These metrics should help benchmarking of different designs from resilience perspective in more informative and easy to understand approaches. Therefore, this work introduces a new multi-phase metric for quantifying the building overall thermal resilience (i.e. thermal resilience of whole building).

1.3. Contribution of this paper

As described above, the frequency and severity of extreme events increase because of climate change. Therefore, resilient building design is essential to face disruptive events. This paper introduces a methodology to quantify the overall building thermal resilience in case of disruptive events. The methodology aims to (i) develop a test framework for building thermal resilience quantification, (ii) quantify the overall thermal resilience for buildings, (iii) label the building thermal resilience, which can be included in energy performance certificates (EPCs) [32]. A new single metric for resilience quantification, called the weighted unmet thermal performance (WUMTP), is defined within the proposed methodology and allows the identification of the building resilience class. Indeed, the main novelty of this work is the introduction of the resilience test framework and quantification metric, with which a single value can summarise and weight all aspects affecting the building thermal resilience. There are two main considerations for this metric:

- The boundary conditions for metric quantification with respect to the building is focusing on building characteristics (including building envelope and systems) and occupancy in multi-zones with different thermal condition limits. This means that the developed metric can capture the changes in thermal resilience based on variations of these conditions not only for one zone but also for the whole building.
- The scope of metric quantification with respect to the disruptive event focuses on the phase of the event, the hazard level of the event, and the exposure time to the event. Changing one of these factors can affect the thermal resilience of a building.

As stated before, the scope of the developed test framework was on evaluating the thermal resilience of residential buildings during heating seasons. Residential buildings have been selected here because it is supposed that during the abnormal condition, which is needed for resilience evaluation, occupants will spend most of their time at homes. In Norway as a country with a cold climate, buildings are mostly heating dominated. For this reason, the suggested metric with the developed test framework was assessed for a case study of a Norwegian single-family house with two different designs which appropriately fits the scope of this study. Furthermore, the impact of design options and resilience enhancement strategies, such as battery storage and a photovoltaic (PV) system, on thermal resilience was evaluated. The paper is structured as follows. Section 2 describes the development of the test framework for the building thermal resilience evaluation. In addition, the thermal resilience quantification, WUMTP formulation, and resilience classification and labelling are described. In Section 3, the case study building is described along with different building designs and resilience enhancement strategies. Section 4 presents the results of the application of the resilience quantification and labelling methods for the case study. The impact of two resilience enhancement strategies was evaluated for the case study building. The paper concludes by outlining the practical implications of resilience quantification in building thermal performance predictions and explaining how this quantification of resilience can be helpful for building designers and decision-makers (Section 5).

2. Methodology

2.1. Multi-phase resilience curve associated to an event

In general, the performance of systems concerning a disruptive event as a function of time can be shown by two concepts: resilience triangle [19] and resilience trapezoid [9], which have widely been used in different fields such as seismic engineering, power engineering, etc [9,19]. The concept of the resilience triangle is the foundation for the analytical assessment of resilience, and it describes the deterioration of a system's functionality over the disruptive event timeline [33]. In this concept, immediate restoration actions are assumed to be taken at the end of the disturbance. The concept of the resilience triangle has been extended by resilience trapezoid, which considers the degraded state that the systems experience when facing a disruptive event. Being inspired by these two concepts, analysis of pre-simulation results of building performance during a disruptive event shows that buildings as dynamic systems are experiencing an exponential degradation when they are faced with disruptive events. So, in this paper, the performance of building concerning a disruptive event as a function of time is plotted with a curve. Similar to the resilience triangle [19], immediate restoration actions are assumed to be taken at the end of the disturbance. The plotted curve named the "multi-phase resilience curve" because of the two phases of the disruptive event — phase I, namely "during the disruptive event", and phase II, "after the disruptive event". Furthermore, two states are also represented in the multi-phase resilience curve to show the performance of building in initial and final states. Based on the definition of resilient buildings, the building is able to prepare in the initial state, absorb and adapt during the disruptive event (phase I) and recover after the disruptive event (phase II). The multi-phase resilience curve is a simulation-based curve. The performance of building in the initial state, during and after the disruptive event, and in the final state has been simulated by modelling the building using a dynamic whole building simulation tool. Building simulation has been selected here because it creates the possibility of easily controlling building boundary conditions and evaluating building performance under the disruptive event, which is not an easy task when it comes to the experimental methods. The performance of the building is simulated under a typical metrological year (TMY) weather file, which can properly show the most typical pattern of weather during a

year. Furthermore, the disruptive event applies during a specific part of the heating season, for a specific time period, which will be elaborated later in Section 3.2. By running the building performance simulation during the period of the multi-phase resilience curve, performance of the building during the normal and abnormal conditions (i.e., states and phases) will be determined and form the multi-phase resilience curve. The implemented building performance simulation tool in this work is IDA Indoor Climate and Energy software (IDA ICE) [34], which applies equation-based modelling in Neutral Modelling Format (NMF) and has been validated using several validation tests [35,36]. The performance across different phases in the multi-phase resilience curve can be quantitatively measured by the application of suitable indicators of various performance criteria. Here, the "building indoor operative temperature" resulting from the simulation was used as a performance indicator to create the multi-phase resilience curve for the thermal resilience evaluation. It is noteworthy that other important factors such as humidity can influence the evaluation of thermal resilience, but in this study for the sake of simplicity thermal resilience has only been evaluated concerning the temperature. The indoor operative temperature is what humans perceive thermally in a space; it is a simplified measure of human thermal comfort derived from the mean radiant temperature and air temperature [37]. Furthermore, the curve experiences different temperature thresholds in case of a disruptive event. The conceptual illustration of the multi-phase thermal resilience curve, along with states, phases, and different performance thresholds, is shown in Fig. 1. Solid lines in this figure represent a fixed parameter, while dashed lines are case-dependent variables. The states and phases can be described as follows:

- Initial state ($0 \leq t < t_0$: In this state, the building operates based on the set point temperature (which is considered the target) before the disruptive event. Based on the resilient building definition, the building is preparing for the disruptive event in this state.
- Phase I($t_0 \leq t < t_1$): This phase is placed between the initiation and the end of the disruptive event, during which the indoor operative temperature is usually decreasing continuously. Based on the definition of resilient building, the building absorbs the impact of and then adapts to the disruptive event in this phase.
- Phase II ($t_1 \leq t < t_2$): This phase starts after the end of the disruptive event and lasts until the building reaches the same performance level in initial state. During this phase, the indoor operative temperature is usually increasing continuously. Based on the definition of the resilient building, the building recovers from the disruptive event in this phase.
- Final state ($t > t_2$): This state starts after the full recovery of the building. In this state, the building operates based on the setpoint temperature like in the initial state.

In addition to these phases and states, four different performance thresholds are in the multi-phase thermal resilience curve:

- T_{SP} is the set target (the setpoint temperature), which is needed for the desired performance of the building.
- T_{RT} is the performance robustness threshold. Any performance (i.e. operative temperature) higher than this value will indicate a robust performance, and if the operative temperature is less than T_{RT}, the performance will not be robust from the thermal point of view.
- T_{HT} is the performance threshold for habitability. Any performance (i.e. operative temperature) lower than this value will create an uninhabitable condition for the building occupants.
- T_{min} is the minimum experienced performance (i.e., operative temperature) during phase I.

By considering these four performance thresholds, three performance levels are created. Values between T_{SP} and T_{RT} indicate an acceptable performance (acceptable level). Between T_{RT} and T_{HT}, the performance will be in the habitable level, and any value less than T_{HT} indicates an uninhabitable level. Every level is shown with a different colour in Fig. 1.

To quantify building thermal resilience based on a multi-phase resilience curve, a test framework is introduced in the next section, establishing the requirements for thermal resilience quantification.

2.2. Resilience test framework

The purpose of the thermal resilience test framework is to determine the effect of a given disruptive event with a fixed duration on the building thermal performance. In developing each test framework, three factors should be considered:

1. The disruptive event (The occurrence time (t_0) and the event duration($t_1 - t_0$)): Literature shows that various source of disruptive events such as fires, windstorms and hurricanes, flooding, heatwaves, ice storms, power outage, and the pandemic situation can influence building performance [38]. In the suggested test framework, it is assumed that the disruptive event will last during a fixed duration. This fixed duration and the initiation time of disruptive event are important parameters that should be considered when developing a test framework.
2. Duration of phase II ($t_2 - t_1$) — The thermal performance of the building after the disruptive event should also be simulated in order to determine how can it recover after the disruptive event. For the suggested test framework, it is assumed that phase II will last as long as phase I to capture how the building recovers from the disruptive event. During this phase, the time duration that takes the building to reach its pre-disturbance state called recovery time, and shown with t_R in Fig. 1. t_R shows how fast the building can recover from the disruptive event.
3. Performance levels: The range of different performance levels that have been defined in the previous section should also be specified when developing the test framework.

The suggested resilience test framework involves a fixed-duration disruptive event and simulates the performance of the building during and after the disruptive event. The application of an appropriate set of metrics for the developed test framework leads to thermal resilience quantification.

2.3. Thermal resilience quantification

2.3.1. Boundary conditions with respect to the building

In this paper, a new metric WUMTP was developed for thermal resilience quantification. WUMTP is a multi-zone metric that not only focuses on phase I but also represents the thermal performance during phase II. This metric can capture the abilities of absorption and adaptation during the disruptive event and recovery after the disruptive event. However, WUMTP does not capture the ability of preparation directly, but preparation affects the other abilities by default. For instance, if the building is more prepared for the disruptive event, it can absorb and adapt better and recover faster from the disruptive event. Furthermore, the focus of this metric is the thermal resilience of the whole building level and not focusing on the individual abilities. Unlike the previously mentioned metrics (e.g. overheating hours at a specified temperature), WUMTP is introduced so that different levels of thermal conditions for different zones can be considered, taking into account specific hours when the building is occupied. The boundaries of the thermal resilience evaluation are kept within the building characteristics (including building envelope and systems) and also the occupants who are using the building, as shown in Fig. 2. WUMTP is determined by calculating the thermal performance deviation from the temperature targets during the occupied hours and penalising them based on where they have been placed in the test framework. A lower WUMTP indicates the building is more thermal resilient.
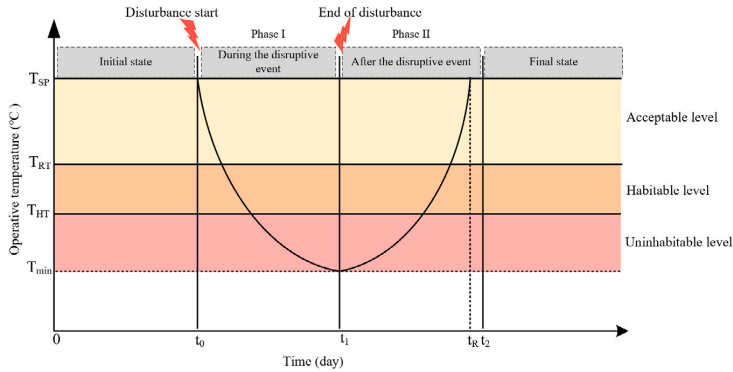
Fig. 1. Illustration of multi-phase thermal resilience curve of buildings.
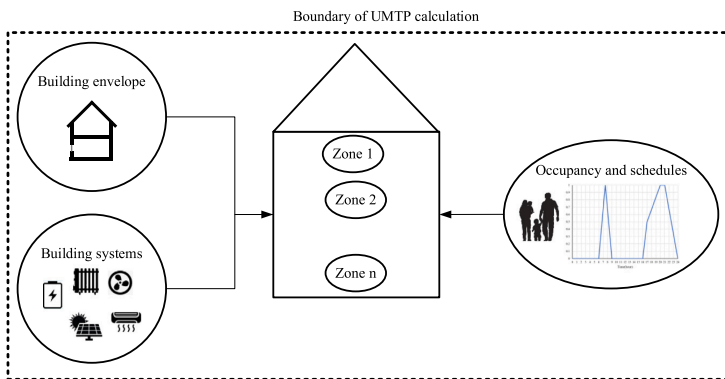
Fig. 2. Illustration of the boundary of WUMTP calculation.

2.3.2. Scope with respect to the event

The calculation of the WUMTP varies in the different phases and thermal performance levels of the test framework. Furthermore, the calculation of WUMTP is not the same for different exposure times within each level. For instance, the first few hours inside the uninhabitable level have a different impact in comparison to the remaining hours. The new metric is, therefore, more sensitive regarding the performance deviation in different parts of the resilience test framework. The quality of performance deviation in different parts can be differentiated by penalising it regarding the following factors, which indicate the scope of WUMTP quantification with respect to the event:

1. The phase of the event differentiates between the WUMTP in phases I and II. The toleration of the performance deviation during the disruptive event is more difficult in comparison to after the disturbance. This is a result of the mental condition that the occupants may experience during each phase. In phase I, the temperature is continuously decreasing, and occupants are facing a pessimistic condition. In contrast, in phase II, the temperature increases continuously, and occupants are facing an optimistic situation, which is easier to bear. The application of different penalties to these phases means the calculation of WUMTP is different as well.
2. The hazard level of the event differentiates between three different performance levels (acceptable, habitable and uninhabitable). The calculation of WUMTP in each of these levels differs with the application of various penalties.

3. The exposure time to the event: which differentiates the WUMTP in different exposure time duration. This differentiation creates two various sections (i.e., easy and difficult exposure sections) inside each phase and level, in which different penalties will be applied for them.

2.3.3. WUMTP metric

The application of two phases, three hazard levels and two exposure time sections results in 12 segments in the resilience test framework, as shown in Fig. 3. The lighter version of each colour indicates the easy exposure sections, and the darker version shows the difficult exposure sections in each level. Three penalty types are needed to be considered for each segment: phase penalty, hazard penalty, and exposure time penalty. The details of these penalties are shown in Table 1. The assigned values for each penalty in Table 1, are based on the logical assumptions that have been made by authors. To the best of the authors' knowledge, little is known in this context in the literature, and establishing a set of penalties still needs further attempts in the field of physiological research. When defining the phase penalty, the hazard level penalty, and the exposure time penalty for each segment, it should be noted that where the segment has been placed. For example, a segment in phase I will get a higher phase penalty in comparison to phase II. Regarding hazard level penalty, a segment in uninhabitable level will be penalised more in comparison to the habitable level, and that will be penalised more in comparison to the acceptable level. When it comes to the exposure time penalty, it should be noted where the segment has been placed regarding the phase, hazard level, and exposure time. The phase penalty is assigned as 0.6 for phase I and 0.4

Fig. 3. Differentiation of 12 various segments in resilience test framework.

Table 1
Associated penalties for different segments inside the resilience test framework.

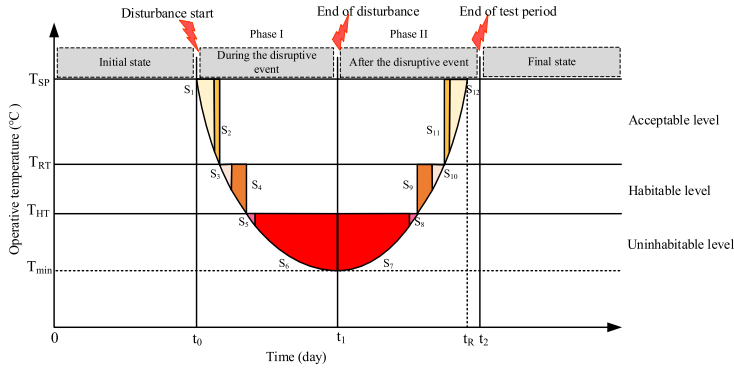| Segment	Penalties		
	Phase penalty (W_P)	Hazard penalty (W_H)	Exposure time penalty (W_E)
S1	0.6	0.1	2
S2	0.6	0.1	8
S3	0.6	0.2	10
S4	0.6	0.2	20
S5	0.6	0.7	20
S6	0.6	0.7	40
S7	0.4	0.7	40
S8	0.4	0.7	20
S9	0.4	0.2	20
S10	0.4	0.2	10
S11	0.4	0.1	8
S12	0.4	0.1	2

for phase II. A hazard penalty of 0.1 is applied for an acceptable level, and 0.2 and 0.7 for the habitable and uninhabitable levels, respectively. The exposure time penalty is different for each section in each level. In order to obtain comparable and informative results from the WUMTP calculation, note that the exposure time penalty is not on the same scale as the two previous penalties. For example, in phase I and in the acceptable level, the assigned penalty for S_1 (easy exposure) is 2, and for S_2 (difficult exposure) is 8. The summation of exposure time penalties in each phase is 100. The assigned penalties can be changed easily based on the priorities of each phase, the hazard level and exposure time.

Considering the specified penalties in Table 1 and the area of each segment resulted in the simulation-based test framework, the definition of WUMTP for a single zone (WUMTP) will be as follows:

$$WUMTP = \sum_{i=1}^{12} S_i W_{P,i} W_{H,i} W_{E,i} \qquad \text{[Degree hours]} \qquad (1)$$

where i is the counter for 12 segments and S_i shows the area of segment i during the occupancy hours, which has been calculated based on the hourly indoor operative temperature resulted in the building performance simulation. $W_{P,i}$, $W_{H,i}$ and $W_{E,i}$ represent the phase penalty, the hazard penalty and the exposure time penalty of the segment i, respectively. Inside each segment, only occupied hours are accounted for in the calculation of the segment area. A building consists of different thermal zones, and different performance levels can be defined based on standards or even the occupants' desires for each zone. WUMTP allows the consideration of these performance levels separately for each zone, but one overall metric is needed to evaluate the overall building. Based on the calculated WUMTP for each zone,

the overall WUMTP of the building can be calculated based on the following equation:

$$WUMTP_{Overall} = \frac{\sum_{z=1}^{Z} WUMTP_z}{\sum_{z=1}^{Z} A_z} \qquad \text{[Degree hours/m}^2\text{]} \qquad (2)$$

where z is the building zone counter, Z is the total number of zones in the building, and A_z is the area of each zone.

2.4. Resilience labelling

In order to rate a building in a specific resilience class, the same approach as energy labelling is used. The objective of building energy labelling is to unfold the building's energy consumption and to promote potential energy-saving measures. Building energy labelling consists of assigning an energy performance label to buildings and it is based on the development of a scale for the labelling index. Since its introduction in early 2000, the scheme has been used to classify buildings on a scale from A to G, with A-rated buildings the most energy-efficient and G the least [39]. The energy labelling can be evaluated based on the simulated or measured energy performance of buildings [40]. Energy labelling based on calculations is mostly used for the new buildings, while energy labelling based on the measurements is used for the existing buildings. In the energy labelling method, first, the energy performance of a reference building, which is derived from the actual building, but is according to standards and regulations is evaluated. In the second step, the performance of the actual building will be evaluated and be compared with the reference building. The next step is to assign a label, and this needs the development of a scale related to the labelling index. The labelling index is the ratio of the energy performance of the actual building to the energy performance of the reference building. Limits between labels can be set on a scale [39]. The same strategy has been used for the resilience labelling of the buildings in this study. The steps toward this approach are shown in Fig. 4. The first step is to select one ideal reference building design based on the standards or regulations. The characteristics of this reference building regarding building envelope, systems, occupancy schedules and internal load can be defined based on the recommendations from standards in each country. The second step is to select the building design to be rated for resilience. In the third step, the location of the building should be selected. Both the reference building and the building of interest should be located in the same place. In step 4, both the reference building and the desired building are subjected to the same test framework, such that they are exposed to the same disruptive event, starting at a specified time and lasting for a specified duration. Step 5 deals with the selection of the thermal performance levels for the different zones of the building. In steps 6 and 7, the $WUMTP_{overall}$ is calculated for both the reference and desired buildings. The calculated
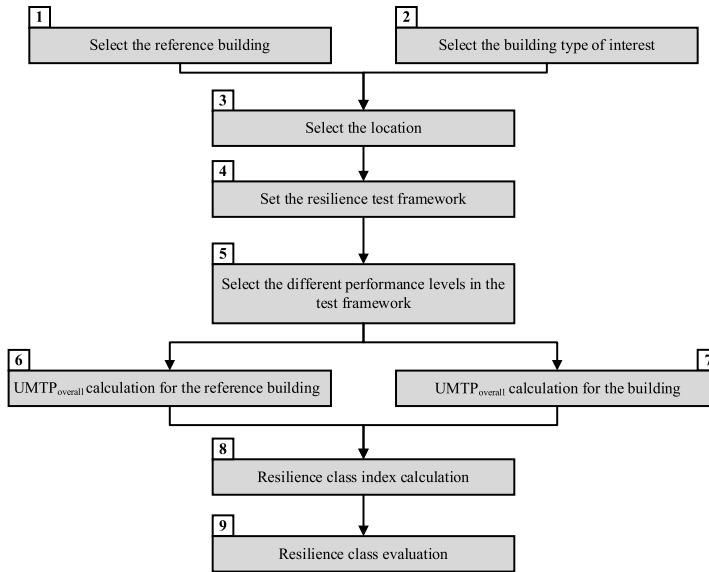
Fig. 4. Steps to implement resilience labelling methodology.

Table 2
Resilience classes for buildings labelling.

<3.6	RCI		Class A^+
<2.4	RCI	≤ 3.6	Class A
<1.5	RCI	≤ 2.4	Class B
<0.9	RCI	≤ 1.5	Class C
<0.6	RCI	≤ 0.9	Class E
	RCI	≤ 0.6	Class F

$WUMTP_{overall}$ for the reference building is assumed to have a medium WUMTP level, set in class C. In step 8, the resilience class index (RCI) is determined by dividing the $WUMTP_{overall}$ of the reference building by the $WUMTP_{overall}$ of the desired building as Eq. (3).

$$RCI = \frac{WUMTP_{overall,ref}}{WUMTP_{overall}} \qquad (3)$$

In step 9, the resilience class of the desired design is determined as presented in Table 2, where the subdivisions are multiples of 0.3. The range of class D is 0.3, but the ranges of classes C, B, A increase to 0.6, 0.9, and 1.2, respectively. Therefore, switching from class B to A is more difficult than switching from class C to B.

3. Case study

The suggested methods for resilience quantification and labelling are demonstrated using a representative model of Norwegian single-family houses in order to analyse the impact of different building designs and resilience enhancement strategies on a building's thermal resilience.

3.1. Description of case study

A representative model of a Norwegian single-family house was selected to be studied [41]. It is a two-storey building with a floor area of 162.4 m², located in Oslo. The building model was divided into three thermal zones (living room, bedroom, bathroom) to simulate the performance of each zone from energy and comfort perspectives in a detailed model in IDA Indoor Climate and Energy software

(IDA ICE) [34], which was validated using the BESTEST: Test Procedures [42]. The building is all-electric, equipped with direct-electric heating systems. The occupancy schedules are based on the Norwegian standard (NS3031) [43], and domestic hot water distribution and internal heat gains were based on [41]. Heating set points, window opening strategy and window shading aligned with the first scenario in [41], and the International Weather for Energy Calculations (IWEC) weather file from the library of IDA ICE was used for running the simulations. Two building designs and two categories of resilience enhancement strategies were considered for the case study building and are described in the following subsections.

3.1.1. Building designs

The two designs are based on the acceptable designs in the Norwegian standards. The first design, called "standard design" in this work, is based on the conventional Norwegian building code from 2017 (TEK17) [44]. TEK17 is the current minimum energy requirement in Norway. The second design, called "passive design" in this work, is based on the Norwegian passive house standard NS3700 [45]. The building element characteristics for the TEK17 standard and passive house standard designs are shown in Table 3. The TEK17 standard states that the total net specific energy use (kWh/m²) – which includes space heating, heating for ventilation air, space cooling, domestic hot water, ventilation, lighting systems and appliances – for a single-family house is derived from the following equation [44]:

$$Net\ specific\ energy = 100 + \frac{1600}{heated\ floor\ area}\ [kWh/m^2] \qquad (4)$$

Considering this equation, the total energy use for the first design (standard design) of the case study building should not exceed 110 kWh/m².

Based on NS3700 [45], the annual energy used for space heating is based on the useful floor area and local annual mean temperature. For the case study building located in Oslo, the annual energy for space heating should be calculated based on the following equation [45]:

$$Annual\ space\ heating = 15 + 5.4 * \frac{250 - A_{FA}}{100}\ [kWh/m^2] \qquad (5)$$

Which A_{FA} shows the floor area in m². This equation set the annual space heating equal to 19.75 kWh/m² for the case study building.

Table 3
Building element characteristic for the standard and passive design.

	Standard design (TEK17 standard)	Passive design (Passive House standard)
U_{wall} [W/m² K]	0.19	0.12
U_{roof} [W/m² K]	0.13	0.09
U_{floor} [W/m² K]	0.1	0.08
U_{window} [W/m² K]	0.8	0.8
Thermal bridge [W/m² K]	0.07	0.03
Heat exchanger efficiency (%)	80	80
SFP ventilation [kW/m³ s]	1.5	1.5
Air leakage 50 Pa [Air change/h]	0.6	0.6

Table 4
Heating capacity of different zones in the two designs.

	Heating capacity (W)	
	Standard design	Passive design
Living room	2000	1300
Bedroom	1300	900
Bathroom	900	600

Table 5
Cost-effective battery size for the standard and passive designs.

	Standard design	Passive design
Cost-effective battery size (kWh)	48	31

The heating capacity of each zone is compared for the two designs in Table 4.

3.1.2. Applied resilience enhancement strategies for the case study

Two categories of resilience enhancement strategies were evaluated for their impact on the introduced designs of the case study building. The first enhancement strategy is the application of batteries as the storage system, and the second is the implementation of the PV systems for the two building designs.

i. Batteries as a storage system

Literature shows that storage systems can be implemented as one of the resilience enhancement strategies in different scales such as grid scale or building scale. Even though small-scale batteries are still relatively expensive, they can be a potential solution to render home resilience [46]. For instance, Mehrjerdi [47] studied the impact of battery swapping mechanisms in a vehicle-to-home operation to evaluate the building energy resilience enhancement. Kosai et al. [48] investigated the role of storage capacity on the resilience of hybrid renewable energy systems. Homaei and Hamdy [49] proposed a new approach for battery sizing in all-electric buildings, called "cost-effective battery sizing". This sizing approach is based on the strategy of shifting heating demand in all-electric buildings based on a signal coming from dynamic pricing tariffs. Norwegian regulators proposed three business models of dynamic pricing tariffs to incentivise load shifts and peak load reduction [50]. Homaei and Hamdy [49] developed cost-effective battery sizing strategies for these three tariffs. In this work, the cost-effective battery size needed for shifting the heat load based on the "time of use" tariff was implemented as a resilience enhancement option. At the start of the disruptive event, batteries were assumed to be ready to use with full capacity. The evaluation of building thermal performance in case of battery implementation was performed with IDA ICE. First, the duration in which the battery capacity could provide the total space heating demand of the building, or "delay time (t_d)", was calculated, i.e. the disruptive event was assumed to be delayed by t_d. This delay in the disruptive event will affect the thermal performance of the building during and after the disruptive event. It will absorb a part of the event's impact, and the minimum temperature will be higher compared to the case without a battery. The battery capacities based on cost-effective battery sizing for each of the two designs are reported in Table 5.

ii. Implementation of PV systems

Electricity generation from renewable sources, such as solar PVs, can provide resilience for buildings or, on larger scales, for grids. Even more effective is electricity generation from PV combined with storage systems. For example, Gupta et al. [51] evaluated the extent of energy resilience through the application of PVs and smart batteries at a community level. In the current work, the impact of PV systems on resilience enhancement was considered without storage systems. Hence, the generated electricity from PV systems, used only for space heating in the building, would be directly used during the disruptive event. A PV configuration with a total area of 40 m², which is typical for similar buildings [52], was added for the two suggested designs of the case study building to understand how the implementation of the PV system can be helpful in resilience enhancement.

3.2. Establishing the test framework for case study building: four-day test framework

As mentioned before, different disruptive events can be considered in the suggested resilience test framework. In this paper, the suggested test framework was applied for an all-electric case study building, and for this reason, a fixed duration of power failure was considered as the disruptive event. This power failure lasted for four days and took place during the four days with the highest heating demand (starting on 14 January). The resilience test framework is called the "four-day test framework" for the considered case study. The duration of power failure was specified based on iterative simulations, which showed how long a power failure needed to be to move a reference building (based on Norwegian standards) out of the habitability range. Furthermore, the same duration was used for phase II. To gain a full perspective of building performance in the initial and final states, these two states were simulated for a duration of one day. This means that the performance of the building was simulated for a total of ten days: one day in the initial state, four days during the power failure, four days after power failure and one day in the final state. Performance levels in the four-day test framework could be set based on the standards and regulations in Norway. In this paper, the four days test framework focused on a power failure as a disruptive event and implemented operative temperature as the performance indicator. This framework can be customised easily and used for other disruptive events and other performance criteria. As stated in Section 2, three performance levels are in the multi-phase resilience curve and consequently in the test framework. These performance levels are variant for each thermal zone in the building. The case study building had three thermal zones, and the performance levels for these thermal zones are described here:

- The first performance threshold is T_{SP}, which shows the setpoint temperature for each thermal zone. Acceptable heating set points in the Norwegian context were selected from [53] for different zones in the case study building. The setpoint temperatures for the living room, bedroom and bathroom were 21.5 °C, 18 °C, 23 °C, respectively.
- The second performance threshold is T_{RT}, which differentiates between the robust and non-robust performance. Based on the recommendations of the World Health Organization (WHO) [54], 18 °C is a safe and well-balancing temperature to protect the health of general populations during cold seasons in countries with temperate or cold climates. Therefore, 18 °C was selected as T_{RT} for the living room zone. This created a 3.5 °C margin from the setpoint temperature for the robust performance in the living room. The same margin was applied for other zones, resulting in a T_{RT} of 14.5 °C for the bedroom and 19.5 °C for the bathroom. Selecting different robustness threshold for different zones has been inspired by different setpoint temperature in each zone and based on the cultural habits that occupants may have. For example, in Scandinavia, more people prefer to have colder

Table 6

Three performance thresholds for different zones of the case study building.

Performance level	Zones		
	Living room	Bedroom	Bathroom
T_{SP} (°C)	21.5	18	23
T_{SP} (°C)	18	14.5	19.5
T_{SP} (°C)	15	11.5	16.5

bedrooms and instead they try to protect themselves by using warmer clothes and thicker blankets [55]. For this reason, it is assumed that occupants can tolerate colder temperature in bedrooms. The opposite is happening for zones such as bathrooms and this creates the idea behind assigning different robustness threshold for different zones.

- The last performance threshold is T_{HT}, which differentiates between habitable and uninhabitable condition for the occupant. A temperature of 15 °C was selected as the habitability threshold for the living room based on a comprehensive review on the effect of low temperatures on elderly morbidity [56]. This created a 3 °C margin from the robustness threshold for the habitable performance in the living room. The same margin was applied for other zones, resulting in T_{HT} of 11.5 °C for the bedroom and 16.5 °C for the bathroom.

The performance thresholds for the three different zones are summarised in Table 6.

Another factor in the test framework is the impact of exposure time to hazard, which is indicated with two sections: easy and difficult exposure. Literature shows that exposure between one to two hours to low temperatures, such as 10 °C [57], 11 °C [58] and 12 °C [59] (all of which are in uninhabitable levels), has a significant impact on human health, such as changes in blood pressure, a decrease of body temperature, changes in heart rate and decrease in plasma level [60]. Therefore, the easy exposure section in the uninhabitable level was assumed to last for one hour, and the rest formed the difficult exposure section. For the habitable level, the first two hours formed the easy exposure section, and the rest was the difficult exposure section. At the acceptable level, the easy section would last for three hours, and the rest was the difficult exposure section.

4. Result and discussion

This study considers four-days power failure as a low probable high impact event for the case study building and tries to quantify thermal resilience using a simulation-based test framework as one structural-based resilience quantification method. The results of the multi-phase resilience curve, resilience quantification, and labelling have been shown in the following sections:

4.1. Multi-phase resilience curve for considered designs

Fig. 5 represents the multi-phase resilience curve for the two designs: standard design (Fig. 5a) and passive design (Fig. 5b) in the living room zone. The thermal performances of these two designs with the enhancement strategies are also shown in Fig. 5. The standard design clearly experiences the uninhabitable level in its base condition (without using any resilient enhancement strategies) and in the case of using enhancement strategies. In contrast, the passive design does not experience the uninhabitable level even in its base condition. This shows that upgrading design from standard to passive design plays an important role in case of facing power failure during cold winter days. The blue curves in Fig. 5a and b show the design performance when the battery is used for storage capacity, and the effect of the battery is shown by the delayed period t_d that postpones the power failure. In the case of the application of the PV system, the temperature fluctuation
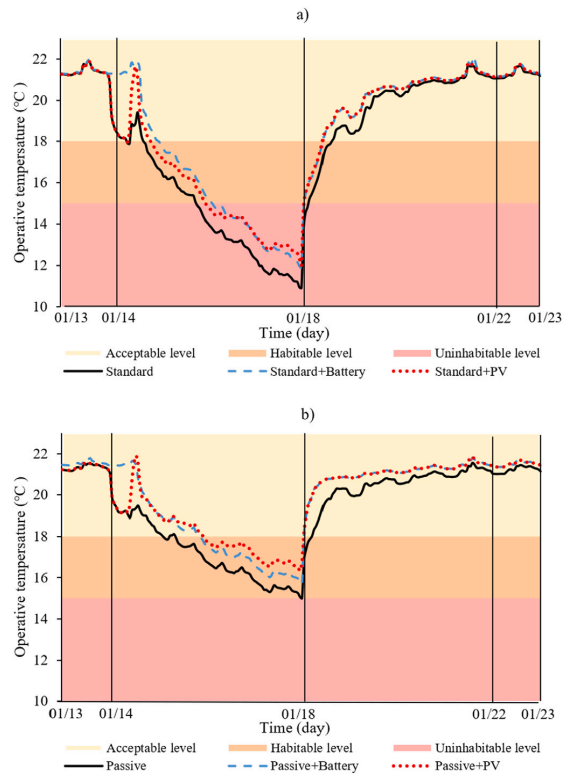
Fig. 5. Impact of the resilience enhancement strategies on the multi-phase resilience curve of (a) standard design, (b) passive design. (For interpretation of the references to colour in this figure legend, the reader is referred to the web version of this article.)

in the daytime during the disruptive event shows the impact of the implementation of the PV system (red curves), which was providing electricity to be used directly for space heating demand in the building, and when the electricity production was high, the temperature increased even in the power failure condition. Furthermore, Fig. 5 shows that in both of the designs during phase II, the performances with the battery and with the PV system are approximately the same. The building designs with the battery and with the PV system are identical in phase II, and the minimum experienced temperature in these two cases are near to each other. Therefore, their performances during recovery would be similar. The effects of the enhancement strategies or design upgrade on the thermal performance of the building during the test days are described in detail in the following sections.

4.1.1. Building envelope influence

The influence of the building envelope on the multi-phase resilience curve was evaluated through the comparison of designs based on the TEK17 (standard design) and passive house standards (passive design), without the implementation of resilience improvement strategies. Fig. 6 shows the multi-phase resilience curve for the living room zone for the two designs based on TEK17 and passive house standards. The building envelope upgrade clearly had a huge impact on the resilience curve and consequently on the WUMTP calculation and resilience class evaluation. The multi-phase resilience curve of the standard design shows that this design experienced the uninhabitable level in the case of four days of power failure. In contrast, the passive house design did not experience the uninhabitable level in the case of four days of
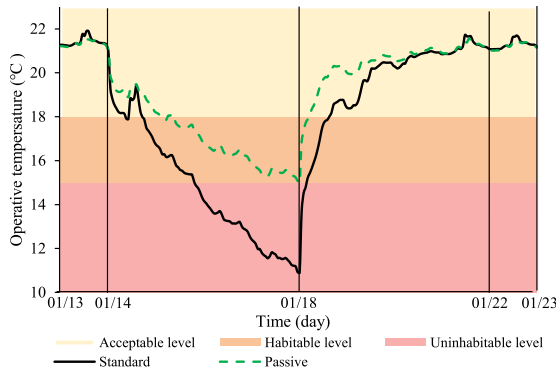
Fig. 6. Comparison of multi-phase resilience curve for standard and passive design without any enhancement strategies.

power failure in Oslo. The minimum temperature in the living room for the standard and passive designs were approximately 11 °C and 15 °C, respectively. Despite this difference, the recovery time (the time it takes to reach the set point temperature after the power failure) is approximately the same for both cases. This means that the recovery speed for passive design is slower than the standard design.

4.1.2. Battery storage influence

Fig. 7 clearly shows that implementation of the batteries as a storage system plays an important role when the building is facing an event that can disrupt its performance. To evaluate the impact of the application of battery storage in the case of a four-day power failure, the two building designs with and without a battery were compared, as shown in Fig. 7. In the standard design, the implementation of the cost-effective battery creates a delay time of 15 h and postpones the power failure for 15 h. A higher delay time results in a smaller temperature drop during the power failure. A 15-hour delay increased the minimum experienced temperature from 11 °C to 12 °C. Furthermore, the application of the cost-effective battery did not shift the resilience curve of the standard design out of the uninhabitable level. For the passive design, the application of the cost-effective battery leads to a 13-hour delay in the power failure, which increased the minimum experienced temperature from 15 °C to 15.7 °C. In addition, the application of the battery also did not change the experienced levels for the passive design. Therefore, even after adding the battery, the resilience curve still travelled through the acceptable and habitable levels.

4.1.3. PV system influence

The effect of the PV systems on the resilience of the two suggested designs was investigated. In this case, the generated electricity by the PV systems was assumed to be directly used for heating during the power failure and it will not be used any more after the power connection. The electricity production from the PV system during the ten-day test is shown in Fig. 8a. Only the electricity generation in the dark grey area was used by the building in the simulation. Fig. 8b and c show multi-phase resilience curves in the living room for the standard and passive designs with and without the PV systems. When the PV system was implemented, both standard and passive designs faced peak temperatures on 15 January. This peak in temperature aligned with the higher PV production the same day compared to the other days during the power failure. The application of the PV system for the standard design increased the minimum experienced temperature from 11 °C to 12.5 °C, without moving the resilience curve from uninhabitable level. For the passive design, the minimum experienced temperature increased from 15 °C to 16.5 °C. The minimum temperature difference in both standard and passive designs was 1.5 °C when the PV was added to the design as an enhancement strategy.
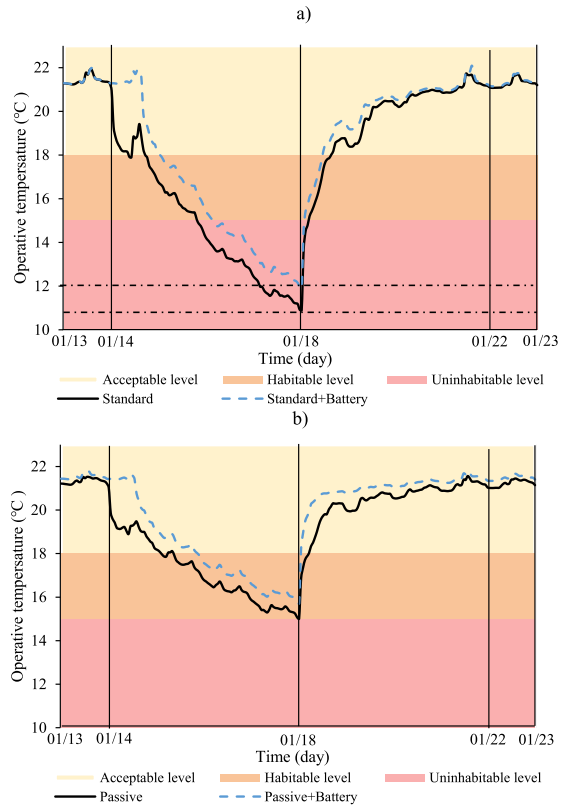
Fig. 7. Influence of the battery storage on the (a) standard design and (b) passive design.

4.2. Quantification of WUMTP

The metric for resilience quantification ($WUMTP_{overall}$) was calculated for the different designs of the considered case study. This metric is multi-zone, and three different thermal zones were in the case study building. Therefore, the suggested performance levels in Table 6 were used for the calculation of $WUMTP_{overall}$. The values of $WUMTP_{overall}$ are reported in Table 7 for the six designs. The upgrade of the standard design to the passive design decreased the $WUMTP_{overall}$ by 80 degree-hours, a 71% reduction. This means that in the case of power failure during cold winter days, the passive design performs more closely to the targets compared to the standard design. In this work, the suggested test framework and calculation of $WUMTP_{overall}$ focused on a cold event during winter. So, the WUMTP during summer was not evaluated here and is out of the scope of the considered test framework. However, it is possible to change the event type to a hot event, such as a heatwave, but the framework need specific adjustment regarding this kind of events. Although the passive design had a lower $WUMTP_{overall}$ than the standard design against a cold event, the situation may be different when a hot event is implemented in the test framework. The lower $WUMTP_{overall}$ of the passive design in the current test framework is not a surprising result and is in line with what was expected regarding the performance of standard and passive designs. Similar work has been done by O'Brien and Bennet [24] who tried to evaluate the impact of building envelope on the thermal resilience of Canadian high-rise residential buildings

Table 7
Calculated $WUMTP_{overall}$ for the six designs of the case study building.

Num	Design	WUMTP (Degree hours)	Improvement (Degree hours)
1	Standard	113	–
2	Standard+Battery	91	22 (compared to standard)
3	Standard+PV	63	50 (compared to standard)
4	Passive	33	–
5	Passive+Battery	24	9 (compared to passive)
6	Passive+PV	13	20 (compared to passive)

are placed and how easily or difficultly they can be tolerated. These issues tried to be shown by defining the hazard levels, and exposure times, and penalties in WUMTP. The developed test framework and calculation of the $WUMTP_{overall}$ considering the event phase, hazard levels, and exposure time helps the designers and decision-makers to compare designs and enhancement strategies, such as adding battery storage or PV systems.

Regarding the enhancement strategies, the addition of battery storage and PV systems decreased the $WWUMTP_{overall}$ for both standard and passive designs. For the standard design, the battery addition changed the $WUMTP_{overall}$ from 113 to 91 degree-hours, a 19% reduction. When PV was added to the standard design, the $WUMTP_{overall}$ changed from 113 to 63 degree-hours, a 44% reduction. For the passive design, the battery application decreased the $WUMTP_{overall}$ by 9 degree-hours (27% reduction), and the PV addition changed the $WUMTP_{overall}$ from 33 to 13, a drop by 60%. The absolute improvement values in degree-hours are higher for the standard design in the case of both enhancement strategies. Hence, if the building is less resilient (e.g. standard design), the improvements will be more significant. Furthermore, the result showed that the application of PV systems had a greater impact than the cost-effective battery storage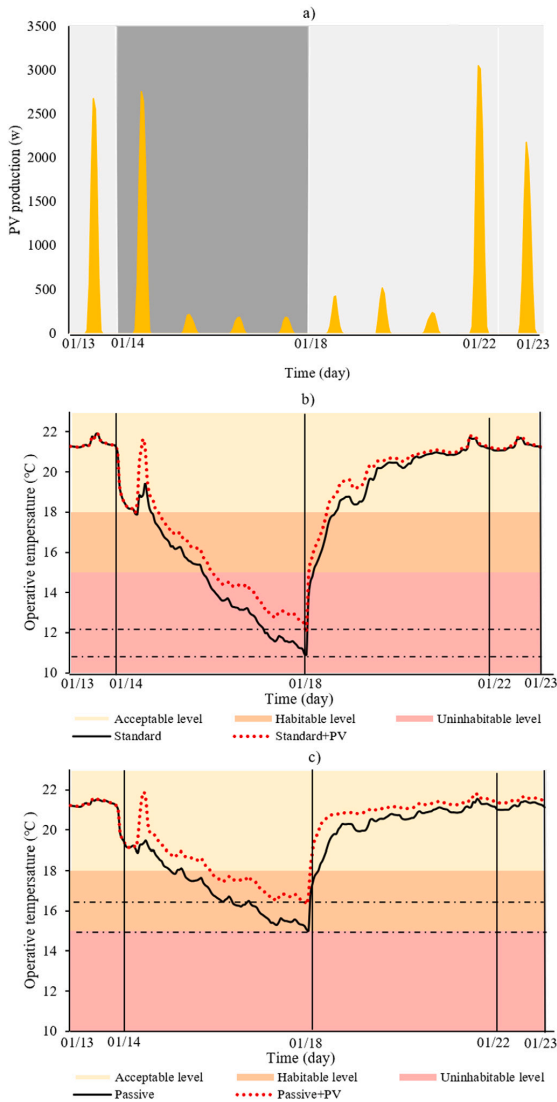 for both standard and passive design for the considered case study. The resilience enhancements achieved by the application of PV systems and batteries in this study is in line with other findings in the literature. For example, Gupta et al. [51] confirm that the application of PV systems can enhance energy resilience at the community level. However, they have not mentioned that how they have quantified resilience and they have implemented more general measures related to PV such as self-consumption. Furthermore, their focus was more on energy resilience and they did not separate total energy to its subcategories such as heating, etc. Another example is the work of Mehrjerdi [47], who has tried to study the impact of batteries in the vehicle-to-home battery swapping mechanics. The result of this study also shows that batteries are able to improve resilience and reduce energy cost. The focus of this work is also on the resilience of total energy consumed in the building without separating it into subcategories. In this study, resilience is evaluated based on the number of hours in which the total energy demand of the building can be provided by batteries. Using this approach does not reveal any information about the different phase of the disruptive event and the level of hazard that the building can be exposed to.

4.3. Resilience labelling for the considered designs

The building designs were classified based on their resilience according to the resilience classes introduced in Table 2. As stated in Fig. 4, the first step for resilience labelling is to select a reference design for the considered building. For the considered case study building, design based on TEK 17 standard (standard design) [44], which is the minimum requirement in Norway has been selected as the reference design. The simulation of this design has been done under the recommendations of NS3031 standard [43] with respect to the internal loads, etc. This makes the RCI for the standard design to be equal to 1 and its resilience will be placed in class C as shown in Fig. 9. The RCI of other designs are also been calculated by dividing the $WUMTP_{overall}$ of

Fig. 8. (a) PV production during test days, (b) Influence of the PV system on the standard design, (c) Influence of the PV system on the passive design.

during power outages. They have used two metrics for thermal resilience quantification: passive survivability and thermal autonomy. They approved that the high-performance envelopes significantly reduce the frequency of conditions that are too cold, which is in line with our findings. However, passive survivability and thermal autonomy are only evaluating the performance of buildings during the event, and they have no considerations regarding after event phase. In addition, the passive survivability metric only considers the performance of building until the survivability threshold and it does not include any observation of building performance after survivability threshold, which has been captured by WUMTP metric. Furthermore, passive survivability and thermal autonomy do not reveal any information about the quality of performance deviations from the temperature targets. For example, they do not capture in which hazard level the performance deviations
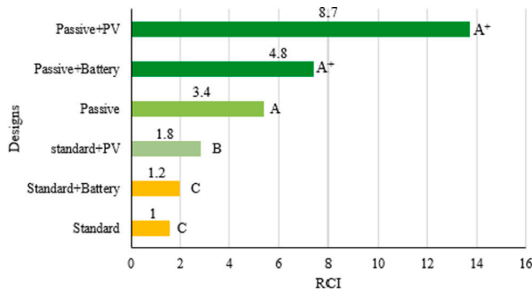
Fig. 9. Calculated RCI and resilience class for the combination of designs and enhancement strategies.

the reference design by the studied designs in this paper. According to Fig. 9 that adding the battery to the standard design does not changing the resilience class of the standard design . Furthermore, with the application of the PV systems, the resilience class of the standard design will be upgraded from class C to class B. The same building with the passive standards by itself is in resilience class A, and the application of the battery and PV systems moved the passive design to class A^+. The resilience classes of the six considered designs for the case study building are distributed from class C to A^+. The maximum resilience class improvement occurred when the design changed from standard to passive equipped with PV panels. Furthermore, if the standard design was upgraded to the passive design without any other improvement options, the resilience level would improve by two levels (from class C to A).

4.4. Strength and limitations

We are not aware of studies that aimed to evaluated thermal resilience on a building scale involving multiple phases of disruptive events, various hazard levels, and varying exposure times to the disruptive event. In addition, the suggested methodology creates a great potential for benchmarking the thermal resilience of residential buildings with respect to the building's characteristics and occupants. Despite its scientific approach, the methodology can be easily used by different stakeholders involving in real projects such as building designers, engineers, decision-makers, and even building occupants. However, we acknowledge that the methodology has some limitations, which should be mentioned: this methodology is focusing on the quantification of thermal resilience for residential buildings during heating seasons. The positive point regarding this methodology is that it can be implemented for thermal resilience quantification, wherever that there is a need for heating during cold seasons, but when it comes to evaluation of thermal resilience during the cooling season, the methodology needs to be adjusted and it may not be applicable for evaluation of thermal resilience during cooling seasons in, for example, regions with hot and humid weather. Further considerations regarding thresholds, penalties and etc needed to be considered with respect to the evaluation of thermal resilience during cooling seasons. Furthermore, this methodology only takes temperature into account in the evaluation of thermal resilience, while other factors such as humidity can also influence thermal resilience evaluation, which needs further research. In addition, the application of this methodology is limited to the residential buildings and its extension to other kinds of buildings such as educational buildings, office buildings, hospitals, and care homes can be achieved by setting a new set of assumptions regarding the thermal comfort conditions in each kind of these buildings.

5. Summary and conclusions

As a step toward protecting building performance against uncertainties, changes and disturbances, this paper proposes a methodology to quantify the thermal resilience of buildings and label these buildings according to their resilience level. The thermal resilience quantification is based on the introduction of a single metric, WUMTP, which calculates the deviation from the thermal targets for the whole building and penalises them based on three factors: the phase of the event, the hazard level of the event and the exposure time to the event. Given the dependency of resilience quantification on the scope of the disruptive event, a test framework was also developed for thermal resilience quantification, which considers the type and duration of the event, the time duration for each event phase, and different thermal performance levels. Furthermore, a whole-building dynamic performance simulation was also performed in order to easily control the boundary conditions of the building and predict the building performance during normal and abnormal conditions.

The developed test framework and new metric were used for a case study building of a Norwegian single-family house to determine how the building would perform during a four-day power failure during a typically cold winter. Two designs were considered for the case study building based on the Norwegian standards: a standard design, based on the TEK 17 standard (a minimum requirement in Norway), and a passive design, based on the Norwegian passive house standard. Furthermore, two resilience enhancement strategies – battery storage and PV systems – were considered to evaluate their impact on the designs thermal resilience.

- The developed test framework can guide building designers in establishing the requirements that are needed for resilience quantification. In this paper, the developed framework was used to evaluate thermal resilience in the case of power failure. However, different event types, performance criteria, and thresholds can be implemented for further evaluation.
- The developed metric for thermal resilience quantification is a multi-zone metric, which represents the thermal resilience for the whole building by considering different performance thresholds for different thermal zones inside the building.
- The developed metric is a multi-phase metric. Unlike most existing metrics, it can quantify resilience during and after the disturbance.
- The boundaries of thermal resilience evaluation with the developed metric are within the building characteristics (including building envelope and systems) and occupancy of the building. Therefore, the difference created in thermal resilience due to the building characteristics and occupancy can be captured by the developed metric.
- The results of the case study building show a significant influence from the building upgrade from a standard to passive design on the building's thermal resilience against a power failure in winter. This result was expected from the performance of standard and passive designs, but the resilience quantification can be more insightful for resilience comparison of competitive designs or resilience enhancement strategies
- The implementation of the battery storage and PV systems as resilience enhancement strategies can improve resilience level for the considered case study in the range of 9–22 degree.hours and 20–50 degree.hours, respectively.
- A less resilient design (e.g. standard design) will gain more significant improvements in the WUMTP when equipped with the resilience enhancement strategies.

The application of resilience quantification and labelling methods that are analysed in this paper can be an effective step for building designers and decision-makers to design resilient buildings to be prepared

for, absorb the impact of, adapt to and recover from disruptive events. Incorporating thermal resilience labels in the design, planning and operation phases of existing and newly-built buildings and including them in the energy performance certificates (EPCs) can be valuable. This information can provide a better understanding of the building performance under disruptive events and facilitate a design selection that not only performs well under design conditions but also it is a safe design for upcoming uncertainties and changes in the future.

Declaration of competing interest

The authors declare that they have no known competing financial interests or personal relationships that could have appeared to influence the work reported in this paper.

Acknowledgements

References

[1] A. Katal, M. Mortezazadeh, L.L. Wang, Modeling building resilience against extreme weather by integrated CityFFD and CityBEM simulations, Appl. Energy 250 (2019) 1402–1417.

[2] H. Li, N. Nord, Transition to the 4th generation district heating-possibilities, bottlenecks, and challenges, Energy Procedia 149 (2018) 483–498.

[3] S. Cao, The impact of electric vehicles and mobile boundary expansions on the realization of zero-emission office buildings, Appl. Energy 251 (2019) 113347.

[4] S. Roostaie, N. Nawari, C. Kibert, Sustainability and resilience: A review of definitions, relationships, and their integration into a combined building assessment framework, Build. Environ. 154 (2019) 132–144.

[5] S. Hosseini, K. Barker, J.E. Ramirez-Marquez, A review of definitions and measures of system resilience, Reliab. Eng. Syst. Saf. 145 (2016) 47–61.

[6] I.P. on Climate Change, Technical summary IPCC SR1.5, 2018.

[7] USGCRP, Our changing planet: The U.S. global change research program for fiscal year 2020. URL https://www.globalchange.gov/browse/reports/our-changing-planet-fy-2020.

[8] C.C.C.S. C3S, C3S releases European state of the climate to reveal how 2019 compares to previous years. URL https://climate.copernicus.eu/c3s-releases-european-state-climate-reveal-how-2019-compares-previous-years.

[9] M. Panteli, P. Mancarella, Modeling and evaluating the resilience of critical electrical power infrastructure to extreme weather events, IEEE Syst. J. 11 (3) (2015) 1733–1742.

[10] The texas tribune. URL https://www.texastribune.org/series/winter-storm-power-outage/.

[11] A.-T. Nguyen, S. Reiter, P. Rigo, A review on simulation-based optimization methods applied to building performance analysis, Appl. Energy 113 (2014) 1043–1058.

[12] L.T. Graham, T. Parkinson, S. Schiavon, Lessons learned from 20 years of CBE's occupant surveys, Build. Cities 2 (1) (2021).

[13] F.H. Jufri, V. Widiputra, J. Jung, State-of-the-art review on power grid resilience to extreme weather events: Definitions, frameworks, quantitative assessment methodologies, and enhancement strategies, Appl. Energy 239 (2019) 1049–1065.

[14] R.J. Campbell, S. Lowry, Weather-Related Power Outages and Electric System Resiliency, Congressional Research Service, Library of Congress, Washington, DC, 2012.

[15] S. Homaei, M. Hamdy, Developing a Test Framework for Assessing Building Thermal Resilience, Building Simulation 2021 Conference, Bruges, Belgium, 2021, Accepted for publication.

[16] N.W. Resources, E. Directorate, Energy consumption 2012 household energy consumption, 2012.

[17] A. Sharifi, Y. Yamagata, Principles and criteria for assessing urban energy resilience: A literature review, Renew. Sustain. Energy Rev. 60 (2016) 1654–1677.

[18] V.M. Nik, A. Perera, D. Chen, Towards climate resilient urban energy systems: A review, Natl. Sci. Rev. (2020).

[19] M. Bruneau, S.E. Chang, R.T. Eguchi, G.C. Lee, T.D. O' Rourke, A.M. Reinhorn, M. Shinozuka, K. Tierney, W.A. Wallace, D. Von Winterfeldt, A framework to quantitatively assess and enhance the seismic resilience of communities, Earthq. Spectra 19 (4) (2003) 733–752.

[20] M. Panteli, P. Mancarella, D.N. Trakas, E. Kyriakides, N.D. Hatziargyriou, Metrics and quantification of operational and infrastructure resilience in power systems, IEEE Trans. Power Syst. 32 (6) (2017) 4732–4742.

[21] J. Liu, L. Jian, W. Wang, Z. Qiu, J. Zhang, P. Dastbaz, The role of energy storage systems in resilience enhancement of health care centers with critical loads, J. Energy Storage (2020) 102086.

[22] S.C. Shandiz, G. Foliente, B. Rismanchi, A. Wachtel, R.F. Jeffers, Resilience framework and metrics for energy master planning of communities, Energy (2020) 117856.

[23] B. Pickering, R. Choudhary, Quantifying resilience in energy systems with out-of-sample testing, Appl. Energy 285 (2021) 116465.

[24] W. O'Brien, I. Bennet, Simulation-based evaluation of high-rise residential building thermal resilience, ASHRAE Trans. 122 (1) (2016).

[25] P. Trimintzios, Measurement frameworks and metrics for resilient networks and services: technical report, Eur. Netw. Inf. Secur. Agency (2011) 109.

[26] K.J. Lomas, Y. Ji, Resilience of naturally ventilated buildings to climate change: Advanced natural ventilation and hospital wards, Energy Build. 41 (6) (2009) 629–653.

[27] E. Burman, J. Kimpian, D. Mumovic, Reconciling Resilience and Sustainability in Overheating and Energy Performance Assessments of Non-domestic Buildings, Centre for Urban Sustainability and Resilience, UCL (University College London), 2014.

[28] K. Sun, M. Specian, T. Hong, Nexus of thermal resilience and energy efficiency in buildings: A case study of a nursing home, Build. Environ. 177 (2020) 106842.

[29] S. Flores-Larsen, C. Filippín, Energy efficiency, thermal resilience, and health during extreme heat events in low-income housing in Argentina. Energy Build. 231 110576.

[30] E. Rosales-Asensio, M. de Simón-Martín, D. Borge-Diez, J.J. Blanes-Peiró, A. Colmenar-Santos, Microgrids with energy storage systems as a means to increase power resilience: An application to office buildings, Energy 172 (2019) 1005–1015.

[31] M. Hamdy, S. Carlucci, P.-J. Hoes, J.L. Hensen, The impact of climate change on the overheating risk in dwellings—A dutch case study, Build. Environ. 122 (2017) 307–323.

[32] Directive (EU) 2018/844 of the European parliament and of the council of 30 May 2018 amending Directive 2010/31/EU on the energy performance of buildings and Directive 2012/27/EU on energy efficiency, https://eur-lex.europa.eu/eli/dir/2018/844/oj.

[33] E. Hossain, S. Roy, N. Mohammad, N. Nawar, D.R. Dipta, Metrics and enhancement strategies for grid resilience and reliability during natural disasters, Appl. Energy 290 (2021) 116709.

[34] EQUA solutions AB Ida indoor climate and energy (version 4.8). URL https://www.equa.se/en/ida-ice.

[35] Validation of IDA Indoor Climate and Energy 4.0 build 4 with Respect to ANSI/ASHRAE Standard 140-2004, Tech. rep., Equa Simulation AB, 2010.

[36] Validation of IDA Indoor Climate and Energy 4.0 with Respect to CEN Standards EN 15255-2007 and EN 15265-2007, Tech. rep., Equa Simulation AB, 2010.

[37] F. Kalmár, Summer operative temperatures in free running existing buildings with high glazed ratio of the facades, J. Build. Eng. 6 (2016) 236–242.

[38] S. Attia, R. Levinson, E. Ndongo, P. Holzer, O.B. Kazanci, S. Homaei, C. Zhang, B.W. Olesen, D. Qi, M. Hamdy, et al., Resilient cooling of buildings to protect against heat waves and power outages: key concepts and definition, Energy Build. (2021) 110869.

[39] L. Pérez-Lombard, J. Ortiz, R. González, I.R. Maestre, A review of benchmarking, rating and labelling concepts within the framework of building energy certification schemes, Energy Build. 41 (3) (2009) 272–278.

[40] P. Rajagopalan, C. Leung Tony, Progress on building energy labelling techniques, Adv. Build. Energy Res. 6 (1) (2012) 61–80.

[41] S. Homaei, M. Hamdy, A robustness-based decision making approach for multi-target high performance buildings under uncertain scenarios, Appl. Energy 267 (2020) 114868.

[42] A.S. of Heating, Refrigerating, A.-C. Engineers, Standard Method of Test for the Evaluation of Building Energy Analysis Computer Programs, Vol. 140, American Society of Heating, Refrigerating and Air-Conditioning Engineers . . ., 2001.

[43] StandardNorge(2016)SN/TS3031:2016 calculation of energy needs and energy supply. URL https://www.standard.no/nyheter/nyhetsarkiv/bygganlegg-og-eiendom/2016/snts-30312016-for-beregning-av-energibehov-og-energiforsyning/.

[44] Byggteknisk forskrift (TEK 17), 2020, https://dibk.no/byggereglene/byggteknisk-forskrift-tek17/14/14-2/.

[45] Criteria for passive houses and low energy buildings - Residential buildings. URL https://www.standard.no/no/Nettbutikk/produktkatalogen/Produktpresentasjon/?ProductID=636902.

[46] E. Chatterji, M.D. Bazilian, Battery storage for resilient homes, IEEE Access 8 (2020) 184497–184511.

[47] H. Mehrjerdi, Resilience oriented vehicle-to-home operation based on battery swapping mechanism, Energy 218 (2021) 119528.

[48] S. Kosai, J. Cravioto, Resilience of standalone hybrid renewable energy systems: The role of storage capacity, Energy 196 (2020) 117133.

[49] S. Homaei, M. Hamdy, Quantification of energy flexibility and survivability of all-electric buildings with cost-effective battery size : Methodology and indexes, Energies 14 (10) (2021) 2787.

[50] H. Hansen, T. Jonassen, K. Løchen, V. Mook, Høringsdokument nr 5-2017: Forslag Til Endring i Forskrift om Kontroll av Nettvirksomhet, Tech. rep., Norges vassdrags- ogenergidirektor, 2017.

[51] R. Gupta, A. Bruce-Konuah, A. Howard, Achieving energy resilience through smart storage of solar electricity at dwelling and community level, Energy Build. 195 (2019) 1–15.

[52] A.H. Wiberg, L. Georges, T.H. Dokka, M. Haase, B. Time, A.G. Lien, S. Mellegård, M. Maltha, A net zero emission concept analysis of a single-family house, Energy Build. 74 (2014) 101–110.

[53] I.S. Øystein Rønneseth, Method for Modelling Norwegian Single-Family House in IDA ICE, The research centre on zero emission neighbourhoods (ZEN) in smart cities, 2018.

[54] W. health organization, WHO Housing and Health Guidelines, World health organization, 2018.

[55] J. Clauß, S. Stinner, I. Sartori, L. Georges, Predictive rule-based control to activate the energy flexibility of norwegian residential buildings: Case of an air-source heat pump and direct electric heating, Appl. Energy 237 (2019) 500–518.

[56] K. Collins, Low indoor temperatures and morbidity in the elderly, Age Ageing 15 (4) (1986) 212–220.

[57] J.A. Wagner, S.M. Horvath, K. Kitagawa, N.W. Bolduan, Comparisons of blood and urinary responses to cold exposures in young and older men and women, J. Gerontol. 42 (2) (1987) 173–179.

[58] J.B. Mercer, B. Østerud, T. Tveita, The effect of short-term cold exposure on risk factors for cardiovascular disease, Thromb. Res. 95 (2) (1999) 93–104.

[59] K. Collins, J. Easton, H. Belfield-Smith, A. Exton-Smith, R. Pluck, Effects of age on body temperature and blood pressure in cold environments., Clin. Sci. (Lond. Engl.: 1979) 69 (4) (1985) 465–470.

[60] P.H. England, Minimum Home Temperature Thresholds for Health in Winter – A Systematic Literature Review, Public Health England, 2014.
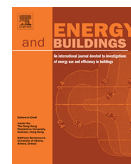
Paper V

Resilient cooling of buildings to protect against heat waves and power outages: Key concepts and definition
Shady Attia, Ronnen Levinson, Eileen Ndongo, Peter Holzer, Ongun Berk Kazanci, Shabnam Homaei, Chen Zhang, Bjarne W. Olesen, Dahai Qi, Mohamed Hamdy, Per Heiselberg
Building and Environment. 2021 Jun 2.

Resilient cooling of buildings to protect against heat waves and power outages: Key concepts and definition

Shady Attia [a,*], Ronnen Levinson [b], Eileen Ndongo [a,c], Peter Holzer [d], Ongun Berk Kazanci [e], Shabnam Homaei [f], Chen Zhang [g], Bjarne W. Olesen [e], Dahai Qi [h], Mohamed Hamdy [f], Per Heiselberg [g]

[a] Sustainable Building Design Lab, Department UEE, Applied Sciences, University of Liège, Belgium
[b] Heat Island Group, Lawrence Berkeley National Laboratory, Berkeley, CA, USA
[c] EPF Graduate School of Engineering, Montpellier, France
[d] Institute of Building Research & Innovation, Vienna, Austria
[e] International Centre for Indoor Environment and Energy – ICIEE, Technical University of Denmark, Denmark
[f] Department of Civil and Environmental Engineering, NTNU Norwegian University of Science and Technology, Trondheim, Norway
[g] Department of the Built Environment, Aalborg University, Denmark
[h] Department of Civil and Building Engineering, Université de Sherbrook, Canada

ARTICLE INFO

ABSTRACT

The concept of climate resilience has gained extensive international attention during the last few years and is now seen as the future target for building cooling design. However, before being fully implemented in building design, the concept requires a clear and consistent definition and a commonly agreed framework of key concepts. The most critical issues that should be given special attention before developing a new definition for resilient cooling of buildings are (1) the disruptions or the associated climatic shocks to protect against, (2) the scale of the built domain, (3) the timeline of resilience, (4) the events of disruption, (5) the stages of resilience, (6) the indoor climate limits and critical comfort conditions, and (7) the influencing factors of resilient cooling of buildings. This paper focuses on a scoping review of the most of the existing resilience definitions and the various approaches, found in 90 documents, towards possible resilient buildings. In conclusion, the paper suggests a definition and a set of criteria —vulnerability, resistance, robustness, and recoverability— that can help to develop intrinsic performance-driven indicators and functions of passive and active cooling solutions in buildings against two disruptors of indoor thermal environmental quality—heat waves and power outages.

1. Introduction

The resilience of the built environment against climate change impacts and associated disruptions is an important topic that has received increasing attention in recent years [1]. Resilience is a central feature of the United Nations (UN) Sustainability Development Goals (SDGs) and is reflected in a range of SDG targets [2]. According to the UN General Assembly Resolution 71/276 [3], the term "resilience" describes "the ability of a system, community or society exposed to hazards to resist, absorb, accommodate, adapt to, transform and recover from the effects of a hazard in a timely and efficient manner, including through the preservation and restoration of its essential basic structures and functions through risk management." The European Green Deal identified

climate-proof buildings and low-carbon buildings as key levers to achieve a resilient and carbon–neutral continent [4]. The need for resilient building design and construction is urgent to anticipate climate change and disruptions caused by weather extremes, increasing carbon emissions, and resource depletion [5]. Our well-being depends on reducing the carbon emissions in our built environment and other sectors [6]. While solving the root-cause problem of climate change, we need to address its effects. Avoiding excessive temperatures induced by overheating is one of the most critical challenges that the building industry will face worldwide in the coming decades [7,8].

Increasing electricity demand during heat stresses can lead to blackouts and grid failures. This can leave buildings out of thermal comfort range and threaten the lives of vulnerable people at risk, as happened during the 2003 Europe heat wave [9]. As building disruptions may have severe and long-term economic impacts, resilient building cooling solutions are an essential strategy to mitigate

threats to occupants [10]. There is an urgent need for resilient cooling solutions in buildings to keep comfort despite extreme weather events due to climate change [11]. Meanwhile, the use of fuel-intensive mechanical cooling should be reduced to slow climate change [12]. Greenhouse gas (GHG) emissions from buildings air conditioning stand at around 210–460 gigatonnes of carbon dioxide equivalent ($GtCO_2e$) over the next four decades, based on 2018 levels [13].

It is of principal importance to define buildings' resilient cooling to maintain indoor environmental quality against unexpected events, e.g., extreme weather conditions, heat waves, power outages, etc. However, the definition of resilience and resilient cooling is challenging and complex [14]. Research on resilience associated with human-nature interactions is still in an explorative stage with few practical methods for real-world applications [15,16].

This article presents the main concepts of resilience. It proposes a definition of resilient cooling of buildings based on the discussion taking place in the International Energy Agency (IEA) - Energy in Buildings and Communities Programme (EBC) research project "Annex 80: Resilient Cooling of Buildings" [11]. The essence of this paper is to define resilience against overheating and power outage. It seeks to answer the following research questions:

- What are the existing concepts of resilience in the built environment?
- How to define resilient cooling of buildings?

The article presents a definition framework based on reviewing almost 90 studies of resilience, including RELi 2.0 Rating Guidelines for Resilient Design and Construction [17]. One of the challenges of this study is to define resilience on the building scale beyond what is present in literature, which mainly addresses the definition of resilience on an urban scale. Most of the studies we reviewed investigated the term "resilience" on the urban scale against disruptions such as hurricanes, flooding, earthquakes, and a long duration [18]. In this context, most studies tend to address the urban scale's resilience for an extended period with less focus on the building scale [18]. The proliferation of urban- or community-scale investigations limits attention paid to indoor environmental quality and overheating buildings' problems. One interpretation for that could be that heat waves and power outages are specific shock events that occur briefly on a few summer days. However, we found many studies confirming that climate change increases the frequency and magnitude of heat waves, making heat waves rise in the ranking of the most significant disruptions in the built environment [19]. This reinforces the importance of resilient cooling as an integral approach for building design and operation concerning comfort (including indoor environmental quality), carbon neutrality, and environmental friendliness [6].

2. Methodology

Fig. 1 shows the research methodology of this study, including its conceptual framework. The methodology is similar to that used by Attia to define main concepts and definitions of adaptive facades [20,21]. Our research methodology is qualitative and relies on the literature review, focus group discussions, and individuals' follow-up discussions. The research methodology of this study has four significant steps, each detailed in the following sections.

2.1. Literature review

A literature review was conducted, aiming to define resilience against different climate change associated disruptions in the built
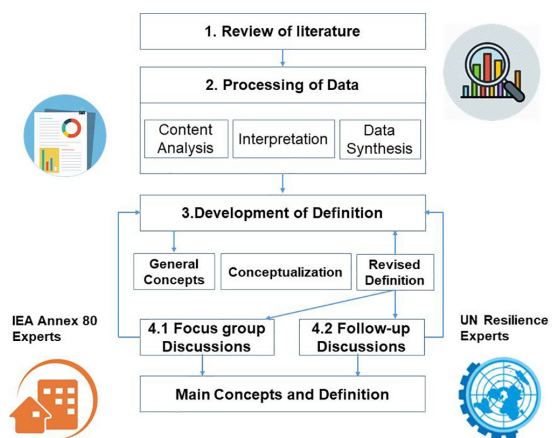
Fig. 1. Study conceptual framework.

environment worldwide. The publications included scientific journal articles, reports, books, building rating systems, and grey literature (government reports, policy statements, and papers. We opted for large databases and quality web sources with complete bibliographic data. Our initial *Scopus* and *Web of Science* research resulted in almost 90 publications relevant to the built environment's resilience and resilience criteria. To examine the definitions of resilience and the associated resilience criteria such as vulnerability, resistance, robustness, and recoverability, we surveyed resilience in ecology, resilience in engineering, and resilience in psychology as inclusion criteria. These domains cover the body of knowledge and discourse concerning resilience in general. We then narrowed the research scope to focus on the overheating and power outage disruptions and the resilience of cooling strategies and technologies in buildings. The exclusion criteria were twofold, aiming to eliminate publications that define resilience on an urban scale and infrastructure. The exclusion criteria included terms such as "city", "urban", "structure", "infrastructure", and "flooding". The search language was mainly English and looked back to 1995, in which the term resilience first appeared in literature related to the built environment, until 2020. The publication information was imported to the software HistCite 12.3.17 for analysis and grouped into two categories [22]: resilience on the building scale and resilience on the urban scale. The results of the literature review are presented in Section 3 and Appendix A.

2.2. Data processing

We analyzed the content of every identified article's full text and developed an analysis protocol and coding schema to record its content attributes. The entire text of the full article was read multiple times as they search for coding words was completed by the coders (authors). Coding is a way of indexing or categorizing the text to establish a framework of its themes [23]. We used the framework method commonly used to manage and analyze qualitative data in health research [24,25]. The framework method involves reading the manuscripts carefully and applying a code or label that describes important phrases or paragraphs. The documents are labeled and systematically to develop a dataset of codes. After coding the manuscripts, the codes were compared and classified. Codes were then grouped together in categories. After several categorization iterations, an analytical framework or structure for the main domain and concepts was created under which the codes

and labels are grouped. With the help of ATLAS.ti software (version 9) the framework is charted grouping all codes, concepts and categories [26]. The tagging system summarizes and interprets the manuscripts interrogating the theoretical concepts and the connection between categories in a structured way. A detailed description of text processing can be found in Attia's videos [27,28].

2.3. Development of definition

We used the framework method for the definition development, which is the most commonly used technique for the management and analysis of qualitative data in health research [24,25]. The framework method allows systematic analysis of the text data to produce highly structured outputs and summarized data. It can also compare and identify patterns, relevant themes, and contradictory data [24]. We categorized the codes (resilience concepts) by theme. Our classification resulted in four concepts that define the resilient cooling of buildings.

2.4. Focus group and follow-up-discussions

Qualitative research is primarily a subjective approach as it seeks to understand human perceptions and judgments. However, it remains a reliable exploratory scientific method if bias is avoided. The suggested definition validated through focus group discussions to provide consistent and dependable results. Several validation measures were implemented, including member checking, memo logs, and peer examination following the work of Attia [29] and Attia et al. [21]. The study validation allowed emphasizing credibility and strengthening the relevance of the conducted study and results. Focus groups were convened during IEA-EBC Annex 80's first expert meeting in Vienna, Austria (21 October 2019) and during its second expert meeting, held online (21 April 2020). Each focus group comprised of 15 people. IEA-EBC Annex 80 members aim to support a rapid transition to an environment where resilient, low energy and low carbon cooling systems are the mainstream and preferred solutions for cooling and overheating issues in buildings [11]. The invited experts for the focus-group discussion represented the scientific and professional experts in the field of building performance assessment and comfort. A list of the IEA-EBC Annex 80 participants can be found on the Annex website [30]. The focus group discussions' goal was to validate the suggested definition and main associated criteria [29].

Follow-up discussions with RELi steering committee members and UN resilience experts helped articulate and validated the framework and included detailed elaboration of some criteria. The RELi Rating System is a holistic, resilience-based rating system that combines innovative design criteria with the latest integrative design processes for next-generation neighborhoods, buildings, homes, and infrastructure (see further explanation Section 3.3). The follow-up discussions took place between the first authors and some of the co-authors via teleconference and emails.

3. General concepts of resilience

The definitions of resilience concern with the interplay of continuity and change of objects/systems subject to internal or external disruption(s). Whatever the field of application of the resilience concept, the study of resilience entails adapting to crisis associated with the assumption of vulnerability in the context of climate change [31]. Vulnerability has been used as the "flip side" of resilience [32]. Some researchers separate resilience and vulnerability [33], while others consider resilience related to one of the components of vulnerability [34]. In the following two subsections, we

explain resilience concepts in different domains and review papers that assess resilient comfort in buildings.

3.1. Resilience in different domains

The concept of resilience varies by discipline [35]. The first definition, found in ecological literature, is a system's ability to absorb a shock without changing its pre-shock structure, identity, and function. Holling [36] defined resilience to disruptions in ecosystems. His resilience concept assumes that the system's absorptive resilience or "ability to bounce back" can handle shocks and find an alternative (equilibrium) state or form that is less good than the system's pre-shock state.

The second definition of resilience, found in the behavioral psychology literature, focuses on positive adaptability resilience or "ability to absorb" [37]. Resilience is defined as individuals' coping capacity to maintain or regain psycho-pathological well-being following trauma, personal stress, or crisis [35]. In this definition, individuals are expected to demonstrate dynamic self-renewal and adjustment capacity to neutralize the shock and its impacts.

The third definition of resilience, found in the engineering and economics literature, is focused on the ability to "bounce forward" or "recover; fast following a disruption [35]. This was termed "engineering resilience" due to the human-made nature of engineering [36]. It is defined as "how fast a system that has been displaced from equilibrium by a disturbance or shock returns to that equilibrium and continues performing." This interpretation was also found in the physical sciences and economics literature. This definition of resilience led some authors to refer to it as "evolutionary resilience" due to the ability of the system to "bounce forward" rather than just absorb the shock or "bounce back" [38–40]. Table 1 summarizes the different definitions and concepts of resilience under three categories.

3.2. Resilience as "bounce forward" from shocks

There is a plethora of studies that employed the term "resilience'. However, very few studies have defined the term 'resilience' in the built environment [42]. Therefore, we deliberately chose the third definition of resilience (see Table 1). The third definition of resilience is already used differently by researchers and professionals in different engineering domains (structural and energy engineering) and is focused on the ability to "bounce back" or recover following a disruption of some kind [38,43,44]. As shown in Fig. 2, the definition of resilience in engineering and economy is a process that involves several elements. The first element is vulnerability (the sensitivity of a building system to different types of shocks). According to literature, vulnerability is a central concept in climate change research. Vulnerability describes the system associated with hazards of concern and attributes of concern [45,46]. The UN general definitions define vulnerability

Table 1
Different concepts and definitions of resilience in different domains [35]

| Fields	Definition Interpretations
In ecology:Resilience is the "ability to absorb shocks" or" bounce back"	Ability of an ecosystem to rearrange its organization outside of its equilibrium state to another one when facing a perturbation [36].
In psychology:Resilience is "positive adaptability" in anticipation of/in response to shocks	Capacity of an individual to endure and develop in the context of adverse conditions and to recover [37].
In engineering and economics: Resilience the ability to "bounce forward" from shocks	Ability of a system to resist perturbations outside of its equilibrium state and its speed to come back to it [35,41].

Stages of Resilience
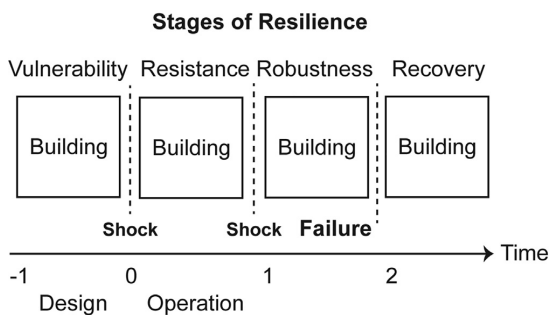
Fig. 2. The stages and timeline of the resilience process.

as risks "expected losses [...] resulting from interactions between natural or human-induced hazards and vulnerable conditions" [47]. The second element is resistance (the building system's ability to maintain the initial design conditions). The third element is robustness (how the building system, including occupants, adjusts and adapts to shocks under critical performance conditions). The fourth element is recoverability (the extent and nature of recovery from shocks). If the building cooling design involves a vulnerability assessment, it can resist shocks, then falls under the influence of a shock and recovers from the shock; only then we can call it a resilient.

To define a building or system as resilient, it must be vulnerable (sensitive) to disruptions or shocks and experience failure. Failure is essential in any definition of resilience because the latter is built upon it. A failure can be temporary or permanent and can partial or full. The failure to protect occupants against heat waves or power outages, resulting in heat-related deaths or morbidity, are examples of building failures [19]. Unfortunately, several studies in the field of building engineering investigated the robustness of the building's performance against heat waves without addressing the broader definition of resilience and its stages illustrated in Fig. 2 [48–50].

Thus, there is a lack of understanding of the term "resilience" and the conditions and stages associated with this complex term. The fundamental definition of resilience necessitates the occurrence of a shock. Only the presence of a shock can ascertain whether, and to what extent, the robustness (adaptation) of a system or building has imbued it with resilience [38].

3.3. Resilience in the built environment

The literature about resilience in the built environment can be classified by scale—*urban* or *building*.

Ernsstson et al. [51] published one of the earliest studies defining urban resilience within human-dominated ecosystems. Using three case cities, the study explored the resilience of urban governance concerning ecosystem services. Similarly, Meerow et al. [52] proposed a general definition of urban resilience without focusing on any specific disruption in the built environment. In contrast, Godschalk [53] focused on urban hazards in cities and specifically on terrorism. The study was initiated due to the terrorist attack on the World Trade Center in September 2001 in New York and presented resilience in this context.

Liao [15] presented a definition of urban resilience addressing floods and the surrogate measure of percent floodable area for assessing potential to flood. Stead [54] evaluated Rotterdam's resilience (Netherlands) with a focus on water management and climate change. Sharifi & Yamagata [55] developed a framework for assessing urban energy resilience, identifying planning and design

criteria, and examining these criteria' relationshiBased on their framework, to be resilient, and urban energy system needs to be capable of "planning and preparing for," "absorbing," "recovering from," and "adapting to" future adverse events.

The previous studies addressed resilience and vulnerability on the urban scale. Other reviewed studies have addressed the concept of resilience for individual buildings. Most focused on blast resilience, seismic resilience, and hurricane or wind resilience. Takewaki et al. [43] sought to reduce the unexpected incidents in building structural design and define robustness and resilience against earthquakes in buildings. Cormie et al. [57] assessed the whole-building response against blasts and the influence of the building form and façade. Tokgoz & Gheorghe [56] quantified the resilience of residential buildings against hurricane winds.

Lomas and Ji [58] published one of the earliest studies on thermal resilience in buildings. In a special issue of *Building and Environment*, Lomas & Giridharan [59] measured internal temperatures and thermal resilience to climate change of free-running hospital wards. De Wilde & Coley [60] conducted a literature review investigating climate change's implication on buildings. Burman et al. [61] presented another early investigation on overheating resilience using evidence gathered from two educational buildings in London. They proposed a theoretical framework with three main criteria: vulnerability (sensitivity and exposure), resilience (capacity of response), and adaptation (long-term adjustment). Holmes et al. [62] proposed an indoor heat index for evaluating heat stress and passive habitability in residential buildings. Coley et al. [63] presented a new comfort equation for resilient building design that considers weather and probabilistic adaptive comfort measures variability. Hamdy et al. [64] investigated the impact of climate change on the overheating risk in dwellings and the potential for ventilative cooling to mitigate climate change effects. Vulnerability to overheating and sensitivity of the building response were used to assess the investigated dwellings' resilience.

Version 4.1 of the United States Green Building Council (USGBC) Leadership in Energy and Environmental Design (LEED) rating system introduced a "Thermal Resilience" pilot credit that aims to assess passive survivability and thermal resilience [65]. The credit was developed initially within the RELi rating system. RELi is a building and community rating system wholly based on resilient design [17] and has been adopted by the USGBC. Under the Thermal Resilience pilot credit, a space qualifies as thermally resilient if it can provide indoor thermal comfort in the event of a power outage. Comfort thresholds are based on standard effective temperature degree-days [66].

Table 2 summarizes documents found in the literature explicitly addressed and used the term "resilience" concerning comfort. The studies mentioned above are the beginning to define the thermal resilience of buildings. However, the studies listed in Table 2 proposed neither a consistent definition of thermal resilience nor an assessment framework for buildings' resilient cooling. The literature review confirms the need to establish a definition of resilient cooling for buildings.

4. Conceptualization of resilient cooling for buildings

4.1. Resilience against what?

One critical prerequisite for a comprehensive definition and assessment of resilience is identifying threats (shocks) or disruptions to the stability of these systems. An essential question to answer is "resilience against what?".

As shown in Table 3, several types of disruptions or emergencies can lead to buildings' systemic failure to be resilient—e.g., air

Table 2
A list of documents found in literature in direct relation with the thermal resilience of buildings based on Appendix I

Scientific Article	Reference	Definition Paper	Review Paper	Calculation Method
Lomas (2009)	[58]			✔
Lomas et al. (2012)	[59]			
De Wilde et al. (2012)	[60]		✔	
Burman et al. (2014)	[61]			✔
Holmes et al. (2017)	[62]			✔
Lomas et al. (2017)	[67]		✔	
Coley et al. (2017)	[63]			✔
Hamdy et al. (2017)	[64]			✔
Rating System				
USGBC (2018)	[65,66]	✔		✔
USGBC (2019)	[17]	✔		✔

* Search Keywords: resilient, resilience, thermal, overheating, building

Table 3
Different types of disruptions affecting the built environment

Disruption	Description
Air Pollution	- **Outdoor air pollution** refers to the air pollution experienced by populations living in and around urban areas. Air pollution derives from poor combustion of fossil or biomass fuels (e.g., exhaust fumes from cars, furnaces, or wood stoves) or wildfires [69]. Buildings require efficient air filters and ventilation systems that mitigate the impact of air pollution.
Fire	- **Wildfires** are sweeping and destructive conflagrations, especially in a wilderness or a rural area, that cause significant damage. Most building codes adequately addresses common fire hazards with mandatory fire-resistant stairwells, fire-resistant building materials, and proper escape methods.
Earthquakes	- **Earthquakes** are the most common disruptions covered in all building codes. They are trembling of the ground caused by the passage of seismic waves through the earth's rocks. This natural disaster can damage a building by knocking it off its foundations and harm the occupants. Seismic testing should be used on components of buildings to determine their resilience to earthquakes.
Wind storms and hurricanes	- **Hurricane** has the potential to harm lives and property via storm surge, heavy rain, or snow, causing flooding or road impassibility, lightning, wildfires, and vertical wind shear.
Flooding	- **Flooding** is the inundation of land or property in a built environment, particularly in more densely populated areas, caused by rainfall overwhelming the drainage systems' capacity, such as storm sewers.
Heat waves	- **Heat waves** are a period of excessively hot weather accompanied by high humidity [70]. They cause overheating in the building and intensify the urban heat island effect [71]. This event can potentially risk the health and lives of occupants if no measures are taken.
Power outages	- **Power outages** and blackouts are common occurrences caused by natural disasters cited earlier, like floods or hurricanes. It can lead to overheating in buildings when air conditioners do not operate.
Water shortages	- **Water shortage** is the lack of freshwater resources to meet water demand. Lack of water has a significant impact on irrigation and urban use, degrading food security, public health, and overall stability.
Pandemic	- **Pandemics** can impact societies' built environment is how spatial and social aspects are intertwined to constitute everyday lives mutually. During active outbreaks, such as COVID-19, minimizing the risk of disease spread in buildings starts with keeping people out of them. For those who occupy a building, increasing the ventilation and filtration of the inside air is essential.

pollution, fires, and earthquakes. Disruptions are increasingly presented by unexpected phenomena outside or inside the building [60]. The rate and pace of disturbances that the built environment faces have been accelerating significantly over the past three decades [68]. Understanding and identifying the phenomena that disrupt a building and threaten the well-being of its occupants is fundamental.

For this study, heat waves and power outages were identified as major disruptions that can influence occupant indoor thermal quality conditions on the building scale [72]. The frequency and severity of extreme weather events have increased in the last 30 years. Increased ambient temperature during heat waves can directly influence the thermal performance of buildings by decreasing the efficiency of energy systems. This direct impact makes the extreme weather event and associated power outages major sources of disruptions for resilience evaluation. In addition to the direct impact, heat waves can have some cascading impacts such as power failure, access to clean water, and acceptable indoor air quality. There are other potential disruptions to the indoor environment detailed in Table 3. However, of these only heat waves and power outages directly affect the indoor thermal quality. For example, heat from wildfires might affect the indoor environment, but buildings are typically evacuated if a wildfire is close enough to heat them.

Therefore, the paper is focused on the definition of resilient cooling of buildings as part of the IEA-EBC Annex 80 activities that aim to define resilience. Crawley et al. [73] identified heat waves as the significant climate change disruption in buildings. Baniassadi et al. [74] identified the frequency and duration of power outages as a significant cause of disruption for buildings in the near future. Both studies confirmed that the increase of mean outdoor temperatures and the frequent and intensive nature of heat waves disrupt power and degrade comfort.

Disruptions are shocks or events with an origin, a nature, an incidence, a scale, and duration. Therefore, we define disruptions in buildings as shocks that degrade the indoor environment and require resilient cooling strategies and technologies to maintain it [60].

4.2. Resilience: At which scale? And for how long?

The resilience of a system cannot be studied without examining the system's scale and the relation between the shock cause and its effect(s). Resilient systems function through the interaction of complex processes operating at different scales and times frames [75]. Therefore, it is essential to characterize the scale of the system expected to be resilient in a time-bound way. The definition of resilience should always reflect whether the disturbance affects a single building element's performance or operation, building service, or the entire building [76]. As shown in Fig. 3, the definition of resilience should always characterize the resilience to disturbance of a system to its scale within a specific time frame for the distur-
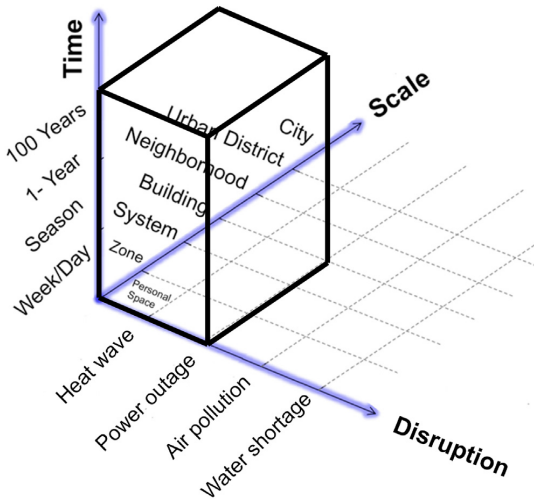
Fig. 3. the components of a resilience definition within a specific field or domain.

The interviewed experts agreed that climate change should be defined as a long-term disruptive event and that heat waves and power outages should be designated short-term disruptive events. Based on our literature review and following Fig. 4, we distinguish four major events categories that can challenge resilient cooling [78]:

1. Event 1: Observed and future extreme weather conditions (extended, spanning years)
2. Event 2: Seasonal extreme weather conditions (extended, spanning months)
3. Event 3: Short extreme weather conditions (short, spanning days)
4. Event 4: Power outages (spanning hours)

Across the literature, several studies identified extended and long climate change associated temperature increase events (Events 1 and 2) [64,79]. Other studies investigated the impact of short-term heat waves and power outages on thermal conditions and cooling systems' resilience [80,81]. For example, the RELi rating system requires thermal safety during emergencies (Events 3 and 4) by maintaining indoor air temperature at or below outdoor air temperature up to seven days [17]. Designers need to demonstrate that the building will maintain safe temperatures during a blackout that lasts four days through thermal zoning and modeling. During a power outage, buildings must provide backup power to satisfy critical loads for 36 h.

We define four major event categories that need to be tested and address in any resilience assessment for comfort in buildings. The following section provides further detailed explanation for Fig. 3 in association with Fig. 4.

bance. According to Fig. 3, this study defines resilient cooling in buildings within certain boundary conditions that are limited to the building scale in response to heat waves and power outages for duration of 100 years.

We select heat waves and power outages as the primary disruptive events to be addressed by resilient cooling for buildings for our study. Our proposed definition considers the indoor environmental conditions on the building scale for long periods. Climate scenarios represent historical and future outdoor conditions and consider both short-term and long-term heat waves. Resilience in the building engineering field is strongly associated with long-term climate projections that encompass both the increase in the average temperature due to a global warming effect or temperature rise due to the urban heat island effect [77].

Defining and identifying disruptions and specifying their associated events that impact healthy and comfortable buildings is the first step to determine a building's resilience. Other issues can degrade the indoor thermal environment, such as the sudden change of indoor occupant numbers during some events. However, in this study, we focus only on climatic disruptions represented into heat waves and power outages. As shown in Fig. 3, heat waves and power outages are events that may impact the thermal conditions in buildings. The identification of heat-wave events is based on their intensity, duration, and frequency coupled with power outages [78]. It is expected that a building with a resistant cooling design (strategy) can withstand short and extensive heat waves. A building with a robust cooling design can withstand short, intense, and prolonged lengthy heat wave. The performance of a building with a resilient cooling design could surpass that of a robust building by reacting to power outages and longer intensive heat waves. The literature review confirms that resilience must be associated with response to system failure [17]. A system is robust when it can continue functioning in the presence of internal and external challenges without a system failure. However, a system is resilient when it can adapt to internal and external challenges by changing its operation method while continuing to function. The ability of the building to recover after disruptive events is a fundamental feature of resilience. Therefore, the ability to model the occurrence and consequences of discrete heat-wave events is crucial to prepare the building for the response.

5. Definition of "resilient cooling for buildings"

Resilient cooling is used to denoting low-energy and low-carbon cooling solutions that strengthen the ability of individuals and our community as a whole to withstand, and also prevent, the thermal and other impacts of changes in global and local climates—particularly concerning rising outdoor temperatures and the increasing frequency and severity of heat waves [61].

Resilient cooling for buildings is a concept that was not approached thoroughly in previous studies. Therefore, we developed the following definition based on the literature review and
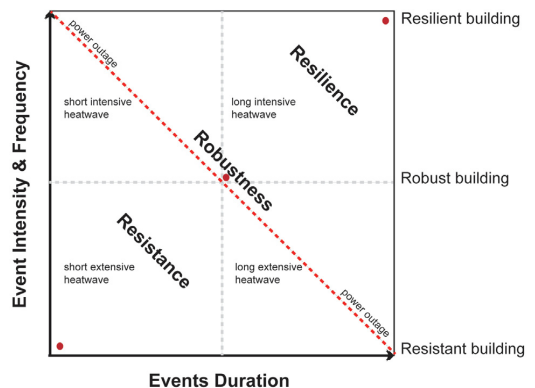

Fig. 4. The components of a resilience definition within a specific field or domain.

validated it through the focus group discussion with members of IEA-EBC Annex 80:

The cooling of a building is resilient when the capacity of the cooling system integrated in the building allows it to withstand or recover from disturbances due to disruptions, including heat waves and power outages, and to adopt the appropriate strategies after failure (*robustness*) to mitigate degradation of building performance (deterioration of indoor environmental quality and /or increased need for space cooling energy (*recoverability*).

Resilience is a process that involves several criteria, including vulnerability, resistance, robustness, and recoverability [35]. Therefore, we include those four criteria in the definition formulation shown in Fig. 5. The vulnerability involves the sensitivity or propensity of the building's comfort conditions to different disruptions. At this stage, it is vital to define disruptions, as discussed in Sections 4.1 and 4.2 (see Figs. 3 and 4).

A resilient building must be conceived based on a vulnerability assessment that considers future climate scenarios and prepares the building system, including occupants, to adapt against failures. The vulnerability assessment should test the building performance against long-term disruptions using average weather conditions, extreme weather conditions, future weather conditions, and worst future weather conditions. It should also test the building against short-term disruptions, including brief heat waves and power outages. A vulnerability assessment stage should be part of the design process. A building cooling system is prepared to go through different disruption scenarios engaging other thermal conditions.

The building cooling system should be able to withstand short-term and long-term disruptive events. As shown in Fig. 5, resistance involves the ability and the depth of reaction to the shock. Under disruptive events, the building may use performance drop-backs to achieve the pre-defined minimal thermal conditions. After the building cooling system's failure, the building's resilience process moves to the most crucial stage—robustness, meaning reaction to failure. Robustness requires the building to be prepared to survive an otherwise-fatal shock by adapting its performance. The survivability of the system relies on its ability to assure the critical thermal conditions to maintain occupants' functional activities during a crisis. As shown in Fig. 5, a robust building will first fail and then adapt its performance conditions meeting critical or minimum thermal requirements to achieve a degree of survivabil-

ity for occupants depending on the vulnerability assessment decisions made during design. The failure time of a robust building will be relatively long before recovery, and the performance will reach only minimum thermal conditions after failure compared to a resilient building. The significant distinction between a resistant building system and a robust building system is that the latter is prepared to adapt based on a backup plan and ecosystem. Robustness involves how the building, including its services and occupants, adjusts and adapts to shocks.

The final stage of resilience involves the recoverability of the system. Recoverability consists of the extent and nature a occupants and building's services to recover, and returns to its equilibrium state and its speed to come back. As shown in Fig. 5, recovering has a duration, performance, and learnability. The necessary speed for recovery and the recovery performance curve should be planned during the vulnerability assessment stage. The users' ability, building, and systems to learn from the event is an integral part of this stage.

While the diagram in Fig. 5 is linear, the process of resilience is cyclic and iterative. Resilient cooling of buildings is a continuous process that involves the commissioning and retro-commission of building elements and systems over the building's life cycle. It also includes the continuous education of occupants and the preparation for the adaptive measures during unforeseeable disruptions.

Fig. 6 provides a complementary definition framework that includes the main criteria of resilience. It presents an example of the factors that influence cooling performance in buildings under the four resilience criteria. Depending on the overheating definition and exposure risk, a resilient cooling design for buildings assures that the designed indoor environmental conditions are secured before the disruption. The risk factors should be identified during the design stage to assess vulnerability. Examples of risk factors include climate change scenarios, heat waves combined with power outages, or urban heat island effects. As shown in Fig. 6, the resistance stage depends mainly on the building's design features and technologies and their ability to keep the building performing under severe overheating exposure until reaching failure. The failure is the essential disruption to start the third stage of resilience, namely robustness. The cooling system's robustness must adapt to cover the critical thermal conditions temporarily until reaching the recovery stage. Adaptively, the ability to respond
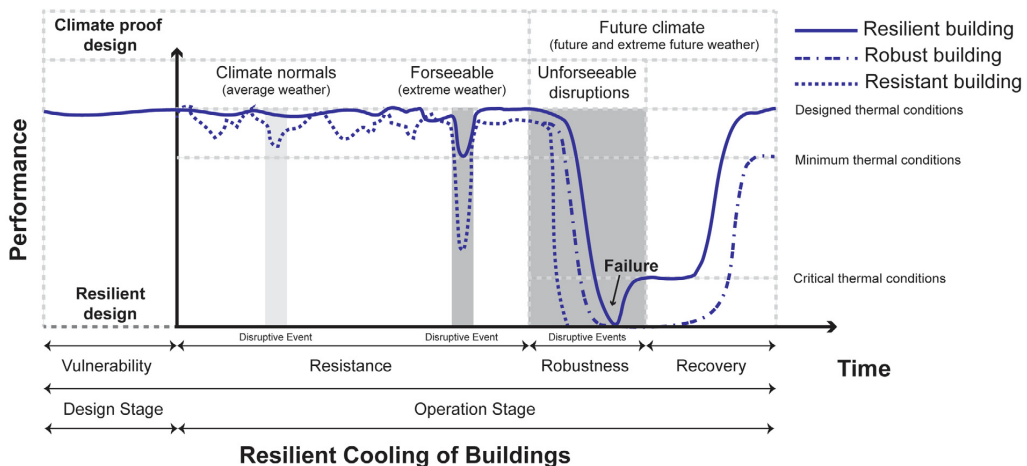

Fig. 5. The components of a resilience definition within a specific field or domain modifying Moazami et al. 's definition in 2019 [50].

Definition of Resilient Cooling Characteristics and Risk Factors

Fig. 6. Factors that influence resilient cooling of buildings.

and apply changes to the original thermal conditions involved occupants and systems adaptability. The presence of energy system backup and an emergency control possibility is part of the building's robustness. This is finally followed by a recovery stage and a shift in the building performance to achieve before designed thermal conditions that reflects adapting to the normal.

6. Discussion

The review of the main concepts on resilience mainly relates to the resilience of ecology, economy, city, and buildings. Therefore, proposing a definition for buildings and assessment framework indicates the complexity of the idea. We found varying and inconsistent definitions of resilience in building comfort and in the context of the overall built environment. The following sections discuss possible questions that we answered in this study.

- What are the existing concepts of resilience?
- How to define resilient cooling for buildings?

6.1. Findings and recommendations

For this study, we defined resilient cooling for buildings and developed a framework used by building designers, authorities, developers, and future occupants. By reviewing the literature, including rating systems and standards and consulting with IEA-EBC Annex 80 members, USGBC members, and UN experts, the proposed definition and criteria intend to identify and group critical performance criteria of buildings cooling resilience. The criteria—vulnerability, resistance, robustness, and recoverability—can help develop intrinsic performance-driven indicators and functions of passive and active cooling solutions in buildings against heat waves and power outages. In this sense, this study aimed to screen, characterize, and structure resilience criteria to provide a logical framework to design and evaluate resilient cooling strategies for buildings.

Few studies and case studies succeeded in defining resilience and applying its principles on a building scale. Across our review, we found some studies that focus mainly on robustness as a proxy for resilience [48,50]. However, none of those reviewed studies embraced a multi-criteria approach for resilience that involves vulnerability, resistance, robustness, and recoverability. Therefore, based on our literature review and focus group discussions, this study's suggested definition and framework is a step forward. The following recommendations can be helpful for designers and building operators that seek to achieve resilient cooling of buildings in a holistic way:

1. Any definition of resilience must be based on the identification of a specific shock or disruption. In the case of resilient cooling of buildings, heat waves and power outages are considered as the main shocks (extreme events). Designers should assess the vulnerability of buildings against those shocks.

2. Any definition of resilience should specify and distinguish, at the same time, the resistance and robustness conditions against heat waves and power outage events. The resistance period involves the building's ability to resist shock(s) with the same pre-shock operation conditions. However, robustness requires failure and adaptation after failure. The robustness mechanism involves building users and building systems adaptation and their ability to adjust after a shock.

3. Thus, the definition of resilient cooling for buildings involves four critical criteria, mainly vulnerability (sensitivity to risk), resistance (absorption), robustness (adaptation after failure), and recovery (remedy). The building design, construction, and operation processes should address these criteria.

4. Resilient cooling design is an urgent requirement for future proof buildings. Weather extremes must be anticipated to assume well-being. The choice of comfort models is elementary to prepare buildings. Resilient cooling design involves combining passive and active cooling design measures, on-site renewable production, and the coupling to storage capacities. Our suggested definition for resilient cooling of buildings can help to develop in the future resilience performance indicators that account for the impacts of glo-

bal warming for long and short assessment periods. This can allow comparing the carbon emissions and primary energy use of different technologies at different stages of the building life stages. As part of the activities of IEA-EBC Annex 80, there is a need to assess the performance of conventional and advanced cooling technologies including advanced solar shading, chromogenic facades, cool materials, ventilated facades, thermal mass utilization including, PCM and off-peak ice storage, ventilative cooling, adiabatic/evaporative cooling, compression refrigeration, absorption refrigeration, natural heat sinks, sky radiative cooling, high-temperature cooling systems, Comfort ventilation, micro-cooling, personal comfort control and high-performance dehumidification including desiccant humidification. Without a multi-stage definition, it will be challenging to develop universal indicators that allow assessing the active and passive cooling technologies listed above.

5. Building operation systems and building management systems will play a significant role in applying the adaptation strategies and risk mitigation plans in collaboration with buildings users. For resilient cooling, HVAC systems and envelope features are a prime target for real-time optimization. Different dynamic control strategies with predictive algorithms should be embedded in building operation systems using a deeply coupled network of sensors. The smart readiness of buildings is part of resilience because it considers the fact that buildings must play an active role within the context of an intelligent energy system [82].

6. Resilience is a process, and its criteria should be addressed following a circular, iterative approach. Extracting learned lessons and integrating user experience during shocks is essential to increase the emergency learnability and feed the preparedness loop.

6.2. Strength and limitations

We are not aware of any studies that aimed to define resilience on a building scale involving the four criteria for resilience: vulnerability, resistance, robustness, and recovery. Two other resilience definition criteria are found in literature and are used on an urban scale: (1) adaptability, efficiency, flexibility, and redundancy; and (2) preparation, adaptation, recovery, and mitigation. However, both groups of criteria (1 and 2) hardly fit and match the indoor environmental performance requirements and challenges of buildings (and their occupants) against overheating and power outages events.

Despite the difficulty of creating a definition and developing a framework, the research benefited from the contributions of IEA-EBC Annex 80 building experts, RELi steering committee members, and UN resilience experts who fostered a consensus for a new definition and framework. The debate on considering "failure "or the "path to failure" fundamental criteria in the interpretation of resilience let us distinguish robustness from resistance [41]. Accordingly, the research aimed to provide a perspective for building professionals and users based on analyzing the existing literature and body of knowledge. The study theme remains novel because it was never discussed extensively in the different fields of use of the definitions of resilience in ecology, psychology, engineering, and economy.

A definition and framework within the scope of the IEA-EBC Annex 80 was proposed and validated. The definition positions "resilient cooling "in the field of engineering and economic resilience concerning climatic disruptions, namely heat waves and power outages. As shown in Fig. 6, it identifies the main criteria and sub-criteria that can be used to design, construct, and operate new and existing buildings [35]. Content analysis of more than 90 publications was conducted to provide insights and establish relevant connections with resilience definitions found in the scientific and professional literature. RELi 2.0 Rating Guidelines for Resilient Design and Construction [17] and its assessment criteria were critically investigated. The identified criteria will improve the understanding of practitioners and allow for comparison, discussion, and learning. The paper developed in-depth criteria that provide valuable strategies for resilient building design. It can help researchers and designers identify and reduce the risk of overheating during heat waves and power outages to protect occupants. The definition and criteria will allow benchmarking of resilient cooling buildings, including systems, solutions, and building control strategies.

However, the most challenging search activity was to find representative case studies. At the beginning of this study, defining resilient building cooling through case studies or reference buildings similar to developing the European sustainability reporting framework Levels [83,84] was planned. Failing to find case studies that addressed the concept of resilience partially or entirely forced us to define resilience first. The complexity and novelty of this concept makes its understanding, by building professional, challenging. The adoption of the resilience definition in this paper is influenced by the interpretation found in literature in engineering and economic sciences. Also, relevant publications that focus on building resilience against overheating risks could not be found. The suggested definition and framework are complete or can eliminate risks. However, they represent an adequate and initial knowledge base that can be consolidated and refined with standards and local regulations.

One of the main questions that we have answered in the resilience definition is "Resilience to what?" So, any future resilience framework must focus on a specific disruptive event. The current framework does not address all disruptions that can degrade the indoor thermal environment in one resilience evaluation framework, unless we are developing a multi-disruptive framework, which is not our case. The literature review and the experts provided insights and in-depth knowledge elaborated by the authors to develop a framework that defines resilience against "heat waves" and "power outages". The study would have benefited more from a broader focus group involving practitioners in the building industry and stakeholders of the built environment. However, the study topic remains novel because it can establish a quantitative evaluation framework for building cooling resilience.

6.3. Implication on practice and research

While the design for resilience is a consolidated procedure in other fields, this is not a common approach in the architectural engineering and construction industries—especially on the building scale. In this study, the resilience of building cooling and developed a framework that should be used in practice is defined. Despite the presence of RELi 2.0 Rating Guidelines for Resilient Design and Construction [17], there is a need to develop a standard that defines the resilience on the building scale concerning different disruptions. Practitioners and building professionals are confused about the term resilience, and they use it many times to replace other meanings, such as resistance or robustness. The other problem with many building designers is that they wish to assess the cooling system's resilience separately from the building and occupants. Resilience should be applied to integrated systems that involve occupants, systems, and building operators [85]. The term is related to holistic systems and cannot be used on parts of a system.

Therefore, there is a strong need to identify case studies that embrace this concept of building scale resilience. Case studies evaluating the buildings vulnerability, resistance, robustness, and recovery attributes are required to articulate and validate the resilience key performance indicators. These case studies should investigate real-time building management systems that predict

approaching heat waves and suggest adaptation strategies following building operators and occupants [62]. At the same time, governments and green building councils should promote exemplary buildings' design and construction as showcases of resilient buildings. Rating systems such as LEED, BREEAM, DGNB, and Levels should learn from RELi 2.0 Rating Guidelines and allow the development of further projects that adopt the concept of resilience [86]. The smart readiness indicator developed by the EU could also be used to measure the resilience of the cooling of buildings. The capacity of a building to use information and communication technologies and electronic systems to adapt its buildings services operation is essential. The same applies to adapt to the occupants' needs and the grid signals to improve indoor environmental quality during heat waves and power outages [82,87].

Finally, regional priorities regarding the climatic disruptions potential and investigate the possibility of passive resistance mechanisms of buildings (e.g., ventilative cooling and thermal storage technologies) and their adaptability robustness mechanisms should be addressed. There is a need for lateral thinking and experimental research approaches to apply the concept of resilience and assess the optimal solutions for the people and the planet.

7. Conclusions

A definition of resilient cooling for buildings is developed and discussed in this paper as part of the IEA-EBC Annex 80 research activities. The definition's main concepts and criteria are based on qualitative research methods. The paper presents a set of recommendations to adopt the definition in practice and research. Future research should build on our findings and create more consistent frameworks with useful quantifiable indicators, quantitative metrics, and performance threshold limits. Additional definitions of overheating and modeling of overheating events are required for different building types and climates. The research should be extended to identify benchmarks and case studies with reference values, threshold ranges, and to seek tools and reporting mechanisms for buildings' resilient cooling. Our suggested framework should evolve as research and experience build a greater understanding of resilient and sustainable buildings.

CRediT authorship contribution statement

Shady Attia: . **Ronnen Levinson:** Conceptualization, Validation. **Eileen Ndongo:** Software, Data curation, Validation, Visualization. **Peter Holzer:** Validation. **Ongun Berk Kazanci:** . **Shabnam Homaei:** Conceptualization. **Chen Zhang:** . **Bjarne W. Olesen:** Conceptualization. **Dahai Qi:** . **Mohamed Hamdy:** . **Per Heiselberg:** Conceptualization, Methodology, Validation.

Declaration of Competing Interest

The authors declare that they have no known competing financial interests or personal relationships that could have appeared to influence the work reported in this paper.

Appendix A

Table A-1

Table A-1

List of critical publications found in literature directly related to the four criteria of resilience against overheating and power outages in buildings. None of the listed studies proposed a definition of resilience applied for cooling buildings except reference [55].

	Vulnerability	Resistance	Robustness	Recovery	Resilience
Sander et al. (2003) [72]					✔
Lomas et al. (2009, 2012, 2017) [58,59,67]	✔	✔ *			✔
De Wilde et al. (2012) [60]		✔			✔
Olsen et a. (2012) [66]		✔	✔	✔	✔
Hassler et al. (2014) [76]		✔	✔	✔	✔
Burman et al. (2014) [61]		✔			
Anderies et al. (2014) [88]					✔
Nicol et al. (2014) [89]	✔		✔	✔	✔
Martin et al. (2015) [35]	✔	✔	✔	✔	
Buso et al. (2015) [90]		✔	✔ *		
Holmes et al. (2016) [62]		✔			✔
Coley et al. (2017) [63]		✔			
Hamdy et al. (2017) [64]	✔	✔			
Acione et al. (2017) [91]		✔ *	✔ *		
Kotireddy et al. (2018) [48]	✔	✔	✔ *		
Wilson (2018) [92]	✔	✔	✔	✔	✔
USGBC RELi (2018) [17]	✔	✔	✔	✔	✔
USGBC (2019) [65]		✔	✔		✔
Moazami et al. (2019abc) [50,79,93]	✔	✔	✔ *		*
Gupta et al. (2019) [94]		✔ *			*
Sun et al. (2020) [95]	✔	✔	✔ *		*
Homaei et al. (2020) [49]			✔ *		

* Studies that define resilience or robustness in disagreement with the definition proposed in this study. The studies do not consider failure as an essential event to assess the robustness and o resilience.

References

[1] T. McAllister, T. McAllister, Developing guidelines and standards for disaster resilience of the built environment: A research needs assessment, US Department of Commerce. National Institute of Standards and Technology, 2013.

[2] A. Jacob et al., 'Transformation towards sustainable and resilient societies in Asia and the Pacific', 2018.

[3] '71/276. Report of the open-ended intergovernmental expert working group on indicators and terminology relating to disaster risk reduction', United Nations, New York, UN General Assembly 71/276 Resolution, 2017. [Online]. Available: https://www.un.org/en/ga/search/view_doc.asp?symbol=A/RES/71/276.

[4] European Commission, 'The European Green Deal', Brussels, Belgium, Chapter 2.1.4, 2019. Accessed: May 12, 2020. [Online]. Available: https://ec.europa.eu/info/strategy/priorities-2019-2024/european-green-deal_en.

[5] S. Attia, Net Zero Energy Buildings (NZEB): Concepts, frameworks and roadmap for project analysis and implementation, Butterworth-Heinemann, 2018.

[6] S. Attia, Regenerative and positive impact architecture: Learning from case studies, Springer, 2018.

[7] R. Gupta, L. Barnfield, M. Gregg, Overheating in care settings: magnitude, causes, preparedness and remedies, Build. Res. Inf. 45 (1–2) (2017) 83–101.

[8] T. Kjellstrom, I. Holmer, B. Lemke, Workplace heat stress, health and productivity–an increasing challenge for low and middle-income countries during climate change, Glob. Health Action 2 (1) (2009) 2047.

[9] A. De Bono, Peduzzi, S. Kluser, and G. Giuliani, 'Impacts of summer 2003 heat wave in Europe', 2004.

[10] R. Gupta, M. Kapsali, Empirical assessment of indoor air quality and overheating in low-carbon social housing dwellings in England, UK, Adv. Build. Energy Res. 10 (1) (2016) 46–68.

[11] Holzer and Cooper, 'IEA EBC Annex 80 on Resilient Cooling for Residential and Small Non-Residential Buildings', IEA, Paris, 10.13140/RG.2.2.33912.47368, 2019. [Online]. Available: https://annex80.iea-ebc.org/Data/Sites/10/media/documents/supporting/ebc-annex-80-annex-text-190616.pdf.

[12] 'The Future of Cooling: Opportunities for energy-efficient air conditioning', IEA, Paris, France, 2018. [Online]. Available: https://www.iea.org/reports/the-future-of-cooling.

[13] S. O. Andersen et al., 'Cooling Emissions and Policy Synthesis Report: Benefits of Cooling Efficiency and the Kigali Amendment Workplace', 2020.

[14] I. Kelman, J.C. Gaillard, J. Lewis, J. Mercer, Learning from the history of disaster vulnerability and resilience research and practice for climate change, Nat. Hazards 82 (1) (2016) 129–143.

[15] K.-H. Liao, 'A theory on urban resilience to floods—a basis for alternative planning practices', Ecol. Soc., vol. 17, no. 4, 2012.

[16] S.R. Carpenter, C. Folke, Ecology for transformation, Trends Ecol. Evol. 21 (6) (2006) 309–315.

[17] USGBC, RELi 2.0 Rating Guidelines for Resilient Design & Construction, U.S. Green Building Council, Washington, USA, 2018.

[18] K. Nelson, L. Gillespie-Marthaler, H. Baroud, M. Abkowitz, and D. Kosson, 'An integrated and dynamic framework for assessing sustainable resilience in complex adaptive systems', Sustain. Resilient Infrastruct., 1–19, 2019.

[19] S. Attia, A.M.E.S. Mustafa, M.K. Singh, 'Assessment of thermal overheating in free-running buildings in Cairo', in PROCEEDINGS OF THE 1ST INTERNATIONAL CONFERENCE ON COMFORT AT THE EXTREMES: ENERGY, Economy and Climate (2019) 902–913.

[20] S. Attia, S. Bilir, T. Safy, C. Struck, R. Loonen, F. Goia, Current trends and future challenges in the performance assessment of adaptive façade systems, Energy Build. 179 (2018) 165–182.

[21] S. Attia, R. Lioure, Q. Declaude, Future trends and main concepts of adaptive facade systems, Energy Sci. Eng. (2020).

[22] E. Garfield, S. Paris, W.G. Stock, HistCiteTM: A software tool for informetric analysis of citation linkage, Inf. Wiss. Prax. 57 (8) (2006) 391.

[23] G. R. Gibbs, 'Thematic coding and categorizing', Anal. Qual. Data Lond. Sage, 38–56, 2007.

[24] N.K. Gale, G. Heath, E. Cameron, S. Rashid, S. Redwood, Using the framework method for the analysis of qualitative data in multi-disciplinary health research, BMC Med. Res. Methodol. 13 (1) (2013) 117.

[25] A. Lacey, D. Luff, Qualitative data analysis, Trent Focus Sheffield (2001).

[26] S. Friese, Qualitative data analysis with ATLAS. ti. SAGE Publications Limited, 2019.

[27] S. Attia, 'Content Analysis', Qualitative Research Methods, Mar. 01, 2020. https://tinyurl.com/qorc2x3 (accessed Oct. 10, 2019).

[28] S. Attia, 'In-depth Interviews', Qualitative Research Methods, May 01, 2020. https://tinyurl.com/ycacmljt (accessed Oct. 10, 2019).

[29] S. Attia, 'Focus group discussion', Qualitative Research Methods, 2020. https://tinyurl.com/y8l5xv4r (accessed Jun. 01, 2020).

[30] Holzer, 'Annex 80 Participants', Annex 80 Participants, 2019. https://annex80.iea-ebc.org/participants (accessed Jun. 01, 2020).

[31] T. Cannon, D. Müller-Mahn, Vulnerability, resilience and development discourses in context of climate change, Nat. Hazards 55 (3) (2010) 621–635.

[32] C. Folke, S. Carpenter, T. Elmqvist, L. Gunderson, C.S. Holling, B. Walker, Resilience and sustainable development: building adaptive capacity in a world of transformations, AMBIO J. Hum. Environ. 31 (5) (2002) 437–440.

[33] S.B. Manyena, The concept of resilience revisited, Disasters 30 (4) (2006) 434–450.

[34] G.C. Gallopín, Linkages between vulnerability, resilience, and adaptive capacity, Glob. Environ. Change 16 (3) (2006) 293–303.

[35] R. Martin, Sunley,, On the notion of regional economic resilience: conceptualization and explanation, J. Econ. Geogr. 15 (1) (2015) 1–42.

[36] C.S. Holling, Resilience and stability of ecological systems, Annu. Rev. Ecol. Syst. 4 (1) (1973) 1–23.

[37] R. Graber, F. Pichon, E. Carabine, Psychological resilience, Lond. Overseas Dev. Inst. (2015).

[38] J. Simmie, R. Martin, The economic resilience of regions: towards an evolutionary approach, Camb. J. Reg. Econ. Soc. 3 (1) (2010) 27–43.

[39] R. Boschma, Towards an evolutionary perspective on regional resilience, Reg. Stud. 49 (5) (2015) 733–751.

[40] C.M. Sgro, A.J. Lowe, A.A. Hoffmann, Building evolutionary resilience for conserving biodiversity under climate change, Evol. Appl. 4 (2) (2011) 326–337.

[41] C.S. Holling, Engineering resilience versus ecological resilience, Eng. Ecol. Constraints 31 (1996) (1996) 32.

[42] Y. Jabareen, Planning the resilient city: Concepts and strategies for coping with climate change and environmental risk, Cities 31 (2013) 220–229.

[43] I. Takewaki, A. Moustafa, K. Fujita, Improving the earthquake resilience of buildings: the worst case approach, Springer Science & Business Media, 2012.

[44] S. L. Cox, E. L. Hotchkiss, D. E. Bilello, A. C. Watson, and A. Holm, 'Bridging climate change resilience and mitigation in the electricity sector through renewable energy and energy efficiency: emerging climate change and development topics for energy sector transformation', National Renewable Energy Lab.(NREL), Golden, CO (United States), 2017.

[45] H.-M. Füssel, Vulnerability: A generally applicable conceptual framework for climate change research, Glob. Environ. Change 17 (2) (2007) 155–167.

[46] J.X. Kasperson, R.E. Kasperson, B. Turner, W. Hsieh, A. Schiller, 'Vulnerability to global environmental change', in The social contours of risk: volume II: risk analysis, in: corporations and the globalization of risk, Taylor and Francis, 2012, pp. 245–285.

[47] D.R.C. Asian, 'Living with risk, A global review of disaster reduction initiatives. Preliminary version', United Nations, 2002.

[48] R. Kotireddy, P.-J. Hoes, J.L. Hensen, A methodology for performance robustness assessment of low-energy buildings using scenario analysis, Appl. Energy 212 (2018) 428–442.

[49] S. Homaei, M. Hamdy, A robustness-based decision making approach for multi-target high performance buildings under uncertain scenarios, Appl. Energy 267 (2020) 114868.

[50] A. Moazami, S. Carlucci, S. Geving, Robust and resilient buildings: A framework for defining the protection against climate uncertainty, in: IOP Conference Series, Materials Science and Engineering 609 (2019) 072068.

[51] H. Ernstson et al., Urban transitions: on urban resilience and human-dominated ecosystems, Ambio 39 (8) (2010) 531–545.

[52] S. Meerow, J. Newell, M. Stults, Defining urban resilience: A review, Landsc. Urban Plan. 147 (2016) 38–49.

[53] D.R. Godschalk, Urban hazard mitigation: creating resilient cities, Nat. Hazards Rev. 4 (3) (2003) 136–143.

[54] D. Stead, Urban planning, water management and climate change strategies: adaptation, mitigation and resilience narratives in the Netherlands, Int. J. Sustain. Dev. World Ecol. 21 (1) (2014) 15–27.

[55] A. Sharifi, Y. Yamagata, Principles and criteria for assessing urban energy resilience: A literature review, Renew. Sustain. Energy Rev. 60 (2016) 1654–1677.

[56] B.E. Tokgoz, A.V. Gheorghe, Resilience quantification and its application to a residential building subject to hurricane winds, Int. J. Disaster Risk Sci. 4 (3) (2013) 105–114.

[57] D. Cormie, G. Mays, and Smith, Blast effects on buildings. ICE publishing, 2019.

[58] K.J. Lomas, Y. Ji, Resilience of naturally ventilated buildings to climate change: Advanced natural ventilation and hospital wards, Energy Build. 41 (6) (2009) 629–653.

[59] K.J. Lomas, R. Giridharan, Thermal comfort standards, measured internal temperatures and thermal resilience to climate change of free-running buildings: A case-study of hospital wards, Build. Environ. 55 (2012) 57–72.

[60] De Wilde, D. Coley, The implications of a changing climate for buildings, Elsevier (2012).

[61] E. Burman, J. Kimpian, and D. Mumovic, 'Reconciling Resilience and Sustainability in Overheating and Energy Performance Assessments of Non-domestic Buildings', 2014.

[62] S.H. Holmes, T. Phillips, A. Wilson, Overheating and passive habitability: indoor health and heat indices, Build. Res. Inf. 44 (1) (2016) 1–19.

[63] D. Coley, M. Herrera, D. Fosas, C. Liu, M. Vellei, Probabilistic adaptive thermal comfort for resilient design, Build. Environ. 123 (2017) 109–118.

[64] M. Hamdy, S. Carlucci, P.-J. Hoes, J.L. Hensen, The impact of climate change on the overheating risk in dwellings—A Dutch case study, Build. Environ. 122 (2017) 307–323.

[65] USGBC, Leadership in energy and environmental design v4 (2019) 1.

[66] E. Olsen, J. Kuo, and A. Tazi, 'Resilient Design: Putting thermal resilience in the LEED pilot credits to the test', 2012. https://www.resilientdesign.org/putting-thermal-resilience-in-the-leed-pilot-credits-to-the-test/.

[67] K.J. Lomas, S.M. Porritt, Overheating in buildings: lessons from research, Taylor & Francis, 2017.

[68] L. Bull-Kamanga et al., From everyday hazards to disasters: the accumulation of risk in urban areas, Environ. Urban. 15 (1) (2003) 193–204.

[69] W. H. Organization, 'Background information on urban outdoor air pollution', WHO Accessed April, vol. 21, 2017.

[70] S. Carlucci, L. Pagliano, A review of indices for the long-term evaluation of the general thermal comfort conditions in buildings, Energy Build. 53 (2012) 194–205.

[71] C. Di Napoli, F. Pappenberger, H.L. Cloke, Verification of Heat Stress Thresholds for a Health-Based Heat-Wave Definition, J. Appl. Meteorol. Climatol. 58 (6) (2019) 1177–1194.

[72] C.H. Sanders, M.C. Phillipson, UK adaptation strategy and technical measures: the impacts of climate change on buildings, Build. Res. Inf. 31 (3–4) (2003) 210–221.

[73] A. Jones, Indoor air quality and health, Atmosph. Environ. 33 (28) (1999) 4535–4564.

[74] A. Baniassadi, J. Heusinger, D.J. Sailor, Energy efficiency vs resiliency to extreme heat and power outages: The role of evolving building energy codes, Build. Environ. 139 (2018) 86–94.

[75] T. Swanstrom, 'Regional resilience: a critical examination of the ecological framework', working paper, 2008.

[76] U. Hassler, N. Kohler, Resilience in the built environment, Taylor & Francis, 2014.

[77] M. Palme, L. Inostroza, G. Villacreses, A. Lobato-Cordero, C. Carrasco, From urban climate to energy consumption. Enhancing building performance simulation by including the urban heat island effect, Energy Build. 145 (2017) 107–120.

[78] A. Laouadi, A. Gaur, M.A. Lacasse, M. Bartko, M. Armstrong, Development of reference summer weather years for analysis of overheating risk in buildings, J. Build. Perform. Simul. 13 (3) (2020) 301–319.

[79] A. Moazami, V. Nik, S. Carlucci, and S. Geving, 'Impacts of the future weather data type on the energy simulation of buildings–Investigating long-term patterns of climate change and extreme weather conditions', 2019.

[80] D.J. Sailor, Risks of summertime extreme thermal conditions in buildings as a result of climate change and exacerbation of urban heat islands, Build. Environ. 78 (2014) 81–88.

[81] C.A. MacKenzie, K. Barker, Empirical data and regression analysis for estimation of infrastructure resilience with application to electric power outages, J. Infrastruct. Syst. 19 (1) (2012) 25–35.

[82] T. Märzinger, D. Österreicher, Supporting the Smart Readiness Indicator—A Methodology to Integrate A Quantitative Assessment of the Load Shifting Potential of Smart Buildings, Energies 12 (10) (1955) 2019.

[83] A.S. Cordero, S.G. Melgar, J.M.A. Márquez, Green Building Rating Systems and the New Framework Level (s): A Critical Review of Sustainability Certification within Europe, Energies 13 (1) (2019) 1–25.

[84] N. Dodd, S. Donatello, E. Garbarino, and M. Gama-Caldas, 'Identifying macro-objectives for the life cycle environmental performance and resource efficiency of EU buildings', JRC EU Comm. Luxemb., 117, 2015.

[85] K. Beckmann and S. Roaf, 'Workshop Report: Climate Resilience for the Scottish Built Environment', in Report for ClimateXChange Scotland, 2013.

[86] N. Dodd, M. Cordella, M. Traverso, S. Donatello, Level (s)–A common EU framework of core sustainability indicators for office and residential buildings, JRC Sci. Policy ReEur. Comm. (2017).

[87] E. Parliament, Directive 2018/844/EU of the European Parliament and of the council of 19 June 2018 on the energy performance of buildings (recast), Off. J. Eur. Communities 61 (156) (2018) 75–91.

[88] J.M. Anderies, Embedding built environments in social–ecological systems: resilience-based design principles, Build. Res. Inf. 42 (2) (2014) 130–142.

[89] L.A. Nicol, Knoepfel,, Resilient housing: a new resource-oriented approach, Build. Res. Inf. 42 (2) (2014) 229–239.

[90] T. Buso, V. Fabi, R.K. Andersen, S. Corgnati, Occupant behaviour and robustness of building design, Build. Environ. 94 (2015) 694–703.

[91] F. Ascione, N. Bianco, R.F. De Masi, G.M. Mauro, G. Vanoli, Resilience of robust cost-optimal energy retrofit of buildings to global warming: A multi-stage, multi-objective approach, Energy Build. 153 (2017) 150–167.

[92] A. Wilson, 'Resilience as a driver of passive design', in *Activism in Architecture*, Routledge (2018) 155–164.

[93] A. Moazami, S. Carlucci, V.M. Nik, S. Geving, Towards climate robust buildings: An innovative method for designing buildings with robust energy performance under climate change, Energy Build. 202 (2019) 109378.

[94] R. Gupta, A. Bruce-Konuah, A. Howard, Achieving energy resilience through smart storage of solar electricity at dwelling and community level, Energy Build. 195 (2019) 1–15.

[95] K. Sun, M. Specian, T. Hong, Nexus of thermal resilience and energy efficiency in buildings: A case study of a nursing home, Build. Environ. 106842 (2020).

Paper VI

**Simulation-Based Framework to Evaluate Climate
Resistivity of Buildings**
Ramin Rahif, Mohamed Hamdy, Shabnam Homaei, Chen Chang, Peter Holzer,
Shady Attia
Building and Environment. 2021 November 19.

Simulation-based framework to evaluate resistivity of cooling strategies in buildings against overheating impact of climate change

R. Rahif [a,*], M. Hamdy [b], S. Homaei [b], C. Zhang [c], P. Holzer [d], S. Attia [a]

[a] Sustainable Building Design Lab, Dept. UEE, Faculty of Applied Science, Université de Liege, Belgium
[b] Department of Civil and Environmental Engineering, Norwegian University of Science and Technology, Norway
[c] Aalborg University, Department of the Built Environment, Thomas Manns Vej 23, 9220, Aalborg Øst, Denmark
[d] Institute of Building Research and Innovation, Wipplingerstraße, 23/3, 1010, Vienna, Austria

ARTICLE INFO

ABSTRACT

Over the last decades overheating in buildings has become a major concern. The situation is expected to worsen due to the current rate of climate change. Many efforts have been made to evaluate the future thermal performance of buildings and cooling technologies. In this paper, the term "climate change overheating resistivity" of cooling strategies is defined, and the calculation method is provided. A comprehensive simulation-based framework is then introduced, enabling the evaluation of a wide range of active and passive cooling strategies. The framework is based on the Indoor Overheating Degree (IOD), Ambient Warmness Degree (AWD), and Climate Change Overheating Resistivity (CCOR) as principal indicators allowing a multi-zonal approach in the quantification of indoor overheating risk and resistivity to climate change.

To test the proposed framework, two air-based cooling strategies including a Variable Refrigerant Flow (VRF) unit coupled with a Dedicated Outdoor Air System (DOAS) (C01) and a Variable Air Volume (VAV) system (C02) are compared in six different locations/climates. The case study is a shoe box model representing a double-zone office building. In general, the C01 shows higher *CCOR* values between 2.04 and 19.16 than the C02 in different locations. Therefore, the C01 shows superior resistivity to the overheating impact of climate change compared to C02. The maximum CCOR value of 37.46 is resulted for the C01 in Brussels, representing the most resistant case, whereas the minimum CCOR value of 9.24 is achieved for the C02 in Toronto, representing the least resistant case.

1. Introduction

During the last decade, the concept of resistivity of buildings and cooling strategies emerged in several studies [1]. The term resistivity appeared under different names including: Resistance, Resilience, Robustness, and other terms. For example, Attia et al. [1] defines cooling resistance as the building system's ability to maintain the initial design conditions during the disturbances such as heatwaves or power outages. This paper defines so-called "climate change overheating resistivity" as the ability of building cooling strategies to resist the increase of indoor overheating risk against the increase of outdoor thermal severity in a changing climate. In other words, the climate change overheating resistivity shows to what extend the indoor overheating risk will increase with the increase of outdoor thermal stress under future climate scenarios. This definition targets the ability of cooling strategies in

buildings to maintain an acceptable thermal environment against the gradual worsening of weather conditions due to climate change, whereas the definition in Ref. [1] targets the ability of cooling strategies to suppress the short-term overheating incidents. There is a universal need to understand the notion of climate change overheating resistivity as a key factor in characterizing the future thermal performance of cooling strategies in buildings.

Despite the important role of opting for the implementation of climate change overheating resistive cooling strategies in buildings, it is being overlooked in the fight against climate change. Climate change overheating resistive cooling strategy improves the preparedness of the building for more intense and frequent overheating events in the future. The more the cooling strategy is resistant, the higher it is able to maintain a comfortable and healthy environment for the occupants in buildings. The concept of climate change overheating resistivity must be

---

standardized through the regulation and policies to be strictly implemented in the building cooling requirements.

Several studies highlighted the importance of cooling strategies in mitigating the overheating impacts of climate change [2–4]. The cooling demand in buildings is predicted to encounter unprecedented growth with the continuation of global warming [5–7]. The increase in cooling demand will be further aggravated with the increase of internal gains related to growing occupancy densities [8]. The cooling strategies will become inexorable to remove sensible/latent heating loads, prevent heat gains to the indoor environment, or enhance personal comfort. Therefore, the cooling strategies are expected to play the main role in reducing the overheating risks in buildings and hence ensure comfortable environments in future climates.

The first question considered in evaluating the scientific literature is, *"what are the simulation-based studies that assessed the performance of cooling strategies in relation to climate change?"*. In response to the first question, some relevant studies are presented as follows. O'Donovan et al. [9] investigated ten passive cooling control strategies applied on a Nearly Zero Energy Building (NZEB). Each strategy uses different combinations of passive cooling systems such as day-time ventilation, nighttime ventilation, and dynamic solar shading. For different combinations of passive cooling systems, an increase in indoor operative temperature between $0.1°C$ and $0.3°C$ in Dublin (maritime climate) and between $1°C$ and $1.9°C$ in Budapest (continental climate) was resulted by 2050s. It was also mentioned that the passive cooling strategies (and their combination) are able to maintain 57–95% comfortable occupied hours. Chiesa & Zajch [10] investigated the sensitivity of Earth-to Air Heat Exchangers (EAHE) to climate change in nine different locations across Northern America. Using Local and Residual Cooling Degree Hour (CDH_{loc} and CDH_{res}) to calculate the virtual control of EAHE, they found a significant reduction in the cooling potential of the EAHE system for Representative Concentration Pathway (RCP) 4.5 and 8.5 scenarios by 2061–2090. Rey-Hernández et al. [11] studied the impact of climate change on the indoor operative temperature of a zero energy and carbon office building located in Valladolid, Spain. The cooling system consists of a chiller system backed up with an adsorption chiller connected to an Air Handling Unit (AHU). By using the CCWorldWeatherGen tool to produce future weather files, they found an increase in indoor air temperature of $\sim 1°C$ between 2020 and 2050 and $\sim 1.7°C$ between 2050 and 2080. Ibrahim & Pelsmakers [12] investigated the increase in indoor overheating risk in a PassivHaus retrofit case study using PassivHaus Planning Package (PHPP) [13] metric. For the period between High Emission Scenarios (HiES) of 2050 and 2080, the study results show an increase in overheating frequency by 6% for roof insulation, 7% for wall insulation, 6% for reduced glazing size, 5% for nighttime ventilation, 5% for internal and external shading devices, and 3% for reduced glazing G-value.

There is a study by Hamdy et al. [14] that introduced the Overheating Escalation Factor (OEF) metric corresponding to the inverse of climate change overheating resistivity factor within this paper. The *OEF* shows the sensitivity of a building to increasing outdoor thermal severity. By morphing the historical data (1964/1965 and 2003), they generated future and worst future weather scenarios. By applying in total 4 weather scenarios, they found the *OEF* values between 0.1 and 0.989 in Dutch dwellings. It means that there are some dwellings (with only natural ventilation) that are very close to become overheated in the future.

The second question considered in evaluating the scientific literature is, *"do those studies allow for a universal and comprehensive evaluation of the resistivity of cooling strategies against the overheating impact of climate change?"*. In response to the second question, four criteria are set for a systematic analysis as follows.

- **Universality:** this criterion evaluates whether the study is conducted for a universal evaluation of cooling strategies. Most studies focus on a specific location and climate based on the national or regional

standards for comfort models and definition of building characteristics.
- **Function-independency:** this criterion investigates whether the study is focused on a specific building typology and function mode. Function-dependent studies focus on specific residential or non-residential buildings. Therefore, they do not contain full guidance on how to define the operational properties, schedules, and comfort categories for different building types.
- **Comfort model-independency:** this criterion evaluates whether the study has provisions regarding the flexible selection of the static and adaptive comfort models. Such a provision enables the evaluation of both active and passive cooling strategies with different cooling modes (air conditioned, non-air conditioned, and mixed/hybrid modes).
- **Resistivity evaluation:** this criterion examines whether the study contains resistivity evaluation against overheating impact of climate change. The main factor for the resistivity evaluation is the use of specific metrics (e.g. *OEF*, *CCOR*, etc.) that relate the indoor and outdoor thermal environments while incorporating multiple historical and future weather scenarios. Such metrics show, via a single value, to what extend the thermal performance of the cooling strategies in buildings are affected due to the changes in outdoor thermal conditions over time.

The results of the literature analysis based on the four abovementioned criteria are presented in Table 1.

Until now, there is a lack of comprehensive universal method to evaluate and compare the climate change overheating resistivity of cooling strategies. As part of the International Energy Agency (IEA) EBC Annex 80 – "Resilient cooling of buildings" project activities, this paper is developed to address the abovementioned knowledge gaps. The aim of this research is to broaden the comparative analysis among cooling strategies to global scales. The main research question is:

- How to evaluate the climate change overheating resistivity of cooling strategies worldwide?

The main research question can be divided into:

- Q1: How to characterize the climate data and building models in a consistent way to universally compare the cooling strategies?

Table 1
A list of studies in the literature concerning the thermal performance evaluation of buildings/cooling strategies under future climate scenarios.

Scientific article	Universality	Function-independency	Comfort model-independency	Resistivity evaluation
O'Donovan et al. [9]	✗	✗	✗	✗
Lomas & Ji [15]	✗	✗	✗	✗
Hanby & Smith [16]	✗	✗	✓	✗
K.J. Lomas & Giridharan [17]	✗	✗	✗	✗
Gupta & Gregg [18]	✗	✗	✗	✗
Sajjadian et al. [19]	✓	✗	✗	✗
Hamdy et al. [14]	✗	✗	✓	✓
Ibrahim & Pelsmakers [12]	✗	✗	✗	✗
Pagliano et al. [20]	✗	✗	✓	✗
Chiesa & Zajch [10]	✓	✗	✗	✗

- Q2: How to quantify and evaluate the climate change overheating resistivity of cooling strategies in buildings?
- Q3: How to test the evaluation framework?

This paper provides a generic simulation-based framework contributing to the body of knowledge in several ways. First, the framework is based on universally applicable standards enabling, with common boundary conditions, a universal comparison of cooling strategies in different climatic regions. Second, the framework is comprehensive; it allows for the comparison of a wide range of active and passive cooling strategies by providing systematic guidance on how to select the comfort models for the zones with different cooling modes (air conditioned, non-air conditioned, and mixed/hybrid mode). The framework is also not limited to any building typology and operation type; it encompasses residential and non-residential buildings, whether they are newly built or existing buildings. Third, the framework identifies and includes a multi-zonal and climate-change sensitive approach in the quantification of overheating risks in buildings. More importantly, a new fit-to-purpose metric called "Climate Change Overheating Resistivity (CCOR)" is introduced to quantify the resistivity of cooling strategies against overheating impacts of climate change. Finally, a Variable Refrigerant Flow (VRF) unit coupled with a Dedicated Outdoor Air Supply (DOAS) and a Variable Air Volume (VAV) system are compared in six reference cities to test the framework. Detailed information on their sizing is also presented.

The proposed framework can provide strong support for the building professionals to assess and compare different cooling strategies in the early design stage and retrofit of the new and existing buildings, respectively. Implementing the methodology may yield to thermal resiliency benefits in the buildings. Also, the research outcomes can inform the cooling industry regarding the resistivity of cooling strategies against climate change in different regions. It can instigate technical improvements towards more resistive cooling concepts. It also sheds light on the importance of resistivity requirements to be embedded in the regional and national building codes in defining thermal comfort requirements. The current paper is organized as follows. In Section 2, the methodology, including the framework is provided (Section 2.1) and the demonstration case (Section 2.2). Section 3 presents the results. Section 4 discusses the key findings, recommendations, strengths, limitations, and implications on the practice of the study and suggests potential future research. And, Section 5 concludes the paper.

2. Methodology

Fig. 1 shows the research methodology of the current paper. The methodology consists of two main parts. In the first part, the framework is introduced relying on the literature review, International standards, focus-group discussions, and follow-up discussions among the authors. In the second part, a demonstration case to test the proposed framework is provided.
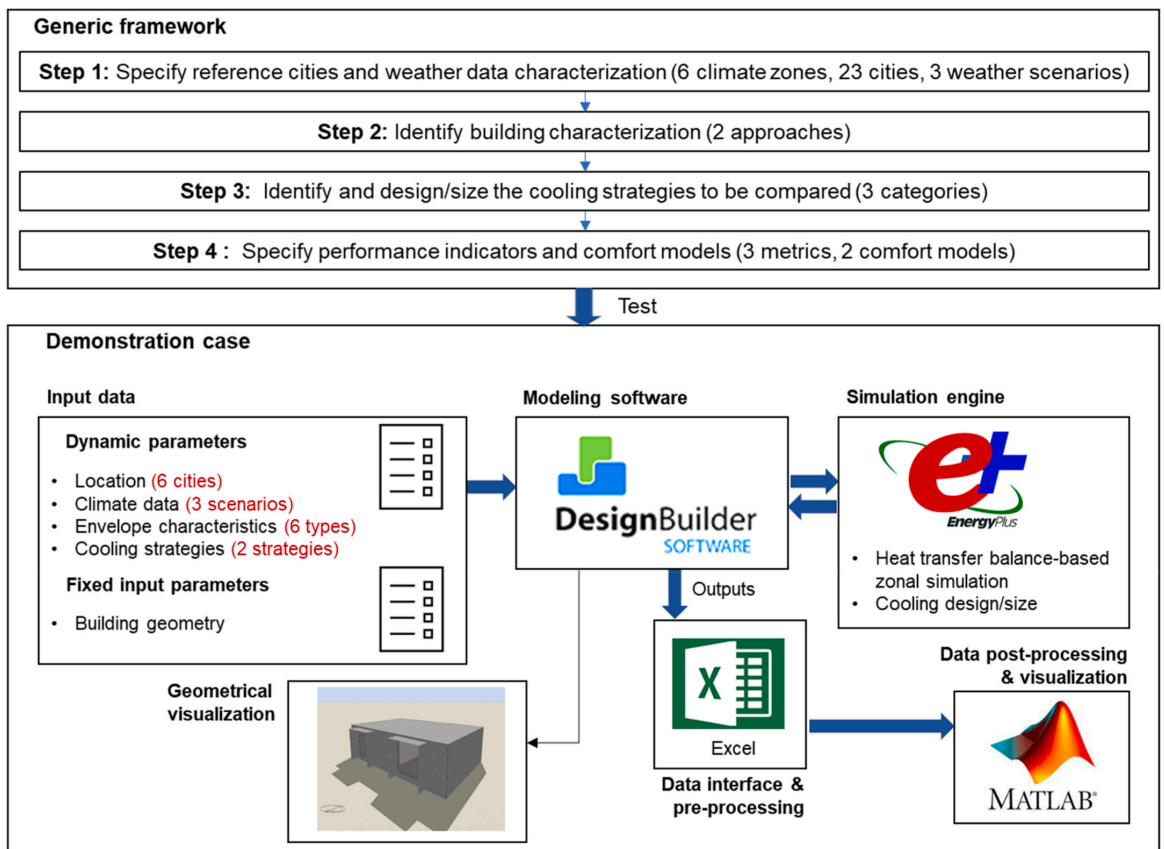

Fig. 1. Study conceptual framework (SCF).

2.1. Generic framework

Thermal discomfort in buildings can be divided into overheating discomfort and overcooling discomfort. Many researchers highlighted that with the continuation of global warming, overheating will become the increasing cause of thermal discomfort in buildings in most regions [21–25]. Therefore, the scope of the current framework is narrowed to the overheating discomfort and the evaluation of cooling strategies. In other words, the overcooling discomfort and heating system performance are excluded.

As shown in Fig. 2, the proposed framework consists of four main steps, 1) specify reference cities and weather data characterization (Section 2.1.1), 2) identify building characterization (Section 2.1.2), 3) identify and design/size the cooling strategies to be compared (Section 2.1.3), and 4) specify performance indicators and comfort models (Section 2.1.4). The framework allows a universal comparison of a wide range of active and passive cooling strategies. It encompasses almost the entire building typologies and function modes. The framework is also flexible to be used as a fast decision-support tool with recommending simple shoe box models as well as to more sophisticated analysis via reference building models. As mentioned earlier, the principal aim of the framework is to provide a standardized method (based on Internationally applicable standards) for a universal (different locations and climates) comparison of cooling strategies. However, for practical use, one can select a specific location and building and follow the suggested procedure to compare a set of applicable cooling strategies.

2.1.1. Step 1: specify reference cities and weather data characterization

Weather files are major prerequisites in any study related to climate change. The weather data requirements for the current framework is inspired by the work of (IEA) EBC Annex 80 - Weather Data Task Force. First, it necessitates the use of one contemporary (i.e. 2010s) and two future (i.e. 2050s and 2090s) weather scenarios. Future weather data projections are grouped according to the concentration and emission scenarios that are called Representative Concentrations Pathways (RCPs) to represent the 21st century. RCPs are based on energy, land use and cover, technological, socioeconomic, Green House Gas (GHG) emissions, and air pollutant assumptions [26]. With the current climate change mitigation efforts, the actual temperatures expected to be much higher than the projections in RCP2.6 (low emission scenario), RCP4.5 (medium-low emission scenario), and RCP6 (medium-high emission scenario) [27]. So, the framework requires future weather files based on RCP8.5 (high emission scenario). Current state-of-the-art approaches and tools to produce future global projections and weather files are widely discussed in Refs. [28–30].

Second, the framework recommends 23 cities (see Fig. 2) representing the climate zones 1 to 6 in ASHRAE 169.1 [31] classification. Multiple reference cities are assigned for each climate zone based on the population and the rate of growth.

Third, the framework allows both UHI effect included and excluded weather data. Including the UHI effect, especially in urban-related studies, quantifies the anthropogenic impacts on the evolution of outdoor thermal conditions [32]. Doing so contributes to more realistic weather data input for the simulations. However, due to limitations in obtaining such accurate weather data, the framework allows the use of weather files without UHI effects as an alternative.

2.1.2. Step 2: identify building characterization

The framework is applicable for evaluations in both new and existing buildings. The "existing buildings" are the buildings that are already in existence or constructed and authorized prior to the effective date of the current national or regional building regulations. Differently, the "new buildings" are the buildings that are already constructed or will be constructed after the effective date of the current national or regional building regulations. The framework provides two approaches for the selection of the building simulation models, the shoe box model (new buildings) and the reference building model (new and existing buildings).

The shoe box model is a basic and simplified model of a building that represents a building or its division as a rectangular box. The shoe box models can be made very quickly and therefore valuable to make early design decisions. In the case of shoe box models, the envelope characteristics must comply with ASHRAE 90.1 [33]. It is a widely accepted standard that specifies requirements for building envelope thermal properties for high-performance buildings (except for low-rise residential buildings) for each climate zone. The International standards ISO 18523- [34] and ISO 18253–2 [35] as well as ISO 17772–1 [36] are suggested to define schedules and condition of building, zone and space usage, including occupancy, operation of technical building systems, hot water usage, internal gains due to occupancy, lighting and equipment.

The reference building models are "*buildings characterized by and representative of their functionality and geographic location, including indoor and outdoor climate conditions*" (Annex III of the EPBD recast). The reference buildings can be created statistically (theoretical model) or by expert assumptions and previous studies (example model) or by selecting a real typical building [37]. Consequently, all the input parameters regarding the geometry, envelope properties, and operational conditions (schedule and condition of building, zone and space usage) can be derived by statistical analysis or expert assumptions or should reflect real typical conditions. Establishing reference building models provides a credible and robust model to evaluate the energy needs and retrofit measures [38] as well as thermal comfort and climate change adaptation measures. There are several studies that developed reference building models such as for educational buildings in Belgium [39], in Italy [40], in Ireland [41], in Australia [42], for office buildings in Korea [43], in England and Wales [44], for commercial buildings and residential buildings in the United States [33,45,46], and for residential buildings in thirteen European countries (Germany, Greece, Slovenia, Italy, France, Ireland, Belgium, Poland, Austria, Bulgaria, Sweden, Czech Republic, and Denmark) within the TABULA IEE-EU followed by EPISCOPE IEE-EU projects. In the case of reference building models, the users should create or select (e.g. from the above studies) representing a specific building typology and vintage (i.e., constructed during a specific new or old period) in the target reference city.

2.1.3. Step 3: identify and design/size the cooling strategies to be compared

Choosing a cooling strategy for buildings is challenging, especially when the designers are concerned with the impact of their choices on the resistivity against climate change. The framework lists a set of active and passive cooling strategies that are categorized by Ref. [4] as part of (IEA) EBC Annex 80 - Subtask B activities into four main categories (A, B, C, and D) based on their approaches in cooling the people or the indoor environment.

In category A, there are cooling strategies that reduce heat gains to the indoor environment and the occupants. It consists of solar shading and chromogenic glazing technologies, cool envelope materials, green roofs, roof ponds, green facades, ventilated roofs and facades, and thermal mass utilization. In category B, there are cooling strategies that remove sensible heat from indoor environments. It consists of absorption refrigeration (including desiccant cooling), ventilative cooling including Natural Ventilation (NV) and Mechanical Ventilation (MV), adiabatic/evaporative cooling, compression refrigeration, ground source cooling, sky radiative cooling, and high-temperature cooling (including radiant cooling). In category C, there are cooling strategies that enhance personal comfort apart from space cooling such as personal comfort systems. In category D, there are cooling strategies that remove latent heat from indoor environments such as high-performance dehumidification (including desiccant humidification). However, the framework cannot be used for category D due to the lack of relative humidity factor within the performance indicators (Step 4).

The cooling strategy (C_n) selected to be evaluated through the framework can be an individual or any combination of active and

(1) Climate and location

Weather data for *contemporary 2010s, mid-future 2050s (RCP8.5), and future 2090s (RCP8.5)* (IEA EBC Annex 80 - Weather Data Task Force)

Reference cities (ASHRAE 169.1):

Lagos (1A)	Barcelona (3A)	Los Angeles (3B)	Brussels (4A)	Vienna (5A)
Guayaquil (1A)	Rome (3A)	Santiago (3C)	Xian (4B)	Montreal (6A)
New Delhi (1B)	Buenos Aires (3A)	Paris (4A)	Vancouver (4C)	Stockholm (6A)
Sao Paulo (2A)	Busan (3A)	London (4A)	Toronto (5A)	
Cairo (2B)	Tehran (3B)	Gent (4A)	Copenhagen (5A)	

Urban heat island effect included   Urban heat island effect excluded

(2) Building characterization

Shoe box model (new buildings)   Reference model (new & old buildings)

Residential   Non-residential

Climate-zone based envelope characteristics (ASHRAE 90.1):

- Zone 1 (A,B)   • Zone 3 (A,B,C)   • Zone 5 (A,B,C)
- Zone 2 (A,B)   • Zone 4 (A,B,C)   • Zone 6 (A,B)

Reference envelope characteristics

Operational properties and schedules (ISO 18523-1 & 2):

Office	Residential, apartment, retired	Restaurant
Educational		Hospital
Day-care, kindergarten	Residential, apartment	Meeting room
Department store	Residential, detached	Shop
Restaurant	Attached spaces Library	Theatre
Hospital	Museum	
Religious	Sports and amusement	

Reference operational properties and schedules

(3) Cooling strategy selection and design/size

Cooling strategy categorization (IEA EBC Annex 80 - Subtask B):

Category A	Category B	Category C
• Solar shading and chromogenic glazing technologies • Cool envelope materials • Thermal energy storage systems including PCMs • Green roofs, roof ponds, green facades • Ventilated roofs and ventilated facades	• Absorption refrigeration including desiccant cooling • Ventilative cooling (NV & MV) • Adiabatic/evaporative cooling • Compression refrigeration • Ground source cooling • Sky radiative cooling • High temperature cooling system including radiant cooling	• Personal comfort systems

Scheme A:

Cooling strategy C_n; n=1,…,N

Design and size per city based on "*contemporary weather scenario*"

Scheme B:

Cooling strategy C_n; n=1,…,N

Design and size per city based on "*contemporary weather scenario*"

Design and size per city based on "*mid-future weather scenario*"

Design and size per city based on "*future weather scenario*"

(4) Performance indicators and comfort models

Climate data   Simulations

Outdoor air temperature ($T_{out,a,i}$)   Indoor operative temperature ($T_{in,o,z}$)

Ambient Warmness Degree (*AWD*)   Climate Change Overheating Resistivity (*CCOR*)   Indoor Overheating Degree (*IOD*)

Air conditioned   else   Mixed/Hybrid   else   Non-air conditioned   if   z = 1,…,Z   Thermal comfort limit ($T_{comf,z}$)

High expectancy   Energy-conservative

No   Sedentary activities   Yes   No   Adjustable clothing   Yes   No   Operable openings   No

PMV/PPD comfort model (ISO 17772-1: Cat I,II, III, and IV)   Adaptive comfort model (ISO 17772-1: Cat I,II, III, and IV)

Additional indicators (optional) e.g., *Exceedance Hours (EH), Degree hours (Dh), Weighted PPD (PPDw), Averaged PPD (AvgPPD), Heat Exposure Index (HEI), and other discomfort/overheating indicators.*
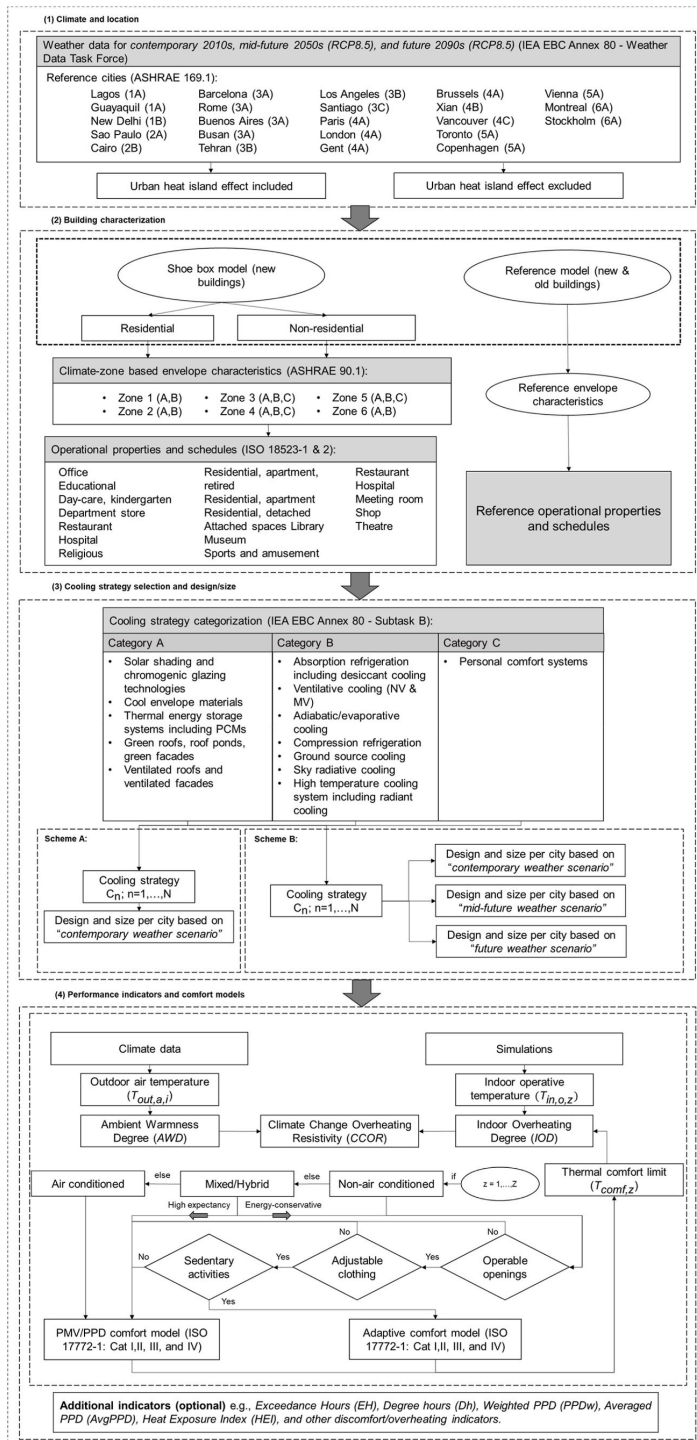
Fig. 2. The generic simulation-based framework to evaluate the climate change overheating resistivity of cooling strategies in buildings.

passive cooling strategies. The applicability of the selected cooling strategy in the target climates must be ensured while incorporating the different locations. Also, most active cooling systems have a life span of 15–25 years, depending on the type of the system and other contributing factors. Therefore, the framework allows for system adjustments through the long-term analysis period. It means that the cooling strategy characteristics can be changed in the mid-future and future scenarios.

Two schemes for cooling strategy adjustment is proposed within the framework. Scheme A: the C_n is designed or sized to provide an acceptable thermal environment in each reference city based on the *"contemporary weather scenario 2010s"* and is kept or replaced with the same for future scenarios, Scheme B: the C_n is adjusted at the end of its life span considering the changes in weather conditions, and thus is designed or sized based on future weather scenarios. In this case, it is possible to predict the thermal performance of the building if the cooling strategy design is not climate change-responsive (scheme A) or is climate change-responsive (scheme B).

Attaining the indoor thermal conditions always within the comfort limits can lead to oversizing the building cooling strategies. For the active strategies, the cooling strategy must be sized to summer design days. While for passive cooling strategies, the design should comply with the strict acceptable deviations criteria by Ref. [47]. It allows weekly 20%, monthly 12%, and yearly 3% deviations from the maximum comfort limits (Section 2.1.4.2) during the occupied hours. For mixed/hybrid mode cooling strategies, it is recommended that the building first operates via non-air conditioned cooling technology and use air conditioning to temper the weather extremes [48].

2.1.4. Step 4: specify performance indicators and comfort models

2.1.4.1. Performance indicators.
There are several metrics introduced in the standards and scientific literature to quantify the time-integrated overheating in buildings. The time-integrated overheating indices describe, in a synthetic way, the extend of discomfort over time and predict the uncomfortable phenomena. Those indicators were extensively reviewed by Refs. [49,50]. Following the recommendations of [49], a climate change-sensitive overheating calculation method developed by Ref. [14] is selected that fits the scope of the current paper. Hamdy et al. [49] introduced a methodology based on two principal indicators, namely, Indoor Overheating Degree (IOD) (for the indoor environment) and Ambient Warmness Degree (AWD) (for the outdoor environment).

The *IOD* metric provides a multi-zonal approach in the quantification of intensity and frequency of overheating risks in buildings. Such a multi-zonal approach allows the implementation of zonal thermal comfort models (i.e., PMV/PPD and adaptive models) and requirements (i.e., comfort categories). Therefore, it is possible to assign variable comfort models with regard to the cooling mode and occupant adaptation opportunities in different zones of a building. It also tracks the zonal occupancy profiles and therefore excludes the effect of unoccupied zones in overheating calculations. The *IOD* [°C] is the summation of positive values of the difference between zonal indoor operative temperature $T_{in,o,z}$ and the zonal thermal comfort limit $T_{comf,z}$ (PMV/PPD or adaptive comfort limits) averaged over the sum of the total number of zonal occupied hours $N_{occ}(z)$ [−],

$$IOD \equiv \frac{\sum_{z=1}^{Z}\sum_{i=1}^{N_{occ}(z)}\left[\left(T_{in,o,z,i} - T_{comf,z,i}\right)^{+} \times t_{i,z}\right]}{\sum_{z=1}^{Z}\sum_{i=1}^{N_{occ}(z)} t_{i,z}} \tag{2}$$

where t is the time step (1h), i is occupied hour counter [−], z is building zone counter [−], Z is total building zones [−].

The *AWD* [°C] metric is used to quantify the severity of outdoor thermal conditions by averaging the Cooling Degree hours (*CDh*) calculated for a base temperature (T_b) of 18 °C [14] over the total number of building occupied hours,

$$AWD \equiv \frac{\sum_{i=1}^{N}\left[\left(T_{out,a,i} - T_b\right)^{+} \times t_i\right]}{\sum_{i=1}^{N} t_i} \tag{3}$$

where $T_{out,a,i}$ is the outdoor dry-bulb air temperature and N is the total number of building occupied hours. Only the positive values of $\left(T_{out,a,i} - T_b\right)^{+}$ are taken into account in the summation.

In this paper, the Climate Change Overheating Resistivity (CCORF) metric is introduced to couple the outdoor and indoor environments quantifying the climate change overheating resistivity of cooling strategies in buildings. The *CCOR* [−] shows the rate of change in the *IOD* with an increasing *AWD* due to the impact of climate change. It can be calculated using the linear regression methods assuming linearity between the *IOD* and *AWD*,

$$\frac{1}{CCOR} = \frac{\sum_{Sc=1}^{Sc=M}\left(IOD_{Sc} - \overline{IOD}\right) \times \left(AWD_{Sc} - \overline{AWD}\right)}{\sum_{Sc=1}^{Sc=M}\left(AWD_{Sc} - \overline{AWD}\right)^{2}} \tag{4}$$

where *Sc* is the weather scenario counter, *M* is the total number of weather scenarios, and $\overline{IOD}$ and $\overline{AWD}$ are the average of total *IODs* and *AWDs*. *CCOR* > 1 means that the building is able to suppress the increasing outdoor thermal stress due to climate change, and *CCOR* < 1 means the building is unable to suppress increasing outdoor thermal stress due to climate change.

The framework is also open for the implementation of additional user-specific metrics such as Exceedance Hours (EH), Degree hours (Dh), Weighted PPD (PPDw) [47,51], Averaged PPD (AvgPPD) [52], Heat Exposure Index (HEI) [53], and other discomfort/overheating indicators.

2.1.4.2. Thermal comfort models.
The evaluation of overheating risks in buildings requires the determination of thermal comfort criteria. Thermal comfort defined as *"that condition of mind which expresses satisfaction with the thermal environment"* [52] has two main approaches: PMV/PPD (static) and adaptive.

The PMV/PPD comfort model assumes the human body as a passive recipient of its immediate environment [54], thus defining static thermal criteria. It has been shown that the PMV/PPD comfort model works well in air-conditioned spaces [55–57]. The framework suggests the use of the Category-based PMV/PPD model of [36] for the air-conditioned zones (Table 2).

The adaptive comfort model, however, allows a chance for occupant adaptation (e.g. operable openings, activity and clothing adjustments) and provides variable thermal comfort limits based on outdoor running mean temperature T_{rmo} [36],

$$T_{rmo} = (1-\alpha)\cdot\left\{T_{ed-1} + \alpha T_{ed-2} + \alpha^2 T_{ed-3+\ldots}\right\} \tag{1}$$

where α is reference value between 0 and 1, T_{ed-i} is daily mean outdoor air temperature for $i - th$ previous day [°C]. The adaptive comfort model presents a valuable alternative in an energy-constrained world and is recommended by most standards to non-air conditioned buildings [58, 59]. Therefore, the framework suggests the use of the Category-based adaptive comfort model of [36] for non-air conditioned zones (Table 3). In the adaptive comfort model, the occupants should have access to operable openings (e.g. windows, vents, and doors etc.) and

Table 2
PMV/PPD comfort model ranges by ISO 17772–1.

Categories	PPD [%] & PMV [−]
I (high-quality environment)	$PPD\% < 6$, $− 0.2 < PMV < + 0.2$
II (medium-quality environment)	$PPD\% < 10$, $− 0.5 < PMV < + 0.5$
III (moderate-quality environment)	$PPD\% < 15$, $− 0.7 < PMV < + 0.7$
IV (low-quality environment)	$PPD\% < 25$, $− 1.0 < PMV < + 1.0$

Table 3
Adaptive comfort model ranges by ISO 17772–1.

Categories	Upper limit [$^\circ C$]	Lower limit [$^\circ C$]	T_{rmo} range [$^\circ C$]
I (high-quality environment)	$0.33T_{rmo} + 18.8 + 2$	$0.33T_{rmo} + 18.8 - 3$	10–30
II (medium-quality environment)	$0.33T_{rmo} + 18.8 + 3$	$0.33T_{rmo} + 18.8 - 4$	10–30
III (moderate-quality environment)	$0.33T_{rmo} + 18.8 + 4$	$0.33T_{rmo} + 18.8 - 5$	10–30

mainly sedentary activities (~ 1.2 *met*). They should also be able to adjust their clothing.

Different categories reflect the expected indoor environmental quality [50]. Category I is recommended for the high level of expectancy that is expected by very sensitive and fragile occupants such as the elderly, very young, and sick. Category II corresponds to the normal level of expectation and should be used for new buildings and renovations. Category III is the acceptable and moderate level of expectation and may be used for existing buildings. Category IV (only for the PMV/PPD model) defines the out of the range values that can be accepted for a limited part of the year.

So far, there is no sufficient Internationally applicable comfort model for mixed/hybrid cooling operation mode [48]. For mixed/hybrid cooling mode zone, the framework suggests the selection of either PMV/PPD model (high levels of expectancy or vulnerability of occupants) or the adaptive comfort model (energy-conservative purposes). The comfort Category (I, II, III, and IV) should be selected depending on building typology, occupant expectation, and climate context.

2.2. Demonstration case

To test the framework, in this section a demonstration case is provied to compare the climate change overheating resistivity of two cooling strategies, 1) Variable Refrigerant Flow (VRF) unit coupled with Dedicated Outdoor Air Supply (DOAS) system, and 2) Variable Air Volume (VAV) system. Those strategies applied on a double-zone office building under the operation of two cooling technologies in six different locations/climates.

2.2.1. Simulation program

In this paper, the DesignBuilder software based on EnergyPlus v8.9 simulation engine is used to conduct the simulations. EnergyPlus is developed by the U.S. Department Of Energy (U.S. DOE) as one of twenty major building energy simulation programs to run the simulations [60]. EnergyPlus contains an integrated heat and mass balance module and a building system module. Zone heating and cooling loads are calculated based on heat balance method recommended by Ref. [61]. The calculated loads are then passed to building HVAC module to calculate heating and cooling system, plant, and electric system response [62]. The HVAC simulation results via EnergyPlus have shown a close agreement with well-known simulation tools such as TRNSYS, ESP-r, and DOE-2.1E [63,64]. The simulations' results are then post-processed using a MATLAB script to calculate the *IOD*, *AWD*, and *CCOR*.

2.2.2. Weather data

To demonstrate the first step of the framework, six cities are selected including New Delhi, Cairo, Buenos Aires, Brussels, Toronto, and Stockholm covering zones 1 to 6 in ASHRAE 169.1 climatic classification [31]. Heating and Cooling Degree Days (HDD10°C and CDD18°C) averaged over 2016–2020 for the selected cities are summarized in Table 4.

Three weather scenarios are generated for each city. *Scenario 01* is the TMY [65] weather data constructed based on the recorded data in

Table 4
Weather station location and climate characteristics of New Delhi, Cairo, Buenos Aires, Brussels, Toronto, and Stockholm (HDD10°C and CDD18°C averaged over 2016–2020).

City	Country	Coordinates (weather station)	Climate zone	HDD10°C	CDD18°C
New Delhi	India	28.6° N, 77.2° E	1B	24	3130
Cairo	Egypt	30.1° N, 31.3° E	2B	5	2327
Buenos Aires	Argentina	34.8° S, 58.5° W	3A	75	1034
Brussels	Belgium	50.9° N, 4.5° E	4A	780	258
Toronto	Canada	43.7° N, 79.4° W	5A	1630	494
Stockholm	Sweden	59.3° N, 18.1° E	6A	1501	171

each weather station. It includes the solar radiation values for 1996–2015 and other parameters (i.e. air temperature, dew-point temperature, wind speed, wind direction, and precipitation properties) for 2000–2019. *Scenario 02* and Scenario 03 are future weather projections based on RCP8.5 defined by IPCC Fifth Assessment Report (AR5) [66]. To generate the future weather data, a representative subset (10 out of 35) of CMIP5 models are used for averaging the weather parameters [67]. All weather files are derived from Meteonorm v8 which is a combination of climate database, spatial interpolation tool and a stochastic weather generator, with global radiation data obtained from the Global Energy Balance Archive (GEBA) [28,29].

2.2.3. Case study

The case study is assumed to be a double-zone office building formed by two adjacent identical zones (i.e., office room and administration room). Different comfort categories (i.e., comfort Category II and I) and operational conditions (i.e., occupancy density and heat loads by equipment) are considered for each zone. Each zone corresponds to the BESTEST 630 model [68]. It has east- and west- oriented windows (3 m $\times$ 2 m) with permanent solar shading devices (overhang and sidefins). The total building area is 96 m^2. The envelope characteristics are

Table 5
Building envelope characteristics for six cities (ASHRAE 90.1).

		Assembly maximum [W/m^2K]	Insulation Min. R-value [m^2K/W]
New Delhi	Roof	U-0.048	R-20 c.i.*
	Walls	U-0.089	R-13
	Floors	U-0.282	–
	Windows	U-0.45	–
Cairo	Roof	U-0.039	R-25 c.i.
	Walls	U-0.089	R-13
	Floors	U-0.033	R-30
	Windows	U-0.36	–
Buenos Aires	Roof	U-0.039	R-25 c.i.
	Walls	U-0.089	R-13
	Floors	U-0.033	R-30
	Windows	U-0.32	–
Brussels	Roof	U-0.029	R-35 c.i.
	Walls	U-0.058	R-13.0 + R-7.5 c.i.
	Floors	U-0.030	R-38.0
	Windows	U-0.32	–
Toronto	Roof	U-0.029	R-35 c.i.
	Walls	U-0.046	R-13.0 + R-12.5 c.i.
	Floors	U-0.030	R-38.0
	Windows	U-0.29	–
Stockholm	Roof	U-0.029	R-35 c.i.
	Walls	U-0.046	R-13.0 + R-12.5 c.i.
	Floors	U-0.024	R-38.0+ R-7.5 c.i.
	Windows	U-0.29	–

● Continuous insulation.

defined per city (climate zone) based on [33] and are summarized in Table 5. The case study is illustrated in Fig. 3.

The occupancy densities of 0.1 $person/m^2$ and 0.025 $person/m^2$ are set for the office room and the administration room. Heat gains by the lighting and appliances of 12 W/m^2 is considered for the office room. Heat gains by the lighting and appliances of 12 W/m^2 and 4 W/m^2 are assigned for the administration room. It is also assumed that the occupants have the generic winter 1 clo and summer 0.5 clo clothing, and metabolic rate of 1.2 met (sedentary activity). All the information regarding the lighting, equipment, and occupancy schedules can be found in Ref. [34].

2.2.4. Cooling strategies

2.2.4.1. VRF + DOAS system.
The first cooling strategy (C01) includes the Variable Refrigerant Flow (VRF) air-conditioning unit coupled with a Dedicated Outdoor Air Supply (DOAS). The VRF system uses an electric expansion valve and a variable-speed compressor to vary the refrigerant flow rate to each terminal unit to meet the zonal thermal loads. There are two types of VRF systems: Heat Pump (HP) and Heat Recovery (HR). In VRF-HP, all zones must be either in heating or cooling mode. In VRF-HR, the system is able to operate in the heating and cooling modes simultaneously. This paper applies VRF-HR system by default performance curves in the EnergyPlus such as the polynomial performance curve (VRFCoolCapFTBoundary) for the cooling capacity ratio boundary curve from the manufacturer's data [69]. The VRF-HR is implemented in v8.6. EnergyPlus and validated by Ref. [70]. The default input values are mostly used for the VRF-HR system as described in Table 6 [62,70]. However, some input values are modified in this study, including the increase of maximum outdoor air temperature in cooling only mode to 50°C to avoid the system disruption in the hot climates of New Delhi and Cairo. The Coefficient Of Performance (COP) values of 3.23 and 3.2 are set for cooling and heating, respectively, as minimum efficiency requirements [33,62]. The VRF-HR unit is operated by load priority master thermostat control type. It means that the total zone load is used to vary the zonal operating mode as being either heating or cooling. A Constant Air Volume (CAV) Air Handling Unit (AHU) is coupled to the VRF-HR system as DOAS to handle the latent loads and provide ventilation rates as per [36,71]. The input values for DOAS system are also presented in Table 6.

2.2.4.2. VAV system.
The second cooling strategy (C02) is Variable Air Volume (VAV) system that consists of an AHU and Air Distribution Units (ADUs). The supply air is heated or cooled with heating and cooling coils centrally in AHU and the thermal capacity is controlled by varying the supply air volume via the dampers installed in the zonal ADUs. At full cooling capacity, the damper is fully open and the fan operates at maximum speed to supply the maximum air flow rate. With decreasing the cooling demand, the damper closes until it reaches the zone minimum ventilation air requirements as per [36]. In this study, the default AHU is used for the VAV system which contains a variable speed fans. Such AHU supplies variable airflow at a constant temperature having additional precision in temperature control [72]. The VAV models in EnergyPlus have been validated by Ref. [73]. In this paper, the VAV system is modeled using mostly the default input values or the values derived from Refs. [62,74,75] as listed in Table 6.

For both C01 and C02, all thermal capacities and design flow rates are auto-sized to design days by EnergyPlus based on the reference cities' external design conditions and the building configuration. Assuming a non climate change-responsive design (scheme A), the cooling strategies are not re-sized for future climates. The C01 and C02 are schematically shown in Fig. 4. The two technologies are among widely available (TRL~9) and applicable cooling technologies for the selected climate zones [4,62].

2.2.5. Zonal comfort criteria

Two air conditioned cooling strategies are selected for the case study. Therefore, the PMV/PPD comfort model is considered for both zones [36]. A Distinct comfort categories for the office room and the administration room are considered. The comfort Category II is set for the office room due to the normal level of expectation that should be used for the new buildings [76]. It corresponds to a fixed maximum indoor operative temperature limit of 26°C. The minimum ventilation rate requirement for Category II is 1.4 l/s.m². Assuming a high level of expectation for the occupants in the administration room, the comfort Category I is selected for this zone. It corresponds to a fixed maximum indoor operative temperature limit of 25.5°C. The minimum ventilation rate requirement for Category I is 2 l/s.m². The cooling and heating
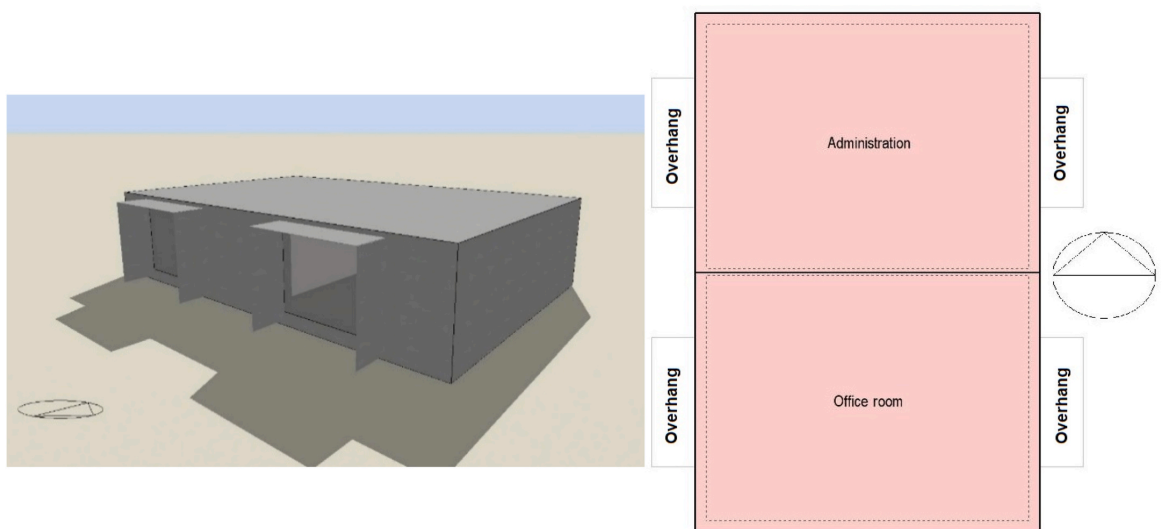

Fig. 3. The case study 3D view (left) and floor plan (right).

Table 6
The HVAC model inputs for C01 (VRF + DOAS) and C02 (VAV).

	C01 (VRF + DOAS)	C02 (VAV)
Set-points temperatures (occupied hours)	$24.5°C$ for cooling/$22°C$ for heating	$24.5°C$ for cooling/$22°C$ for heating
Set-back temperatures (unoccupied hours)	$26.6°C$ for cooling/$15.5°C$ for heating	$26.6°C$ for cooling/$15.5°C$ for heating
Minimum fresh air	1.4 l/s.m^2 (office room)/ 2 l/s.m^2 (Administration)	1.4 l/s.m^2 (office room)/ 2 l/s.m^2 (Administration)
Fuel type	Electricity	Electricity (cooling)/Gas (heating)
Defrost strategy/ capacity	Resistive/Auto-sized	N/A
Condenser type	Air-cooled	Air-cooled
Heating	VRF outdoor unit	Gas furnace inside the packaged air conditioning unit
Cooling	VRF outdoor unit	Air-cooled chiller inside the packaged air conditioning unit
Total cooling capacity	Auto-sized to design days per city	Auto-sized to design days per city
Cooling COP	3.23	3.39
Total heating capacity	Auto-sized to design days per city	Auto-sized to design days per city
Heating COP	3.20	0.8 (gas burner efficiency)
Minimum outdoor temperature in cooling mode	$-6°C$	N/A
Maximum outdoor temperature in cooling mode	$50°C$	N/A
Minimum outdoor temperature in heating mode	$-20°C$	N/A
Maximum outdoor temperature in heating mode	$40°C$	N/A
Indoor unit supply air flow rates	Auto-sized to design days per city	Auto-sized to design days per city
Indoor fan efficiency/ type/pressure rise	0.7/constant volume/100 pa	N/A
Indoor cooling coil	VRF DX cooling coil	N/A
Indoor heating coil	VRF DX heating coil	N/A
AHU type	CAV	VAV
AHU supply air flow rates	Auto-sized to design days per city	Auto-sized to design days per city
AHU fan efficiency/ type/pressure rise	0.7/constant volume/600 pa	0.7/variable volume/600 pa
Supply air set-point manager	Preheat coil: Always $5°C$	Air loop cooling: Always $14°C$
AHU cooling coil	N/A	Water cooling coil
AHU heating coil	Electric heating coil	Water heating coil

set-point temperatures of $24.5°C$ and $22°C$ are set, respectively [36].

3. Results

Following the instructions given by the framework (see Fig. 2), this section is allocated to show the results of totally 36 simulation cases which are the combination of two cooling strategies (C01 and C02) and three weather scenarios (2010s, 2050s, and 2090s) in six locations (New Delhi, Cairo, Buenos Aires, Brussels, Toronto, and Stockholm). The simulations are run for annual period to cover the overheating incidents in winter and intermediate seasons as well. It should be mentioned that the heating system performance and cold discomfort is not in the scope of the current study.

3.1. Outdoor thermal conditions

The annual distribution of hourly outdoor air temperature for Scenario 01, Scenario 02, and Scenario 03 are illustrated in Fig. 5. The

minimum, maximum, and average outdoor air temperature, Direct Normal Irradiance (DNI), Diffuse Horizontal Irradiance (DHI), $HDD10°C$, and $CDD18°C$ over the annual period as well as AWD are summarized in Table 7. The increase in average and maximum outdoor air temperature is about 2.97–$5.97°C$ and 3.5–$6.5°C$ for the six reference cities by 2090s. In the cooling-dominated climates of New Delhi and Cairo, the AWD increases by 23% and 30% in the 2090s. It corresponds to $CDD18°C$ variation of $+42\%$ and $+62\%$, respectively, and $HDD10°C$ tends to be zero in the future (i.e., 2050s and 2090s). New Delhi has the highest average and maximum outdoor air temperature of $29.15°C$ and $49.9°C$, and has the highest AWD of $14.87°C$ in the 2090s. In the heating-dominated climates of Toronto and Brussels, both are expected to shift to cooling-dominated zones by increasing 248% and 224% in CDD18 °C and a decrease of 59% and 56% in $HDD10°C$ by 2090s, respectively. In Toronto, higher maximum outdoor air temperature of around 2–$4.1°C$ and higher $CDD18°C$ of around 208–643 are resulted compared to Brussels. Therefore, Toronto shows higher AWD by $1.32°C$ in the 2010s, $2.7°C$ in the 2050s, and $3.89°C$ in the 2090s than in Brussels. Toronto has the highest increase in average outdoor air temperature by $5.97°C$, maximum outdoor air temperature by $6.5°C$, and AWD by $4.06°C$ in the 2090s. In Stockholm, although the $CDD18°C$ increases by 313% in the 2090s, it still remains as a heating-dominated city with $HDD10°C$ of 824 and $CDD18°C$ of 413. Stockholm has the lowest average and maximum outdoor air temperature of $7.53°C$ and $30.20°C$ and therefore has the lowest AWD of $3.84°C$ in the 2010s.

3.2. Indoor operative temperature and exceedance hours (EH)

Fig. 6 shows the distribution of annual indoor operative temperature and Exceedance Hours (EH) (additional indicators) over the cooling set-point of $24.5°C$ in the office room and the administration room. The maximum indoor operative temperature fixed thresholds of $25.5°C$ of Category I (administration room) and $26°C$ of Category II (office room) are illustrated based on the static comfort model of ISO 17772–1. Table 8 summarizes the IOD, maximum indoor operative temperature, and EH for each scenario in six cities under the operation of C01 and C02.

In this study, the highest maximum indoor operative temperature of $34.98°C$ and the highest increase in maximum indoor operative temperature of $6.91°C$ are resulted for Toronto by 2090s. The highest EH of 625 and the highest increase in EH of 576 are also calculated for Toronto during the same period. It is due to the fact that, first, even though Toronto is classified as cool-humid climate (5A), more extreme up to $40.60°C$ and frequent hot weather conditions are expected by 2090s (similar to Buenos Aires) (see Table 7). Second, in line with the findings of [14,77], higher insulation levels in Toronto based on ASHRAE 90.1 requirements exacerbate the intensity and frequency of high indoor temperatures.

The ranges of the maximum indoor operative temperature difference between the office room and the administration room are 0.96–$1.98°C$ for C01 and 0.63–$2.07°C$ for C02. The ranges of the difference between the EH in the office room and the administration room are 16–143 for C01 and 19–131 for C02. The office room experiences higher maximum indoor operative temperatures and more overheating hours than the administration room. It is normal because of the higher internal gains by the office equipment and the higher number of occupants. However, the C01 shows more consistent zonal temperature control and therefore lower zonal temperature gradients [73]. The difference in the number of exceedance hours among the office room and administration room increases with global warming up to 346% (in Cairo). As a result, the office room is expected to have a relatively higher increase in the frequency of high indoor temperatures than the administration room due to climate change.

The C01 shows a lower maximum indoor operative temperature by 0.5–$2.74°C$ in the office room (except for New Delhi) and 0.5–$2.67°C$ in the administration room than C02. It shows that the C01 performs better
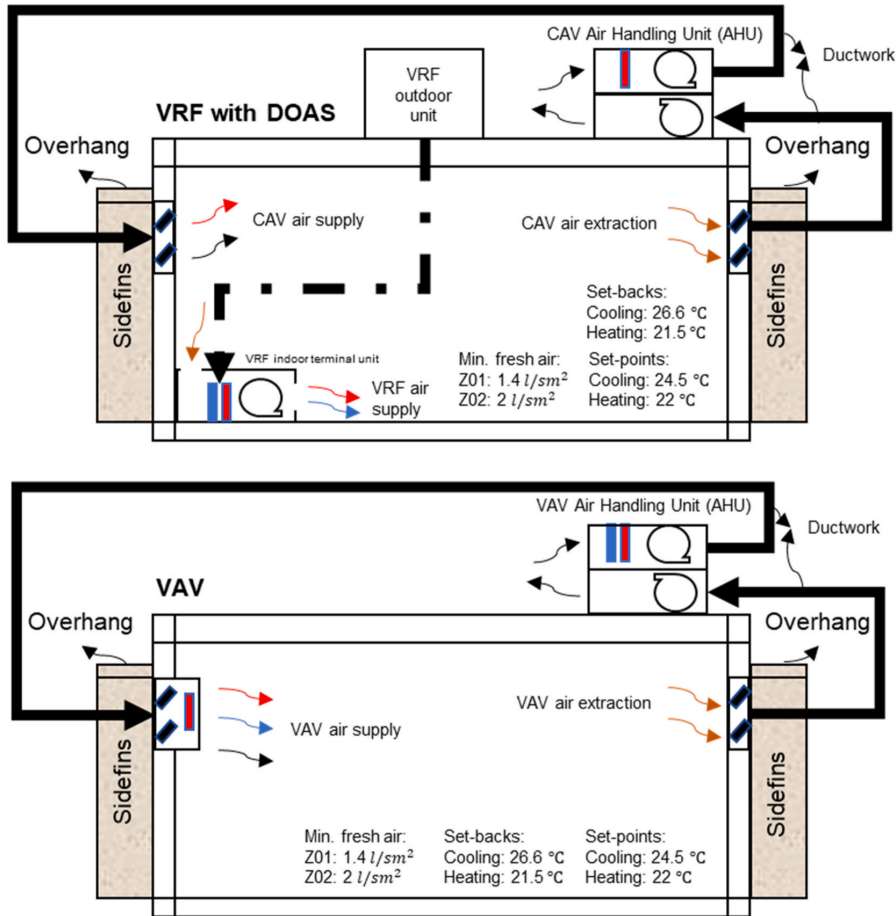
Fig. 4. Graphical representation of C01 (VRF with DOAS) (upper) and C02 (VAV) (lower).

in dampening the maximum indoor operative temperatures. The C01 results in higher *EH* between 1 and 56 (in office room) and 3–82 (in administration room) in relatively warmer climates of New Delhi, Cairo, and Buenos aires. However, the C02 shows lower *EH* between 2 and 57 (in office room) and 2–122 (in administration room) in Brussels, Toronto, and Stockholm. Both the above differences regarding the maximum indoor operative temperature and *EH* between the C01 and C02 increase with global warming. Overall, C01 performs better in reducing the maximum indoor operative temperatures in all climates and *EH* in Brussels, Toronto and Stockholm. At the same time, C02 has better performance in reducing the *EH* in New Delhi, Cairo, and Buenos Aires.

3.3. Overheating risk and climate change overheating resistivity

This section presents the results of the Indoor Overheating Risk (IOD) and Climate Change Overheating Resistivity (CCOR) of the selected cooling strategies. The *IOD* represents the intensity and frequency of overheating in buildings considering zonal comfort criteria. The *CCOR* quantifies the increase in the *IOD* corresponding to an increase in the *AWD*. Fig. 7 shows the linear regression models representing *IOD* as *AWD*. It shows a direct correlation between *IOD* and *AWD*; that is, when the *AWD* increases, overheating risk increases as well. The climate

scenarios, namely 2010s, 2050s, and 2090s are represented by their *AWD* in each city.

Fig. 7 shows that the overheating conditions are becoming more intense and frequent with the increase of *AWD*. Since the C01 and C02 are sized to design days based on the *"Contemporary weather scenario 2010s"*, very low *IOD* values between 0.005 and 0.012 are calculated for this scenario.

In this study, the highest value of *IOD* $0.46°C$ is calculated for Toronto by 2090s associated with the maximum indoor operative temperature of $34.98°C$ and the *EH* of 589 under the operation of C02. It means that the current building configuration (i.e., the envelope complying with ASHRAE 90.1 standard and C02 as the cooling strategy) in Toronto is expected to have the highest risk of overheating in the future. In all cases, with the continuation of global warming the difference of *IOD* between C01 and C02 increases, especially in Brussels, Toronto, and Buenos Aires where higher differences up to 0.182 are observed. It shows that C02 is more affected by climate change than C01.

The *CCOR* values vary between 9.24 and 37.46 depending on the city and cooling strategy. However, it is > 1 for all cases. It shows that the cooling strategies (C01 and C02) selected and sized for the current weather conditions will be able to maintain an acceptable thermal environment and suppress global warming [14]. It is normal since the case study is equipped with active cooling systems, making it more
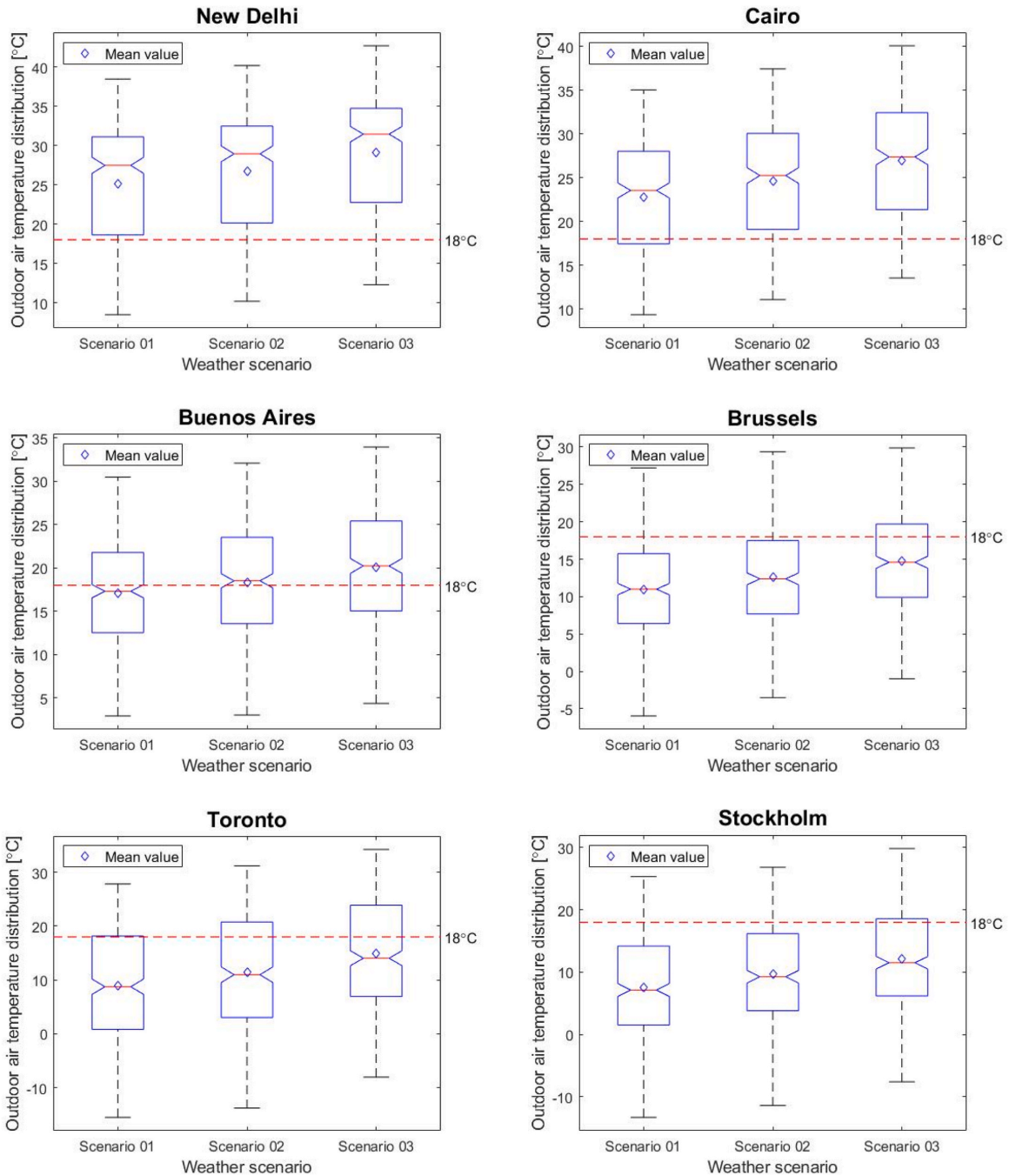
Fig. 5. Distribution of annual outdoor air temperature for Scenario 01 (2010s), Scenario 02 (2050s), and Scenario 03 (2090s).

resistant to climate change impacts but with different levels of success. The case study with C02 in Toronto has the lowest *CCOR* of 9.24 representing the case that affected most by climate change. On the other hand, the case study with C01 in Brussels has the highest *CCOR* of 37.46 and therefore is the most resistant case in this paper. In the analysis, the

C01 always has higher *CCOR* values than C02, showing its superior resistance toward climate change. Especially in relatively cold climates of Brussels, Toronto, and Stockholm, the differences between the *CCOR* values among C01 and C02 are 19.16, 6.04, and 14.41, respectively. It was shown that most design variants such as internal heat gain, building

Table 7
Summary of average, minimum, and maximum outdoor air temperature, Direct Normal Irradiance (DNI), Diffuse Horizontal Irradiance (DHI), HDD10°C, CDD18°C, and AWD for three scenarios in all cities.

		Scenario 01	Scenario 02	Scenario 03
New Delhi	$T_{out.ave}$ [°C]	25.11	26.65	29.15
	$T_{out.max}$ [°C]	44.90	46.80	49.9
	$T_{out.min}$ [°C]	3.70	5.30	7.50
	DNI [W/m^2]	166.93	147.47	142.28
	DHI [W/m^2]	99.08	100.75	102.71
	AWD [°C]	12.12	13.05	14.87
	$HDD10°C$	2.51	0	0
	$CDD18°C$	2911	3355	4149
Cairo	$T_{out.ave}$ [°C]	22.80	24.63	26.99
	$T_{out.max}$ [°C]	41.80	44	46.9
	$T_{out.min}$ [°C]	5.60	7.40	9.30
	DNI [W/m^2]	185.36	176.62	179.95
	DHI [W/m^2]	94.24	96.88	95.69
	AWD [°C]	9.39	10.59	12.16
	$HDD10°C$	1	0	0
	$CDD18°C$	2052	2581	3325
Buenos Aires	$T_{out.ave}$ [°C]	17.11	18.33	20.08
	$T_{out.max}$ [°C]	37.50	39.10	41
	$T_{out.min}$ [°C]	−2.70	−1.70	−0.50
	DNI [W/m^2]	198.75	189.61	187.88
	DHI [W/m^2]	77.53	80.43	82.12
	AWD [°C]	6.49	7.40	8.42
	$HDD10°C$	135	109	55
	$CDD18°C$	777	1048	1446
Brussels	$T_{out.ave}$ [°C]	10.93	12.58	14.70
	$T_{out.max}$ [°C]	32.10	33.90	36.50
	$T_{out.min}$ [°C]	−7	−5.70	−3.40
	DNI [W/m^2]	101.95	115.44	117.58
	DHI [W/m^2]	65.94	65.03	66.47
	AWD [°C]	3.64	4.59	5.13
	$HDD10°C$	804	572	325
	$CDD18°C$	134	264	467
Toronto	$T_{out.ave}$ [°C]	8.99	11.40	14.96
	$T_{out.max}$ [°C]	34.10	36.60	40.60
	$T_{out.min}$ [°C]	−18.90	−16.40	−11.10
	DNI [W/m^2]	138.58	143.01	141.83
	DHI [W/m^2]	71.80	72.68	73.30
	AWD [°C]	4.96	7.29	9.02
	$HDD10°C$	1794	1405	782
	$CDD18°C$	342	663	1110
Stockholm	$T_{out.ave}$ [°C]	7.53	9.63	12.20
	$T_{out.max}$ [°C]	30.20	32.10	34.60
	$T_{out.min}$ [°C]	−15.70	−13.30	−10.60
	DNI [W/m^2]	130.22	133.42	138.46
	DHI [W/m^2]	53.30	54	52.31
	AWD [°C]	3.84	4.53	5.96
	$HDD10°C$	1742	1280	824
	$CDD18°C$	100	189	413

archetype, construction period, orientation, solar shading option are not key aspects to describe the resistivity to climate change [14]. However, the study shows that the selection of the active cooling system has a sound effect in determining the comfort conditions in buildings in the future. The relative potential to adapt to climate change metric P is quantified via the difference between the IOD resulted by C01 and C02 in the 2090s ($IOD_{C01,2090s}$ - $IOD_{C02,2090s}$)$^+$ over the Max [$IOD_{C01,2090s}$, $IOD_{C02,2090s}$] [14]. By calculating the P, the C02 shows to have 13%, 29%, 8%, 51%, 39%, and 49% more potential to adapt compared to C01

in New Delhi, Cairo, Buenos Aires, Brussels, Toronto, and Stockholm, respectively.

4. Discussion

4.1. Findings and recommendations

More intense and frequent overheating events are expected with the continuation of global warming. Comparative building performance simulations seek to evaluate different strategies or measures in buildings concerning climate change with identical boundary conditions. Therefore, a generic simulation-based framework is developed that allows performing a relative comparison of individual or multiple cooling technologies in the frame of the (IEA) EBC Annex 80 – "Resilient cooling of buildings" project. The framework considers all function types (i.e., residential and non-residential), comfort categories (i.e., I, II, III, and IV), and cooling strategies (i.e., conditioned air, non-conditioned air, and mixed/hybrid mode). And, the selection of weather data and comfort criteria are based on unique approaches for climate change overheating resistivity evaluations in buildings.

Through the efforts to assign the building models in the framework, it was found that while in the North America especially in the United States, the creation of benchmark building models has consistently evolved [78–80], it is a recently emerging concept in other regions [39, 40,43,81]. For example, after introducing the Energy Performance of Building Directive (EPBD) in Europe in 2003 which was implemented after in 2008, the projects such as the TABULA and the EPISCOPE started to create a central and structured depository of building stocks. However, there is still a substantial knowledge gap in the reliable benchmark models for different building typologies, vintages, and functions. Therefore, the framework is open to the implementation of the shoe box models for basic early design decisions and reference models for more sophisticated analyses.

The framework uses IOD, AWD, and $CCOR$ as principal indicators to calculate the indoor overheating risk, the severity of the outdoor thermal environment, and climate change overheating resistivity of cooling strategies in buildings. The IOD metric allows a multi-zonal approach representing the real situations in buildings including zones with variable thermal comfort models (i.e., PMV/PPD and adaptive models) and requirements (e.g., comfort categories) tracing the occupied hours in each zone of the building (Section 2.1.4.2). Therefore, the framework is flexible and allows for personalization to evaluate cooling strategies under real and artificial conditions at zone levels. The AWD is a useful metric to quantify the severity of outdoor thermal conditions. However, it does not take into account the effect of solar radiation. As a result, it underestimates the severity of the outdoor thermal environment during the days with high solar radiation and low air temperatures.

The proposed methodology is tested by comparing C01 (VRF unit with DOAS) and C02 (VAV system) cooling strategies on a double-zone (i.e., office room and administration room) shoe box model in New Delhi, Cairo, Buenos Aires, Brussels, Toronto, and Stockholm (Section 2.2). Both systems are able to suppress the outdoor warming conditions by the end of this century. The C01 showed reduced maximum indoor operative temperature as well as EH compared to C02 leading to lower overheating risks (Table 8) and higher climate change overheating resistivity (Fig. 7). It shows that the C02 system is more prone to outdoor temperature increase and thus has less potential to overcome the climate change impacts. Although the VAV system cooling capacity can be increased by an increase in the amount of inlet air or by decreasing the inlet air temperature, it can lead to droughts and cold discomfort due to excessively high air velocities associated with low air temperatures [82]. The superior performance of C01 over C02 is more evident in Brussels, Toronto, and Stockholm. However, it should be mentioned that in this paper, a maximum temperature of 50°C is set as the temperature above the VRF system does not operate. Such assumption ensures the operation of the VRF system throughout the year in the selected reference cities
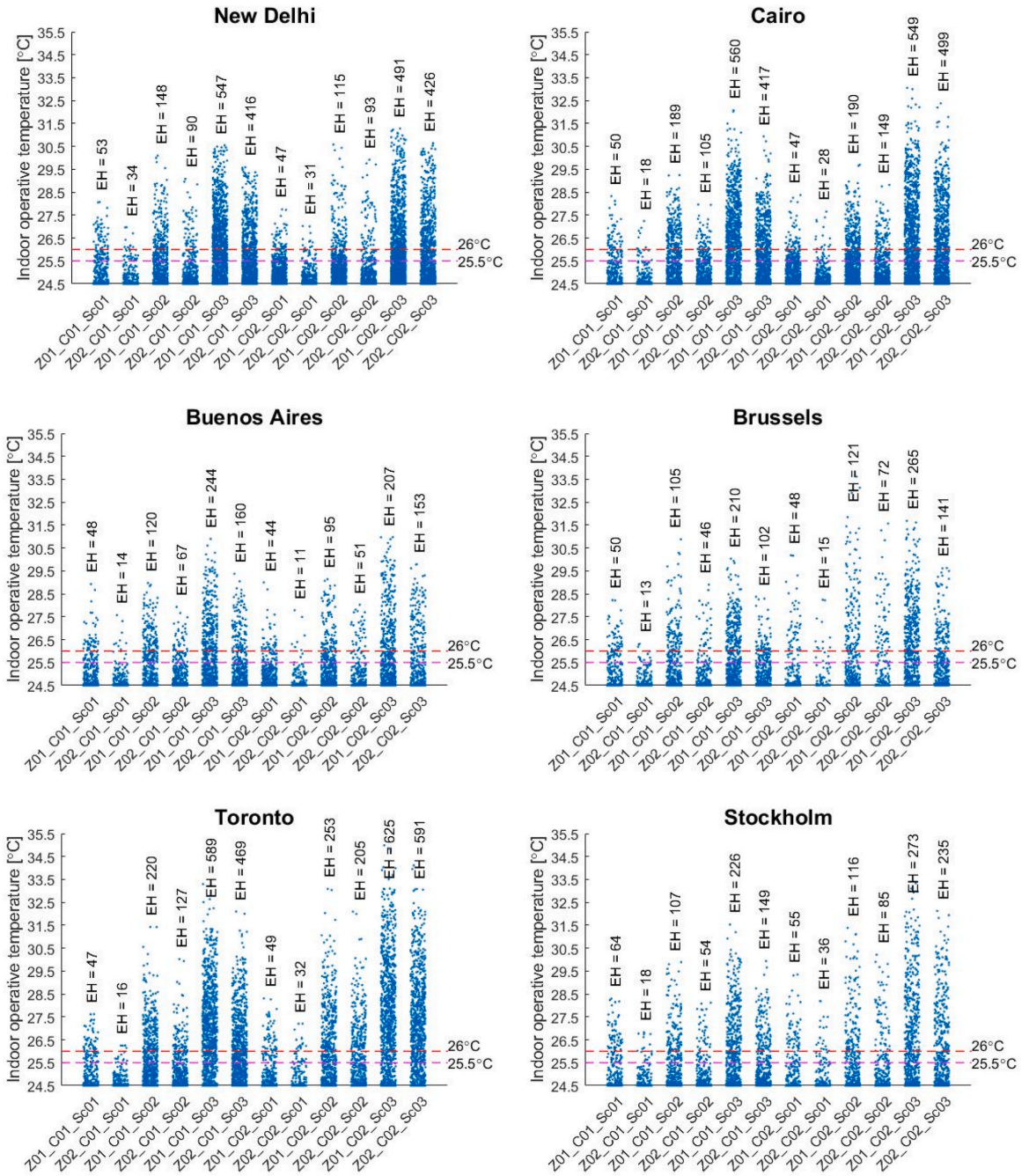
Fig. 6. Annual distribution of indoor operative temperature over cooling set-point of 24.5°C in office room and administration room for C01 and C02 during the occupied hours. The maximum indoor operative temperature threshold of 25.5°C is assigned for comfort Category I (administration room) and 26°C for Category II (office room). Exceedance Hours (EH) are shown for each zone per cooling strategy per scenario.

considering the weather data used in this study. Also, a previous study by Ref. [73] showed the energy-saving potential of the VRF system between 14 and 39% over the VAV system in all climatic zones across the U.S. Consequently, the VRF unit with DOAS seems to offer better performance in comparison to the VAV system in both energy-saving and thermal comfort aspects.

To summarize the significant recommendations, the list below is provided:

Table 8

Summary of IOD, exceedance hours, and maximum indoor operative temperature during occupied hours in the office room and the administration room.

			C01		C02	
			Office room (Z01)	Administration room (Z02)	Office room (Z01)	Administration room (Z02)
New Delhi	Scenario 01	IOD [$°C$]	0.0075		0.0058	
		EH [$-$] ($T_{i,max}$) [$°C$]	47 (28.07)	31 (26.97)	53 (27.75)	34 (27.02)
	Scenario 02	IOD [$°C$]	0.0362		0.0361	
		EH [$-$] ($T_{i,max}$) [$°C$]	115 (30.09)	93 (29.07)	148 (30.58)	90 (29.91)
	Scenario 03	IOD [$°C$]	0.1891		0.2162	
		EH [$-$] ($T_{i,max}$) [$°C$]	491 (30.54)	426 (29.58)	547 (31.27)	416 (30.64)
Cairo	Scenario 01	IOD [$°C$]	0.0066		0.0075	
		EH [$-$] ($T_{i,max}$) [$°C$]	50 (28.32)	18 (27.24)	47 (28.37)	28 (27.65)
	Scenario 02	IOD [$°C$]	0.0357		0.0447	
		EH [$-$] ($T_{i,max}$) [$°C$]	189 (29.24)	105 (27.96)	190 (29.69)	149 (28.81)
	Scenario 03	IOD [$°C$]	0.2087		0.2946	
		EH [$-$] ($T_{i,max}$) [$°C$]	560 (32.07)	417 (30.93)	549 (33.05)	499 (32.37)
Buenos Aires	Scenario 01	IOD [$°C$]	0.0063		0.0050	
		EH [$-$] ($T_{i,max}$) [$°C$]	44 (28.92)	11 (27.57)	48 (28.99)	14 (27.78)
	Scenario 02	IOD [$°C$]	0.0235		0.0229	
		EH [$-$] ($T_{i,max}$) [$°C$]	95 (28.97)	51 (27.93)	120 (29.13)	67 (28.02)
	Scenario 03	IOD [$°C$]	0.0792		0.0862	
		EH [$-$] ($T_{i,max}$) [$°C$]	207 (30.89)	153 (29.37)	244 (30.97)	160 (29.78)
Brussels	Scenario 01	IOD [$°C$]	0.0055		0.0107	
		EH [$-$] ($T_{i,max}$) [$°C$]	48 (28.22)	15 (26.31)	50 (30.18)	13 (28.24)
	Scenario 02	IOD [$°C$]	0.0261		0.0544	
		EH [$-$] ($T_{i,max}$) [$°C$]	121 (30.87)	72 (28.89)	105 (33.61)	46 (31.56)
	Scenario 03	IOD [$°C$]	0.0461		0.0935	
		EH [$-$] ($T_{i,max}$) [$°C$]	265 (30.03)	141 (28.37)	210 (31.68)	102 (29.61)
Toronto	Scenario 01	IOD [$°C$]	0.0046		0.0081	
		EH [$-$] ($T_{i,max}$) [$°C$]	49 (27.62)	32 (26.25)	47 (28.30)	16 (27.20)
	Scenario 02	IOD [$°C$]	0.0558		0.1087	
		EH [$-$] ($T_{i,max}$) [$°C$]	253 (31.42)	205 (30.02)	220 (33.08)	127 (32.09)
	Scenario 03	IOD [$°C$]	0.2810		0.4636	
		EH [$-$] ($T_{i,max}$) [$°C$]	625 (33.29)	591 (32.09)	589 (34.98)	469 (34.11)
Stockholm	Scenario 01	IOD [$°C$]	0.0088		0.0122	
		EH [$-$] ($T_{i,max}$) [$°C$]	55 (28.29)	36 (26.82)	64 (29.34)	18 (28.19)
	Scenario 02	IOD [$°C$]	0.0259		0.0461	
		EH [$-$] ($T_{i,max}$) [$°C$]	116 (29.88)	85 (28.11)	107 (31.38)	54 (30.21)
	Scenario 03	IOD [$°C$]	0.0819		0.1602	
		EH [$-$] ($T_{i,max}$) [$°C$]	273 (31.53)	235 (29.93)	226 (33.33)	149 (32.12)

● It is recommended to use the proposed framework to assess the indoor overheating risks in buildings and conduct comparative studies on the climate change overheating resistivity of different cooling strategies in buildings.

● It is also recommended to implement *IOD*, *AWD*, and *CCOR* as three principal indicators in climate change sensitive overheating evaluations. Designers and decision-makers can use these indicators for a multi-zonal comparison of building designs and their cooling strategies in the context of climate change.

● It is recommended to include additional weather files with intermediate periods (e.g., 2030s, 2040s, 2060s, etc.), which contributes to the CCOR's accuracy as the inverse slope of the linear regression line between the *IOD* and the *AWD*.

● It is recommended to further explore the potential of the VRF unit coupled with the DOAS as a promising strategy in enhancing the resistivity of buildings against overheating impacts of climate change.

4.2. Strength and limitations

There is an ongoing concern regarding the overheating risks that will be encountered more in future climates. There is no common guidance so far for evaluating the climate change overheating resistivity of cooling strategies to overcome the potential overheating issues in buildings. For this aim, the paper develops a comprehensive framework that can be followed step by step to compare the climate change overheating resistivity of a wide range of cooling strategies in buildings. The first strength of the study relies on the strong intellectual support via long-lasting brainstorming sessions by the members of (IEA) EBC Annex 80 – "Resilient cooling of buildings" project. The study provides a well-established framework based on universally applicable standards and state-of-the-art methods. This paper also provides the basis to compare different cooling strategies worldwide. The study's strength also relates to the implementation of a multi-zonal and climate change sensitive approach in the quantification of overheating risk as well as quantification of climate change overheating resistivity of cooling strategies. The proposed framework is also tested by comparing the C01 (VRF with DOAS) and C02 (VAV) cooling strategies in six reference cities. Despite the numerous previous studies on both above systems [83–87], there is no comparative study on their impact on the climate change overheating resistivity with detailed information on the system design and sizing.

However, the study has some limitations. First, this paper considers a shoe box model as the case study due to the restrictions in obtaining region-specific reference models. Second, the focus was on the thermal
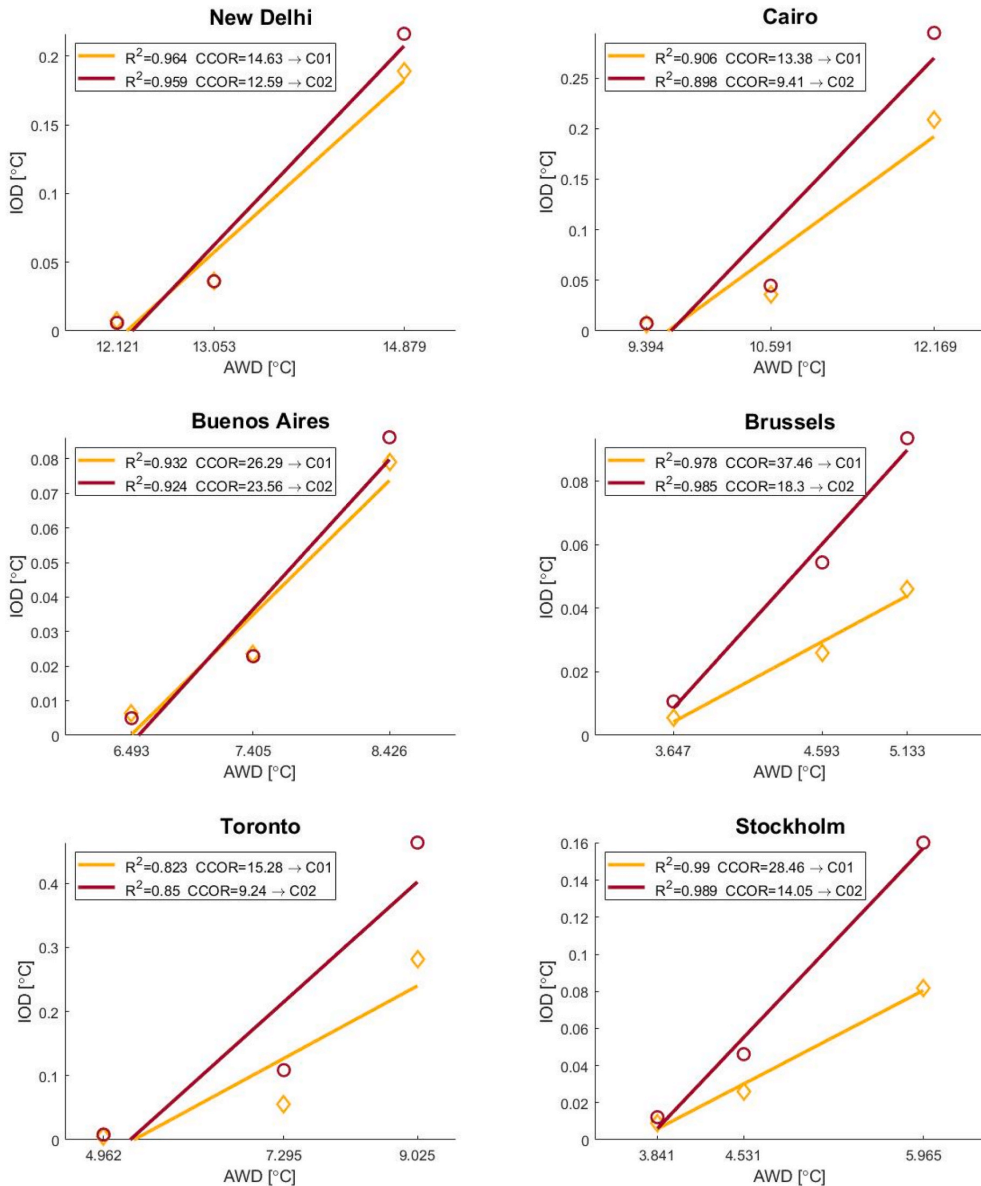
Fig. 7. IOD versus AWD. The slope of the regression line inverse shows the CCOR per city per cooling strategy.

comfort aspect, neglecting the energy performance of the selected cooling strategies. Third, spatial, cultural, and occupant behavioural differences are not considered in the selected cities to accurately define simulation parameters such as clothing factor, metabolic rate, control strategies, etc. Fourth, the weather data applied in the current study are generated using an autoregressive model very similar to the morphing technique [88]. It means that the same weather events are assumed to occur in the future in the same way as they do under the current climate, with the only difference being a linear shift in temperature throughout the year. Fourth, the effect of heat stress is not only dependent on air temperature or operative temperature. Considerations for relative humidity and other comfort parameters such as clothing factor, metabolic

rate, and air velocity are also important in determining thermal comfort. Those parameters are neglected within the evaluation framework of the current study. Therefore, more accurate studies are suggested to overcome the limitations of this paper.

4.3. Implication on practice and future research

One of the implications of the current work is to interpret and include the proposed framework and recommendations in future revisions of national, regional, or local building regulations. Most regulations, such as the EPBD in Europe, do not provide a straightforward method to assess the indoor overheating risk and have no considerations for

climate change. Consequently, the indoor overheating risks arising from global warming are undermined in building designs. Also, the study establishes the foundation for the experts of the field such as the members of (IEA) EBC Annex 80 – "Resilient cooling of buildings" project to compare the resilient cooling strategies in different climate zones worldwide. The results will be communicated publicly to disseminate knowledge and raise community awareness to adapt the buildings to worsening outdoor conditions.

As some areas of the framework yet remain undemonstrated, some potential research recommendations are provided. First, future research is recommended to incorporate other reference cities specified in the framework using more accurate and reliable weather files. Second, even though the use of multi-zonal shoe box models provides preliminary but valuable insights into the performance of cooling strategies in a simple and fast way, the future research is recommended to apply real residential and non-residential reference building models developed for local, provincial or national building stocks for more realistic evaluations. Third, through the demonstration case in this paper, only the performance of two active cooling systems are compared. Therefore, future research is recommended to use the framework for the evaluation of other active cooling strategies and passive cooling strategies (see Section 2.1.3) as well as their combinations. Forth, future studies are suggested to implement additional discomfort/overheating indices besides the primary ones (i.e., *IOD*, *AWD*, and *CCOR*) to complement the overheating assessments.

In addition to the research recommendations on undemonstrated parts of the framework, future research is recommended to improve the performance indices suggested by the framework (i.e., *IOD* and *AWD*). The new metric for the indoor environment and occupant comfort should include more comfort parameters such as relative humidity, metabolic rate, clothing factor, and air velocity to better reflect the occupant's thermal sensation. At the same time, the new metric for the outdoor environment should include more outdoor thermal parameters such as solar radiation, relative humidity, etc. Future research is also encouraged to define a well-defined post-processing procedure to establish sensitivity and optimization analysis. It further extends the functionality of the current framework to optimize the cooling strategies for the buildings in different typologies and climates.

5. Conclusion

In this paper, a generic simulation-based framework is developed to evaluate the climate change overheating resistivity of cooling strategies in varying climates. Following the framework yields consistent results contributing to comparative studies among cooling strategies. The framework requires four key decisions: 1) specify weather data characterization (Section 2.1.1), 2) identify building characterization (Section 2.1.2), 3) identify and design/size the cooling strategies to be compared (Section 2.1.3), and 4) specify performance indicators and comfort models (Section 2.1.4). 23 cities are suggested as reference cities worldwide based on the rate of growth and population covering zones 1 to 6 in ASHRAE 169.1 classification. The framework considers all function types (i.e., residential and non-residential), comfort categories (i.e., I, II, III, and IV), cooling strategies (i.e., conditioned air, non-conditioned air, and mixed/hybrid mode). Three metrics are implemented namely, Indoor Overheating Degree (IOD), Ambient Warmness Degree (AWD), and Climate Change Overheating Resistivity (CCOR) allowing for a multi-zonal approach in the quantification of intensity and frequency of overheating during the zonal occupied hours.

Subsequently, the framework is tested by comparing sufficiently-sized VRF unit with DOAS and VAV cooling strategies in New Delhi, Cairo, Buenos Aires, Brussels, Toronto, and Stockholm. It was concluded that the VRF unit with DOAS results in reduced maximum indoor operative temperature and Exceedance Hours (EH) compared to VAV system. More importantly, the results showed that the building equipped with the former are more resistant to overheating impact of climate. It

should be mentioned that the demonstration case is aimed to show that the framework is working well in conducting a universal comparison among cooling strategies. The validation of the results achieved in this study is required by using the framework in real multi-zonal reference buildings by using more reliable and accurate future climate data.

Declaration of competing interest

The authors declare that they have no known competing financial interests or personal relationships that could have appeared to influence the work reported in this paper.

References

[1] S. Attia, et al., Resilient cooling of buildings to protect against heat waves and power outages: key concepts and definition, Energy Build. (Mar. 2021) 110869, https://doi.org/10.1016/j.enbuild.2021.110869.

[2] H. Hooyberghs, S. Verbeke, D. Lauwaet, H. Costa, G. Floater, K. De Ridder, Influence of climate change on summer cooling costs and heat stress in urban office buildings, Climatic Change 144 (4) (Oct. 2017) 721–735, https://doi.org/10.1007/s10584-017-2058-1.

[3] R. Khosla, et al., Cooling for sustainable development, Nat. Sustain 4 (3) (2021) 201–208, https://doi.org/10.1038/s41893-020-00627-w.

[4] C. Zhang et al., "Resilient cooling strategies- a critical review and qualitative assessment," *Energy Build.* , In press., 2021.

[5] U. Berardi, P. Jafarpur, Assessing the impact of climate change on building heating and cooling energy demand in Canada, Renew. Sustain. Energy Rev. 121 (2020) 109681, https://doi.org/10.1016/j.rser.2019.109681.

[6] J. Izar-Tenorio, P. Jaramillo, W.M. Griffin, M. Small, Impacts of projected climate change scenarios on heating and cooling demand for industrial broiler chicken farming in the Eastern US, J. Clean. Prod. 255 (2020) 120306, https://doi.org/10.1016/j.jclepro.2020.120306.

[7] M.A.D. Larsen, S. Petrović, A. Radoszynski, R. McKenna, O. Balyk, Climate change impacts on trends and extremes in future heating and cooling demands over Europe, Energy Build. 226 (2020) 110397, https://doi.org/10.1016/j.enbuild.2020.110397.

[8] W. Luan, X. Li, Rapid urbanization and its driving mechanism in the Pan-Third Pole region, Sci. Total Environ. 750 (Jan. 2021) 141270, https://doi.org/10.1016/j.scitotenv.2020.141270.

[9] A. O' Donovan, M.D. Murphy, P.D. O'Sullivan, Passive control strategies for cooling a non-residential nearly zero energy office: simulated comfort resilience now and in the future, Energy Build. 231 (Jan. 2021) 110607, https://doi.org/10.1016/j.enbuild.2020.110607.

[10] G. Chiesa, A. Zajch, Contrasting climate-based approaches and building simulations for the investigation of Earth-to-air heat exchanger (EAHE) cooling sensitivity to building dimensions and future climate scenarios in North America, Energy Build. 227 (2020) 110410, https://doi.org/10.1016/j.enbuild.2020.110410.

[11] J.M. Rey-Hernández, C. Yousif, D. Gatt, E. Velasco-Gómez, J. San José-Alonso, F. J. Rey-Martínez, Modelling the long-term effect of climate change on a zero energy and carbon dioxide building through energy efficiency and renewables, Energy Build. 174 (2018) 85–96, https://doi.org/10.1016/j.enbuild.2018.06.006.

[12] A. Ibrahim, S.L. Pelsmakers, Low-energy housing retrofit in North England: overheating risks and possible mitigation strategies, Build. Serv. Eng. Technol. 39 (2) (Mar. 2018), https://doi.org/10.1177/0143624418754386. Art. no. 2.

[13] W. Feist, B. Kaufmann, J. Schnieders, O. Kah, Passive House Planning Package, Passive House Institute, Darmstadt, Germany, 2015.

[14] M. Hamdy, S. Carlucci, P.-J. Hoes, J.L.M. Hensen, The impact of climate change on the overheating risk in dwellings—a Dutch case study, Build. Environ. 122 (Sep. 2017) 307–323, https://doi.org/10.1016/j.buildenv.2017.06.031.

[15] K.J. Lomas, Y. Ji, Resilience of naturally ventilated buildings to climate change: advanced natural ventilation and hospital wards, Energy Build. 41 (6) (Jun. 2009) 629–653, https://doi.org/10.1016/j.enbuild.2009.01.001.

[16] V.I. Hanby, S.T. Smith, Simulation of the future performance of low-energy evaporative cooling systems using UKCP09 climate projections, Build. Environ. 55 (2012) 110–116, https://doi.org/10.1016/j.buildenv.2011.12.018.

[17] K.J. Lomas, R. Giridharan, Thermal comfort standards, measured internal temperatures and thermal resilience to climate change of free-running buildings: a case-study of hospital wards, Build. Environ. 55 (Sep. 2012) 57–72, https://doi.org/10.1016/j.buildenv.2011.12.006.

[18] R. Gupta, M. Gregg, Using UK climate change projections to adapt existing English homes for a warming climate, Build. Environ. 55 (2012) 20–42, https://doi.org/10.1016/j.buildenv.2012.01.014.

[19] S.M. Sajjadian, J. Lewis, S. Sharples, The potential of phase change materials to reduce domestic cooling energy loads for current and future UK climates, Energy Build. 93 (2015) 83–89, https://doi.org/10.1016/j.enbuild.2015.02.029.

[20] L. Pagliano, S. Carlucci, F. Causone, A. Moazami, G. Cattarin, Energy retrofit for a climate resilient child care centre, Energy Build. 127 (Sep. 2016) 1117–1132, https://doi.org/10.1016/j.enbuild.2016.05.092.

[21] R. Barbosa, R. Vicente, R. Santos, Climate change and thermal comfort in Southern Europe housing: a case study from Lisbon, Build. Environ. 92 (Oct. 2015) 440–451, https://doi.org/10.1016/j.buildenv.2015.05.019.

[22] P.M. Congedo, C. Baglivo, A.K. Seyhan, R. Marchetti, Worldwide dynamic predictive analysis of building performance under long-term climate change conditions, J. Build Eng. 42 (Oct. 2021) 103057, https://doi.org/10.1016/j.jobe.2021.103057.

[23] A. Dodoo, L. Gustavsson, F. Bonakdar, Effects of future climate change scenarios on overheating risk and primary energy use for Swedish residential buildings, Energy. Procedia 61 (Jan. 2014) 1179–1182, https://doi.org/10.1016/j.egypro.2014.11.1048.

[24] C.A. Alves, D.H.S. Duarte, F.L.T. Gonçalves, Residential buildings' thermal performance and comfort for the elderly under climate changes context in the city of São Paulo, Brazil, Energy Build. 114 (Feb. 2016) 62–71, https://doi.org/10.1016/j.enbuild.2015.06.044.

[25] A.D. Peacock, D.P. Jenkins, D. Kane, Investigating the potential of overheating in UK dwellings as a consequence of extant climate change, Energy Pol. 38 (7) (Jul. 2010) 3277–3288, https://doi.org/10.1016/j.enpol.2010.01.021.

[26] D.P. Van Vuuren, et al., The representative concentration pathways: an overview, Climatic Change 109 (1) (2011) 5–31, https://doi.org/10.1007/s10584-011-0148-z.

[27] A. Cibse Guide, A. Cibse Guide, Environmetnal Design, 2006, Chartered Institution of Building Services Engineers, London, UK, 2006.

[28] M. Herrera, et al., A review of current and future weather data for building simulation, Build. Serv. Eng. Technol. 38 (5) (2017) 602–627, https://doi.org/10.1177/0143624417705937.

[29] A. Moazami, V.M. Nik, S. Carlucci, S. Geving, Impacts of future weather data typology on building energy performance – investigating long-term patterns of climate change and extreme weather conditions, Appl. Energy 238 (Mar. 2019) 696–720, https://doi.org/10.1016/j.apenergy.2019.01.085.

[30] J. Bravo Dias, G. Carrilho da Graça, P.M.M. Soares, Comparison of methodologies for generation of future weather data for building thermal energy simulation, Energy Build. 206 (Jan. 2020) 109556, https://doi.org/10.1016/j.enbuild.2019.109556.

[31] Ansi/Ashrae Standard 169.1, Standard 169.1-2013: climatic data for building design standards, Climatic Data. Build. Des. Stand. (2013).

[32] A. Mohajerani, J. Bakaric, T. Jeffrey-Bailey, The urban heat island effect, its causes, and mitigation, with reference to the thermal properties of asphalt concrete, J. Environ. Manag. 197 (2017) 522–538, https://doi.org/10.1016/j.jenvman.2017.03.095.

[33] Ansi/Ashrae Standard 90.1, Standard 90.1-2013: energy standards for buildings except low-rise residential buildings, Climatic Data. Build. Des. Stand. (2019).

[34] ISO 18523-1, "'ISO 18523-1: Energy Performance of Buildings — Schedule and Condition of Building, Zone and Space Usage for Energy Calculation — Part 1: Non-residential buildings.," P. Geneva, Switzerland, 2016.

[35] ISO 18523-2, "'ISO 18523-2: Energy Performance of Buildings — Schedule and Condition of Building, Zone and Space Usage for Energy Calculation — Part 2: Residential buildings.," P. Geneva, Switzerland, 2017.

[36] ISO 17772-1, "ISO 17772-1: Energy Performance of Buildings - Indoor Environmental Quality. Part 1: Indoor Environmental Input Parameters for the Design and Assessment of Energy Performance in Buildings". Geneva, Switzerland, 2017.

[37] S.P. Corgnati, E. Fabrizio, M. Filippi, V. Monetti, Reference buildings for cost optimal analysis: method of definition and application, Appl. Energy 102 (2013) 983–993, https://doi.org/10.1016/j.apenergy.2012.06.001.

[38] Erika Guolo, Lorenza Pistore, Piercarlo Romagnoni, The role of the reference building in the evaluation of energy efficiency measures for large stocks of public buildings, E3S Web Conf. 111 (2019) 3017, https://doi.org/10.1051/e3sconf/201911103017.

[39] S. Attia, N. Shadmanfar, F. Ricci, Developing two benchmark models for nearly zero energy schools, Appl. Energy 263 (Apr. 2020) 114614, https://doi.org/10.1016/j.apenergy.2020.114614.

[40] P. Marrone, P. Gori, F. Asdrubali, L. Evangelisti, L. Calcagnini, G. Grazieschi, Energy benchmarking in educational buildings through cluster analysis of energy retrofitting, Energies 11 (3) (2018) 649, https://doi.org/10.3390/en11030649.

[41] P. Hernandez, K. Burke, J.O. Lewis, Development of energy performance benchmarks and building energy ratings for non-domestic buildings: an example

for Irish primary schools, Energy Build. 40 (3) (Jan. 2008) 249–254, https://doi.org/10.1016/j.enbuild.2007.02.020.

[42] M. Khoshbakht, Z. Gou, K. Dupre, Energy use characteristics and benchmarking for higher education buildings, Energy Build. 164 (2018) 61–76, https://doi.org/10.1016/j.enbuild.2018.01.001.

[43] H.S. Park, M. Lee, H. Kang, T. Hong, J. Jeong, Development of a new energy benchmark for improving the operational rating system of office buildings using various data-mining techniques, Appl. Energy 173 (2016) 225–237, https://doi.org/10.1016/j.apenergy.2016.04.035.

[44] M. Shahrestani, R. Yao, G.K. Cook, A review of existing building benchmarks and the development of a set of reference office buildings for England and Wales, Intell. Build. Int. 6 (1) (2014) 41–64, https://doi.org/10.1080/17508975.2013.828586.

[45] Us Doe, Commercial prototype building models, Build. Energy. Codes. Progr. (2020) [Online]. Available: https://www.energycodes.gov/development/commercial/prototype_models.

[46] Us Doe, Residential prototype building models, Build. Energy. Codes. Progr. (2020) [Online]. Available: https://www.energycodes.gov/development/residential/iecc_models.

[47] ISO 17772-2, "ISO 17772-2: Energy Performance of Buildings - Overall Energy Performance Assessment Procedures. Part 2: Guideline for Using Indoor Environmental Input Parameters for the Design and Assessment of Energy Performance of Buildings". Geneva, Switzerland, 2018.

[48] T. Parkinson, R. de Dear, G. Brager, Nudging the adaptive thermal comfort model, Energy Build. 206 (2020) 109559, https://doi.org/10.1016/j.enbuild.2019.109559.

[49] R. Rahif, D. Amaripadath, S. Attia, Review on time-integrated overheating evaluation methods for residential buildings in temperate climates of Europe, Energy Build. 252 (Dec. 2021) 111463, https://doi.org/10.1016/j.enbuild.2021.111463.

[50] S. Carlucci, L. Pagliano, A review of indices for the long-term evaluation of the general thermal comfort conditions in buildings, Energy Build. 53 (Oct. 2012) 194–205, https://doi.org/10.1016/j.enbuild.2012.06.015.

[51] ASHRAE, ANSI/ASHRAE Standard 55-2017, Thermal Environmental Conditions for Human Occupancy, ASHRAE, Atlanta, 2017.

[52] ISO 7730, ISO 7730: Ergonomics Of the Thermal Environment. Analytical Determination and Interpretation of Thermal Comfort Using Calculation of the PMV and PPD Indices and Local Thermal Comfort Criteria, International Standards Organization Geneva, 2004.

[53] M. Hendel, K. Azos-Diaz, B. Tremeac, Behavioral adaptation to heat-related health risks in cities, Energy Build. 152 (Oct. 2017) 823–829, https://doi.org/10.1016/j.enbuild.2016.11.063.

[54] L. Yang, H. Yan, J.C. Lam, Thermal comfort and building energy consumption implications – a review, Appl. Energy 115 (Feb. 2014) 164–173, https://doi.org/10.1016/j.apenergy.2013.10.062.

[55] W.A. Andreasi, R. Lamberts, C. Cândido, Thermal acceptability assessment in buildings located in hot and humid regions in Brazil, Build. Environ. 45 (5) (May 2010), https://doi.org/10.1016/j.buildenv.2009.11.005. Art. no. 5.

[56] R. De Dear, G.S. Brager, "Developing an adaptive model of thermal comfort and preference," UC Berkeley: center for the Built Environment [Online]. Available: https://escholarship.org/uc/item/4qq2p9c6, 1998. (Accessed 3 February 2020).

[57] P.O. Fanger, J. Toftum, Extension of the PMV model to non-air-conditioned buildings in warm climates, Energy Build. 34 (6) (2002) 533–536, https://doi.org/10.1016/S0378-7788(02)00003-8.

[58] D. Khovalyg, et al., Critical review of standards for indoor thermal environment and air quality, Energy Build. (2020) 109819, https://doi.org/10.1016/j.enbuild.2020.109819.

[59] S. Carlucci, L. Bai, R. de Dear, L. Yang, Review of adaptive thermal comfort models in built environmental regulatory documents, Build. Environ. 137 (Jun. 2018) 73–89, https://doi.org/10.1016/j.buildenv.2018.03.053.

[60] D.B. Crawley, J.W. Hand, M. Kummert, B.T. Griffith, Contrasting the capabilities of building energy performance simulation programs, Build. Environ. 43 (4) (2008) 661–673, https://doi.org/10.1016/j.buildenv.2006.10.027.

[61] ANSI/ASHRAE Handbook, "Handbook—2017: Fundamentals," American Society of Heating, Refrigerating and Air Conditioning Engineers: Atlanta, GA, USA, 2009.

[62] D. Kim, S. J. Cox, H. Cho, and P. Im, "Evaluation of energy savings potential of variable refrigerant flow (VRF) from variable air volume (VAV) in the U.S. climate locations," Energy Rep., vol. 3, pp. 85–93, Nov. 2017, doi: 10.1016/j.egyr.2017.05.002.

[63] M.J. Witte, R.H. Henninger, D.B. Crawley, Experience testing energyplus with the iea hvac bestest E300-E545 series and iea hvac bestest fuel-fired furnace series, Proc. Sim. Build 2 (1) (2006) 1–8.

[64] X. Zhou, T. Hong, D. Yan, Comparison of HVAC System Modeling in EnergyPlus, DeST and DOE-2.1 E, 7, 2014, pp. 21–33, https://doi.org/10.1007/s12273-013-0150-7, 1.

[65] ISO 15927-4, "'ISO 15927-4: Hygrothermal Performance of Buildings — Calculation and Presentation of Climatic Data — Part 4: Hourly Data for Assessing the Annual Energy Use for Heating and cooling'." P. Geneva, Switzerland, 2005.

[66] Ipcc and Core Writing Team, Summary for policymakers, Clim. Change 2014: Synthesis Report. Contribution of Working Groups I, II and III to the Fifth Assessment Report of the Intergovernmental Panel on Climate Change (2014) 2–34.

[67] K.E. Taylor, R.J. Stouffer, G.A. Meehl, An overview of CMIP5 and the experiment design, Bull. Am. Meteorol. Soc. 93 (4) (2012) 485–498, https://doi.org/10.1175/BAMS-D-11-00094.1.

[68] R. Judkoff, J. Nevmark, International Energy Agency Building Energy Simulation Test (BESTEST) and Diagnostic Method (No. NREL/TP–472-6231), National Renewable Energy Lab. Colorado, United States, 1995.

[69] R.A. Raustad, A Variable Refrigerant Flow Heat Pump Computer Model in EnergyPlus, Univ. of Central Florida, Orlando, FL (United States), 2013.

[70] R. Zhang, K. Sun, T. Hong, Y. Yura, R. Hinokuma, A novel Variable Refrigerant Flow (VRF) heat recovery system model: development and validation, Energy Build. 168 (Jun. 2018) 399–412, https://doi.org/10.1016/j.enbuild.2018.03.028.

[71] H. Holder, DOAS & humidity control, ASHRAE J. 50 (5) (2008) 34.

[72] D.B. Lu, D.M. Warsinger, Energy savings of retrofitting residential buildings with variable air volume systems across different climates, J. Build Eng. 30 (Jul. 2020) 101223, https://doi.org/10.1016/j.jobe.2020.101223.

[73] T.N. Aynur, Y. Hwang, R. Radermacher, Simulation of a VAV air conditioning system in an existing building for the cooling mode, Energy Build. 41 (9) (2009) 922–929, https://doi.org/10.1016/j.enbuild.2009.03.015.

[74] S. Goel, et al., "Enhancements to ASHRAE Standard 90.1 Prototype Building Models," Pacific Northwest National Lab.(PNNL), Richland, WA (United States), 2014.

[75] B.A. Thornton, et al., "Achieving the 30% Goal: Energy and Cost Savings Analysis of ASHRAE Standard 90.1-2010," Pacific Northwest National Lab.(PNNL), Richland, WA (United States), 2011.

[76] S.P. Corgnati, E. Fabrizio, D. Raimondo, M. Filippi, Categories of Indoor Environmental Quality and Building Energy Demand for Heating and Cooling, 4, 2011, pp. 97–105, https://doi.org/10.1007/s12273-011-0023-x, 2.

[77] S. Attia, Net Zero Energy Buildings (NZEB): Concepts, Frameworks and Roadmap for Project Analysis and Implementation, Butterworth-Heinemann, Quebec, Canada, 2018.

[78] N. Fumo, P. Mago, R. Luck, Methodology to estimate building energy consumption using EnergyPlus Benchmark Models, Energy Build. 42 (12) (2010) 2331–2337, https://doi.org/10.1016/j.enbuild.2010.07.027.

[79] R. Hendron, R. Anderson, C. Christensen, M. Eastment, P. Reeves, Development of an Energy Savings Benchmark for All Residential End-Uses, National Renewable Energy Lab., Golden, CO (US), 2004.

[80] P. Torcelini, et al., DOE Commercial Building Benchmark Models, National Renewable Energy Lab.(NREL), Golden, CO (United States), 2008.

[81] X. Luo, T. Hong, Y. Chen, M.A. Piette, Electric load shape benchmarking for small- and medium-sized commercial buildings, Appl. Energy 204 (2017) 715–725, https://doi.org/10.1016/j.apenergy.2017.07.108.

[82] J. Evers, C. Struck, R. van Herpen, J. Hensen, A. Wijsman, W. Plokker, Robuustheid voor klimaatvariaties: een vergelijking van klimatiseringsconcepten met behulp van gebouwsimulatie, Bouwfysica 20 (3) (2009) 2–7.

[83] N. Eskin, H. Türkmen, Analysis of annual heating and cooling energy requirements for office buildings in different climates in Turkey, Energy Build. 40 (5) (2008) 763–773, https://doi.org/10.1016/j.enbuild.2007.05.008.

[84] M.-T. Ke, K.-L. Weng, C.-M. Chiang, Performance evaluation of an innovative fan-coil unit: low-temperature differential variable air volume FCU, Energy Build. 39 (6) (2007) 702–708, https://doi.org/10.1016/j.enbuild.2006.06.011.

[85] Y. Pan, H. Zhou, Z. Huang, Y. Zeng, W. Long, Measurement and simulation of indoor air quality and energy consumption in two Shanghai office buildings with variable air volume systems, Energy Build. 35 (9) (2003) 877–891, https://doi.org/10.1016/S0378-7788(02)00245-1.

[86] S. Sekhar, C.J. Yat, Energy simulation approach to air-conditioning system evaluation, Build. Environ. 33 (6) (1998) 397–408, https://doi.org/10.1016/S0360-1323(97)00056-5.

[87] S. Yuan, R. Perez, Multiple-zone ventilation and temperature control of a single-duct VAV system using model predictive strategy, Energy Build. 38 (10) (2006) 1248–1261, https://doi.org/10.1016/j.enbuild.2006.03.007.

[88] V.M. Nik, S. Coccolo, J. Kämpf, J.-L. Scartezzini, Investigating the importance of future climate typology on estimating the energy performance of buildings in the EPFL campus, Energy. Procedia 122 (2017) 1087–1092, https://doi.org/10.1016/j.egypro.2017.07.434.

Paper VII

Assessing responsive building envelope designs through robustness-based multicriteria decision making in zero-emission buildings

Roberta Moschetti, Shabnam Homaei, Ellika Taveres-Chacat, Steinar Grynning

Assessing Responsive Building Envelope Designs through Robustness-Based Multi-Criteria Decision Making in Zero-Emission Buildings

Roberta Moschetti [1,*] 🄳**, Shabnam Homaei** [2]**, Ellika Taveres-Cachat** [1] **and Steinar Grynning** [1]

1   SINTEF Community, 7465 Trondheim, Norway; ellika.cachat@sintef.no (E.T.-C.);
steinar.grynning@sintef.no (S.G.)

2   Department of Civil and Environmental Engineering, Norwegian University of Science and
Technology (NTNU), 7491 Trondheim, Norway; shabnam.homaei@ntnu.no

*   Correspondence: roberta.moschetti@sintef.no

Abstract: Responsive building envelopes (RBEs) are central to developing sustainability strategies for zero emission/energy buildings (ZEBs). RBEs are a large group of complex technologies and systems, which is why multi-criteria decision making (MCDM) methods are helpful to navigate sustainability assessments considering various performance indicators. This article first provides a literature review of assessment criteria and key performance indicators for RBEs and an analysis of existing robustness-based MCDM methods. Then, a methodological approach to assess RBE designs in ZEB projects is proposed as an extension of a novel robustness-based MCDM method that normalizes the objective functions according to defined targets and combines them into one comprehensive indicator (MT-KPI), thereby eliminating the need to weight objectives. The proposed methodological approach is finally tested on a case study of a Norwegian ZEB, where five competitive RBE designs (including building integrated photovoltaics, phase change material, and electrochromic windows) and eight occupancy and climate scenarios are investigated considering three main performance areas: energy use, thermal comfort, and load matching. The results in the case study show that with the proposed MCDM approach the different designs have MT-KPI values between 1.4 and 12.8, where a lower value is better. In this specific case, the most robust building RBE alternative was identified as the one with electrochromic windows and a control based on incident solar radiation and indoor air temperature.

Keywords: building envelope; responsive; zero-emission buildings; robust designs; multi-criteria assessment; decision making; uncertainty scenarios

1. Introduction

1.1. Strategies and Technologies for Zero-Emission Buildings

Improving the building sector is central to achieving the sustainability development goals and creating positive environmental, economic, and social impacts [1]. Zero-energy/emission building (ZEB) continue to be investigated worldwide as a pathway to decrease energy use and greenhouse gas (GHG) emissions in future buildings, reduce future energy-related costs, and improve indoor comfort [2,3]. Recently, the scope of ZEBs was progressively extended from a micro-level of independent single buildings to a meso-level that includes clusters of interconnected buildings and services such as neighbourhoods [4]. Therefore, the concept of zero-energy/emission neighbourhoods (ZEN) is increasingly explored as a way to achieve very low to null GHG emissions and energy use during the neighbourhood's lifetime [5–7]. In Norway, the Research Centre on Zero Emission Neighbourhoods in Smart Cities (ZEN Research Centre) was established in 2017 to develop solutions for future buildings and neighbourhoods with no GHG emissions towards a low carbon society [8]. The design of highly energy efficient building envelopes

is crucial to achieving a zero-energy/emission balance at the building level [9] and has led to a growing emphasis on developing new building envelope concepts. Smart, adaptive, intelligent, dynamic, kinetic, advanced and responsive envelopes are some of the terms used to refer to building envelope systems that integrate new technologies and adopt complex behaviours [10–12]. In this article, we refer to these systems as responsive building envelopes (RBEs), using the same extension of the definition of climate adaptive building shells (CABS) [12] proposed in [13].

Examples of RBEs investigated in the past decade include double skin facades, Trombe walls, envelope-integrated phase change material (PCM), green walls, switchable windows, and dynamic solar shadings [14]. RBEs can provide many benefits ranging from improving environmental aspects and reducing energy use and GHG emissions [15] to increasing indoor environmental quality (IEQ) and leveraging higher building energy flexibility [16]. The latter benefit becomes particularly relevant when analysing ZEBs in a broader context, such as when they are part of ZENs, where implementing coordinated RBE strategies has an even larger potential for action due to the effect of scale.

In ZEBs and ZENs, as much as possible, building envelopes need to be designed to harvest renewable energy—either as electricity or heat—in addition to fulfilling energy and comfort requirements. Achieving a zero-energy/emission level then requires combining different types of RBEs, renewable energy technologies and energy storage solutions so that individual buildings, or ultimately a group of buildings at a neighbourhood scale, can reach a net-zero balance. These analyses are challenging and require systematic and integrated approaches based on multi-criteria decision making (MCDM) to assess overall performance. MCDM methods are widely used to support balanced evaluations considering various performance criteria [17,18]. They are often used in different methods to assess building performance and design, including methodologies focusing on performance robustness [19,20].

1.2. Novelty of the Proposed Research

This paper investigates the use of MCDM for analysing RBE designs in ZEB projects by addressing the following research questions:

- How to evaluate and compare performance of RBE designs with respect to different performance criteria using quantifiable indicators in the context of ZEBs?
- How can MCDM support the selection of the most robust RBE design solution considering operational uncertainties (such as climate change, occupant behaviour, etc.) in ZEBs?

The main contribution of this article is to demonstrate the combined use of a classification of quantifiable performance criteria and indicators with an overall MCDM methodology for analysing and assessing RBE performance in existing or future ZEB projects. The article's novelty lies in the investigation of the possibility of extending a verified robustness-based MCDM approach previously developed by one of this article's authors [21] to the assessment of RBEs. The method leads to a complete evaluation of RBE options under uncertainty by comparing alternative designs based on specific performance targets (set by standards and/or project's requirements) and yields a comprehensive multi-target indicator which accounts for any deviations from targets. The main advantage of this method is that it reduces the decision-making process to a single indicator regardless of the number of assessed performance criteria selected, eliminating the need for criteria weighting, which can be complex and biased.

The paper contributes to the development of systematic methodologies to aid decision-makers involved in ZEB projects to select the most suitable RBE solution among several design alternatives, considering stakeholder needs and available resources to reach ZEB targets. The application of the proposed methodology is demonstrated using a real ZEB located in a Norwegian neighbourhood intended to become a ZEN. This adds to the novelty of this research since the developed methodology is illustrated on a real building where the envelope designs, uncertainty scenarios, and KPIs are meaningful. Our methodology can

easily be applied to other ZEB and/or ZEN projects, where various design alternatives and scenarios, different from those of this article, could be assessed.

The remainder of the paper is organised as follows. Section 2 presents a literature review of performance criteria and indicators for RBEs in ZEBs, including an overview of robustness-based MCDM approaches. Section 3 introduces a classification of performance criteria and indicators for RBE assessments in ZEB projects. Then, the MCDM approach adopted in this study is presented together with the overall methodological approach, the case study used, the performance criteria, and the key performance indicators (KPIs) assessed with their targets. In Section 4, the results of this article are presented and critically discussed. Finally, the main conclusions and future outlooks are given in Section 5.

2. Theoretical Background

2.1. Assessment Criteria and Indicators for Responsive Building Envelope Solutions

The assessment of RBE designs can be challenging because of the dynamic nature of RBE technologies and their simultaneous influence on multiple physical domains [14,22]. For this reason, several recent studies focused on defining criteria and indicators to assess the performance of responsive façades [23–25]. Attia et al. [23] investigated current adaptive façades (AF) trends, with a focus on their performance assessment. They identified the gaps in the performance evaluation of AFs and proposed an assessment framework with five main categories: maintenance durability and life cycle, user control and experience, building control and service, protective performance, energy and environmental performance. Each category includes several KPIs aiming at defining the assessment of requirements, performance criteria, and qualitative technical characteristics of AFs. Loonen et al. [24] proposed an analysis of existing classification approaches for AFs to identify their requirements and challenges. A new matrix to characterise AFs was proposed as a result. In this matrix, six main goals/purposes of AFs are identified, i.e., thermal comfort, indoor air quality, visual performance, acoustic quality, energy generation, and personal control. The authors state that one or several of the identified goals should be achieved by AFs, in addition to considering the overall energy use, CO_2 emissions, and life cycle cost. The goals proposed by the authors can be expressed using performance indicators and are often based on building codes or standards. Aelenei et al. [25] presented the findings of an analysis of existing concepts and case studies of AFs and proposed a new approach to characterising their performance. The specific purposes of façade/components with adaptive capacity were defined, aiming at recognizing the reasons behind the adoption of these façades. The identified purposes were the following: thermal comfort, energy performance, indoor air quality (IAQ), visual performance, acoustic performance, and control. Assessing the performance of RBEs in ZEBs and ZENs can be even more challenging than in the context of ordinary buildings, since it requires considering additional factors such as the interactions with a larger grid system. Taveres-Cachat et al. [13] identified three main (non-mutually exclusive) design purposes for RBEs in ZENs, i.e., energy performance, user needs, and demand side management (DSM). Such classification is also relevant for ZEBs as they are often connected to local energy grids and interact with a broader context. The addition of DMS to assess RBEs on a ZEB or ZEN scale as proposed in [13] aims to integrate strategies for intelligent energy management to increase grid-friendliness at larger scales, a concept also researched under the name "energy flexibility". The IEA EBC Annex 67 project "Energy Flexible Buildings" defines the energy flexibility of a building as: "The ability to manage its demand and generation according to local climate conditions, user needs, and grid requirements. Energy Flexibility of buildings will allow for demand side management/load control and thereby demand response based on the requirements of the surrounding grids" [26]. In ZEBs and ZENs, energy flexibility requires assessing the simultaneity of energy needs versus supply (i.e., load matching) and the match between import and export of energy with respect to the grid needs (i.e., grid interaction) [27]. Energy flexibility indicators can allow investigating alternative design solutions but they often lack specific target values because, for instance, increasing the load match may or may

not be appropriate depending on the circumstances on the grid side [28]. The Norwegian ZEN Research Centre identified assessment categories, criteria, and KPIs based on previous project experience, existing assessment frameworks, and cross stakeholder inputs given in workshops. This resulted in a combination of quantitative and qualitative key assessment criteria and indicators described in [29]. The identified criteria and KPIs can be evaluated either on building-level or neighbourhood scale, and in some cases, on both levels.

2.2. Robustness-Based MCDM

Assessing multiple criteria in building designs inevitably creates design trade-offs. MCDM is a general concept consisting of different techniques to manage performance trade-offs due to conflicting criteria. This is based on the ranking or prioritization of alternatives, where each alternative cannot meet all the criteria on the same level, but the highest-ranking option will lead to the highest net profit. In MCDM, stakeholders differentiate various performance criteria by weighting them to show that achieving different criteria has a different value for the project actors. The decision-making step gets more complicated as more conflicting criteria are added and requires expertise to accurately weigh all criteria [21]. For example, Invidiata et al. [30] ranked the design strategies regarding comfort, environmental, and economic perspectives in an MCDM using input from 30 experts from different fields to define priorities and weightings for suggested criteria. Other multi-criteria decision-making techniques were also implemented in building design such as Multi-Attribute Utility Theory (MAUT), Analytical Hierarchy Process (AHP), Fuzzy Set Theory, Weighted Sum Method, and Weighted Product Method. For instance, AHP was used to select intelligent building systems [31], rank and compare energy management control algorithms for residential buildings [32], and select an optimal PCM to store heat from a ground source heat pump [33]. In addition to selecting a design package regarding different criteria, considering the impact of uncertainties (that influence the performance of different designs) is also a challenging issue. This procedure is known as decision-making under uncertainty. It shows that the building designs should perform well regarding multiple criteria under the current conditions and future uncertainties. An example of this is carried out by Rysanek et al. [34] where classical decision theories like the Wald, Savage, and Hurwicz criterion approaches were used to find the optimum building energy retrofits under technical and economic uncertainty. To show the impact of uncertainties in high-performance design selection, Kotireddy et al. [35] implemented performance robustness as a new criterion in addition to the actual performance of the building in a decision-making process. Homaei and Hamdy [21] defined robustness as the ability of a building to perform effectively and remain within the acceptable margins under a majority of possible changes in the internal and/or external environment. Based on this definition, they integrated robustness assessment with MCDM and developed a robustness-based decision-making approach called "T-robust approach". This method selects designs that perform considering multiple criteria under current conditions and future uncertainties. In this approach, the integration of robustness assessment to MCDM is done by introducing a new indicator called the multi-target key performance indicator (MT-KPI). The MT-KPI is defined based on the building's performance for given criteria and deviations from set performance targets. The approach yields a single performance metric and removes the need for weighting different criteria—which is not an easy task in real-world problems—by considering each criterion's target and penalizing the ouput based on the deviation from these targets. The T-robust approach also evaluates the robustness of the MT-KPI under the formulated uncertainties. In a previous article [21], one of the authors of this work evaluated the MT-KPI in a case study where energy use and comfort were the performance criteria. By running the robustness assessment, they succeeded in finding high performance and robust designs under uncertainties. The interested reader is referred to [21] for more details about the T-robust approach and the minimax method.

3. Materials and Methods

3.1. Classification of Performance Criteria and Indicators for RBE Assessment in ZEBs

One of the objectives of this paper is to provide a classification of quantifiable assessment criteria and indicators for simulation-based performance prediction of RBEs in ZEBs, considering three main categories: environmental/energy performance, user needs, and energy flexibility, as discussed in Section 2.1. This classification is meant to help assessing RBE alternatives in the early-design or renovation phase of building projects. The state-of-the-art review of performance criteria and indicators showed limitations that the classification proposed in this paper aims to overcome. Some of the assessment criteria identified in previous studies can only be assessed qualitatively, and even for the quantitative criteria, specific indicators and unit of measurement were not always provided. In this paper, only quantifiable KPIs are considered, to establish objective and comparable RBE performance assessments. Most publications on performance criteria and KPIs for RBE dealt with assessments at material level, whereas studies focusing on building or neighbourhood level performance are limited [23]. The proposed classification is meant to be used at the building scale but can also consider the broader scale of a neighbourhood. The literature review results shown in Table 1 indicate that most articles on RBE performance assessment at the building level focus on one or two evaluation criteria. Many studies on RBEs used single factors, such as energy saving potential [36–38], or coupled factors, such as energy efficiency and visual comfort [39–41] or visual comfort and thermal comfort [42,43]. Only a few studies analysing RBE performance include other additional criteria, such as energy efficiency, visual comfort, and thermal comfort [43,44]. The proposed robustness-based MCDM approach provides the assessment of one or more KPIs in each of the performance categories identified for the RBE performance evaluation (energy/environmental performance, user needs, and energy flexibility). Note that the evaluation of RBE through KPIs in the "energy flexibility" category was not directly deduced from the literature but was included in the proposed classification because they are acknowledged as essential to assess RBE designs in ZEBs, especially when they are part of a broader area that aims to reach a zero-emission target.

Table 1 summarizes quantitative assessment criteria and KPIs under each performance category identified in this article based on the literature review discussed in Section 2.1 and on the authors' personal elaboration. Note that this is meant to be a proposal for criteria and indicators' classification, where specific KPIs might more easily be examined at the building scale, while others might also result as suitable to the neighbourhood scale.

Table 1. Performance criteria and indicators for RBE assessment in ZEBs.

Performance Category	Assessment Criteria	Key Performance Indicators	Unit of Measurement	Ref.
Energy/ Environmental performance	Energy use	- Energy demand (total or per category e.g., heating, cooling, etc.) - Cooling load - Heating load - Embodied energy - Energy generation - Delivered energy - Exported energy - Energy balance (imported— exported energy)	kWh/yr or kWh/m^2/yr kW/yr or kW/ m^2/yr kW/yr or kW/ m^2/yr kWh/yr or kWh/ m^2/yr kWh/yr or kWh/ m^2/yr kWh/yr or kWh/ m^2/yr kWh/yr or kWh/ m^2/yr kWh/yr or kWh/ m^2/yr	[29,45,46]
	Climate change	- Embodied GHG - Energy use-related GHG emissions - Total GHG emission - Energy use related GHG balance	kgCO$_2$eq/yr or kgCO$_2$eq/m^2/yr kgCO$_2$eq/yr or kgCO$_2$eq/m^2/yr kgCO$_2$eq/yr or kgCO$_2$eq/m^2/yr kgCO$_2$eq/yr or kgCO$_2$eq/m^2/yr	[47,48]

Table 1. *Cont.*

Performance Category	Assessment Criteria	Key Performance Indicators	Unit of Measurement	Ref.
User needs	Thermal comfort	Global thermal comfort: - Indoor operative temperature - Predicted Mean Vote (PMV) - Percentage People Dissatisfied (PPD) - Comfort and/or discomfort hours Local thermal comfort: - Draught - Vertical air temperature difference - Radiant temperature asymmetry - Floor temperature	°C - % No. h or % % °C °C °C	[49–51]
	Visual comfort	- Daylight factor - Illuminance level - Glare index - Illuminance uniformity	% Lux - -	[50–53]
	Acoustic comfort	- Airborne sound reduction index - Reverberation time - A-weighted equivalent sound pressure level - Equivalent continuous sound level	dB s dB(A) dB	[50,51,54, 55]
Energy flexibility	Grid interaction	- Grid interaction index - Generation multiple - Capacity factor - Dimensioning rate - Peak power load - Peak power generation - Peak power export - Grid control level	% - % % kW kW kW %	[29,56–58]
	Load matching	- Load match index - Load cover factor (self-generation) - Supply cover factor (self-consumption) - Loss of load probability - Load/Power shifting ability - Utilisation factor - Mismatch compensation factor	% % % - - % -	[29,56–58]

3.2. Extension of the T-Robust Approach

In [21], the T-robust approach was used for two criteria (energy and comfort) and four different robustness assessment methods (Max-min method, Best-case and worst-case method, Minimax regret method, and Taguchi method). In this paper, this approach was applied to select robust and high-performance designs based on three different criteria (energy use, thermal comfort, and load matching) where the minimax regret method was used to assess the robustness of the MT-KPI. The three chosen criteria, performance indicators, and corresponding targets are described in Section 3.7. For each indicator, there is a corresponding performance target and robustness margins ($KPI_{i,m}$) that creates different performance zones based on their feasibility. Note that a distinction should be made between "less is better indicators" and "more is better indicator". In the first case, a KPI_i lower than $KPI_{i,m}$ will lead to a feasible performance but a KPI_i greater than $KPI_{i,m}$ will lead to an unfeasible performance. The opposite will happen for a "more is better indicator". In this paper, among the three analysed performance criteria, the energy use is a "less is better" indicator, and the thermal comfort and energy flexibility are "more is better" indicators. The relative performance ($KPI_{i,rel}$) is defined based on the relationship between KPI_i and $KPI_{i,m}$, as shown in Equation (1).

$$KPI_{i,\,rel} = \frac{KPI_i}{KPI_{i,m}} \times 100 \qquad (1)$$

In this paper, among the three analysed performance criteria, the energy use is a "less is better" indicator, and the thermal comfort and energy flexibility are "more is better" indicators. The relative performance ($KPI_{i,rel}$) is defined based on the relationship between KPI_i and $KPI_{i,m}$, as shown in Equation (1).

$$KPI_{i,rel} = \frac{KPI_i}{KPI_{i,m}} \times 100$$

(1)

The definition of the zones and the calculation of the MT-KPI depend on the number of performance indicators assessed. The different zones identified in this work are visually illustrated in Figure 1, where each color corresponds to one zone. Point (100,100,100) in Figure 1 shows the relative margin point at which the performance of the building considering all indicators is equal to the robustness margin. The eight different performance zones are created around the relative margin point.
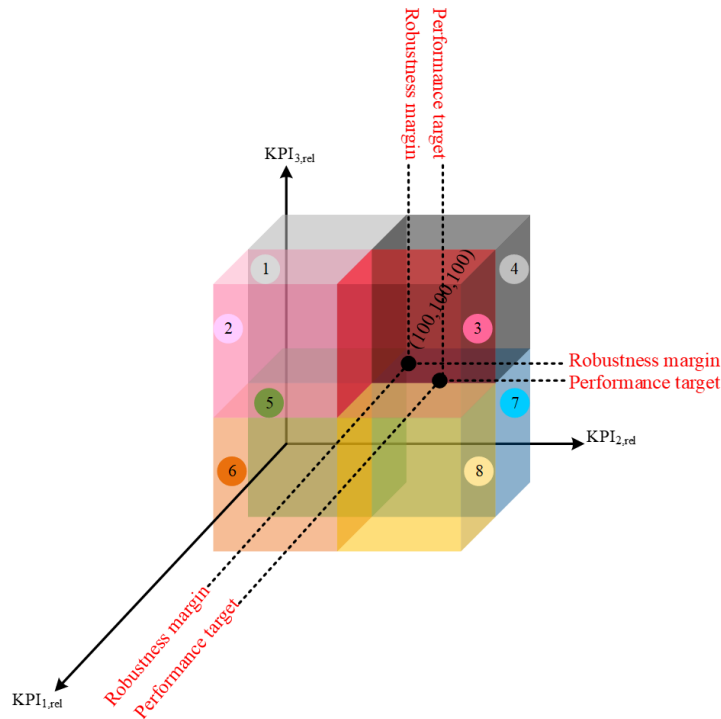

Figure 1. Illustration of performance zones for the MT-KPI.

Table 2 presents the formulas for the MT-KPI calculation for the KPIs considered in this study. The strategy for calculating the MT-KPI is one that penalizes design with a lower performance than the target set for each indicator (i.e., infeasible performance). As shown in Table 2, zone 6 is an extreme case where all indicators are outside the feasible boundaries and in which case the MT-KPI is the sum of the KPIs' difference with their corresponding robustness margins and acts as a penalty for the infeasibility of all three indicators. At the other extreme is zone 4 in which all indicators are within their feasibility bounds and for which the MT-KPI is calculated as the sum of the inverted difference between indicators and their corresponding robustness margins. Inverting the differences is used as a way of differentiating feasible designs. All the other zones are designs with different combinations of performance results which are feasible for some criteria and infeasible for others. In these zones, a penalty is applied for the infeasible indicators and the MT-KPI is defined for each zone based on the formulas shown in Table 2. To give an example, zone 1 has a feasible performance for KPI_1 and KPI_3, and an infeasible performance for KPI_2. Then, for the calculation of the MT-KPI in this zone, a penalty is applied for KPI_2. The calculations of the MT-KPI for each design under each scenario was done in this work by applying an automated MATLAB [59] algorithm. After calculating the MT-KPI, the minimax regret method allowed assessing the difference between the MT-KPI value for each design in each scenario and the minimum performance of each scenario across all designs. Based on the definition of the minimax regret method, this difference is called performance regret.

The maximum performance regret represents the highest deviation in each design, i.e., the largest difference between the worst performance and the best performance. The most robust design is then the one with the smallest maximum performance regret across all scenarios [23]. The calculation related to the minimax regret method was also done using an automated MATLAB algorithm, with the formulas shown in the Appendix A (Tables A1 and A2).

Table 2. Calculation of MT-KPI in different performance zones.

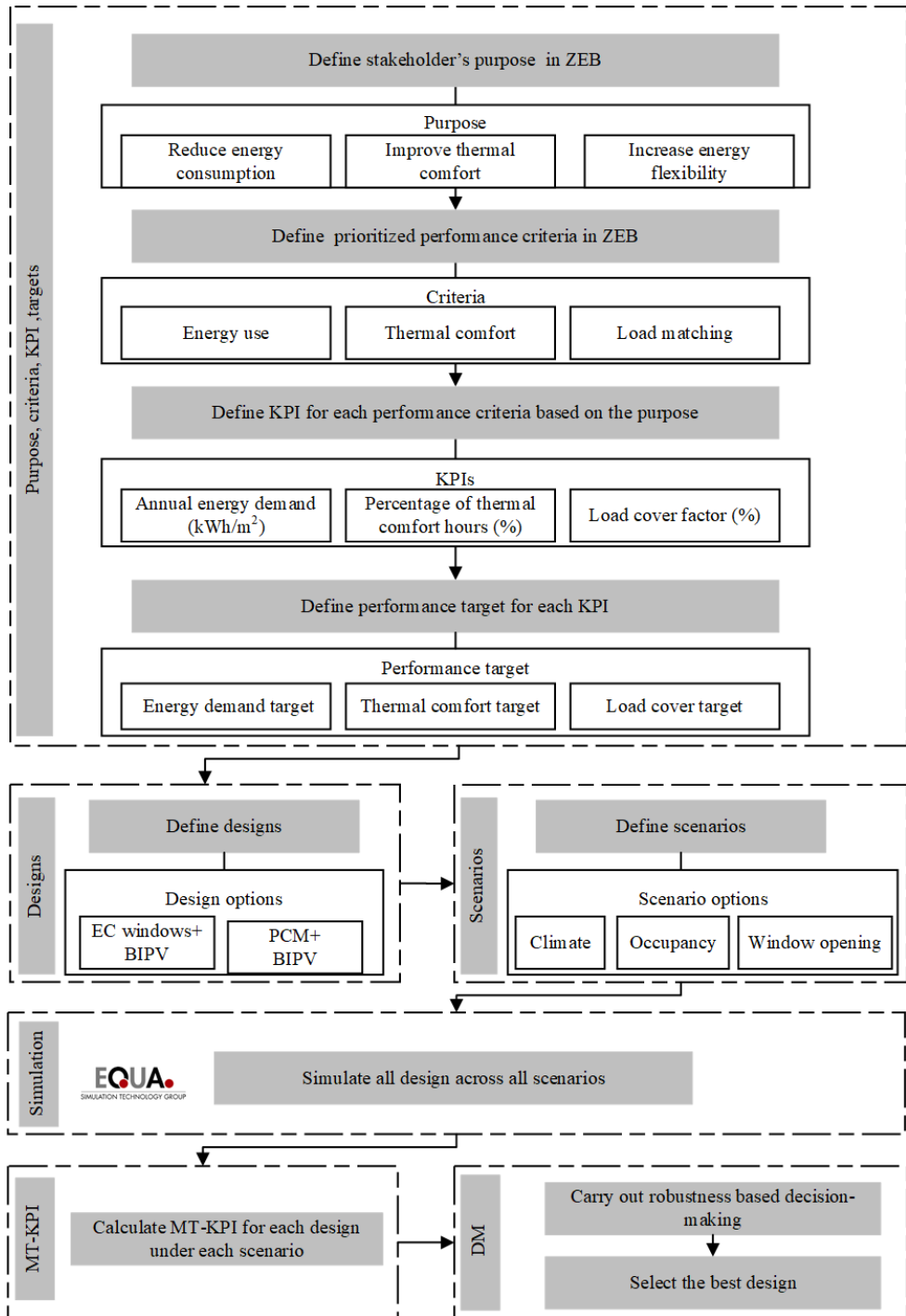| Num.	Performance Zone	Feasibility	MT-KPI
1	$KPI_{1,rel} \leq 100$; $KPI_{2,rel} < 100$; $KPI_{3,rel} \geq 100$	Feasible for KPI_1 and KPI_3	$(1/(100 - KPI_{1,rel})) + (100 - KPI_{2,rel}) + (1/(KPI_{3,rel} - 100))$
2	$KPI_{1,rel} > 100$; $KPI_{2,rel} < 100$; $KPI_{3,rel} \geq 100$	Feasible for just KPI_3	$(KPI_{1,rel} - 100) + (100 - KPI_{2,rel}) + (1/(KPI_{3,rel} - 100))$
3	$KPI_{1,rel} > 100$; $KPI_{2,rel} \geq 100$; $KPI_{3,rel} \geq 100$	Feasible for KPI_2 and KPI_3	$(KPI_{1,rel} - 100) + (1/(KPI_{2,rel} - 100)) + (1/(KPI_{3,rel} - 100))$
4	$KPI_{1,rel} \leq 100$; $KPI_{2,rel} \geq 100$; $KPI_{3,rel} \geq 100$	Completely feasible	$(1/(100 - KPI_{1,rel})) + (1/(KPI_{2,rel} - 100)) + (1/(KPI_{3,rel} - 100))$
5	$KPI_{1,rel} \leq 100$; $KPI_{2,rel} < 100$; $KPI_{3,rel} < 100$	Feasible for just KPI_1	$(1/(100 - KPI_{1,rel})) + (100 - KPI_{2,rel}) + (100 - KPI_{3,rel})$
6	$KPI_{1,rel} > 100$; $KPI_{2,rel} < 100$; $KPI_{3,rel} < 100$	Completely infeasible	$(KPI_{1,rel} - 100) + (100 - KPI_{2,rel}) + (100 - KPI_{3,rel})$
7	$KPI_{1,rel} \leq 100$; $KPI_{2,rel} \geq 100$; $KPI_{3,rel} < 100$	Feasible for KPI_1 and KPI_2	$(1/(100 - KPI_{1,rel})) + (1/(KPI_{2,rel} - 100)) + (100 - KPI_{3,rel})$
8	$KPI_{1,rel} > 100$; $KPI_{2,rel} \geq 100$; $KPI_{3,rel} < 100$	Feasible for just KPI_2	$(KPI_{1,rel} - 100) + (1/(KPI_{2,rel} - 100)) + (100 - KPI_{3,rel})$

3.3. Methodological Approach

Figure 2 shows the methodological approach proposed in this paper to assess RBE designs in ZEB projects. Note that the main general steps of the methodology are shown in the grey boxes, while the specific steps adopted in this work for the case study are in the white boxes.

Primarily, the main purpose and criteria for RBEs in the studied project should be defined based on the priorities of the stakeholders involved. Afterwards, relevant KPIs to assess RBEs in the ZEB project should be identified. The KPIs should be related to the main stakeholders' objectives, including for instance energy use, thermal comfort, and energy flexibility. The choice of the KPIs should be supported by the classification provided in Table 1. Then, specific performance targets should be identified for each KPI to assess how the performance of the building under the design conditions deviate from the defined targets. The performance targets can be based on requirements in building codes, or they can be set specifically based on the preference of stakeholders for a certain project. Based on the assumption in the T-robust approach, the examined designs should comply with a robustness margin of 5% from the target limit to be considered feasible solutions. Such a margin of 5% was selected for this study based on author's assumptions, but it could be changed depending on the preferences of the decision makers in the studied project. Several designs with RBE solutions for the analysed project should be identified, together with alternative scenarios to assess the effects of different uncertainties, such as changes in occupant behaviour and climate conditions. The next step involves the simulation-based performance prediction of all identified designs across all scenarios through specific software applications according to the chosen KPIs.

The robustness of the designs and scenarios is then assessed with an MT-KPI, which reflects the performance of the designs against multiple criteria and penalizes the solutions that do not meet a specific performance target. The performance robustness of the building designs is evaluated using a specific robustness indicator (i.e., minimax regret method) for the MT-KPI, as described in Sections 2.2 and 3.2, and allows selecting the design with the overall highest and most robust performance.

As shown in Figure 2, energy, thermal comfort, and building energy flexibility were selected as the performance criteria for the case study building in this article. Consequently, the authors chose annual energy demand, percentage of comfortable hours, and the load cover factor as the KPIs for the three mentioned criteria, respectively. These KPIs were selected by the authors to reflect the priorities of the specific project analysed, but other KPIs could be used in other studies to address different objectives and preferences of the decision makers.

Such a margin of 5% was selected for this study based on author's assumptions, but it could be changed depending on the preferences of the decision makers in the studied project. Several designs with RBE solutions for the analysed project should be identified, together with alternative scenarios to assess the effects of different uncertainties, such as changes in occupant behaviour and climate conditions. The next step involves the simulation-based performance prediction of all identified designs across all scenarios through specific software applications according to the chosen KPIs.

Figure 2. Methodological approach proposed in this article. The main general steps are in the grey boxes.

design with the overall highest and most robust performance.

As shown in Figure 2, energy, thermal comfort, and building energy flexibility were selected as the performance criteria for the case study building in this article. Consequently, the authors chose annual energy demand, percentage of comfortable hours, and the load cover factor as the KPIs for the three mentioned criteria, respectively. These KPIs

were selected by the authors to reflect the priorities of the specific project analysed, but other KPIs could be used in other studies to address different objectives and preferences of the decision makers.

3.4. Case Study

To show the application of the approach, the Zero Emission Building Laboratory (ZEB-lab) located on the NTNU university campus in Trondheim (Norway) was used as a case study. This office building was finished in December 2020 and is connected to the local energy grid in an area that is intended to become a ZEN [60]. The building, shown in Figure 3, has 4 stories, with a total floor area of ca. 1725 m². The ZEB-lab was designed to achieve the ZEB-COM level [61] meaning that the building's renewable energy production compensates for total GHG emissions associated with the production of the building materials used, the construction phase, and the building operation [62] in a 60 year perspective. PV-panels are integrated in the entire roof surface and cover extensive parts of the facades to ensure sufficient renewable energy harvesting. The ZEB-lab has a compact volume and a wooden load-bearing system, with a highly insulated and airtight building envelope. The space heating is provided by a waterborne system supplied by an air source heat pump and a local heating grid. The heat pump also provides space cooling to two small research laboratories called the twin rooms. The ZEB Lab uses hybrid ventilation, which combines natural and mechanical ventilation, with a highly efficient heat recovery system. In particular, mechanical ventilation is based on a variable volume air (VAV) system providing temperature and CO_2 demand-controlled air flows. See Tables A3 and A4 in the Appendix A for more details about the building envelope and the technical building systems. A detailed model of the case study building, for all the identified designs and scenarios, was created in the dynamic simulation software "Indoor Climate and Energy software" (IDA ICE), version 4.9 beta [63].
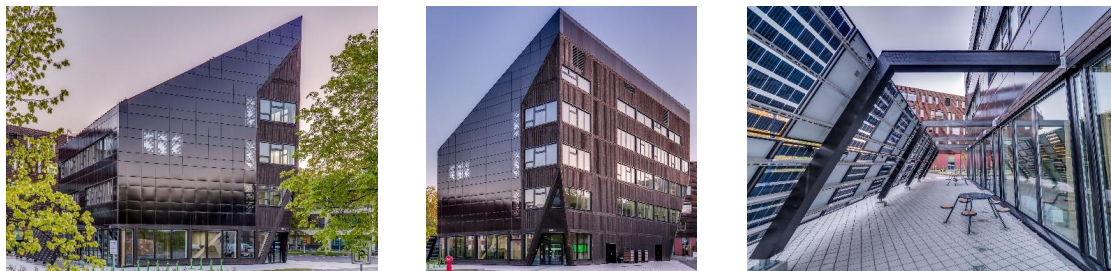

Figure 3. Pictures of the case study building. Copyright: Nicola Lolli/SINTEF.

IDA ICE was validated in several studies with respect to CEN standards and ASHRAE standard [64–66]. The possibility of modeling RBE technologies in IDA ICE, including PCM and electrochromic (EC) windows, was reviewed in several articles, such as Refs. [67,68]. The prediction accuracy of IDA ICE for PCM simulation was tested and validated against experimental results by Mazzeo et al. [69] and Cornaro et al. [70]. EC window modelling in IDA ICE implies the use of a detailed windows' model with dynamic parameters in different states and with various light angles, through custom control macros that can be implemented to activate their shading. Finally, the calculation accuracy of PV energy generation in IDA ICE was also validated, as shown in [71].

3.5. Analysed RBE Technologies

The analysed case study was planned as an arena where new and innovative solutions can be developed, investigated, tested, and demonstrated in a mutual interaction with building's occupants. Energy demand reduction, thermal comfort improvement, and building load covering by on-site energy generation were identified by the stakeholders as the main priorities to be addressed when testing new possible technologies in the building. Therefore, two RBEs, i.e., EC windows and PCM, were selected as alternative designs to be combined with the existing installed RBE technologies, which are building integrated photovoltaics (BIPV) and responsive window screens. The aim was to assess

the possible benefits of new innovative designs with respect to the identified performance objectives. The use of PCM in lightweight buildings characterised by low thermal inertia can lead to a higher thermal storage capacity. Several studies proved the positive effects of PCMs on indoor comfort and energy use [72]. To simulate PCM in walls, IDA ICE uses a PCM model with different temperature-enthalpy equations to determine liquid-solid phase transitions. The cycling between phases is modelled as a hysteresis meaning that the current state depends on past states of the system. The "mode" variable in the model is used to identify the five different physical states, i.e.,: "mode -2" solid phase; "mode 2" liquid phase; "mode -1" solidification phase; "mode 0" inversion during the solidification/fusion process; "mode 1" fusion process. The heat capacity and the temperature of the PCM layer are calculated as a function of the enthalpy and the "mode" variable at each time step.

EC windows are effective in preserving solar gains in winter, while reducing the heat load in summer and glare from the sun. Using EC windows rather than normal windows with external screens arguably provides a better connection to the outdoors for users with smoother and inaudible transitions between different shading states, allowing light to penetrate even in the darkest state [73]. IDA ICE uses a detailed window model for EC window implementation, where the optical and thermal properties of all the panes and spacers are represented. Multiple reflections and solar absorption in each pane are considered to calculate angle-dependent optical properties based on ISO 15099:2003 [74]. The EC glass tint can be automatically controlled by standard or custom control algorithms created directly in the IDA ICE macro interface, which allows changing window optical properties based on, for instance, indoor operative temperature and/or daylighting levels.

3.6. Analysed Designs and Scenarios

Five design configurations were defined for the case study building, as illustrated in Table 3. Table 4 shows an overview over the main parameters used in the designs and scenarios concerning the internal gains, exterior and interior blinds, PCM, and electrochromic windows. Eight scenarios were overall evaluated in this paper, addressing two main parameter categories: climate conditions and occupant behaviour.

i.   Climate scenarios

To assess the influence of climate uncertainties, two weather files were evaluated. The first one was a standard typical meteorological year (TMY) weather file in EPW format for the location of Trondheim (Norway) and represented the current climatic conditions. The second one was obtained by morphing the first weather file using the "CCworldWeather-Gen tool" [76], which is based on the widely accepted General Circulation Model (GCM) HadCM3 and the IPCC's A2 emission representing a medium-high scenario. The resulting weather file accounts for potential impacts of climate change and represented possible future weather conditions for the year 2050 in Trondheim.

Table 3. Details of the five designs considered in the case study demonstration.

Design	Description
D1	As built case study (reference design), with: BIPV on the roof, south, west, and east facing facades; external screens on the south facade, internal curtains on the west and east facades, and no solar protection on the north façade.
D2	Reference design (D1), with PCM added as a layer in all facades and same screens/curtains as D1.
D3	Reference design (D1), with PCM added as a layer in all facades with internal curtains on south/east/west facades.
D4	Reference design (D1), with EC windows on all facades and control macro 1 (different tinting states as a response to incident radiation level and indoor air temperature. See Table 4).
D5	Reference design (D1), with EC windows on all facades and control macro 2 (different tinting states as a response to incident radiation level and daylighting level in the zone. See Table 4).

Table 4. Key parameters for the analysed designs.

Input Category	Value	Reference or Comment
Occupancy schedule and rate	Variable	Schedules based on standard NS/NSPEK 3031:2020 [46]; number of occupants based on as-built seating plan. Daily power profile variation shown in Figure A1 in Appendix A.
Heat gain from occupants	5 kWh/m^2	Average specific value for the whole building, with 1.2 MET per person and people number per room given in Table A5 in Appendix A. This value aligns with [46].
Equipment power	3.2 W/m^2	Average specific value for the whole building, including only typical office electrical equipment (laptop, PC, screens, etc.). Value in line with as-built documentation. Daily power profile variation set as the same as for occupancy. See Figure A1 in Appendix A.
Artificial light power	4.7 W/m^2	Average specific value for the whole building, with dynamic LED lighting strategy in which artificial lighting is used to complement daylighting until an illuminance of 500 lux is reached on the work plan. Value in line with as-built documentation. Daily lighting profile variation based on setpoints and occupancy. See Figure A1 in Appendix A.
Amount of solar radiation on façade to trigger shading signal for exterior and interior blinds	If solar elevation $\leq 29°$ $\rightarrow 79$ W/m^2 If solar elevation $> 29°$ $\rightarrow 198$ W/m^2	As-built control strategy.
PCM	Thickness: 15 mm Melting point: 22–23 °C Cp > 170 kJ/kg (in range 13–28 °C) Density in solid state: 1500 kg/m^3	Melting-solidifying around 20 °C was chosen because it was found to be preferable in heating-dominated climates [75].
Electrochromic windows	U-value: 0.8 W/m^{2}K G-value (min/max): 0.25–0.48	Two control macros: Macro 1 (in D4): proportional shading control based on external solar radiation on window in range 100–300 W/m^2 and KPI control of indoor air temperature (setpoint 24 °C). Macro 2 (in D5): proportional shading control based on external solar radiation on window in range 100–300 W/m^2 and KPI control for daylighting level (500 lux setpoint). See Figures A2 and A3 in Appendix A.

ii. Occupancy schedule

Two occupancy schedule cases were implemented in the model. The first one used occupancy profiles based on those recommended in [46], as shown in the Appendix A, Figure A1. In this schedule, most modelled zones had two main peaks in the occupancy during the hours 9:00–11:00 and 13:00–15:00, and a relatively limited occupancy for the rest of the working hours (7:00–9:00 and 15:00–17:00). The only zone in the building with a different occupancy schedule was the canteen, where occupants were assumed to be present only between 11:00 and 13:00 for lunch. The second occupancy case considered the possibility of people staying longer after regular work hours on the first and third floors. These floors are used by employees and students from the university, a portion of which are likely to work overtime until 20:00. See occupancy schedules in Figure A1 in the Appendix A.

iii. Window opening strategies

Two alternative strategies were used for window opening. The first strategy assumed all windows were always closed, while in the second strategy, the occupants could open all openable windows when the indoor air temperature was higher than a threshold value and the air temperature outside was lower than the indoor air temperature. See more details in Table 5. The second strategy was implemented in IDA ICE through control macros based

on a PI-control. The five designs were analysed across all eight scenarios, leading to a total of forty cases simulated in IDA ICE over a one-year period. Table 5 summarizes the parameters and their combination for all scenarios.

Table 5. Summary of the main parameters for all the scenarios analysed.

Parameters		Scenarios							
		1	2	3	4	5	6	7	8
Climate	1. Current weather	x	x	x	x				
	2. 2050 weather					x	x	x	x
Occupancy schedule	1. Based on NS3031 schedules	x	x			x	x		
	2. Based on NS3031, with longer stay of university employees			x	x			x	x
Window opening strategy	1. All windows closed	x		x		x		x	
	2. All automatically openable windows open if Tindoor > Tout, Tindoor > 24 °C, and room is occupied; all manually openable windows open if Tindoor > Tout, Tindoor > 25 °C, and room is occupied		x		x		x		x

3.7. Analysed KPIs and Targets

To assess the performance of the designs and scenarios defined for the case study, three KPIs from Table 1 were chosen to reflect the main priorities of the project stakeholders.

The first KPI analysed in this article is the annual energy demand of the building for heating, ventilation, cooling, and lighting. The target value for this KPI was based on the requirement of the Norwegian building technical regulation, TEK17 [77], which sets the total energy demand, including energy for space and ventilation heating, space and ventilation cooling, ventilation fans and pump, lighting, domestic hot water (DHW), and electrical equipment. The target value for the first KPI was set to 30 kWh/m^2, which represents a reduction of 60% of the energy demand requirement of TEK17 for office buildings, excluding electrical equipment and DHW energy use. This percentage reduction from the reference value was deducted from the target values for a similar KPI defined in [29], where the highest credit for the energy demand KPI is given to a reduction from 50% to 60%. The robustness margin allows 5% tolerance from the performance target, which leads to 32 kWh/m^2.

The second PI is related to the thermal comfort level in the building, given as the percentage of hours within comfort category II, as defined in EN 15251:2007 [78]. In this latter standard, three main comfort categories are identified, based on an adaptive comfort model where occupants with sedentary physical activities can freely adapt their clothing level to indoor/outdoor thermal conditions. The comfort category II considered in our study represents normal level of expectation in new buildings. The target value for this KPI was set to 100% of occupied hours within thermal comfort category II. The robustness margin allows a 5% tolerance from the performance target, which leads to 95%. The KPI was evaluated first for each one of five representative long-lasting working areas in the case study building and then as an average value for all five rooms. This allowed to have an overall picture of the comfort conditions in the whole building, as the chosen rooms are those mostly occupied and spread across all four floors with different façade expositions. Note that the analysis of hours in category II of EN 15251 focuses on the combination of the thermal comfort hours both in heating and cooling condition, therefore the identification of extreme scenarios is quite complex and is out of the scope of the article.

The third KPI is the load cover factor (self-generation), which represents the percentage of the electricity demand that is covered by on-site electricity generation. This KPI is one of the available load matching factors, which aims to describe the degree of the utilization of on-site energy generation in relation to the actual energy demand. The hourly analysis of the load cover factor offers a useful picture of the correlation between on-site demand and energy supply. An hourly resolution was therefore chosen in this study to evaluate

this KPI for the different RBE designs, and the target value was set to 100% because a high coverage of the energy demand on-site was desired. The robustness margin allows 5% tolerance from the performance target, which leads to 95% as a robustness margin for the load cover factor.

4. Results and Discussion

4.1. Performance Assessment of Designs and Scenarios

Figure 4a shows the results for the energy demand (for heating, cooling, and lighting) for the five designs across the eight analysed scenarios. Scenario 1 and scenario 8 had the highest and the lowest energy demand in all the examined designs, respectively. For designs, D4 showed overall the lowest energy demand values across all scenarios. The energy demand for room and ventilation heating represented the main contribution to the total energy demand (ca. 65–80%), followed by lighting (ca. 20–30%), and cooling (ca. 1–4%). The use of a morphed climate file for 2050 in scenarios 5-8 had the highest impact on the energy demand with a reduction of ~25% compared to results with the TMY weather file (in scenarios 1–4). Figure 4b illustrates the results of the average percentage of hours in category II (according to EN 15251) in the main rooms assessed for the five designs across the eight scenarios. All designs and scenarios had appropriate thermal comfort conditions. Scenario 8 in D2 had the highest percentage of hours in category II (98%) while scenario 1 in D3 had the lowest percentage (89%). In D3, the use of PCM in external walls combined with interior curtains on the south/east/west facades led to the worst thermal comfort among designs, especially for south-facing rooms whose facades are characterised by very large windows leading to high solar gains in summer and significant heat losses in winter. Then, as the case study building is in a heating-dominated climate, a significant part of the unacceptable hours with respect to the thermal comfort is related to underheating hours. Figures 4c illustrate the load cover factor for the five designs across the eight scenarios analysed. The results show that D1 and D2 scored lowest for this KPI, with values in the range 43–48%. D3, D4, and D5 on the other hand yielded higher load cover factors reaching up to 50%. Since the energy generation from the PV system with the two climate files employed is similar in all designs/scenarios, the value for this KPI mainly depends on the size of the building load, its duration, and timing. Generally, the use of the assessed RBE technologies led to a higher load cover compared to the reference design thanks to reducing peak loads and shifting loads. Using PCM combined with external screens on the south facade and interior curtains on east/west facades (D2) led to a small decrease in the energy demand ((−2)–(−3)%), and a slightly better thermal comfort (D2 1.5%) compared to D1, but the load cover factor remained almost the same. Substituting external screens with interior curtains on the south facade in D3 generally led to a lower energy demand (ca. −10%) and a higher load cover factor (4–7%) compared to D1, and D3 performed particularly well in scenarios using the future weather climate file. However, the thermal comfort decreased in all scenarios.

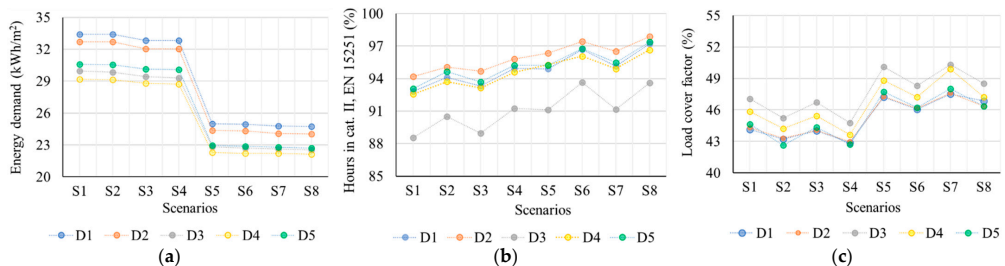**Figure 4.** Results of the three performance indicators for the five analysed designs across the eight scenarios: (**a**) Energy demand results (including only heating, cooling, and lighting). (**b**) Thermal comfort results (average % of hours in cat. II of EN 15251 in five main rooms). (**c**) Load cover factor results.

When using EC windows (D4 and D5), it was possible to improve the performance regarding the energy demand KPI (especially for heating and lighting) and the load cover factor KPI, without significantly reducing the thermal comfort compared to the reference design, D1. The design with the shading control macro for EC windows based on indoor air temperature (D4) was particularly high performing with a lower energy demand ((−10)–(−12)%) and higher load cover factor (1–5%) compared to D1 but did not clearly

When using EC windows (D4 and D5), it was possible to improve the performance regarding the energy demand KPI (especially for heating and lighting) and the load cover factor KPI, without significantly reducing the thermal comfort compared to the reference design, D1. The design with the shading control macro for EC windows based on indoor air temperature (D4) was particularly high performing with a lower energy demand $((-10)–(-12))$% and higher load cover factor (1–5%) compared to D1 but did not clearly outperform D3 in most cases except for thermal comfort.

Based on the performance assessment described in this sub-section, the selection of the best design is not trivial as some designs performed well but with a certain variation across scenarios. Figure 5 shows a closer comparison between D3 and D4, which were the two designs that stood out among all the others in terms of performance. However, even the comparison of only two designs with respect to several KPIs is not straightforward and would also be time- and resource-demanding in real-world problems.
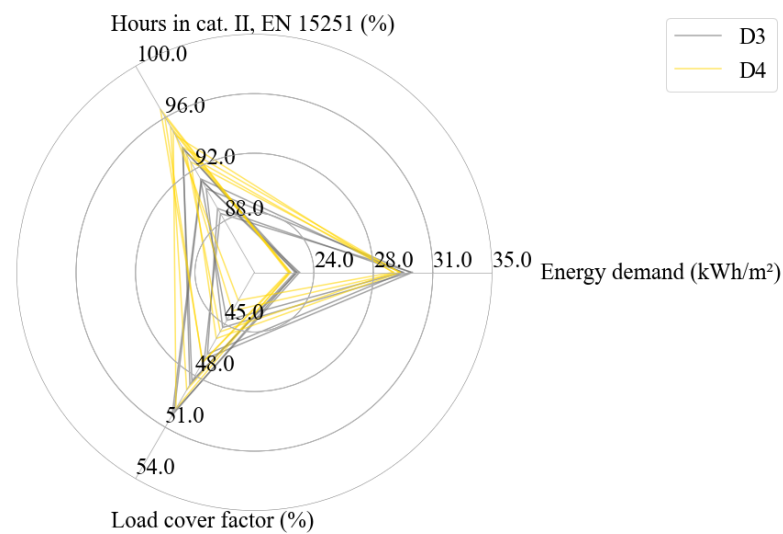
Figure 5. Comparison of the results for all KPIs in D3 and D4 across the eight scenarios.

4.2. Robustness-Based MCDM Assessment

Given the complexity of the performance assessment for the choice of the best design, the robustness-based MCDM assessment was performed to facilitate the selection of the design that was most robust under uncertainties and had optimal actual performance.

In this section, the results of the T-robust approach are presented. Figure 6 summarizes the results for all design and scenarios using the same eight performance zones that were previously introduced in Section 3.2 (see Figure 1 and Table 2). The three highlighted planes inside the graph in Figure 6 are drawn at the robustness target values of each KPI, to visualize the performance zones. As evident in Figure 6, the distribution of the performance of the five designs across the eight scenarios seems categorised into two main groups, which show the performance of the analysed designs in the current and the 2050 weather conditions. The graph in Figure 6 illustrates that a switch from the current to 2050 climate file will lead to a decrease in the energy demand and an increment in the percentage of hours in category II and the load cover factor. An increase in the percentage of underheating hours that can happen during a year. When it comes to the comparison of the designs' performance targets, the following observations can be listed:

- With respect to the energy demand target, all the designs will experience an energy demand higher than 30 kWh/m² at least in one of the suggested scenarios, except for D3 and D4. D1 and D2 also have scenarios with an energy demand higher than the robustness margin for this KPI (32 kWh/m²).

- When it comes to the comfort performance target, which is 100% of hours inside category II, all designs have a performance lower than the target; however, all designs except D3 present scenarios with a performance higher than the robustness margin

- With respect to the energy demand target, all the designs will experience an energy demand higher than 30 kWh/m^2 at least in one of the suggested scenarios, except for D3 and D4. D1 and D2 also have scenarios with an energy demand higher than the robustness margin for this KPI (32 kWh/m^2).
- When it comes to the comfort performance target, which is 100% of hours inside category II, all designs have a performance lower than the target; however, all designs except D3 present scenarios with a performance higher than the robustness margin (95%).

- Regarding the load cover factor target, all the designs across all scenarios experience a performance lower both than the target corresponding to 100 % and the robustness margin of 95%.
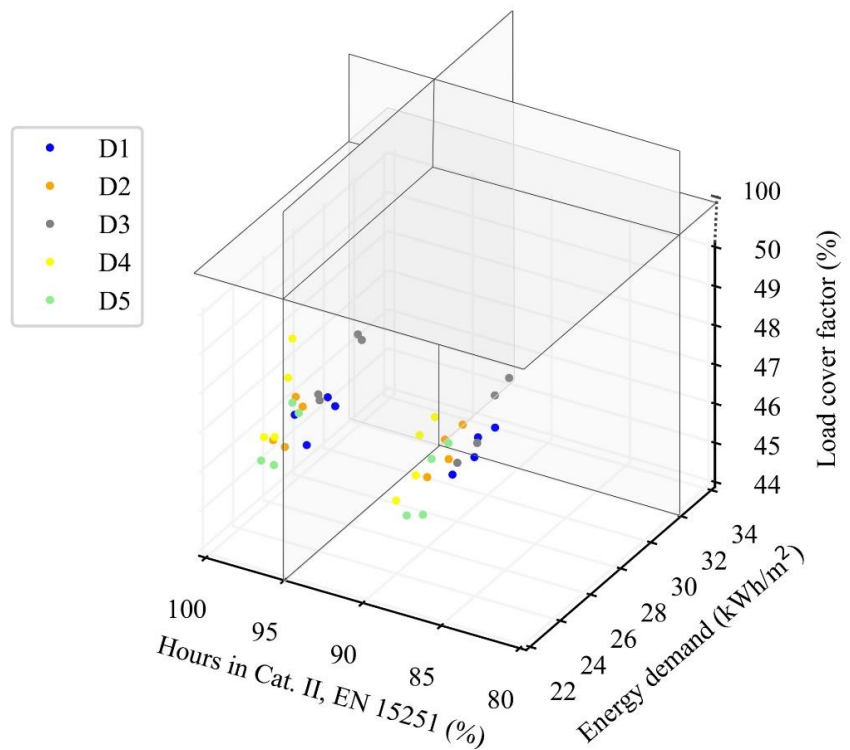

Figure 6. Energy demand vs. percentage of hours in Category II of EN 15251 vs. load cover factor, for the five designs across the eight scenarios. The highlighted planes shows the robustness margins for each indicator.

Based on these observations, the choice of the best design among those analysed in this study is not straightforward and would be even more complex when facing a higher number of designs and scenarios. Therefore, the T-robust approach was developed to help building decision makers in finding a high performance and robust design by benefiting an automated algorithm that can be run by just specifying the design performance targets.

The results of the robustness assessment with MT-KPI are shown in Figure 7. In the T-robust approach, the MT-KPI allowed differentiating between feasible and infeasible designs by considering the performance targets. The robustness of each design was analysed based on the minimax regret method, as described in Section 3.2, where the maximum regret across all scenarios was assessed and its minimum value led to the most robust design.

Figure 7 shows that, among the suggested design, the minimum value of the maximum regret is achieved by D4. As mentioned before, in the T-robust approach, the preferences are automatically incorporated into the MT-KPI by using a performance target. The result of the T-robust approach shows that D4 is a design that is not only performing
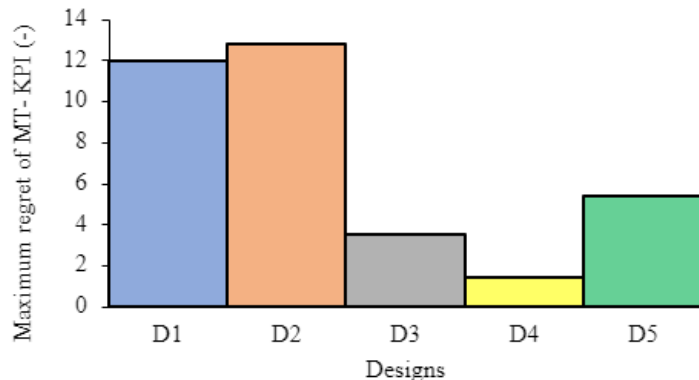
Figure 7. Calculated maximum regret for MT-KPI of the five designs. A low value shows the most robust design.

Figure 7 shows that, among the suggested design, the minimum value of the maximum regret is achieved by D4. As mentioned before, in the T-robust approach, the preferences are automatically generated based on the value of the model in large. The results discussed of the T-robust approach shows that D4 is a design that is not only performing well with respect to the performance targets for the three considered criteria, but it also has the highest robustness when exposed to the considered uncertainty scenarios. This is also in line with the observations which stemmed from the discussion in Section 4.1, as D4 has the lowest energy demand across all scenarios presents a middle range of hours in category II and is one of the designs with the highest load factor.

4.3. Simulation Model Assessment

In this section, the results/simulation of the model in IDA ICE are discussed and assessed against findings in similar studies. The simulation results could not be validated with measurement data, as the case study office was recently built and no data for the real energy use were available for the reference design nor for the other hypothetical RBE-based designs considered in this research. However, specific results obtained in this article are compared with those of similar studies to verify their overall reliability. The heating energy demand of a Norwegian ZEB comparable to the case study building of this research, as described in [79], was in line with that estimated with IDA ICE in the current study for all designs/scenarios (in the range of 20–30 kWh/m² for the reference design). Additionally, the results obtained in the design with EC windows were comparable with those obtained in a similar case study, i.e., [68], where two control strategies based on indoor temperature and lighting were assessed for a representative building in Trondheim. As in this article, the authors of [68] found that the EC window controlled by operative temperature could provide the highest yearly energy saving, up to 20%, compared to a building equipped with reference windows with no control strategies. Finally, the results of the designs with PCM are also compared with those of a similar study, i.e., [75], where a building with PCM layer, integrated backside the interior finish layer of external walls on south façade and internal screens on east/west façades (D2), where PCM layer was assessed in [75], where climate conditions in [75], the authors found that, all heating-dominated buildings, by using a PCM with a melting point at around 20 °C, the annual energy saving was around 2–3% in Nordic climates; this result is in line with what we found out, with the use of PCM in external walls coupled with external screen on south façade and internal screens on east/west façades (D2).

Using a fully planned ZEB-COM building as a case study for this work also allowed determining a more specific threshold for total delivered energy. Based on the project documentation, heating all animated buildings by using a PCM ZEB-COM balance had to be below 20 °C. the annual energy saving CO₂ eq/m²/yr or 35 kWh/m²/yr (including system losses and excluding the PV contribution). This had been calculated during the building planning and construction based on the actual materials used, data records for the construction site emissions, and carbon emissions from the Norwegian energy grids (local district heating grid and electricity). The total annual delivered energy estimated through IDA ICE for the various designs was in the range 29–32 kWh/m², which is consistent with the abovementioned threshold. Note that only for the as-built design, D1, it can be asserted that all its scenarios achieve the zero-energy balance over the entire lifetime, based on the results of the life-cycle assessment available in the project documentation. The other designs, D2–D5, certainly achieve the zero-energy balance in the operational stage, given the very high energy generated by PVs that is over 80 kWh/m²/yr. However, a detailed life-cycle

and construction based on the actual materials used, data records for the construction site emissions, and carbon emissions from the Norwegian energy grids (local district heating grid and electricity). The total annual delivered energy estimated through IDA ICE for the various designs was in the range 29–32 kWh/m^2, which is consistent with the abovementioned threshold. Note that only for the as-built design, D1, it can be asserted that all its scenarios achieve the zero-energy balance over the entire lifetime, based on the results of the life-cycle assessment available in the project documentation. The other designs, D2−D5, certainly achieve the zero-energy balance in the operational stage, given the very high energy generated by PVs that is over 80 kWh/m^2/yr. However, a detailed life-cycle assessment should be performed for D2–D5 designs and scenarios if the objective is to verify the zero-energy/emission balance over the building lifetime, by also including the contribution from the construction and material stages.

5. Conclusions

This article focused on the assessment of responsive building envelope (RBE) designs in zero energy/emission buildings (ZEBs) using a robustness-based multi-criteria decision making (MCDM). A literature review of key assessment criteria and indicators for RBE analysis led to the classification and selection of assessment indicators used in this paper. Unlike in previous research, only quantifiable KPIs were considered to establish objective and comparable performance assessments. The methodological approach proposed was an extension of a novel robustness-based MCDM method that normalizes the objective functions into a single multi-target key performance indicator (MT-KPI). The method combines robustness assessment and decision-making aspects and allows identifying the most appropriate design alternative by not only comparing several designs to each other but also specific performance targets.

The innovative extension of the methodological approach was tested on a case study of a recently built ZEB connected to the local energy grid and located in a Norwegian zone that is intended to become a zero-energy/emission neighbourhood (ZEN). Five competitive designs and eight occupancy and climate scenarios were assessed and compared through three performance indicators focusing on energy use, thermal comfort, and load matching. The analysed designs included a combination of three main RBE technologies, which were building integrated photovoltaics, phase change materials, and electrochromic windows.

The findings of this paper show that the proposed approach helped selecting the most robust building design more easily than if one were to separately compare the performance indicators, without the need for weighting the objectives and with less dependency on the scenario conditions. The results of the performance assessment highlight the difficulty of defining the best design, especially when several scenarios are evaluated under uncertainties in relation, for instance, to building occupation and future climate. This would be even more challenging in real-word projects, where decision makers often have resource and time constraints. Furthermore, as the case study of this article is a real ZEB recently built in Norway, the chosen examined indicators also allowed to gain insight into critical aspects of such buildings, contributing to the definition of benchmark values for explored performance indicators. The flexibility of the method used in this article indicates that it could be applied to other case studies where it could provide insights into design options for new buildings but also for renovation or building extension projects. Indeed, the freedom of choice when it comes to performance criteria and targets make the approach versatile and the single indicator output makes it compatible with parametric performance assessments and even single objective numerical optimization.

This article focuses on assessing RBE designs in ZEB projects, which can support the optimization of the balance between several energy flows at the building and more generally at the neighbourhood scale. This can be useful for the active management of the energy purchased and/or renewably harvested and can also enhance user comfort and acceptance by supplying an interactive interface with the outdoors. As several RBE technologies are available, a systematic breakdown of the properties and requirements

of these technologies is needed to build a portfolio of solutions that can lead to the zero-emission goal for buildings and neighbourhoods. Furthermore, the modelling approach, as well as the modeler's skills and the tool used, represent key aspects when dealing with a system at different scales. The complexity required to simulate clusters of buildings could be handled through lumped capacitance models and grey box approaches, which are less input-intensive than whole building simulation models used in software such as IDA ICE, which was employed in this study.

Several actors involved in a building process could make use of the methodology of this article, including architects, engineers, consultants, and other decision makers. Such actors can be supported in the selection of high performance and robust designs, which should meet specific requirements even under uncertainties that arise in the life cycle of the building.

The study in this article presents some limitations that should be addressed by future research. First, the methodological approach proposed was applied to a single ZEB, but future research could focus on different case studies, including clusters of buildings and neighbourhoods. In this article, a three-criteria robust design problem was addressed, but future studies could extend the analysis to tackle more than three performance indicators. Moreover, the work developed in this study could be developed even further and be integrated with artificial intelligence approaches as part of scenario modelling for digital twins and cyber-physical systems to evaluate the robustness of a system or identify its vulnerabilities [80].

Institutional Review Board Statement: Not applicable.

Informed Consent Statement: Not applicable.

Data Availability Statement: Not applicable.

Conflicts of Interest: The authors declare no conflict of interest.

Nomenclature

AF	Adaptive façade
AHP	Analytical Hierarchy Process
BIPV	Building integrated photovoltaics
CABS	Climate adaptive building shell
CEN	European Committee for Standardization
D_i	Design (with i = 1,2,3,4,5)
DHW	Domestic hot water
DSM	Demand side management
EC	Electrochromic
EN	European norm
GHG	Greenhouse gas emission
IAQ	Indoor air quality
IDA ICE	IDA Indoor Climate and Energy software

IEQ	Indoor environmental quality
IPCC	Intergovernmental panel on climate change
ISO	International Organization for Standardization
KPI	Key performance indicator
LED	Light emitting diode
MAUT	Multi-Attribute Utility Theory
MCDM	Multi-criteria decision making
MET	Metabolic equivalent of task
MT-KPI	Multi-target key performance indicator
PCM	Phase change material
PMV	Predicted mean vote
PPD	Percentage People Dissatisfied
PV	Photovoltaics
RBE	Responsive building envelope
TEK17	Norwegian building regulation
TMY	Typical meteorological year
VAV	Variable air volume
ZEB	Zero emission/energy building
ZEB-COM	ZEB level (C = construction; O = operation; M = materials)
ZEB-lab	Zero Emission Building Laboratory
ZEN	Zero emission/energy neighbourhood
A_m	Maximum performance of design m across all scenarios
B_m	Minimum performance of design m across all scenarios
C_n	Minimum performance of each scenario
C_p	Specific heat capacity
$KPI_{i,rel}$	Relative performance for indicator i
$KPI_{i,m}$	Robustness margin for indicator i
$KPI_{n,m}$	Performance of design m across scenario n
$R_{n,m}$	Performance regret of design m across scenario n

Appendix A

Table A1. Finding the maximum and minimum performance of a design across scenarios and best performance for designs and scenarios [21].

Design	Scenarios					Max and Min Performance Across Scenarios	
	S_1	S_2	...	S_i	S_n	Maximum Performance (A)	Minimum Performance (B)
D_1	KPI_{11}	KPI_{21}	...	KPI_{i1}	KPI_{n1}	$A_1 = \max (KPI_{11}, \ldots, KPI_{n1})$	$B_1 = \min (KPI_{11}, \ldots, KPI_{n1})$
D_2	KPI_{12}	KPI_{22}	...	KPI_{i2}	KPI_{n2}	A_2	B_2
...			...				
D_i	KPI_{1i}	KPI_{2i}	...	KPI_{ii}	KPI_{ni}	A_i	B_i
D_m	KPI_{1m}	KPI_{2m}	...	KPI_{im}	KPI_{nm}	A_m	B_m
Minimum performance for each scenario (C)	$C_1 = \min (KPI_{11}, \ldots, KPI_{1m})$	C_2	...	C_i	C_n		
Best performance of all designs across all scenarios						$D = \min(B) = \min(C)$	

Table A2. Calculation of performance regret of designs across all scenarios [21].

	Performance Regret (R)			
	Scenarios			
Designs	S_1	S_2	. . .	S_n
D_1	$R_{11} = KPI_{11} - C_1$	$R_{21} = KPI_{21} - C_2$	. . .	$R_{n1} = KPI_{n1} - C_n$
D_2	$R_{12} = KPI_{12} - C_1$	$R_{22} = KPI_{22} - C_2$	. . .	$R_{n2} = KPI_{n2} - C_n$
. . .			. . .	
D_i	$R_{1i} = KPI_{1i} - C_1$	$R_{2i} = KPI_{2i} - C_2$	. . .	$R_{ni} = KPI_{ni} - C_n$
D_m	$R_{1m} = KPI_{1m} - C_1$	$R_{2m} = KPI_{2m} - C_2$	. . .	$R_{nm} = KPI_{nm} - C_n$

Table A3. Main envelope parameters for the case study building.

Design Parameters	Value	Note
U-value, external walls	0.15 W/(m^{2}K)	Wooden frame with 300 mm mineral wool insulation
U-value, windows/door	0.77 W/(m^{2}K)	Triple glazed with argon filling and wood frame
Solar factor, g-value, windows	0.53	
Visible transmittance, T-vis, windows	0.71	
U-value, roof	0.09 W/(m^{2}K)	Wooden structure with 450 mm mineral wool insulation
U-value, slab on ground	0.10 W/(m^{2}K)	Concrete slab on 250 mm of EPS insulation. Equivalent U-value for ground transmission
Normalised thermal bridge	0.04 W/(m^{2}K)	
Air leakage at 50 Pa	0.3 h^{-1}	
Window-to-wall ratio	27%	

Table A4. Main building systems' parameters for the case study building.

Design Parameters	Value	Note
Heat pump, COP	3.8	Air-to-water heat pump
Heat pump, total heating capacity	30 kW	
Heating set-point	21 °C 07:00–17:00 Monday-Friday, occupied building 20 °C 17:00–24:00 Monday-Friday, non-occupied building; 15 °C 22:00–07:00 every day	
Heating distribution system (supply/return temperatures)	47/35 °C	Waterborne radiator system
Cooling set-point	24 °C	
Ventilation supply airflow rates	2.5 L/s/m^2	
Ventilation, supply air temperature	17–24 °C	Based on the exhaust air temp.
Ventilation, specific fan power	1 kW/m^3/s °C	
Ventilation, heat recovery efficiency	85%	Rotary heat exchanger
DHW, average hot water use	5 kWh/m^2/year	
PV façade, area	502 m^2	
PV roof, area	456 m^2	
PV façade, average efficiency	16.9%	Monocrystalline silicon
PV roof, average efficiency	21.5%	Monocrystalline silicon
PV facade, installed capacity	83 kWp	
PV roof, installed capacity	98 kWp	

		silicon
PV roof, average efficiency	21.5%	Monocrystalline silicon
PV facade, installed capacity	83 kWp	
PV roof, installed capacity	98 kWp	

— Occupants/El. equipment   — Lighting

Figure A1. Profile schedules used for occupancy, electric equipment, and lighting in the analysed scenarios. * The dashed blue and orange lines denote scenarios 2, 3, 7, and 8, which imply a longer stay of occupants in specific rooms. ** The dotted blue line denotes the occupation profile for the canteen, which is the only zone whose occupation differs from the rest of the modelled zones.

Table A5. Number of occupants set in the models for all rooms, with the profile schedules shown in Figure A1.

Modelled Building Zones	Number of Occupants
Ground floor south, canteen	78
Ground floor, middle zone, auxiliary	1
Ground floor, north zone, auxiliary	1
1st floor south, Tween room 1, working zone	7
1st floor south, Tween room 1, working zone	7
1st floor south, middle zone, auxiliary/meeting	1
1st floor north, working zone	9
1st floor north, auxiliary/lobby	2
2nd floor south, working zone	8
2nd floor south, meeting room 1	3
2nd floor south, meeting room 2	1
2nd floor middle, auxiliary/meeting	3
2nd floor north, working zone	12
2nd floor north, auxiliary/lobby	2
3rd floor north, teaching room	28
3rd floor north, auxiliary/meeting	15
3rd floor middle, auxiliary	0
3rd floor south, auxiliary	0
Secondary stairway	0

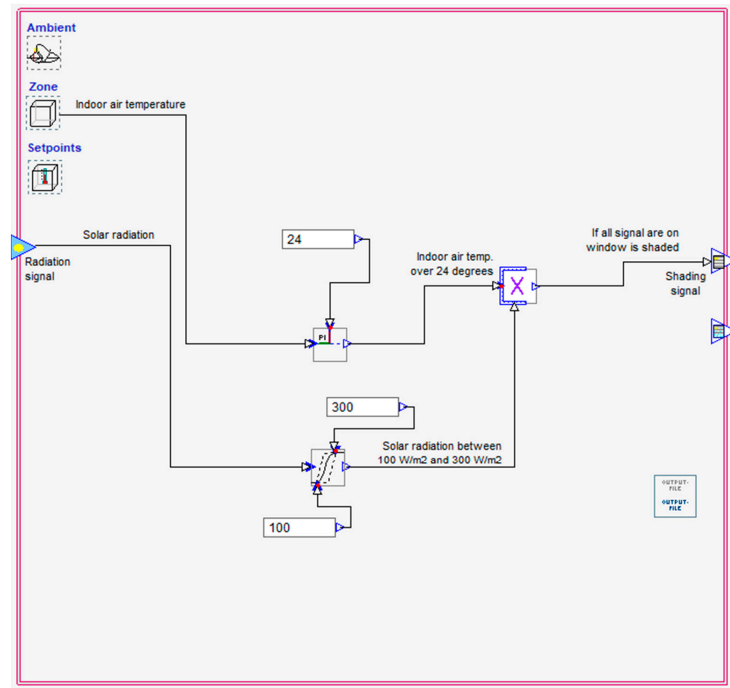|	
2nd floor north, working zone	12
2nd floor north, auxiliary/lobby	2
3rd floor north, teaching room	28
3rd floor north, auxiliary/meeting	15
3rd floor middle, auxiliary	0
3rd floor south, auxiliary	0
Secondary stairway	0

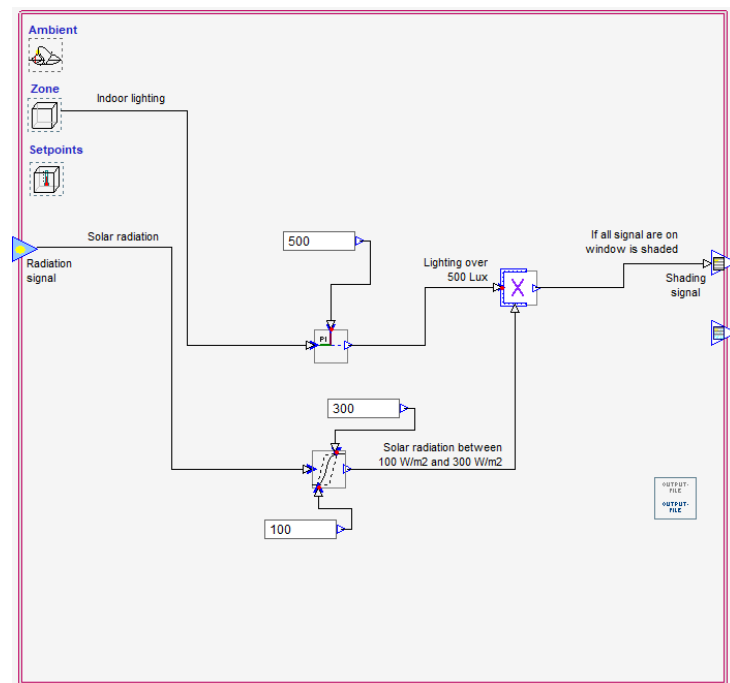**Figure A2.** Control macro used for EC windows in design 4.

Figure A3. Control macro used for EC windows in design 5.

References

1. UN General Assembly. *Transforming Our World: The 2030 Agenda for Sustainable Development*; A/RES/70/1, 21 October 2015. Available online: https://www.refworld.org/docid/57b6e3e44.html [Accessed on 10 November 2021].
2. Moschetti, R.; Brattebø, H.; Sparrevik, M. Exploring the Pathway from Zero-Energy to Zero-Emission Building Solutions: A Case Study of a Norwegian Office Building. *Energy Build.* **2019**, *188–189*, 84–97. https://doi.org/10.1016/j.enbuild.2019.01.047.
3. Li, D.H.W.; Yang, L.; Lam, J.C. Zero Energy Buildings and Sustainable Development Implications—A Review. *Energy* **2013**, *54*,

References

1. UN General Assembly. Transforming Our World: The 2030 Agenda for Sustainable Development; A/RES/70/1. 21 October 2015. Available online: https://www.refworld.org/docid/57b6e3e44.html (accessed on 10 November 2021).
2. Moschetti, R.; Brattebø, H.; Sparrevik, M. Exploring the Pathway from Zero-Energy to Zero-Emission Building Solutions: A Case Study of a Norwegian Office Building. *Energy Build.* **2019**, *188–189*, 84–97. [CrossRef]
3. Li, D.H.W.; Yang, L.; Lam, J.C. Zero Energy Buildings and Sustainable Development Implications—A Review. *Energy* **2013**, *54*, 1–10. [CrossRef]
4. Lützkendorf, T.; Balouktsi, M. Assessing a Sustainable Urban Development: Typology of Indicators and Sources of Information. *Procedia Environ. Sci.* **2017**, *38*, 546–553. [CrossRef]
5. Marique, A.-F.; Reiter, S. A Simplified Framework to Assess the Feasibility of Zero-Energy at the Neighbourhood/Community Scale. *Energy Build.* **2014**, *82*, 114–122. [CrossRef]
6. Nematchoua, M.K.; Marie-Reine Nishimwe, A.; Reiter, S. Towards Nearly Zero-Energy Residential Neighbourhoods in the European Union: A Case Study. *Renew. Sustain. Energy Rev.* **2021**, *135*, 110198. [CrossRef]
7. Skaar, C.; Labonnote, N.; Gradeci, K. From Zero Emission Buildings (ZEB) to Zero Emission Neighbourhoods (ZEN): A Mapping Review of Algorithm-Based LCA. *Sustainability* **2018**, *10*, 2405. [CrossRef]
8. Kjendseth Wiik, M.; Fufa, S.M.; Baer, D.; Sartori, I.; Andresen, I. *The ZEN Definition—A Guideline for the ZEN Pilot Areas*; Research Centre on Zero Emission Neighbourhoods in Smart Cities: Trondheim, Norway, 2018.
9. Perino, M.; Serra, V. Switching from Static to Adaptable and Dynamic Building Envelopes: A Paradigm Shift for the Energy Efficiency in Buildings. *J. Facade Des. Eng.* **2015**, *3*, 143–163. [CrossRef]
10. Böke, J.; Knaack, U.; Hemmerling, M. State-of-the-Art of Intelligent Building Envelopes in the Context of Intelligent Technical Systems. *Intell. Build. Int.* **2019**, *11*, 27–45. [CrossRef]
11. Heiselberg, P. *ECBCS Annex 44: Integrating Environmentally Responsive Elements in Buildings. Project Summary Report*; Energy Conservation in Buildings and Community Systems Programme; International Energy Agency: Paris, France; AECOM Ltd.: St. Albans, UK, 2012.
12. Loonen, R.C.G.M.; Trčka, M.; Cóstola, D.; Hensen, J.L.M. Climate Adaptive Building Shells: State-of-the-Art and Future Challenges. *Renew. Sustain. Energy Rev.* **2013**, *25*, 483–493. [CrossRef]
13. Taveres-Cachat, E.; Grynning, S.; Thomsen, J.; Selkowitz, S. Responsive Building Envelope Concepts in Zero Emission Neighborhoods and Smart Cities—A Roadmap to Implementation. *Build. Environ.* **2019**, *149*, 446–457. [CrossRef]
14. Loonen, R.C.G.M.; Favoino, F.; Hensen, J.L.M.; Overend, M. Review of Current Status, Requirements and Opportunities for Building Performance Simulation of Adaptive Facades. *J. Build. Perform. Simul.* **2017**, *10*, 205–223. [CrossRef]
15. Sadineni, S.B.; Madala, S.; Boehm, R.F. Passive Building Energy Savings: A Review of Building Envelope Components. *Renew. Sustain. Energy Rev.* **2011**, *15*, 3617–3631. [CrossRef]
16. Reynders, G.; Nuytten, T.; Saelens, D. Potential of Structural Thermal Mass for Demand-Side Management in Dwellings. *Build. Environ.* **2013**, *64*, 187–199. [CrossRef]
17. Moghtadernejad, S.; Chouinard, L.E.; Mirza, M.S. Design Strategies Using Multi-Criteria Decision-Making Tools to Enhance the Performance of Building Façades. *J. Build. Eng.* **2020**, *30*, 101274. [CrossRef]
18. Kokaraki, N.; Hopfe, C.J.; Robinson, E.; Nikolaidou, E. Testing the Reliability of Deterministic Multi-Criteria Decision-Making Methods Using Building Performance Simulation. *Renew. Sustain. Energy Rev.* **2019**, *112*, 991–1007. [CrossRef]
19. Hopfe, C.J.; Augenbroe, G.L.M.; Hensen, J.L.M. Multi-Criteria Decision Making under Uncertainty in Building Performance Assessment. *Build. Environ.* **2013**, *69*, 81–90. [CrossRef]
20. Vullo, P.; Passera, A.; Lollini, R.; Prada, A.; Gasparella, A. Implementation of a Multi-Criteria and Performance-Based Procurement Procedure for Energy Retrofitting of Facades during Early Design. *Sustain. Cities Soc.* **2018**, *36*, 363–377. [CrossRef]
21. Homaei, S.; Hamdy, M. A Robustness-Based Decision Making Approach for Multi-Target High Performance Buildings under Uncertain Scenarios. *Appl. Energy* **2020**, *267*, 114868. [CrossRef]
22. Bianco, L.; Cascone, Y.; Avesani, S.; Vullo, P.; Bejat, T.; Koenders, S.; Loonen, R.C.G.M.; Goia, F.; Serra, V.; Favoino, F. Towards New Metrics for the Characterisation of the Dynamic Performance of Adaptive Façade Systems. *J. Facade Des. Eng.* **2018**, *6*, 175–196. [CrossRef]
23. Attia, S.; Bilir, S.; Safy, T.; Struck, C.; Loonen, R.; Goia, F. Current Trends and Future Challenges in the Performance Assessment of Adaptive Façade Systems. *Energy Build.* **2018**, *179*, 165–182. [CrossRef]
24. Loonen, R.C.G.M.; Rico-Martinez, J.M. Favoino Design for Façade Adaptability: Towards a Unified and Systematic Characterization. In Proceedings of the 10th Energy Forum—Advanced Building Skins, Bern, Switzerland, 3–4 November 2015; Economic Forum: Munich, Germany; pp. 1284–1294.
25. Aelenei, D.; Aelenei, L.; Vieira, C.P. Adaptive Façade: Concept, Applications, Research Questions. *Energy Procedia* **2016**, *91*, 269–275. [CrossRef]
26. Reynders, G.; Amaral Lopes, R.; Marszal-Pomianowska, A.; Aelenei, D.; Martins, J.; Saelens, D. Energy Flexible Buildings: An Evaluation of Definitions and Quantification Methodologies Applied to Thermal Storage. *Energy Build.* **2018**, *166*, 372–390. [CrossRef]
27. Salom, J.; Widen, J.; Candanedo, J.; Sartori, I.; Voss, K.; Marszal, A. Understanding Net Zero Energy Buildings: Evaluation of Load Matching and Grid Interaction Indicators. In Proceedings of the 12th Conference of International Building Performance

Simulation Association (Building Simulation 2011), Sydney, Australia, 14–16 November 2011; IBPSA Australasia and AIRAH: Melbourne, Australia, 2011.

28. Sartori, I.; Napolitano, A.; Voss, K. Net Zero Energy Buildings: A Consistent Definition Framework. *Energy Build.* **2012**, *48*, 220–232. [CrossRef]
29. Wiik, M.K.; Fufa, S.M.; Krogstie, J.; Ahlers, D.; Wyckmans, A.; Driscoll, P.; Brattebø, H.; Gustavsen, A. *Zero Emission Neighbourhood in Smart Cities. Definition, Key Performance Indicators and Assessment Criteria*; The Research Centre on Zero Emission Buildings: Trondheim, Norway, 2018.
30. Invidiata, A.; Lavagna, M.; Ghisi, E. Selecting Design Strategies Using Multi-Criteria Decision Making to Improve the Sustainability of Buildings. *Build. Environ.* **2018**, *139*, 58–68. [CrossRef]
31. Wong, J.K.W.; Li, H. Application of the Analytic Hierarchy Process (AHP) in Multi-Criteria Analysis of the Selection of Intelligent Building Systems. *Build. Environ.* **2008**, *43*, 108–125. [CrossRef]
32. Omar, F.; Bushby, S.T.; Williams, R.D. *Assessing the Performance of Residential Energy Management Control Algorithms: Multi-Criteria Decision Making Using the Analytical Hierarchy Process*; National Institute of Standards and Technology: Gaithersburg, MD, USA, 2019; p. NIST TN 2017r1.
33. Yang, K.; Zhu, N.; Chang, C.; Wang, D.; Yang, S.; Ma, S. A Methodological Concept for Phase Change Material Selection Based on Multi-Criteria Decision Making (MCDM): A Case Study. *Energy* **2018**, *165*, 1085–1096. [CrossRef]
34. Rysanek, A.M.; Choudhary, R. Optimum Building Energy Retrofits under Technical and Economic Uncertainty. *Energy Build.* **2013**, *57*, 324–337. [CrossRef]
35. Kotireddy, R.; Hoes, P.-J.; Hensen, J.L.M. Simulation-Based Comparison of Robustness Assessment Methods to Identify Robust Low-Energy Building Designs. In Proceedings of the 15th International Conference of the International Building Performance Simulation Association (Building Simulation 2017), San Francisco, CA, USA, 7–9 August 2017; Curran Associates, Inc.: New York, NY, USA; pp. 892–901.
36. Bui, D.-K.; Nguyen, T.N.; Ghazlan, A.; Ngo, N.-T.; Ngo, T.D. Enhancing Building Energy Efficiency by Adaptive Façade: A Computational Optimization Approach. *Appl. Energy* **2020**, *265*, 114797. [CrossRef]
37. Favoino, F.; Goia, F.; Perino, M.; Serra, V. Experimental Assessment of the Energy Performance of an Advanced Responsive Multifunctional Façade Module. *Energy Build.* **2014**, *68*, 647–659. [CrossRef]
38. Favoino, F.; Overend, M.; Jin, Q. The Optimal Thermo-Optical Properties and Energy Saving Potential of Adaptive Glazing Technologies. *Appl. Energy* **2015**, *156*, 1–15. [CrossRef]
39. Hoffmann, S.; Lee, E.S.; McNeil, A.; Fernandes, L.; Vidanovic, D.; Thanachareonkit, A. Balancing Daylight, Glare, and Energy-Efficiency Goals: An Evaluation of Exterior Coplanar Shading Systems Using Complex Fenestration Modeling Tools. *Energy Build.* **2016**, *112*, 279–298. [CrossRef]
40. Ochoa, C.E.; Aries, M.B.C.; van Loenen, E.J.; Hensen, J.L.M. Considerations on Design Optimization Criteria for Windows Providing Low Energy Consumption and High Visual Comfort. *Appl. Energy* **2012**, *95*, 238–245. [CrossRef]
41. Yun, G.; Yoon, K.C.; Kim, K.S. The Influence of Shading Control Strategies on the Visual Comfort and Energy Demand of Office Buildings. *Energy Build.* **2014**, *84*, 70–85. [CrossRef]
42. Goia, F.; Haase, M.; Perino, M. Optimizing the Configuration of a Façade Module for Office Buildings by Means of Integrated Thermal and Lighting Simulations in a Total Energy Perspective. *Appl. Energy* **2013**, *108*, 515–527. [CrossRef]
43. Nematchoua, M.K.; Noelson, J.C.V.; Saadi, I.; Kenfack, H.; Andrianaharinjaka, A.-Z.F.R.; Ngoumdoum, D.F.; Sela, J.B.; Reiter, S. Application of Phase Change Materials, Thermal Insulation, and External Shading for Thermal Comfort Improvement and Cooling Energy Demand Reduction in an Office Building under Different Coastal Tropical Climates. *Sol. Energy* **2020**, *207*, 458–470. [CrossRef]
44. de Boer, B.J.; Ruijg, G.J.; Bakker, L.; Kornaat, W.; Zonneveldt, L.; Kurvers, S.; Alders, N.; Raue, A.; Hensen, J.L.M.; Loonen, R.C.G.M.; et al. Energy Saving Potential of Climate Adaptive Building Shells—Inverse Modelling of Optimal Thermal and Visual Behaviour. In Proceedings of the International Adaptive Architecture Conference, London, UK, 3–5 March 2011; p. 16.
45. *ISO 52000-1*; Energy Performance of Buildings—Overarching EPB Assessment—Part 1: General Framework and Procedures. ISO: Geneva, Switzerland, 2017.
46. *SN/NSPEK 3031:2020*; Energy Performance of Buildings—Calculation of Energy Needs and Energy Supply. Standards Norway: Lysaker, Norway, 2020. (In Norwegian)
47. *EN 15978*; Sustainability of Construction Works. Assessment of Environmental Performance of Buildings. Calculation Method. CEN: Brussels, Belgium, 2011.
48. *NS 3720*; Method for Greenhouse Gas Calculations for Buildings. Standards Norway: Lysaker, Norway, 2018. (In Norwegian)
49. *ISO 7730*; Ergonomics of the Thermal Environment—Analytical Determination and Interpretation of Thermal Comfort Using Calculation of the PMV and PPD Indices and Local Thermal Comfort Criteria. ISO: Geneva, Switzerland, 2015.
50. *EN 16798-1*; Energy Performance of Buildings—Ventilation for Buildings. Part 1: Indoor Environmental Input Parameters for Design and Assessment of Energy Performance of Buildings Addressing Indoor Air Quality, Thermal Environment, Lighting and Acoustics. CEN: Brussels, Belgium, 2017.
51. *EN 16798-2*; Energy Performance of Buildings—Ventilation for Buildings. Part 2: Interpretation of the Requirements in EN 16798-1. Indoor Environmental Input Parameters for Design and Assessment of Energy Performance of Buildings Addressing Indoor Air Quality, Thermal Environment, Lighting and Acoustics. CEN: Brussels, Belgium, 2017.

52.   *ISO 19454*; Building Environment Design—Indoor Environment—Daylight Opening Design for Sustainability Principles in Visual Environment. ISO: Geneva, Switzerland, 2019.

53.   Carlucci, S.; Causone, F.; De Rosa, F.; Pagliano, L. A Review of Indices for Assessing Visual Comfort with a View to Their Use in Optimization Processes to Support Building Integrated Design. *Renew. Sustain. Energy Rev.* **2015**, *47*, 1016–1033. [CrossRef]

54.   *ISO 717-1*; Acoustics—Rating of Sound Insulation in Buildings and of Building Elements—Part 1: Airborne Sound Insulation. ISO: Geneva, Switzerland, 2020.

55.   *ISO 717-2*; Acoustics—Rating of Sound Insulation in Buildings and of Building Elements—Part 2: Impact Sound Insulation. ISO: Geneva, Switzerland, 2020.

56.   Voss, K.; Sartori, I.; Napolitano, A.; Geier, S.; Gonzalves, H.; Hall, M.; Heiselberg, P.; Widén, J.; Candanedo, J.A.; Musall, E.; et al. Load Matching and Grid Interaction of Net Zero Energy Buildings. In Proceedings of the EuroSun 2010 Conference, Graz, Austria, 28 September–1 October 2010.

57.   Salom, J.; Marszal, A.J.; Widén, J.; Candanedo, J.; Lindberg, K.B. Analysis of Load Match and Grid Interaction Indicators in Net Zero Energy Buildings with Simulated and Monitored Data. *Appl. Energy* **2014**, *136*, 119–131. [CrossRef]

58.   Vigna, I.; Pernetti, R.; Pasut, W.; Lollini, R. Literature Review on Energy Flexibility Definitions and Indicators for Building Clusters. A Technical Report from IEA EBC Annex 67 Energy Flexible Buildings. 2018. Available online: https://www.annex67.org/media/1863/literature-review-on-energy-flexibility-definitions-and-indicators-for-building-clusters.pdf (accessed on 10 November 2021).

59.   *MATLAB*, Version 9.7.; The MathWorks Inc.: Natick, MA, USA, 2019.

60.   Research Centre on Zero Emission Neighbourhood in Smart City. NTNU Campus, Knowledge Axis Trondheim. Available online: https://fmezen.no/knowledge-axis-trondheim/ (accessed on 1 October 2021).

61.   Time, B.; Engebø, A.; Christensen, M.; Dalby, O.; Kvande, T. The Design Process for Achievement of an Office Living Laboratory with a ZEB Standard. *IOP Conf. Ser. Earth Environ. Sci.* **2019**, *352*, 012053. [CrossRef]

62.   Fufa, S.M.; Dahl Schlandbusch, R.; Sørnes, K.; Inman, M.; Andresen, I. *A Norwegian ZEB Definition Guideline*; The Research Centre on Zero Emission Buildings: Trondheim, Norway, 2016.

63.   EQUA Simulation AB, IDA Indoor Climate and Energy (IDA ICE). Available online: https://www.equa.se/en/ida-ice (accessed on 7 October 2021).

64.   Kropf, S.; Zweifel, G. *Validation of the Building Simulation Program IDA-ICE According to CEN 13791 Thermal Performance of Buildings—Calculation of Internal Temperatures of a Room in Summer Without Mechanical Cooling—General Criteria and Validation Procedures*; Hochschule Technik+Architektur Luzern Abt.: Horw, Switzerland, 2010. Available online: https://www.equa.se/en/ida-ice/validation-certifications (accessed on 10 November 2021).

65.   Equa Simulation AB. *Technical Report: Validation of IDA Indoor Climate and Energy 4.0 Build 4 with Respect to ANSI/ASHRAE Standard 140-2004*; Equa Simulation: Solna, Sweden, 2010. Available online: https://www.equa.se/en/ida-ice/validation-certifications (accessed on 10 November 2021).

66.   Equa Simulation AB. *Technical Report: Validation of IDA Indoor Climate and Energy 4.0 with Respect to CEN Standards EN 15255-2007 and EN 15265-200*; Equa Simulation: Solna, Sweden, 2010. Available online: https://www.equa.se/en/ida-ice/validation-certifications (accessed on 10 November 2021).

67.   Cornaro, C.; Pierro, M.; Puggioni, V.; Roncarati, D. Outdoor Characterization of Phase Change Materials and Assessment of Their Energy Saving Potential to Reach NZEB. *Buildings* **2017**, *7*, 55. [CrossRef]

68.   Tällberg, R.; Jelle, B.P.; Loonen, R.; Gao, T.; Hamdy, M. Comparison of the Energy Saving Potential of Adaptive and Controllable Smart Windows: A State-of-the-Art Review and Simulation Studies of Thermochromic, Photochromic and Electrochromic Technologies. *Sol. Energy Mater. Sol. Cells* **2019**, *200*, 109828. [CrossRef]

69.   Mazzeo, D.; Matera, N.; Cornaro, C.; Oliveti, G.; Romagnoni, P.; De Santoli, L. EnergyPlus, IDA ICE and TRNSYS Predictive Simulation Accuracy for Building Thermal Behaviour Evaluation by Using an Experimental Campaign in Solar Test Boxes with and without a PCM Module. *Energy Build.* **2020**, *212*, 109812. [CrossRef]

70.   Cornaro, C.; Pierro, M.; Roncarati, D.; Puggioni, V. Validation of a PCM Simulation Tool in IDA ICE Dynamic Building Simulation Software Using Experimental Data from Solar Test Boxes. In Proceedings of the the 3rd Building Simulation Applications Conference (BSA 2017), Bolzano, Italy, 8–10 February 2017; Bu Press: Bolzano, Italy.

71.   Cornaro, C.; Basciano, G.; Puggioni, V.; Pierro, M. Energy Saving Assessment of Semi-Transparent Photovoltaic Modules Integrated into NZEB. *Buildings* **2017**, *7*, 9. [CrossRef]

72.   Kalnæs, S.E.; Jelle, B.P. Phase Change Materials and Products for Building Applications: A State-of-the-Art Review and Future Research Opportunities. *Energy Build.* **2015**, *94*, 150–176. [CrossRef]

73.   Casini, M. Active Dynamic Windows for Buildings: A Review. *Renew. Energy* **2018**, *119*, 923–934. [CrossRef]

74.   *ISO 15099*; Thermal Performance of Windows, Doors and Shading Services—Detailed Calculations. ISO: Geneva, Switzerland, 2017.

75.   Saffari, M.; de Gracia, A.; Fernández, C.; Cabeza, L.F. Simulation-Based Optimization of PCM Melting Temperature to Improve the Energy Performance in Buildings. *Appl. Energy* **2017**, *202*, 420–434. [CrossRef]

76.   Sustainable Energy Research Group, University of Southampton Climate Change World Weather File Generator for World-Wide Weather Data—CCWorldWeatherGen. Available online: https://energy.soton.ac.uk/climate-change-world-weather-file-generator-for-world-wide-weather-data-ccworldweathergen/ (accessed on 9 October 2021).

77. Norwegian Ministry of Local Government and Modernization and Directorate for Building Quality. Building Technical Regulation, TEK17. 2017. Available online: https://lovdata.no/dokument/SF/forskrift/2017-06-19-840 (accessed on 10 November 2021). (In Norwegian)

78. *EN 15251*; Indoor Environmental Input Parameters for Design and Assessment of Energy Performance of Buildings Addressing Indoor Air Quality, Thermal Environment, Lighting and Acoustics. CEN: Brussels, Belgium, 2007.

79. Lekang Sørensen, Å.; Andresen, I.; Taxt Walnum, H.; Justo-Alonso, M.; Fufa, S.M.; Jenssen, B.; Rådstoga, O.; Hegli, T.; Fjeldheim, H. *Pilot Building Powerhouse Kjørbo. As Built Report*; The Research Centre on Zero Emission Buildings: Trondheim, Norway, 2017.

80. Agostinelli, S.; Cumo, F.; Guidi, G.; Tomazzoli, C. Cyber-Physical Systems Improving Building Energy Management: Digital Twin and Artificial Intelligence. *Energies* **2021**, *14*, 2338. [CrossRef]

NTNU

Norwegian University of
Science and Technology